



NEW APPLICATIONS OF IODINE(III) REACTIVITY: SYNTHESIS AND FUNCTIONALIZATION OF HETEROCYCLES

Laura Fra Fernández

ADVERTIMENT. L'accés als continguts d'aquesta tesi doctoral i la seva utilització ha de respectar els drets de la persona autora. Pot ser utilitzada per a consulta o estudi personal, així com en activitats o materials d'investigació i docència en els termes establerts a l'art. 32 del Text Refós de la Llei de Propietat Intel·lectual (RDL 1/1996). Per altres utilitzacions es requereix l'autorització prèvia i expressa de la persona autora. En qualsevol cas, en la utilització dels seus continguts caldrà indicar de forma clara el nom i cognoms de la persona autora i el títol de la tesi doctoral. No s'autoritza la seva reproducció o altres formes d'explotació efectuades amb finalitats de lucre ni la seva comunicació pública des d'un lloc aliè al servei TDX. Tampoc s'autoritza la presentació del seu contingut en una finestra o marc aliè a TDX (framing). Aquesta reserva de drets afecta tant als continguts de la tesi com als seus resums i índexs.

ADVERTENCIA. El acceso a los contenidos de esta tesis doctoral y su utilización debe respetar los derechos de la persona autora. Puede ser utilizada para consulta o estudio personal, así como en actividades o materiales de investigación y docencia en los términos establecidos en el art. 32 del Texto Refundido de la Ley de Propiedad Intelectual (RDL 1/1996). Para otros usos se requiere la autorización previa y expresa de la persona autora. En cualquier caso, en la utilización de sus contenidos se deberá indicar de forma clara el nombre y apellidos de la persona autora y el título de la tesis doctoral. No se autoriza su reproducción u otras formas de explotación efectuadas con fines lucrativos ni su comunicación pública desde un sitio ajeno al servicio TDR. Tampoco se autoriza la presentación de su contenido en una ventana o marco ajeno a TDR (framing). Esta reserva de derechos afecta tanto al contenido de la tesis como a sus resúmenes e índices.

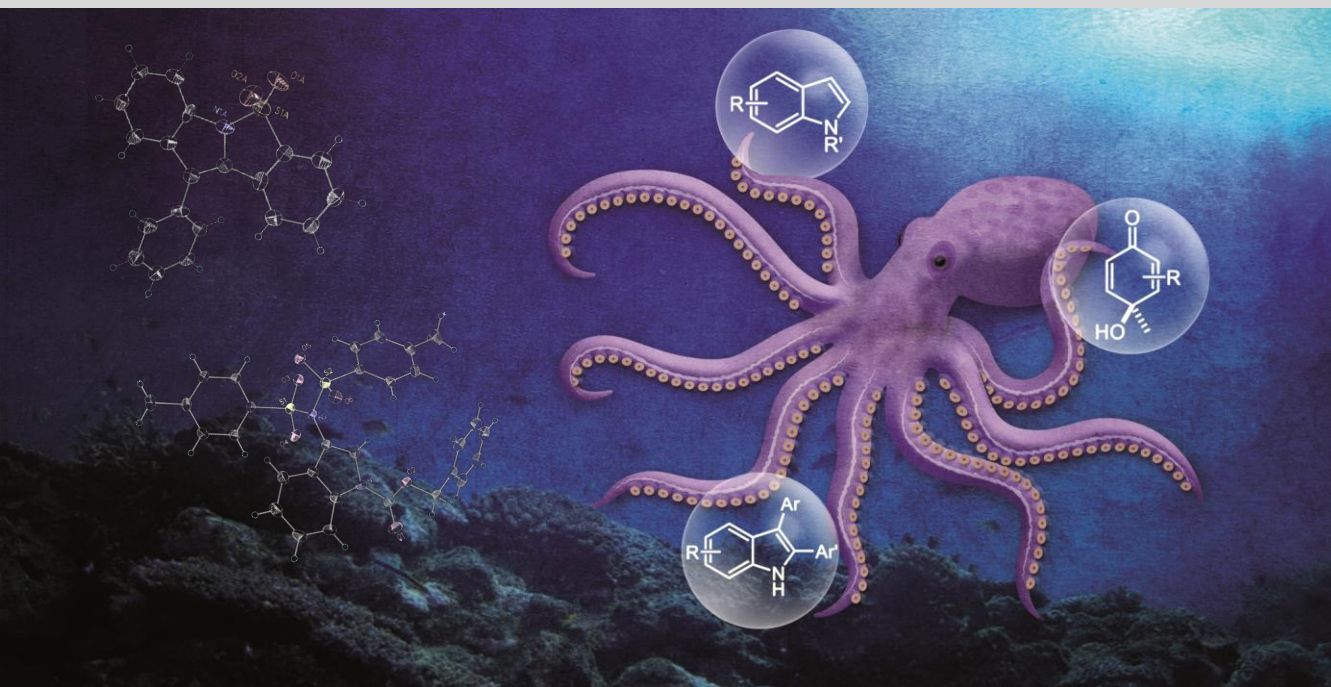
WARNING. Access to the contents of this doctoral thesis and its use must respect the rights of the author. It can be used for reference or private study, as well as research and learning activities or materials in the terms established by the 32nd article of the Spanish Consolidated Copyright Act (RDL 1/1996). Express and previous authorization of the author is required for any other uses. In any case, when using its content, full name of the author and title of the thesis must be clearly indicated. Reproduction or other forms of for profit use or public communication from outside TDX service is not allowed. Presentation of its content in a window or frame external to TDX (framing) is not authorized either. These rights affect both the content of the thesis and its abstracts and indexes.



UNIVERSITAT
ROVIRA I VIRGILI

New Applications of Iodine(III) Reactivity: Synthesis and Functionalization of Heterocycles

Laura Fra Fernández



DOCTORAL THESIS
2017

UNIVERSITAT ROVIRA I VIRGILI

NEW APPLICATIONS OF IODINE(III) REACTIVITY: SYNTHESIS AND FUNCTIONALIZATION OF HETEROCYCLES

Laura Fra Fernández

UNIVERSITAT ROVIRA I VIRGILI

NEW APPLICATIONS OF IODINE(III) REACTIVITY: SYNTHESIS AND FUNCTIONALIZATION OF HETEROCYCLES

Laura Fra Fernández

UNIVERSITAT ROVIRA I VIRGILI

NEW APPLICATIONS OF IODINE(III) REACTIVITY: SYNTHESIS AND FUNCTIONALIZATION OF HETEROCYCLES

Laura Fra Fernández

Laura Fra Fernández

New Applications of Iodine(III) Reactivity: Synthesis and Functionalization of Heterocycles

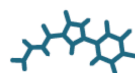
Doctoral Thesis

Supervised by Prof. Kilian Muñiz Klein

Institute of Chemical Research of Catalonia (ICIQ)



UNIVERSITAT ROVIRA I VIRGILI



ICIQ



Institut Català
d'Investigació Química

Tarragona

2017

UNIVERSITAT ROVIRA I VIRGILI

NEW APPLICATIONS OF IODINE(III) REACTIVITY: SYNTHESIS AND FUNCTIONALIZATION OF HETEROCYCLES

Laura Fra Fernández

UNIVERSITAT ROVIRA I VIRGILI

NEW APPLICATIONS OF IODINE(III) REACTIVITY: SYNTHESIS AND FUNCTIONALIZATION OF HETEROCYCLES

Laura Fra Fernández

Acknowledgments

When I accepted this challenge, I would never have imagined all the special things that this great adventure would bring me.

First of all, thanks to my supervisor for giving me the opportunity to carry out this research in a top research institute such as ICIQ. After all these years, he has become more than a thesis supervisor. I would thank him for motivating me to always do my best with perseverance, ambition and enjoyment. His advice has made me grow up little by little, improving my skills and knowledge. Thank you for believing in me from the first minute, even when I didn't know what I might be capable of.

My thanks to Prof. Satoshi Minakata and all my colleagues from the University of Osaka who gave me the possibility to spend three months in Japan. Thanks for making me feel part of your group that is so full of energy, power and happiness. It has been an experience that I will never forget.

I also have to thank Noemi Panadés and Sorania Jiménez for all the administrative and human support given during these years.

Thanks to my family, who have always supported me. From the day when I told them that I would move to Tarragona until the last day of this experience they have been always close to me, helping me in the difficult moments and always encouraging me to follow my dreams. Thanks also to all my friends who, despite the distance, have always been there.

Moreover, in this extraordinary "trip" I have been always surrounded by people who have given to me the strength and support to continue day by day. Special thanks to Dr. Claudio Martínez for all the conversations, discussions and unconditional support from the beginning that made me feel at home. Thanks for being more than a lab partner and becoming part of my family.

Thanks to all my colleagues from the Muñoz group, those who have been over all these years, sharing this experience with me.

Special thanks to Hongwei Zhang and Daniel Bafaluy for sharing the office with me in lab 2.5. We made a good team. I also have to thank Nicola for all the moments (good and bad) and for the mutual support we have given during the end of this experience.

Thanks to Estefanía and Belén for being more than lab mates. I have found real friends in both of you. We will keep in touch, for sure.

Thanks to Dr. Martín Regueiro and Dr. David Esteban from the University of La Coruña, for all they taught me and for their suggestions and support when I made the decision to join the ICIQ. Thanks for trust in me.

Thanks to all ICIQ staff and technicians for their valuable work and their help.

Support from the Institute of Chemical Research of Catalonia (ICIQ) Foundation, from Spanish Ministry for Economy and Competitiveness (FPI grant) and Severo-Ochoa Excellence Accreditation 2014-2018 (SEV-2013-2019) are gratefully acknowledged.



List of Publications

Some of the results presented in this Thesis have been published:

- “Indole Synthesis Based On A Modified Koser Reagent”
Laura Fra, Alba Millán, Jose A. Souto and Kilian Muñiz
Angew. Chem. Int. Ed. **2014**, *53*, 7349.
- “Indole Synthesis through Sequential Electrophilic N-H and C-H Bond Activation Using Iodine(III) Reactivity”
Laura Fra and Kilian Muñiz
Chemistry - A European Journal **2016**, *22*, 4351. Selected as a Hot Paper.
- “Enantioselective 4-Hydroxylation of Phenols under Chiral Organoiodine(I/III) Catalysis”
Kilian Muñiz and Laura Fra
Synthesis, **2017**, *49*, 2901. Highlighted on the journal cover.

UNIVERSITAT ROVIRA I VIRGILI

NEW APPLICATIONS OF IODINE(III) REACTIVITY: SYNTHESIS AND FUNCTIONALIZATION OF HETEROCYCLES

Laura Fra Fernández

*“The future belongs to those who believe
in the beauty of their dreams”*

Eleanor Roosevelt

UNIVERSITAT ROVIRA I VIRGILI

NEW APPLICATIONS OF IODINE(III) REACTIVITY: SYNTHESIS AND FUNCTIONALIZATION OF HETEROCYCLES

Laura Fra Fernández

List of Abbreviations and Acronyms

Ac.....	Acetyl
APCI.....	Atmospheric pressure chemical ionization
Ar.....	Aryl
Bn.....	Benzyl
Boc.....	<i>Tert</i> -butyloxy carbonyl
bpz.....	2,2'-Bipyrazine
Bz.....	Benzoyl
Cbz.....	Benzylcarbamoyl
dba.....	Dibenzylideneacetone
DCE.....	1,2-Dichloroethane
DCM.....	Dichloromethane
DMAP.....	4-Dimethylaminopyridine
DMDO.....	Dimethyldioxirane
DME.....	1,2-Dimethoxyethane
DMF.....	Dimethylformamide
DMP.....	Dess-Martin periodinane
DMSO.....	Dimethylsulphoxide
dppp.....	1,3-Bis(diphenylphosphino)propane
EDA complex.....	Electron donor-acceptor complex
<i>ee</i>	Enantiomeric excess
Equiv.....	Equivalent
ESI.....	Electrospray ionization
ESR.....	Electrospray spin resonance
Fmoc.....	9-Fluorenylmethylloxycarbonyl
GC.....	Gas chromatography
Het.....	Heterocycle

HFIP	1,1,1,3,3,3-Hexafluoroisopropanol
HPLC	High pressure liquid chromatography
HRMS.....	High resolution mass spectrometry
IBX	2-Iodobenzoic acid
IUPAC.....	International Union of Pure and Applied Chemistry
KIE.....	Kinetic isotopic effect
m.p	Melting point
MALDI.....	Matrix-assisted laser desorption ionization
<i>m</i> -CPBA.....	<i>meta</i> -Chloroperbenzoic acid
MHz	Megahertz
Min	Minute
Ms.....	Methanesulphonyl
MTBE	Methyl- <i>tert</i> -butyl-ether
NMO	<i>N</i> -Methylmorpholine <i>N</i> -oxide
NMR	Nuclear Magnetic resonance
°C	Celsius degree
Ph	Phenyl
Phth.....	Phthalimide
PIDA.....	[Bis(diacetoxy)iodo] benzene
PIFA	[Bis(trifluoroacetoxy)iodo] benzene
PMP	<i>Para</i> -methoxy phenyl
Py.....	Pyridine
RT	Room temperature
SET.....	Single electron transfer
TBAI	Tetrabutyl ammonium iodide
TBHP	<i>Tert</i> -butyl hydroperoxide
TBS.....	<i>Tert</i> -Butyldimethylsilyl
TFA	Trifluoroacetic acid
TFE.....	2,2,2-Trifluoroethanol

TIPS.....	Triisopropylsilyl
THF	Tetrahydrofuran
TLC.....	Thin-layer chromatography
TMS	Trimethylsilyl
TOF	Time-of-flight
Tf	Trifluoromethanesulfonyl
t _R	Retention time
Ts	4-Toluenesulphonyl
UV.....	Ultraviolet

UNIVERSITAT ROVIRA I VIRGILI

NEW APPLICATIONS OF IODINE(III) REACTIVITY: SYNTHESIS AND FUNCTIONALIZATION OF HETEROCYCLES

Laura Fra Fernández

Table of Contents

1. Chapter 1: General overview	1
1.1. Introduction	1
1.2. Hypervalent iodine(III) bonding and reactivity	2
1.3. Hypervalent iodine(III)-mediated C-N bond formation	6
1.4. General objectives	13
1.4.1. Synthesis of indoles through C(sp ²)-N bond formation	13
1.4.2. Alternative indole synthesis through C(sp)-N bond formation	14
1.4.3. Searching asymmetric induction using iodine(III) reactivity	15
2. Chapter 2: Indole Synthesis Based on a Modified Koser Reagent	17
2.1. Introduction	17
2.1.1. Classical indole synthesis	18
2.1.2. Metal transition-catalyzed intramolecular cyclization for indole synthesis	21
2.1.3. Hypervalent iodine-mediated intramolecular oxidative C(sp ²)-N bond formation	27
2.2. Objective	40
2.3. Results and discussion	41
2.3.1. Optimization of reaction conditions	41
2.3.2. Kinetic profile of the cyclization	44
2.3.3. Scope of the cyclization reaction	47
2.3.4. Optimization of the catalytic version of the cyclization	50
2.3.5. Mechanistic studies and final proposal	53
2.3.6. Development of a iodine(III)-mediated indole functionalization	56
2.4. Conclusions	57

2.5. Experimental part	58
3. Chapter 3: Indole Synthesis through Sequential Electrophilic N–H/C–H Bond activation Using Iodine(III) Reactivity	95
3.1. Introduction	95
3.1.1. Transition metal-catalyzed cyclization of alkynes and anilines..95	
3.1.2. Hypervalent iodine-mediated intramolecular oxidative C(sp)-N bond formation	103
3.2. Objective	106
3.3. Results and discussion	108
3.3.1. Modular synthesis of starting materials.....	108
3.3.2. Optimization of the reaction conditions	109
3.3.3. Scope of the cyclization reaction	116
3.3.4. Mechanistic studies and final proposal.....	119
3.3.5. Removal of tether and isolation of final indole.....	122
3.4. Conclusions	124
3.5. Experimental part	124
4. Chapter 4: Enantioselective 4-Hydroxylation of Phenols under Chiral Organoiodine(I/III) Catalysis	145
4.1. Introduction	145
4.1.1. Chiral alkene dioxygenation reaction	146
4.1.2. Chiral phenol dearomatization reaction.....	152
4.2. Objective	159
4.3. Results and discussion	160
4.3.1. Optimization of reaction conditions.....	160
4.3.2. Scope of the enantioselective 4-hydroxylation of phenols.....	175

4.3.3. Mechanistic proposal	176
4.3.4. Iodine(I/III)-catalyzed dearomatization of anilines	177
4.4. Conclusions	179
4.5. Experimental part	179
5. Chapter 5: Overall conclusions and outlook	187
5.1. Conclusions	187

UNIVERSITAT ROVIRA I VIRGILI

NEW APPLICATIONS OF IODINE(III) REACTIVITY: SYNTHESIS AND FUNCTIONALIZATION OF HETEROCYCLES

Laura Fra Fernández

Chapter I

General overview

1.1 Introduction

Iodine was first isolated in 1811 from the ash of seaweed during the Napoleonic war by the industrial chemist B. Courtois in 1811 and was later named by J. L. Gay Lussac.¹ Its name derives from the Greek word for violet, reflecting the characteristic deep purple color of resublimed crystalline iodine. History of iodine and all the aspects of its chemistry and applications have been summarized in a detailed review in commemoration of two centuries of iodine research.² Its production comes mostly from the saltpeter deposits in Chile and natural brines in Japan.

Iodine is a very special element not only for its singular color, but also for its characteristics that differs from its halogens equivalents. It is the heaviest non-radioactive element in the Periodic Table classified as a non-metal and it is the largest, the least electronegative and the most polarizable of the halogens. As a result, its chemical behavior resembles a transition metal when used in organic transformations.³ Additional benefits of iodine-based oxidants are their environmentally friendly characteristics due the high stability and easy handling of these compounds.⁴

¹ a) Courtois, B. *Ann. Chim.* **1813**, *88*, 304; b) Gay-Lussac, L.-J. *Ann. Chim.* **1813**, *88*, 311; c) Gay-Lussac, J.-L. *Ann. Chim.* **1813**, *88*, 319; d) Greenwood, N. N.; Earnshaw, A. *Chemistry of the Elements*; Butterworth-Heinemann: Oxford, **1997**.

² Küpper, F. C.; Feiters, M. C.; Olofsson, B.; Kaiho, T.; Yanagida, S.; Zimmermann, M. B.; Carpenter, L. J.; Luther III, G. W.; Lu, Z.; Jonsson, M.; Kloo, L. *Angew. Chem. Int. Ed.* **2011**, *50*, 11598.

³ Zhdankin, V. V. *Hypervalent Iodine Chemistry Preparation, Structure and Synthetic Applications of Polyvalent Iodine Compounds*; Wiley: Chichester, **2013**.

⁴ Dohi, T.; Kita, Y. *Chem. Commun.* **2009**, 2073.

1.2 Hypervalent iodine(III) bonding and reactivity

It was Musher in 1969 who defined “hypervalent” species as ions or molecules of the elements of Groups 15-18 bearing more than eight electrons within a valence shell.⁵ According to this definition, trivalent and pentavalent iodine compounds can be included in this category. In 1886, a German chemist C. Willgerodt prepared the first polyvalent organic iodine compound, (dichloriodo)benzene, PhICl_2 .⁶

Historically, I(III) compounds were called iodinanines, while I(V) compounds were referred to as periodinanines. Nowadays, the IUPAC nomenclature is depicting those compounds as λ^3 -iodanes and λ^5 -iodanes, respectively.

Aryl- λ^3 -iodanes possess a pseudotrigonal bipyramidal geometry, where the aryl and the lone pairs are directing to the equatorial positions (T-shaped structure). The aryl group and the iodine are connected by two σ -bonds described by molecular orbital theory as a three-center-four-electron (3c-4e) system (Figure 1.1).

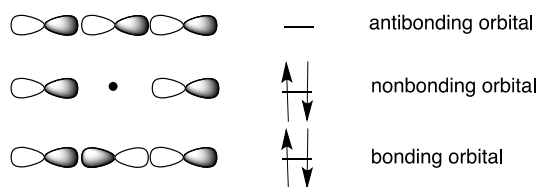


Figure 1.1 Molecular orbital diagram for aryl- λ^3 -iodanes.

Due to the node present in the center of the HOMO orbital, the hypervalent bond shows a highly polarized nature. A partial positive charge is localized on the iodine atom, while a partial negative charge is located on each of the ligands. The electrophilicity is explicitly demonstrated by a strong dipolar moment as well as the apical disposition of the ligands.

The most common classes of aryl- λ^3 -iodanes are depicted in Figure 1.2.⁷ The most known are (diacetoxyiodo)benzene (PIDA), [bis(trifluoroacetoxy)iodo]benzene (PIFA),

⁵ Musher, J. I. *Angew. Chem. Int. Ed.* **1969**, *8*, 54.

⁶ Willgerodt, C. J. *Prakt. Chem.* **1886**, *33*, 154.

⁷ a) Stang, P. J.; Zhdankin, V. V. *Chem. Rev.* **1996**, *96*, 1123; b) *Issue in Honor of Prof. A. Varvoglis*, *Arkivoc* **2003**, *6*, 1.

[hydroxyl(tosyloxy)iodo]benzene (Koser's reagent),⁸ and 3,3-dimethyl-1-(trifluoromethyl)-1,2-benziodoxole (Togni's I reagent).⁹

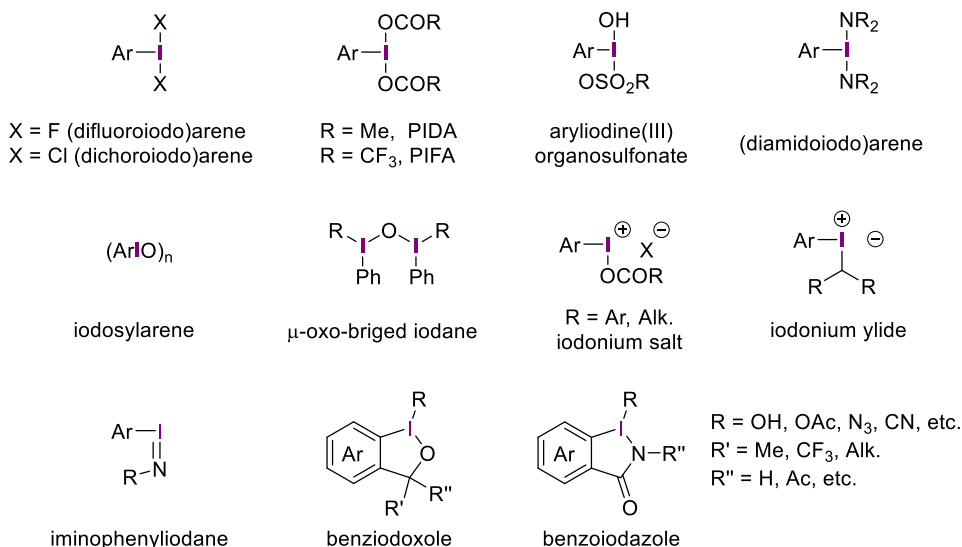


Figure 1.2 Common classes of aryl- λ^3 -iodanes.

On the other hand, iodine(V) compounds presents a square pyramidal geometry with an aryl group in the apical position connected by two σ -bonds to the iodine center. As in aryl- λ^3 -iodanes, these compounds exhibit two orthogonal hypervalent three-center-four-electron bonds with the ligands (Figure 1.3).¹⁰

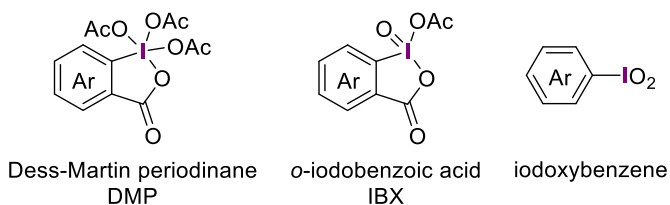


Figure 1.3 Common iodine(V) reagents.

⁸ Moriarty, R. M.; Vaid, R. K.; Koser, G. F. *Synlett* **1990**, 7, 365.

⁹ Charpentier, J.; Früh, N.; Togni, A. *Chem. Rev.* **2015**, 115, 650.

¹⁰ For selected reviews see: a) Skulski, L. *Molecules* **2000**, 5, 1331; b) Zhdankin, V. V.; Stang, P. J. *Chem. Rev.* **2002**, 102, 2523; c) Stang, P. J. *J. Org. Chem.* **2003**, 68, 2997; d) Zhdankin, V. V.; Stang, P. J. *Chem. Rev.* **2008**, 108, 5299; e) Ochiai, M. *Chem. Rec.* **2007**, 7, 12.

Over the last years, a wide variety of organic molecules bearing hypervalent iodine moieties have become a useful and routinely tool for synthetic chemistry.¹¹ Most reactions with these reagents (PhIL_2) involve an initial ligand exchange step on the iodine atom with an external nucleophile (Nu) followed by reductive elimination of iodobenzene. The second step can also proceed as ligand coupling in a concerted manner (Figure 1.4).

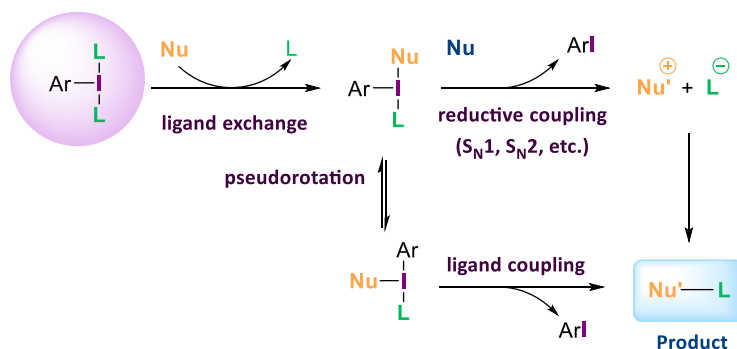


Figure 1.4 Reactivity scheme for aryl- λ^3 -iodanes with nucleophiles.

The reductive coupling step through a S_N1 (dissociative) or S_N2 (associative) mechanism takes place releasing aryl iodide to affording the product. The dissociative pathway seems to be more unlikely due to the instability of a positive-charged intermediate. However, experiments in gas phase or during titrations of $\text{PhI}(\text{OH})\text{OTs}$ and $\text{PhI}(\text{OH})\text{OMs}$ clearly demonstrated by detection of charged intermediates that this could be an alternative pathway.¹²

In the ligand coupling step is required an initial pseudorotation to bring ligands L and Nu to apical and equatorial positions to favor the coupling. Experimental studies on the mechanism of ligand coupling reaction are very limited. This behaviour is characteristic of iodonium salts compounds and occurs in a concerted manner, proceeding with retention of configuration of the ligands. Due to the change of the oxidation state at the iodine center, this chemistry strongly resembles that of transition

¹¹ Wirth, T. *Angew. Chem. Int. Ed.* **2005**, *44*, 3656.

¹² Richter, H. W.; Cherry, B. R.; Zook, T. D.; Koser, G. F. *J. Am. Chem. Soc.* **1997**, *119*, 9614.

metals.¹³ The ligand coupling mechanism for the thermolysis of iodonium salts was discussed and generalized by Grushin.¹⁴

Hypervalent iodine(III) compounds also show single-electron-transfer (SET) oxidation abilities for the activation of electron-rich aromatic systems in polar, non-nucleophilic solvents. In this case, electron-donor and electron-acceptor compounds generate an EDA (electron donor-acceptor) complex (Figure 1.5).¹⁵ Based on this reactivity, Kita found that *para*-substituted phenol ethers, in combination of some nucleophiles in fluoroalcohol solvents reacts with iodine(III) reagents affording products of nucleophilic aromatic substitution via a SET mechanism.¹⁶ A few years later, they determined the involvement of an aromatic cation radical during the reaction by performing detailed mechanistic studies based on UV and ESR spectroscopic measurement.^{16b} Later on, this methodology was further extended to the synthesis of a wide range of biaryls in high yields.¹⁷

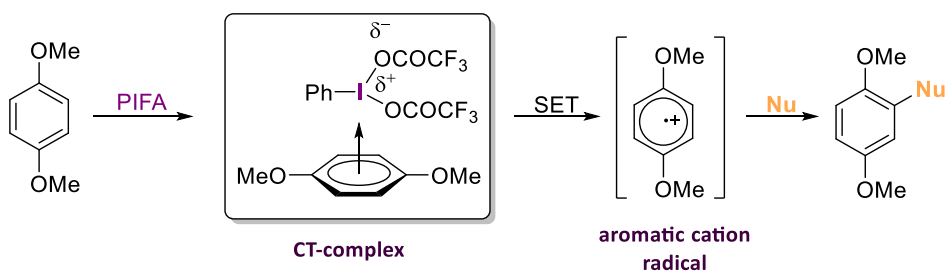


Figure 1.5 Mechanism scheme for aromatic ring activation by SET oxidation.

¹³ a) Moriarty, R. M.; Prakash, O. *Acc. Chem. Res.* **1986**, *19*, 244; b) Ochiai, M. *Top. Curr. Chem.* **2003**, *224*, 5; c) Grushin, V. V. *Acc. Chem. Res.* **1992**, *25*, 529; d) *Ligand Coupling Reactions with Heteroaromatic Compounds*, *Tetrahedron Organic Series Vol. 18*, Ed. P. Finet, Pergamon, Oxford, **1998**.

¹⁴ a) Grushin, V. V.; Demkina, I. I.; Tolstaya, T. P. *J. Chem. Soc., Perkin Trans. 2* **1992**, 505; b) Grushin, V.V. *Chem. Soc. Rev.* **2000**, *29*, 315.

¹⁵ Rathore, R.; Kochi, J. K. *Adv. Phys. Org. Chem.* **2000**, *35*, 193.

¹⁶ a) Kita, Y.; Tohma, H.; Inagaki, M.; Hatanaka, K.; Yakura, Y. *Tetrahedron Lett.* **1991**, *32*, 4321; b) Kita, Y.; Tohma, H.; Hatanaka, K.; Takada, T.; Fujita, S.; Mitoh, S.; Sakurai, H.; Oka, S. *J. Am. Chem. Soc.* **1994**, *116*, 3684; c) Kita, Y.; Takada, T.; Tohma, T. *Pure Appl. Chem.* **1996**, *68*, 627.

¹⁷ a) Tohma, H.; Morioka, H.; Tazikawa, S.; Arisawa, M.; Kita, Y. *Tetrahedron* **2001**, *57*, 345; b) Tohma, H.; Iwata, M.; Maegawa, T.; Kita, Y. *Tetrahedron Lett.* **2002**, *43*, 9241.

Due to its reactivity, hypervalent iodine reagents are used extensively in organic synthesis as efficient and environmentally benign oxidizing reagents with special chemical properties that resembles to heavy metals behavior. Most of them are now commercially available and easily accessible.

1.3 Hypervalent iodine(III)-mediated C-N bond formation

In the early stage of their application, iodine(III) reagents have been used as stoichiometric oxidants with a main focus on palladium and copper catalyzed processes. However, its use is not limited to the role of simply oxidant as many other synthetic transformations have been established based on its reactivity.

Of all the carbon-heteroatom bond formation reactions, the C-N bond-forming methods are of huge importance due to its presence in natural products or in biology or materials science.¹⁸ As a results of its environmental friendly characteristics, they represent an efficient alternatives to toxic and expensive heavy metals for this type of functionalization. Therefore, the development of metal-free amination reactions under iodine(III) reagents represents a big challenge.

Several transformations such aromatic amination, alkene and alkyne amination, cyclizations, α -functionalizations of carbonyl compounds and others have been widely explore over the last years.

Our group contribute strongly in the development of this type of transformations in the area of alkene amination reactions. In 2011, we reported the first enantioselective diamination of styrenes with bismesyimide as a nitrogen source using a chiral iodine(III) reagent based on to lactate arms for enantioinduction (Figure 1.6).¹⁹

¹⁸ a) Henkel, T.; Brunne, R. M.; Müller, H.; Reichel, F. *Angew. Chem. Int. Ed.* **1999**, *38*, 643; b) Fache, F.; Schulz, E.; Tommasino, M. L.; Lemaire, M. *Chem. Rev.* **2000**, *100*, 2159; c) Feher, M.; Schmidt, J. M. *J. Chem. Inf. Comput. Sci.* **2002**, *43*, 218; d) Hili, R.; Yudin, A. K. *Nat. Chem. Biol.* **2006**, *2*, 284.

¹⁹ Röben, C.; Souto, J. A.; González, Y.; Lishchynskyi, A.; Muñiz, K.; *Angew. Chem. Int. Ed.* **2011**, *50*, 9478.

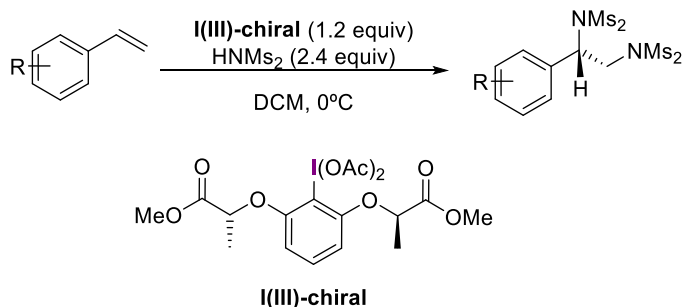


Figure 1.6 First enantioselective iodine(III)-diamination of styrenes under stoichiometric conditions.

While exploring this transformation, a new iodine(III)-reagent was isolated and full characterized (Figure 1.7). The solid-state structure of this new mixed iodine(III) specie formed under ligand-exchange conditions proves the existence of an I^{III}-N covalent bond.

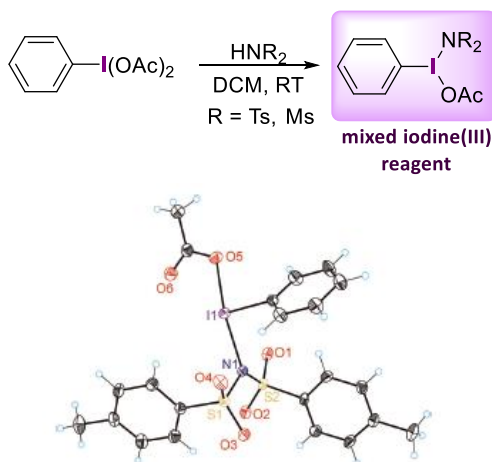


Figure 1.7 Synthesis of a new iodine(III) species and its X-Ray structure.

Based on this finding, a full methodology was developed for alkene diamination reaction. The use of this iodine(III) reagent or its formation *in situ* by combination of PIDA and the corresponding bissulfonamides as a nitrogen source was further expanded to a wide range of alkenes. Over 60 different olefins, terminal and internal alkenes were

converted into the diaminated products in good to high yields, demonstrating the high applicability of this successful combination (Figure 1.8).²⁰

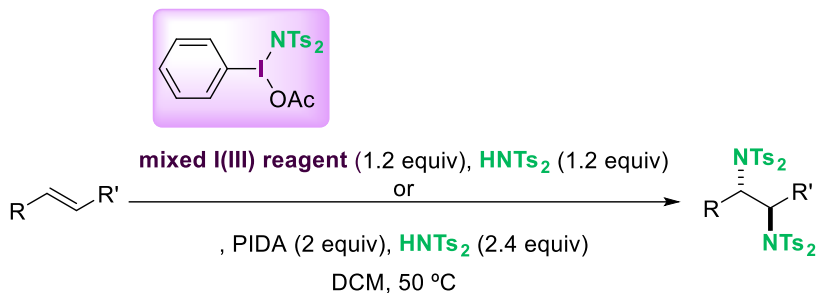


Figure 1.8 Synthetic scheme for the iodine(III)- mediated diamination of alkenes.

This diamination protocol was extended to a variety of butadienes and hexatrienes, an exciting confirmation of the robustness of this methodology. This reaction represents first examples of the metal-free diamination of butadienes expanding the scope to the highly attractive 1,4-installation of two nitrogen atoms within a single step (Figure 1.9).²¹

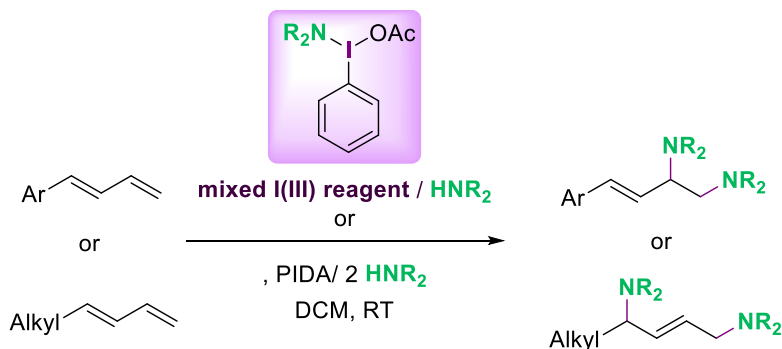


Figure 1.9 Selective diamination of dienes under iodine(III)-reactivity.

²⁰ Souto, J. A.; González, Y.; Iglesias, Á.; Zian, D.; Lishchynskyi, A.; Muñiz, K. *Chem. Asian J.* **2012**, *7*, 1103.

²¹ Lishchynskyi, A.; Muñiz, K. *Chem. Eur. J.* **2012**, *18*, 2212.

Furthermore, this new mixed iodine(III) reagent promotes allylic amination (Figure 1.10 top)²² and moreover, an unprecedented intermolecular amination of terminal alkynes (Figure 1.10 bottom).²³

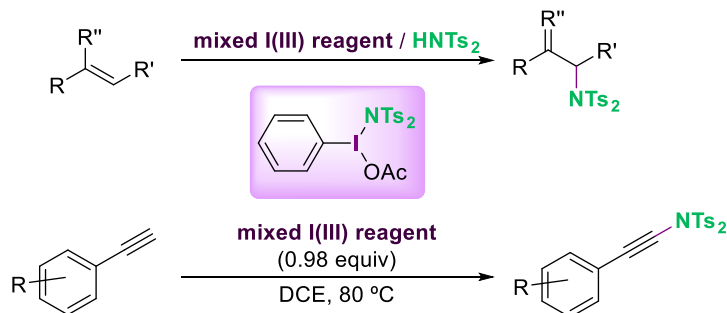


Figure 1.10 Applications of the new mixed iodine(III) reagent in allylic and alkyne amination.

After this great reactivity found using this mixed hypervalent reagent, in 2013 we described the synthesis and isolation of a new hypervalent iodine species bearing two transferable nitrogen groups (Figure 1.11).²⁴ The singular reactivity of this bisimido iodine(III) reagents enabled several new transformations apart from diamination, uncommon α -amination of ketones²⁵ or aromatic amination were achieved with these reagents.

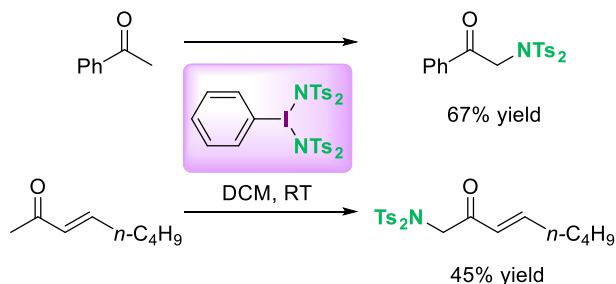


Figure 1.11 Unprecedented α -amination of ketones as an application of new bisimido iodine(III) reagents.

²² Souto, J. A.; Zian, D.; Muñiz, K. *J. Am. Chem. Soc.* **2012**, *134*, 7242.

²³ Souto, J. A.; Becker, P.; Iglesias, Á.; Muñiz, K. *J. Am. Chem. Soc.* **2012**, *134*, 15505.

²⁴ Souto, J. A.; Martínez, C.; Velilla, I.; Muñiz, K. *Angew. Chem. Int. Ed.* **2013**, *52*, 1324.

²⁵ a) Hadjarapoglou, L.; Spyroudis, S.; Varvoglis, A. *Synthesis* **1983**, 207; b) Ye, Y.; Wang, H.; Fan, R. *Org. Lett.* **2010**, *12*, 2802; c) Mao, L.; Li, Y.; Xiong, T.; Sun, K.; Zhang, Q. *J. Org. Chem.* **2013**, *78*, 733.

But the main challenge achieved by our group in alkene amination reactions was the successful development of the first asymmetric diamination reaction of styrenes using chiral organoiodine(I/III)-catalysis (Figure 1.12).²⁶ This methodology further extended to internal alkenes, represents a breakthrough in an active field such the asymmetric iodine(III)-mediated functionalization of alkenes.²⁷

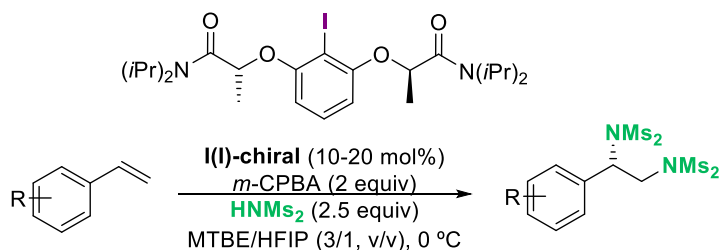


Figure 1.12 First enantioselective iodine(III)-catalyzed diamination of styrenes.

Hypervalent iodine reagents not only act as a good promoters in the alkene diamination, also other functionalization reactions can be achieved.

In 2013, Nevado reported an aminofluorination reaction of styrenes using stoichiometric amounts of a (difluoroiodo)aryl reagent combined with a nitrogen source (Figure 1.13).²⁸ The aminofluorinated products were obtained in good yield, and less than 15% of the corresponding diaminated styrene was observed.

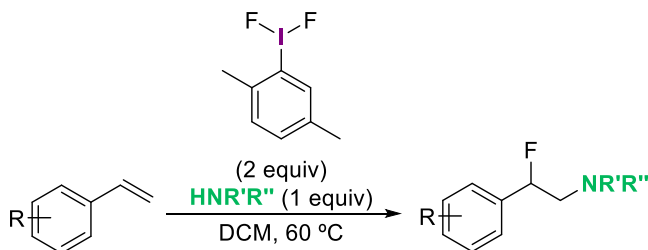


Figure 1.13 Nevado proposal for iodine(III)-mediated aminofluorination of styrenes.

²⁶ Muñiz, K.; Barreiro, L.; Romero, R. M.; Martínez, C. *J. Am. Chem. Soc.* **2017**, *139*, 4354.

²⁷ a) Molnár, I. G.; Gilmour, R. *J. Am. Chem. Soc.* **2016**, *138*, 5004; b) Banik, S. M.; Medley, J. W.; Jacobsen, E. N. *J. Am. Chem. Soc.* **2016**, *138*, 5000; c) Molnár, I. G.; Thiehoff, C.; Holland, M. C.; Gilmour, R. *ACS Catal.* **2016**, *6*, 7167; d) Banik, S. M.; Medley, J. W.; Jacobsen, E. N. *Science* **2016**, *353*, 51.

²⁸ Kong, W.; Feige, P.; Haro, T.; Nevado, C. *Angew. Chem. Int. Ed.* **2013**, *52*, 2469.

Other example of functionalization of styrenes mediated by iodine(III) reagents is the aziridination reaction. For instance, Minakata reported the stoichiometric use of an imidoiodane, *N*-tosyliminophenylidiodane (PhI=NTs), to promote the aziridination of styrenes in combination with catalytic amounts of both molecular iodine I₂ and tetrabutylammonium iodide (TBAI) through a radical mechanism (Figure 1.14).²⁹

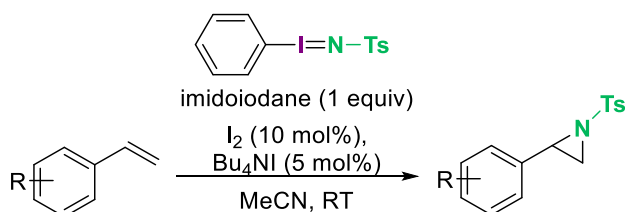


Figure 1.14 Aziridination of styrenes using imidoiodane reagent reported by Minakata.

Aromatic amination reactions can be also accomplished through iodine(III) reactivity.³⁰ One example of the intermolecular version of this transformation has been reported by Antonchick.³¹ They proposed the formation of C-N bond through a cross-coupling of non-prefunctionalized arene, both *N*-arylated and *para*-selective diarylated anilide derivatives were obtained (Figure 1.15).

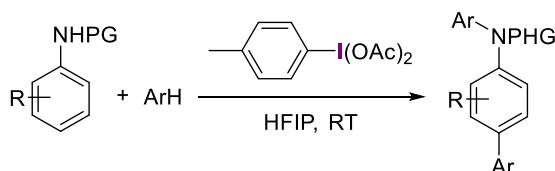


Figure 1.15 Iodine(III)-mediated intermolecular aromatic amination of simple arenes.

The latter methodology require overstoichiometric amounts of both iodine(III) reagent and the arene, so the discovery of catalytic conditions for the aromatic amination could solve part of the problem. In fact, our group also contributed to this field developing a new catalyst for the intermolecular aromatic amination (Figure

²⁹ Kiyokawa, K.; Kosaka, T.; Minakata, S. *Org. Lett.* **2013**, *15*, 4858.

³⁰ a) Cho, S. H.; Yoon, J.; Chang, S. *J. Am. Chem. Soc.* **2011**, *133*, 5996; b) Kim, H. J.; Kim, J.; Cho, S. H.; Chang, S. *J. Am. Chem. Soc.* **2011**, *133*, 16382; c) Kantak, A. A.; Potavathri, S.; Barham, R. A.; Romano, K. M.; DeBoef, B. *J. Am. Chem. Soc.* **2011**, *133*, 19960.

³¹ Samanta, R.; Lategahn, I.; Antonchick, A. P. *Chem. Commun.* **2012**, *48*, 3194.

1.16).³² This compound derived from oxidation of 1,2-diiodobenzene with peracetic acid promote the amination of substituted arenes with up to 66:1 regioisomeric control using an unprecedented low catalyst loading.

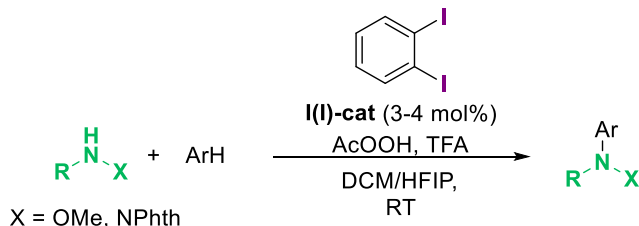


Figure 1.16 Iodine(III)-catalyzed aromatic amination proposed by Muñiz.

A completely different approach for aromatic amination involve the use of diaryl iodonium salts.³³ Recently, we reported the access to 2,6-disubstituted anilines, easily prepared from the direct reaction between amides and diaryliodonium salts (Figure 1.17).³⁴ This methodology of an unusual broad scope regarding the sterically congested arene and the nitrogen source, occurs without the requirement for any additional promoter and proceeds through a direct reductive elimination at the iodine(III) center.

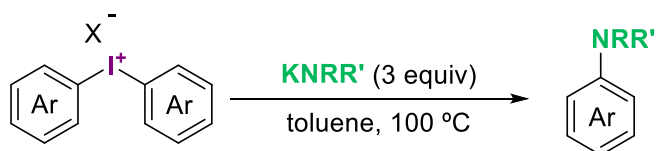


Figure 1.17 Our approach for the synthesis of 2,6-disubstituted anilines using diaryl iodonium salts.

Alkenes, aryls and alkynes have been widely explore as substrates for iodine(III)-mediated C-N bond formation. The intermolecular version of such transformation has

³² Lucchetti, N.; Scalone, M.; Fantasia, S.; Muñiz, K. *Adv. Synth. Catal.* **2016**, *358*, 2093.

³³ a) Tinnis, F.; Stridfeldt, E.; Lundberg, H.; Adolfsson, H.; Olofsson, B. *Org. Lett.* **2015**, *17*, 2688; b) Bergman, J.; Stensland, B. *J. Heterocycl. Chem.* **2014**, *51*, 1; c) Malmgren, J.; Santoro, S.; Jalalian, N.; Himo, F.; Olofsson, B. *Chem. Eur. J.* **2013**, *19*, 10334; d) Carroll, M. A.; Wood, R. A. *Tetrahedron* **2007**, *63*, 11349. f) Li, J.; Liu, L. *RSC Adv.* **2012**, *2*, 10485; i) Peng, J.; Chen, C.; Wang, Y.; Lou, Z.; Li, M.; Xi, C.; Chen, H. *Angew. Chem. Int. Ed.* **2013**, *52*, 7574.

³⁴ Lucchetti, N.; Scalone, M.; Fantasia, S.; Muñiz, K. *Angew. Chem. Int. Ed.* **2016**, *55*, 13335.

been briefly introduced above, but hypervalent iodine reagents can also promote several reactions in an intramolecular manner.

1.4 General objectives

Following the mentioned above, the main objective of this doctoral thesis is the development of new stoichiometric and catalytic methodologies for the metal-free intramolecular amination reaction in heterocycle synthesis. As hypervalent iodine reagents offers a friendly environment, regarding toxicity, mild conditions and more over selectivity, they are the reagent of choice to promote this type of transformations.

As a last challenge, different iodine(III) reactivity was explored in the field of enantioselective intermolecular transformations.

1.4.1 Synthesis of indoles through C(sp²)-N bond formation

In Chapter 2, a novel synthesis of indole under metal-free conditions is described. A modified Koser reagent generated in situ combining iodosobenzene and a sterically congested aryl sulfonic acid promote the intramolecular cyclization of 2-vinyl anilines (Figure 1.18).³⁵

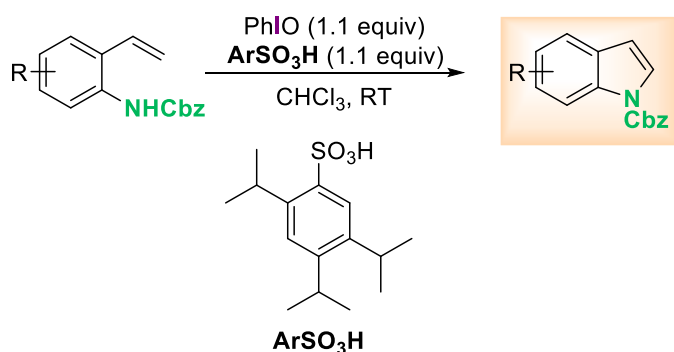


Figure 1.18 Our proposal for indole synthesis through C(sp²)-N bond formation.

³⁵ Fra, L.; Millán, A.; Souto, J. A.; Muñiz, K. *Angew. Chem. Int. Ed.* **2014**, *53*, 7349.

The reaction is of a broad scope broad that surpasses related ones from metal mediated processes. A slightly less efficiency catalytic variant of this oxidative cyclization was also developed, together with a sequential amination reaction with two different iodine(III) reagents demonstrating the robustness of this method and the highly attractive possibilities of its combination with other oxidative processes.

1.4.2 Alternative indole synthesis through C(sp)-N bond formation

In Chapter 3, we proposed an alternative synthesis of indoles through a sequential C-H/C-N bond activation using a tether for reaction control (Figure 1.19).³⁶ This approach allows the access to 2,3-diarylated indoles in a regioselective manner.

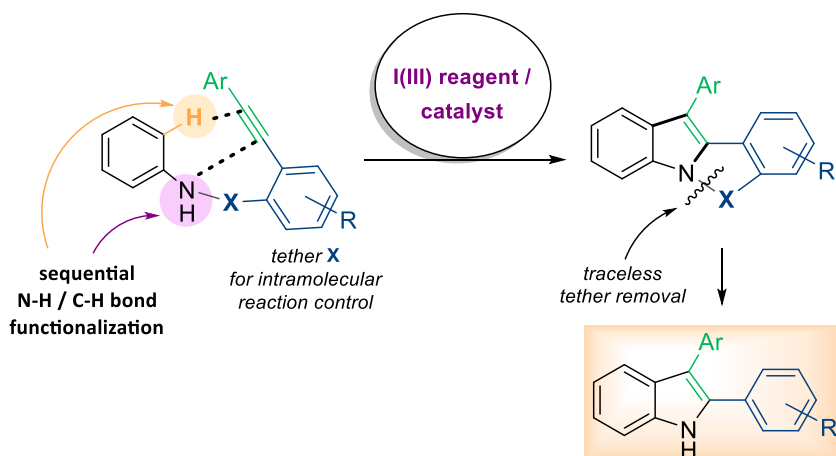


Figure 1.19 Our proposal for the synthesis of 2,3-diarylated indoles using a tether approach.

Four protocols, two stoichiometric and two catalytic, were developed for the preparation of a wide variety of indoles with different substituents at the three arenes rings demonstrating the capacity of the present transformation to act as a general route towards indole synthesis.

³⁶ Fra, L.; Muñiz, K. *Chem. Eur. J.* **2016**, *22*, 4351.

1.4.3 Searching asymmetric induction using iodine(III) reactivity

In Chapter 4, we focused in finding a chiral iodine(III) system to promote enantioinduction. After an extensively investigation, we present the successful development of an asymmetric organoiodine(I/III)-system for the 4-hydroxylation of phenols through phenol dearomatization (Figure 1.20).³⁷

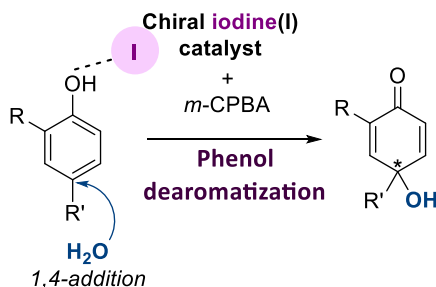


Figure 1.20 Synthetic scheme for the enantioselective dearomatization of phenols under iodine(III) catalysis.

Different phenols were transformed under the corresponding *p*-quinols derivatives using water as an external nucleophile under two mild catalytic protocols. This approach represents the second example of an enantioselective iodine(III)-catalyzed 4-hydroxylation of phenols.

³⁷ Muñiz, K.; Fra, L. *Synthesis*, **2017**, *49*, 2901.

UNIVERSITAT ROVIRA I VIRGILI

NEW APPLICATIONS OF IODINE(III) REACTIVITY: SYNTHESIS AND FUNCTIONALIZATION OF HETEROCYCLES

Laura Fra Fernández

Chapter 2

Indole Synthesis Based on a Modified Koser Reagent

2.1 Introduction

The indole ring system is one of the most abundant and relevant heterocycles in nature. Etymologically, the word indole comes from the combination of *indigo* and *oleum*, because of the original methodology used for its isolation by Baeyer from the natural indigo dye, in 1869 (Figure 2.1).³⁸ Since then, the indole core has been considered as a “privileged structure” in natural products, as well as in medicinal and biological chemistry.³⁹

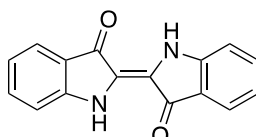


Figure 2.1 Indigo dye

Due to its capability of binding to many receptors with high affinity, indole chemistry has received particular interest. This interest reaches a first high in the 1950's, when the alkaloid reserpine,⁴⁰ which was first synthesized by Woodward in 1956,⁴¹ was found to be active in the treatment of diseases of the central nervous system (CNS), such as anxiety and mental disorders. In the 1960's, vincristine, a highly efficient indolyl-based antitumor agent, was discovered. In subsequent time, the use of indolyl alkaloids was

³⁸ a) Baeyer, A. *Justus Liebigs Ann. Chem.* **1866**, *140*, 295-313; b) Baeyer, A.; Emmerling, A.; *Ber. Dtsch. Chem. Ges.* **1869**, *2*, 679.

³⁹ Sundberg, R. J. *Indoles*, Academic Press, San Diego, **1996**.

⁴⁰ Chen, F.-R.; J. Huang, J. *Chem. Rev.* **2005**, *105*, 4671.

⁴¹ a) Woodward, R. B.; Bader, F. E.; Bickel, H.; Frey, A. J.; Kierstead, R.W. *J. Am. Chem. Soc.* **1956**, *78*, 2023; b) Woodward, R. B.; Bader, F. E.; Bickel, H.; Frey, A. J.; Kierstead, R. W. *J. Am. Chem. Soc.* **1956**, *78*, 2657; c) Woodward, R. B.; Bader, F. E.; Bickel, H.; Frey, A. J.; Kierstead, R. W. *Tetrahedron*, **1958**, *2*, 1.

expanded to include anti-inflammatory, tranquilizing and antihypertensive activities (Figure 2.2).

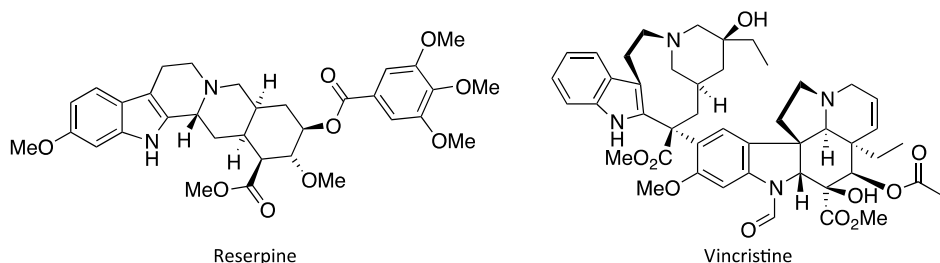


Figure 2.2 Reserpine and Vincristine structures.

Regarding its reactivity, indole is commonly characterised as an electron-rich heteroaromatic system that shows higher reactivity in electrophilic aromatic substitution in comparison to benzene. Although this fact can allow many reactions that cannot be feasible for benzene and other arenes, the reaction conditions and the additives need to be chosen carefully to avoid undesired polysubstitutions in the indolyl ring. The most reactive position of indole towards electrophilic substitution is the C3-site; however, there are other positions that must be taken into account particularly when the C3-position is already functionalized, for example, the C2-position or the N1 (Figure 2.3).

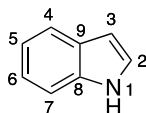


Figure 2.3 Numbering of the indole system.

2.1.1 Classical indole synthesis

The synthesis of indoles has been a major area of focus for synthetic organic chemists for over 100 years, and numerous routes for the access to this class of compounds have been developed.

In 1883, Emil Fischer⁴² discovered the synthesis of indoles, since then, it has become the most important method to prepare a variety of indole intermediates and biologically active compounds (Figure 2.4).

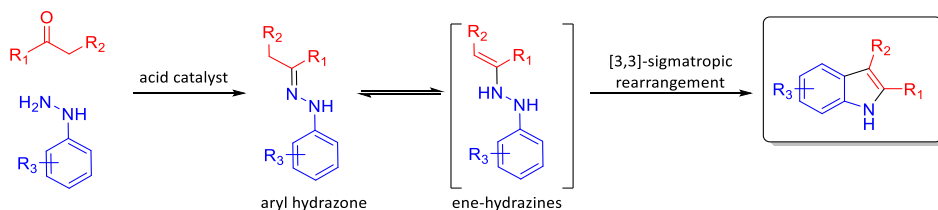


Figure 2.4 Scheme for the Fischer indole synthesis.

The Fischer reaction is extremely useful and often provides a simple and efficient method for the transformation of enolizable *N*-arylhya zones into indoles. In many cases, the reaction is carried out by heating the corresponding ketone or aldehyde and the arylhydrazine with the appropriate acid without the further isolation of the hydrazone intermediate. However, this method suffers from several drawbacks, which lead to introduce a variety of synthetic modifications in order to reduce the environmental impact, such as using mild acids, reusable catalyst and ionic liquids. It is also remarkable that hydrazines are carcinogenic, and some of them are unstable and difficult to prepare, or due to the reaction's requirement for acidic conditions, exhibit only moderate functional group tolerance.

Another example of classical indole synthesis is the Reissert synthesis⁴³ that was discovered in 1896. It is a multistep synthesis that starts from *o*-nitrotoluene, which condenses under basic conditions with an oxalic ester. The resulting *o*-nitrophenyl pyruvic acid is reduced to the corresponding amine, which cyclises without isolation to indol-2-carboxylic acid. Heating the latter above its melting point results in decarboxylation to the final indole (Figure 2.5).

⁴² a) Fischer, E.; Jourdan, F. *Ber. Dtsch. Chem. Ges.* **1883**, *16*, 2241; b) Robinson, B. *Chem. Rev.* **1963**, *63*, 373.

⁴³ a) Reissert, A. *Ber.* **1897**, *30*, 1030; b) Reissert, A. *Ber.* **1896**, *29*, 639; c) Reissert, A.; Scherk, J. *Ber.* **1898**, *31*, 387.

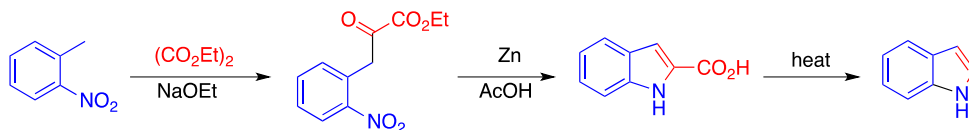


Figure 2.5 Reaction scheme for Reissert indole synthesis.

Later in 1912, W. Madelung reported that by heating *N*-benzoyl-*o*-toluidine with 2 equivalents of sodium ethoxide at high temperatures, the corresponding 2-phenylindole is obtained in the absence of air. Thus, the intramolecular cyclization of *N*-acylated-*o*-alkylanilines to the corresponding substituted indoles in the presence of a strong base at high temperatures (over 250 °C) is known as the Madelung indole synthesis (Figure 2.6).⁴⁴ The temperature can be decreased to room temperature by using alkyllithiums or when the methyl group is substituted with an electron-withdrawing group.⁴⁵

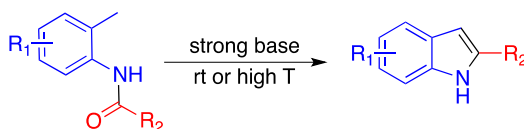


Figure 2.6 Madelung indole synthesis.

In 1973 Gassman and co-workers proposed a very clever indole ring synthesis that includes a [2,3]-sigmatropic rearrangement as the key step (Figure 2.7).⁴⁶ The reaction starts with the *N*-chlorination of the corresponding aniline followed by nucleophilic displacement of the chloride on nitrogen by treatment with different methylsulfides to give the sulfonium salt. Triethylamine generates the corresponding sulfonium ylide that undergoes a [2,3]-sigmatropic rearrangement to afford the aminoketone. The latter cyclized to the corresponding thiomethyl indole, that suffers desulfurization by treatment with Raney nickel to afford as the final product the substituted indole. Although this reaction is not as popular as the Fischer indolization, the Gassman

⁴⁴ Madelung, W. *Ber.* **1912**, *45*, 1128.

⁴⁵ Orlemans, E. O. M.; Schreuder, A. H.; Conti, P. G. M.; Verboom, W.; Reinhoudt, D. N. *Tetrahedron* **1987**, *43*, 3817.

⁴⁶ Gassman, P. G.; van Bergen, T. J. *J. Am. Chem. Soc.* **1973**, *95*, 590; b) Gassman, P. G.; van Bergen, T. J. *J. Am. Chem. Soc.* **1973**, *95*, 591.

synthesis presents many advantages, such as cheap and readily available starting materials, access to many types of substituted indoles, mild reaction conditions and higher yields.

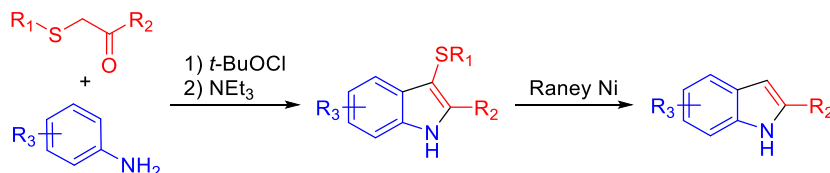


Figure 2.7 Reaction scheme for the Gassman indole synthesis.

2.1.2 Metal transition-catalyzed intramolecular cyclization for indole synthesis

Over the recent years, important contributions in the area of the indole synthesis mediated by catalytic amounts of different transition metals have been developed.⁴⁷

One of the most useful reactions in this particular area is the oxidative cyclization of 2-vinyl anilines and its derivatives to indoles (Figure 2.8). This transformation has been a major challenge in palladium catalysis, although other transition metals have been employed, too. Some selected examples of this intramolecular cyclization through the interaction between an alkene and the nitrogen atom of an aniline derivative are discussed in the following.

⁴⁷ a) Peña-López, M.; Neumann, H.; Beller, M. *Chem. Eur. J.* **2014**, *20*, 1818; b) Zheng, L.; Hua, R. *Chem. Eur. J.* **2014**, *20*, 2352; c) Zhao, D.; Shi, Z.; Glorius, F. *Angew. Chem. Int. Ed.* **2013**, *52*, 12426; d) Wang, C.; Huang, Y. *Org. Lett.* **2013**, *15*, 5294; e) Wei, Y.; Deb, I.; Yoshikai, N. *J. Am. Chem. Soc.* **2012**, *134*, 9098; f) Varela-Fernández, A.; Varela, J. A.; Saá, C. *Synthesis*, **2012**, *44*, 3285; g) Shi, Z.; Zhang, C.; Li, S.; Pan, D.; Ding, S.; Cui, Y. Jiao, N. *Angew. Chem. Int. Ed.* **2009**, *48*, 4572; h) Bernini, R.; Fabrizi, G.; Sferrazza, A.; Cacchi, S. *Angew. Chem. Int. Ed.* **2009**, *48*, 8078; i) Guan, Z.-H.; Yan, Z.-Y.; Ren, Z.-H.; Liu, X.-Y.; Liang, Y.-M. *Chem. Commun.* **2010**, *46*, 2823; j) Shore, G.; Morin, S.; Mallik, D.; Organ, M. G. *Chem. Eur. J.* **2008**, *14*, 1351; k) Barluenga, J.; Jiménez-Aquino, A.; Valdés, C.; Aznar, F. *Angew. Chem. Int. Ed.* **2007**, *46*, 1529; l) Barluenga, J.; Fernández, M. A.; Aznar, F.; Valdés, C. *Chem. Eur. J.* **2005**, *11*, 2276; m) Arcadi, A.; Bianchi, G.; Marinelli, F. *Synthesis*, **2004**, 610.

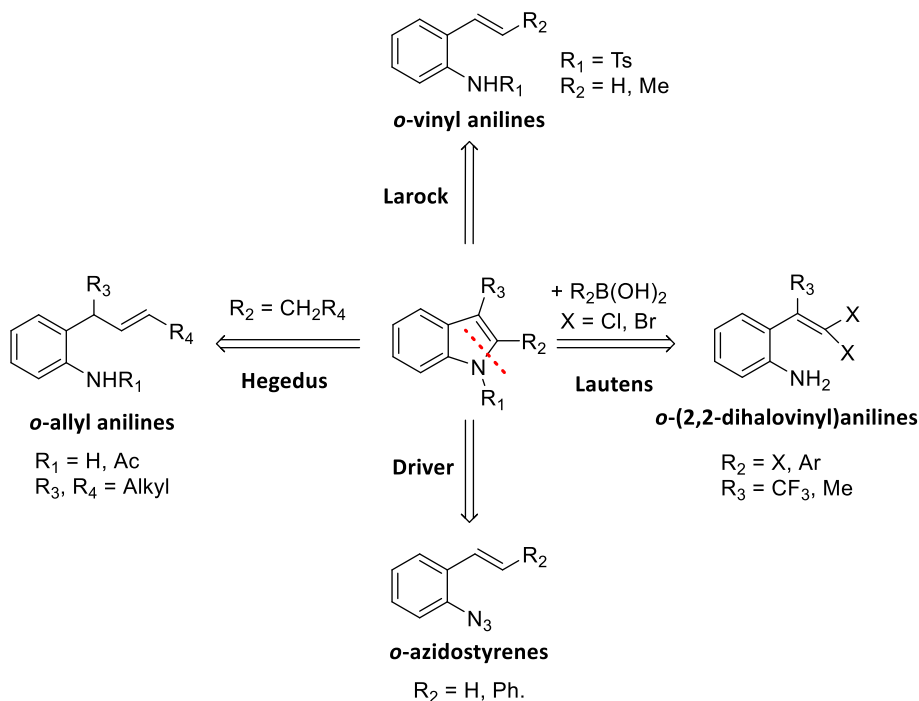


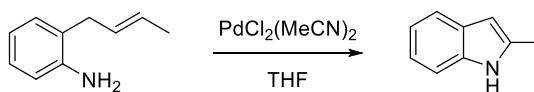
Figure 2.8 Retrosynthetic representation of the main assemblies for the formation of the indole ring starting for 2-vinylanilines and the corresponding derivatives mediated by transition metals.

In 1976, Hegedus reported an intramolecular cyclization starting from *o*-allyl anilines to obtain 2-methylindoles employing a Pd(II)-complex in stoichiometric amounts (Figure 2.9 a).⁴⁸ Later on, in 1978 the same group improved this method developing a catalytic version with benzoquinone as the terminal oxidant (Figure 2.9 b).⁴⁹ Both methods provide a wide variety of indole derivatives in high yields.

⁴⁸ Hegedus, L. S.; Allen, G. F.; Waterman, E. L. *J. Am. Chem. Soc.* **1976**, *98*, 2674.

⁴⁹ Hegedus, L. S.; Allen, G. F.; Bozell, J. J.; Waterman, E. L. *J. Am. Chem. Soc.* **1978**, *100*, 5800.

a) Hegedus, stoichiometric version.



b) Hegedus, catalytic version.

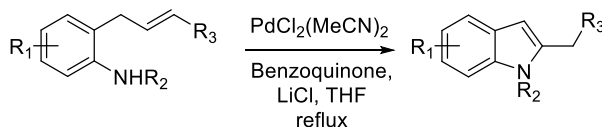


Figure 2.9 Hegedus proposal for the synthesis of indole derivatives.

Although this previous methodology was successfully also applied for the cyclization of different *o*-vinylanilines as an intermediates for the synthesis of alkaloids and related compounds,⁵⁰ Larock proposed in 1996 an alternative synthesis starting from this type of starting materials using $\text{Pd}(\text{OAc})_2$ as a catalyst (Figure 2.10). High temperatures and large reaction times are required for the formation of the corresponding indole, and still the yields remain low.⁵¹

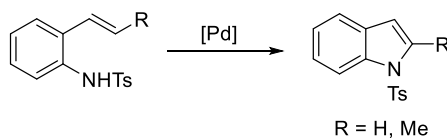


Figure 2.10 Larock synthesis of indoles from 2-vinyl tosylanilides.

Then, in 2010 Buchwald reported the formation of *N*-arylated indoles through a Pd(II)-catalyzed oxidative cyclization. Only a few successful examples were reported and still harsh reaction conditions required.⁵²

⁵⁰ Harrington, P. J.; Hegedus, L. S. *J. Org. Chem.* **1984**, *49*, 2657.

⁵¹ Larock, R. C.; Hightower, T. R.; Hasvold, L. A.; Peterson, K. P. *J. Org. Chem.* **1996**, *61*, 3584.

⁵² Tselikhovsky, D.; Buchwald, S. L. *J. Am. Chem. Soc.* **2010**, *132*, 14048.

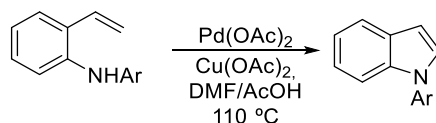


Figure 2.11 Pd-catalyzed oxidative cyclization developed by Buchwald.

In 2013, Copper was found to be an appropriate catalyst for this type of transformation. Chemler suggested the use of a bis(oxazoline)-chelated copper catalyst for the C-N bond formation in combination with MnO₂ as the stoichiometric oxidant (Figure 2.12).⁵³ An *N*-centered radical was proposed as the crucial intermediate for this transformation. Later, the same group improved this methodology introducing TEMPO and O₂ as a co-oxidant and a terminal oxidant respectively.⁵⁴

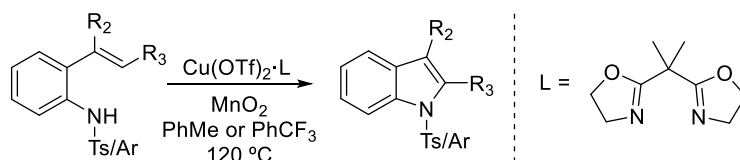


Figure 2.12 Chemler's proposal for the Cu(II)-catalyzed intramolecular amination reaction.

A visible-light-mediated version of this transformation was developed by Zhang in 2012 (Figure 2.13).⁵⁵ They envisioned the formation of an *N*-centered radical cation under visible-light catalysis using [Ru(bpz)₃](PF₆) as the photocatalyst, which undergoes an electrophilic addition to the vinyl moiety. A particular feature of this reaction is the addition of silica gel that might play a role adsorbing oxygen and also serve as a source of protons.

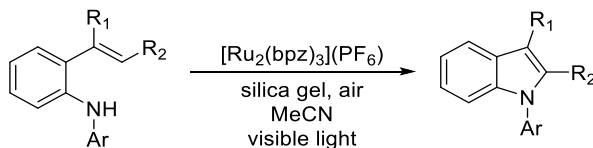


Figure 2.13 Zhang's photocatalytic version for the intramolecular C-N bond formation.

⁵³ Liwosz, T. W.; Chemler, S. R. *Chem. Eur. J.* **2013**, *19*, 12771.

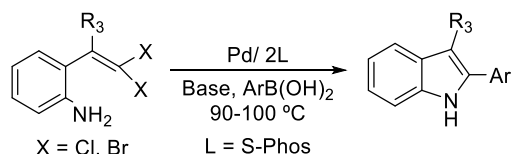
⁵⁴ Liwosz, T. W.; Chemler, S. R. *Synlett* **2015**, *26*, 335.

⁵⁵ Maity, S.; Zheng, N. *Angew. Chem. Int. Ed.* **2012**, *51*, 9562.

One important modification of this methodology was introduced by Lautens in 2005. He proposed the cyclization of different *o*-(2,2-dihalovinyl) unprotected anilines into the correspondent free indoles through a Pd-catalyzed tandem C-N bond formation/Suzuki-Miyaura coupling using an aryl boronic ester (Figure 2.14 a).⁵⁶

By switching the ligand, a variety of *o*-(2,2-dibromovinyl) anilines with different substitution at the aryl moiety were cyclized to the corresponding 2-brominated indole in good yields (Figure 2.14 b).⁵⁷ Although high temperatures are needed in both syntheses, it is remarkable that both methods allow the use of unprotected anilines in the presence of palladium catalysts.

a) Pd-catalyzed tandem C-N/Suzuki-Miyaura coupling



b) Pd-catalyzed synthesis of 2-brominated indoles

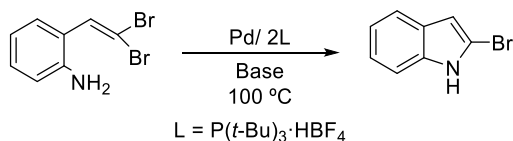


Figure 2.14 Pd-catalyzed cyclization of 2,2-dihalovinyl anilines to 2- and 2,3-substituted indoles and ligand effect proposed by Lautens.

Therefore, palladium catalysis has been widely applied for the synthesis of indoles through an intramolecular cyclization of 2-allyl and 2-vinyl aniline derivatives. These methodologies required high temperatures and, in addition, for most of them long reaction times are needed for the successful formation of the final product.

As an alternative, the use of *o*-azidostyrenes was proposed as a suitable starting materials for this intramolecular cyclization. It was Sundberg in 1972, who initially introduced the thermolysis of this type of starting materials to form indoles via the

⁵⁶ Fang, Y.-Q.; Lautens, M. *Org. Lett.*, **2005**, *7*, 3549.

⁵⁷ Newman, S. G.; Lautens, M. *J. Am. Chem. Soc.* **2010**, *132*, 11416.

formation of a nitrene intermediate (Figure 2.15).⁵⁸ This method has several limitations including the fact that potentially explosive aryl azides are exposed to high temperatures, so a transition-metal catalyzed reaction at reduced temperature would be a good option to this transformation.

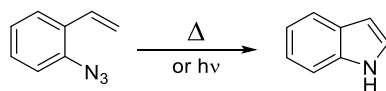
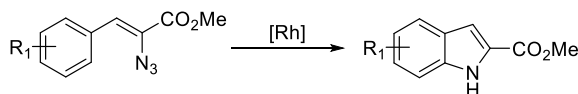


Figure 2.15 Sundberg indole synthesis.

This approach was successfully developed by Driver in 2008. Based on the results that they reported previously for an intramolecular in which azido acrylates were used as starting materials (Figure 2.16 a),⁵⁹ they envisioned an indole synthesis starting from *o*-azidostyrenes through a vinyl C-N bond formation using a Rh(II)-catalyst under relatively mild conditions (Figure 2.16 b).⁶⁰

a) Rh(II)-catalysed aryl C-N bond formation



b) Rh(II)-catalysed vinyl C-N bond formation

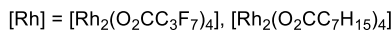
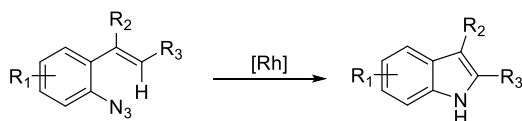


Figure 2.16 Driver's proposals for the Rh(II)-mediated intramolecular cyclization.

⁵⁸ Sundberg, R. J.; Russell, H. F.; Ligon, Jr., W. V.; Lin, L.-S. *J. Org. Chem.* **1972**, *37*, 719.

⁵⁹ Stokes, B. J.; Dong, H.; Leslie, B. E.; Pumphrey, A. L.; Driver, T. G. *J. Am. Chem. Soc.* **2007**, *129*, 7500.

⁶⁰ Shen, M.; Leslie, B. S.; Driver, T. G. *Angew. Chem.* **2008**, *120*, 5134.; *Angew. Chem. Int. Ed.* **2008**, *47*, 5056.

As a summary, transition-metal-catalyzed synthesis of indoles appears to be a suitable tool for the formation of C-N bond through an intramolecular cyclization reaction of 2-vinyl anilines and its derivatives. In fact, this starting material is an appropriate precursor, but still the transformation shows some drawbacks for its application in the pharmaceutical and biological sciences.

2.1.3 Hypervalent iodine-mediated intramolecular oxidative C(sp²)-N bond formation

As described above, transition metals have been extensively used as promoters for the oxidative cyclization via intramolecular C-N bond formation. Due to their costs and toxicity, the application of hypervalent iodine reagents has emerged as a green alternative for this type of transformation. Due to the high electrophilicity at the iodine(III) atom and its ability as a nucleophile, this type of reagents represents an excellent option to choose for the formation of nitrogen-containing heterocycles.

Considering the chemical behaviour of hypervalent iodine reagents, two general reaction pathways can be involved: *a*) the interaction between the double bond and the I(III)-reagent leads to the formation of an iodonium ion intermediate, which is subsequently attacked by the nitrogen, or *b*) the initial oxidation of the amino group to generate a cationic nitrogen that is trapped in an intramolecular fashion through the nucleophilic attack of the double bond (Figure 2.17).

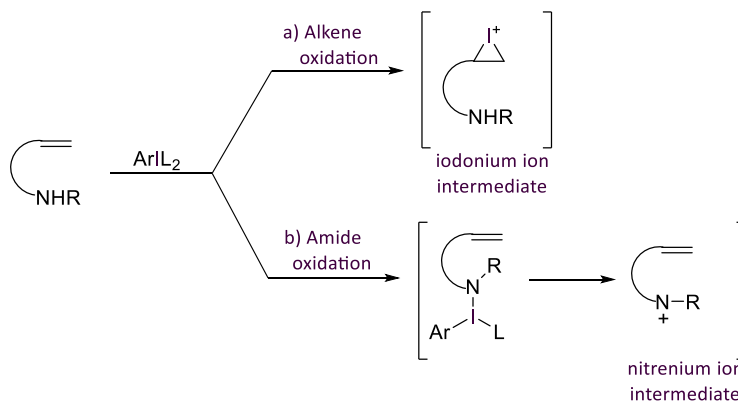


Figure 2.17 Synthetic design of the I(III)-mediated intramolecular amination reaction.

Taking into account these two different strategies, numerous methodologies for the synthesis of *N*-based heterocycles have been developed among the last years.

The formation of a nitrenium ion as the key intermediate plays an important role in the electrophilic aromatic amidation reaction. In 1984, Kikugawa reported the formation of this intermediate through an *N*-chlorination step using *t*-BuOCl, from which the oxidative cyclization takes place in the presence of zinc or silver salts (Figure 2.18 a).⁶¹ Limitations of this method such as the solubility of silver salts or undesired aromatic chlorination, could be overcome by using a hypervalent iodine reagent for the formation of the nitrenium cation and subsequent intramolecular nucleophilic attack by an arene.

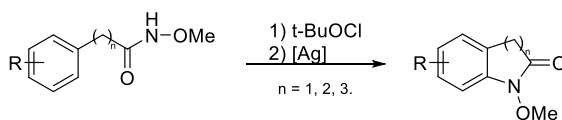
Using this approach, PIFA in combination with *N*-methoxy amides was encountered the reagent of choice for this type of transformations. This methoxy substituent appears to be appropriate for stabilizing the positive charge at the nitrogen. In the 1990's, this strategy was widely applied for the synthesis of different *N*-heterocyclic compounds, for example, *N*-methoxy oxyindoles, dihydroquinolinones (Figure 2.18 b)⁶² and cyclic ureas (Figure 2.18 c),⁶³ among others.

⁶¹ Kikugawa, Y.; Kawase, M. *J. Am. Chem. Soc.* **1984**, *106*, 5728.

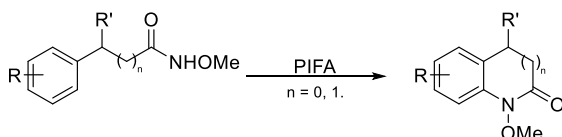
⁶² Kikugawa, Y.; Kawase, M. *Chem. Lett.* **1990**, 581.

⁶³ Romero, A. G.; Darlington, W. H.; Jacobsen, E. J.; Mickelson, J. W. *Tetrahedron Lett.* **1996**, *37*, 2361.

a) Kikugawa, 1984.



b) Kikugawa, 1990.



c) Romero, 1996.



Figure 2.18 Few examples of PIFA-mediated electrophilic aromatic amidation.

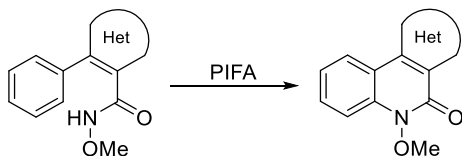
In 2002 Dominguez applied this concept to the development of a PIFA-mediated intramolecular cyclization and a variety of heterocyclic-fused quinolinones (Figure 2.19 a),⁶⁴ 1,4-diazepin-2-ones (Figure 2.19 b)⁶⁵ and pyrrolo(benzo)diazepines, including the antitumor antibiotic DC81 (Figure 2.19 c),⁶⁶ were successfully synthesized in good yields to excellent yields.

⁶⁴ Herrero, M. T.; Tellitu, I.; Domínguez, E.; Hernández, S.; Moreno, I.; SanMartin, R. *Tetrahedron* **2002**, *58*, 8581.

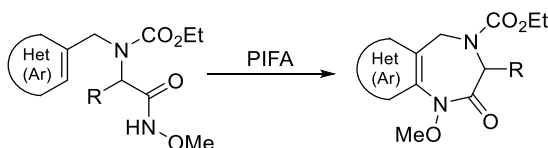
⁶⁵ a) Herrero, M. T.; Tellitu, I.; Domínguez, E.; Moreno, I.; SanMartin, R. *Tetrahedron Lett.* **2002**, *43*, 8273; b) Correa, A.; Herrero, M. T.; Tellitu, I.; Domínguez, E.; Moreno, I.; SanMartin, R. *Tetrahedron* **2003**, *59*, 7103.

⁶⁶ Correa, A.; Tellitu, I.; Domínguez, E.; Moreno, I.; SanMartin, R. *J. Org. Chem.* **2005**, *70*, 2256.

a) PIFA-mediated synthesis of heterocycle-fused quinolinones.



b) PIFA-mediated synthesis of heterocycle-fused 1,4-diazepin-2-ones.



c) PIFA-mediated synthesis of pyrrolobenzodiazepines and heterocycle-fused pyrrolodiazepines.

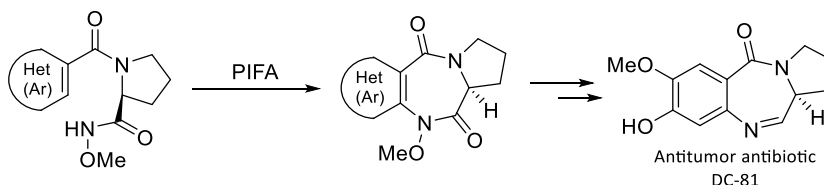


Figure 2.19 Domínguez' approach to the synthesis of *N, S, O*-containing heterocycle-fused quinolinones and pyrrolodiazepines.

This metal-free electrophilic aromatic amidation through the formation of a nitrenium ion was further developed for the synthesis of very important scaffolds such as carbazoles and indoles. It was Antonchick in 2011, who described an organocatalytic method for the synthesis of carbazoles using a 2,2'-diiodo biaryl motif as a catalyst and peracetic acid as the terminal oxidant (Figure 2.20 a).⁶⁷ Indoles could be also obtained through an iodine(III)-mediated aromatic amidation. Recently, Ban reported the synthesis of carbazolone and 3-acetylindole derivatives starting from the corresponding enaminones and using PIFA as oxidant (Figure 2.20 b).⁶⁸

⁶⁷ Antonchick, A. P.; Samanta, R.; Kulikov, K.; Lategahn, J. *Angew. Chem.* **2011**, *123*, 8764; *Angew. Chem. Int. Ed.* **2011**, *50*, 8605.

⁶⁸ Ban, X.; Pan, Y.; Lin, Y.; Wang, S.; Du, Y.; Zhao, K. *Org. Biomol. Chem.* **2012**, *10*, 3606.

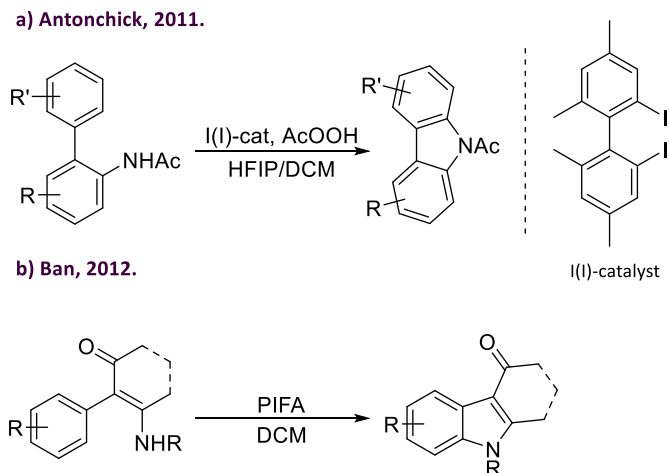


Figure 2.20 Carbazole and indole synthesis through an I(III)-mediated electrophilic aromatic amination reaction.

In all these synthetic strategies, the nitrenium ion is attacked by an arene to form the corresponding heterocyclic product. This concept has been expanded to the use of olefins as the nucleophile for related transformations. It was Domínguez in 2003 who reported a PIFA-mediated aminohydroxylation reaction for the synthesis of isoindolinones and isoquinolinones starting from *o*-allyl and *o*-vinyl substituted benzamides (Figure 2.21).⁶⁹ They explored the reactivity of these substrates and found that by changing the additives, a 6-*endo*-dig cyclization of *o*-vinyl substituted benzamides could take place instead of the corresponding 5-*exo*-trig. The latter could be favoured increasing the nucleophilicity of the styrene fragment introducing two alkoxy groups in the aryl moiety. The reaction takes place through the formation of a *N*-centered cation that is subsequently attack by the double bond leading to the formation of an aziridinium ion that is stabilized by the donating properties of the PMP-protecting group.

⁶⁹ Serna, S.; Tellitu, I.; Domínguez, E.; Moreno, I.; SanMartin, R. *Tetrahedron Lett.* **2003**, *44*, 3483.

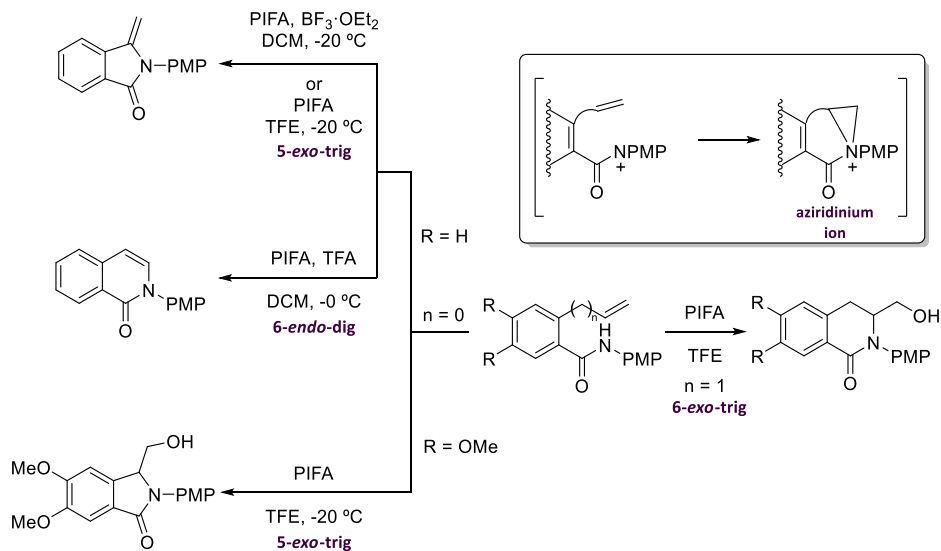


Figure 2.21 Synthetic scheme for the formation of isoindolinones and isoquinolinones proposed by Domínguez.

The specific role of the protecting group at the amide nitrogen to perform the aminohydroxylation process was also studied (Figure 2.22).⁷⁰ It was observed that throughout the course of the cyclization, the nitrenium ion intermediate could be trapped by two internal nucleophiles depending on the nature of the nitrogen substituent. It can be attacked by the arene to form the quinolinone skeleton or, on the other hand, the alkene can attack by forming an aziridinium ion intermediate that is subsequently opened to the final pyrrolidone.

⁷⁰ Serna, S.; Tellitu, I.; Domínguez, E.; Moreno, I.; SanMartín, R. *Tetrahedron* **2004**, *60*, 6533.

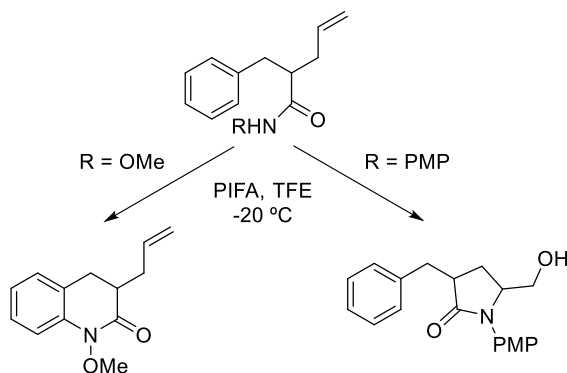


Figure 2.22 Protecting group effect for the chemoselective formation of quinolinones and pyrrolidinones.

It was later, in 2006, when the same group explored the corresponding olefin attack mediated by PIFA for the synthesis of indolines (Figure 2.23).⁷¹ The resulting *N*-acylnitrenium ion was suggested to undergo trapping by the olefin moiety in a 5-*exo*-trig cyclization. The generated intermediate is stabilized as an aziridinium ion as previously proposed, which is opened by a nucleophilic attack of a trifluoroacetate. The resulting ester is then hydrolyzed in the work up and the indoline is obtained as the final product.

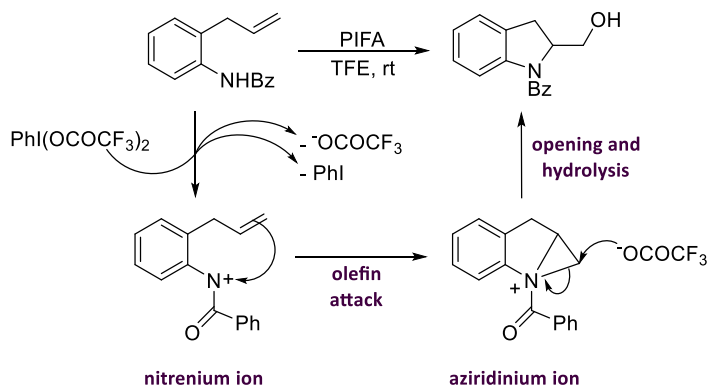


Figure 2.23 Proposed mechanism for the PIFA-mediated olefin amidation for the synthesis of indolines.

⁷¹ Correa, A.; Tellitu, I.; Domínguez, E.; SanMartín, R. *J. Org. Chem.* **2006**, *71*, 8316.

With all these results in hand, the group of Domínguez decided to expand this methodology to the synthesis of a series of pyrrolidinones.⁷² For this purpose, they synthesized different *N*-aryl- and *N*-alkylamides. They found that the PIFA-mediated olefin aminohydroxylation follows different mechanisms depending on the properties of the starting material.

When PIFA reacts with *N*-aryl amides, the corresponding nitrenium cation is formed and trapped intramolecularly by the olefin leading to a primary carbocation, which is stabilized by the adjacent phenyl group. The attack of an acetate moiety, basic work-up and reduction of the resulting hydroxymethylpyrrolidinones with borane end up in the formation of the final pyrrolidines and piperidines (Figure 2.24).

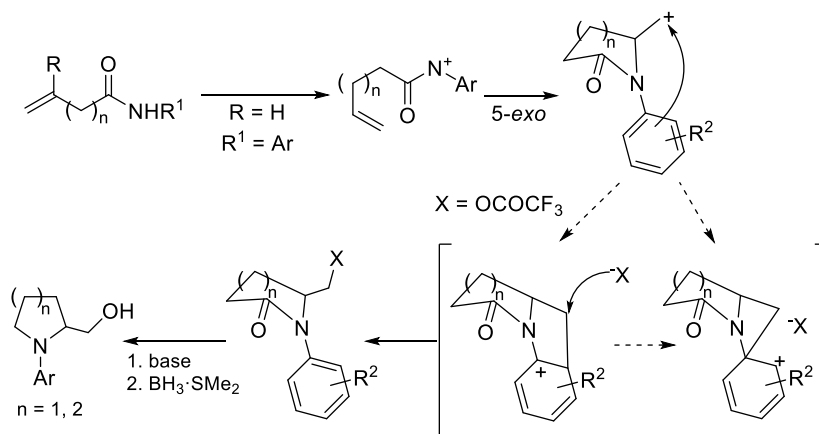


Figure 2.24 Mechanistic proposal for the formation of pyrrolidines and piperidines through a PIFA-mediated olefin amidation.

When an *N*-alkylpentenamide is submitted under the reaction conditions, the reaction proceeds through the formation of an iodonium ion intermediate instead of a less favoured nitrenium cation. It is then intramolecularly attacked by the oxygen atom of the amide entity. After aqueous basic work-up, the final hydroxymethylenyllactone is obtained as the final product (Figure 2.25).

⁷² Tellitu, I.; Urrejola, A.; Serna, S.; Moreno, I.; Herrero, M. T.; Domínguez, E.; SanMartín, R.; Correa, A. *Eur. J. Org. Chem.* **2007**, 437.

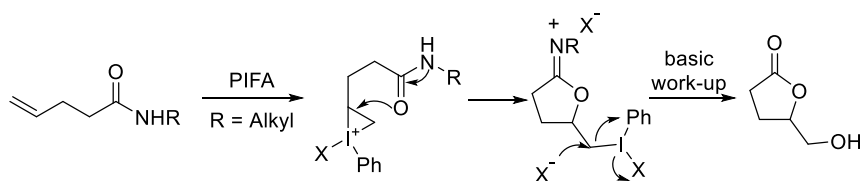


Figure 2.25 Proposed approach for the I(III)-mediated cyclization of *N*-alkylpentenamides.

It is noteworthy that 4-arylpentenamides undergo a specific reaction in the presence of PIFA. First, the nitrenium ion is formed through the action of PIFA and attacked by the olefin, the resulting primary carbocation is stabilized by the aryl ring to form the phenonium ion. Nucleophilic attack of the trifluoroacetate group and subsequent hydrolysis followed by reduction affords a series of 5-amino-2-pentanol (Figure 2.26).

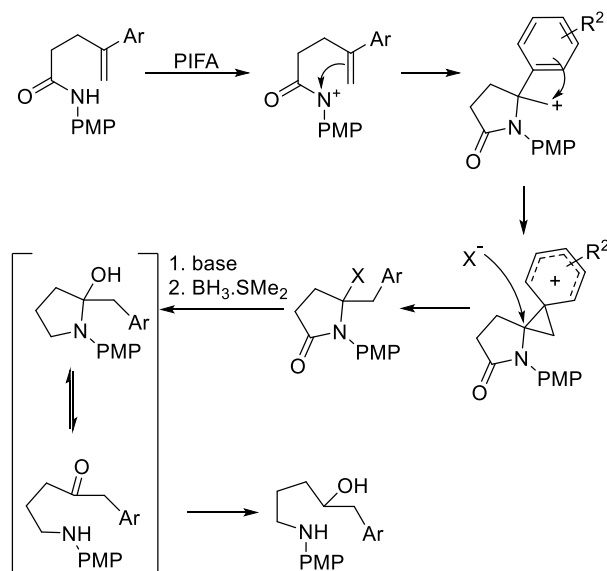
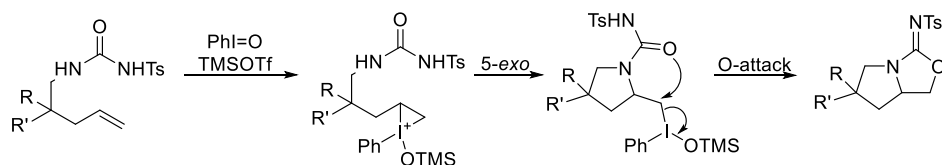


Figure 2.26 Proposed mechanism for the formation of amino alcohols from 4-aryl-4-pentenamides.

As a summary, Domínguez' group developed a full methodology for the synthesis of a large variety of *N*-containing heterocycles through a PIFA-mediated olefin amidation.

Different hypervalent iodine reagents were also used as promoters for the intramolecular olefin amidation. In 2008, Michael proposed the use of iodosobenzene and a Lewis acid to promote an intramolecular oxyamination reaction of ureas. The reaction proceeded through the formation of the iodonium ion followed by 5-*exo*-cyclization. The iodine of the resulting intermediate is displaced intramolecularly by the oxygen due to its high nucleophilicity under the reaction conditions, leading to the final oxyamination product. (Figure 2.27 a).⁷³

a) Michael oxyamination reaction.



b) Barluenga diamination reaction.

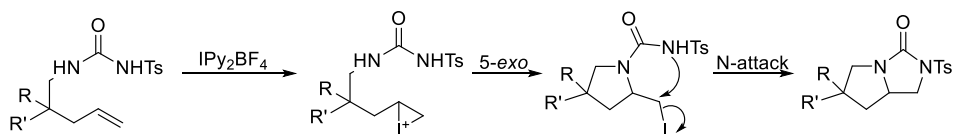


Figure 2.27 Intramolecular cyclization of ureas

Analogously, Barluenga and Muñiz reported the alternative diamination reaction of these substrates using IPy₂BF₄. In this particular case, once the 5-*exo*-cyclization of the iodonium ion occurs, the iodine of the resulting intermediate is displaced by the attack of nitrogen atom and the corresponding cyclic urea is formed (Figure 2.27 b).⁷⁴

Later, Wirth published the stereoselective version of this transformation using chiral hypervalent iodine reagents. Although the optimized conditions afford the oxyamination product in a 99% *ee*, the scope of the reaction remains limited to certain substrates.⁷⁵

⁷³ Cochran, B. M.; Michael, F. E. *Org. Lett.* **2008**, *10*, 5039.

⁷⁴ Muñiz, K.; Hövelmann, C. H.; Campos-Gómez, E.; Barluenga, J.; González, J. M.; Streuff, J.; Nieger, M. *Chem. Asian J.* **2008**, *3*, 776.

⁷⁵ Farid, U.; Wirth, T. *Angew. Chem. Int. Ed.* **2012**, *51*, 3462.

While developing the aminooxygenation reaction of alkenyl ureas, Michael discovered that when a sulfonamidoalkene is treated with PIDA and TFA, the *endo* aminotrifluoroacetoxylation product is preferred, in contrast with the previous methodologies (Figure 2.28).⁷⁶ With these results, they developed an *endo*-selective metal-free cyclization for the synthesis of piperidines. Several trends in diastereoselectivity were observed depending on the chemical nature of the starting material. The overall stereochemical outcome is in favour of a *syn*-addition in *exo*-selective cyclizations and an *anti*-addition in *endo*-selective cyclizations. This observed selectivity is justified with the mechanistic proposal, according to which the *syn*-addition product is formed through the formation of the iodonium ion that is intramolecularly trapped by the sulphonamide and reopened by the trifluoroacetate to form the pyrrolidine. On the other hand, for the less strained and more reactive substrates, an *endo*-cyclization takes place through the intramolecular displacement of the iodine by the nitrogen atom to form the aziridinium ion. The nucleophilic attack onto the higher-substituted carbon generates the corresponding piperidine with *anti*-selectivity.

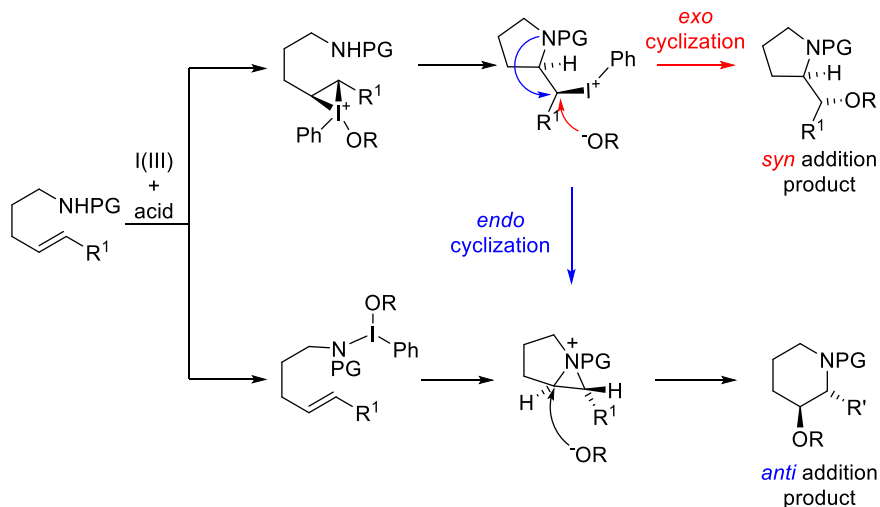


Figure 2.28 Michael mechanistic proposal for the I(III)-mediated intramolecular C-N bond formation for the synthesis of piperidines.

⁷⁶ Lovick, H. M.; Michael, F. E. *J. Am. Chem. Soc.* **2010**, *132*, 1249.

Later, Li applied this concept to the development of an intramolecular aminohalocyclization reaction leading to the synthesis of useful building blocks. A series of alkenyl sulphonamides were cyclized in the present of the hypervalent iodine reagent $\text{PhI}(\text{OPiv})_2$ and $\text{HF}\cdot\text{Pyr}$ as the fluorine source (Figure 2.29).⁷⁷ Based on the previous mechanism, the preferred *cis*-product can be explained proposing two different pathways: a) once the iodonium ion is formed, it is intramolecularly attacked by the tosylamide and rapidly reacts with a fluoride atom through an $\text{S}_{\text{N}}2$ reaction, or b) the nitrogen is oxidized and attacked by the alkene generating a carbocation intermediate, which is stabilized by the neighbouring group participation of the tosyl group in favor of the *cis*-product formation. When the substrate bears a quaternary β -carbon, the axial alkyl group prevent the stabilization by the tosyl group and thus a diastereomeric mixture is obtained.

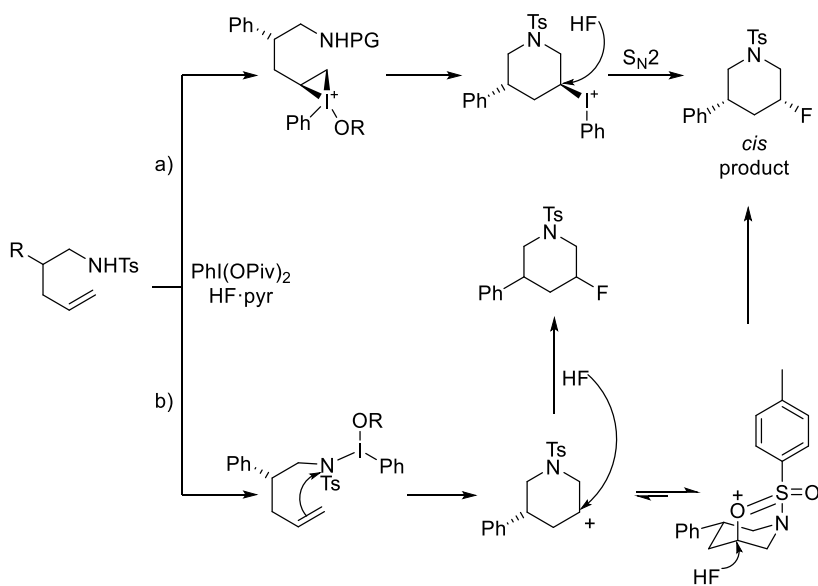


Figure 2.29 Piperidine formation through a diastereoselective aminofluorination cyclization reaction.

In 2013, this halocyclization reaction was furtherly improved by Nevado (Figure 2.30).⁷⁸ They designed the first enantioselective aminofluorocyclization of alkenes by

⁷⁷ Wang, Q.; Zhong, W.; Wei, X.; Ning, M.; Meng, X.; Li, Z. *Org. Biomol. Chem.*, **2012**, *10*, 8566.

⁷⁸ Kong, W.; Feige, P.; Haro, T.; Nevado, C. *Angew. Chem. Int. Ed.* **2013**, *52*, 2469.

using a chiral lactate-derived iodine(III)-difluoride reagent. Based on several mechanistic studies, they suggest that the reaction starts with the activation of the aryliododifluoride reagent with the amine through H-bonding interaction. Then, ligand exchange at the iodine(III) center results in the formation of the crucial I-N intermediate in agreement to the established results from Domínguez. The aminofluoro iodonium intermediate reacts with the alkene to give the aziridinium intermediate that is subsequently opened by fluoride at the more substituted carbon atom to give the *endo*-cyclization product with correct *anti*-selectivity, as previously proposed by Michael.

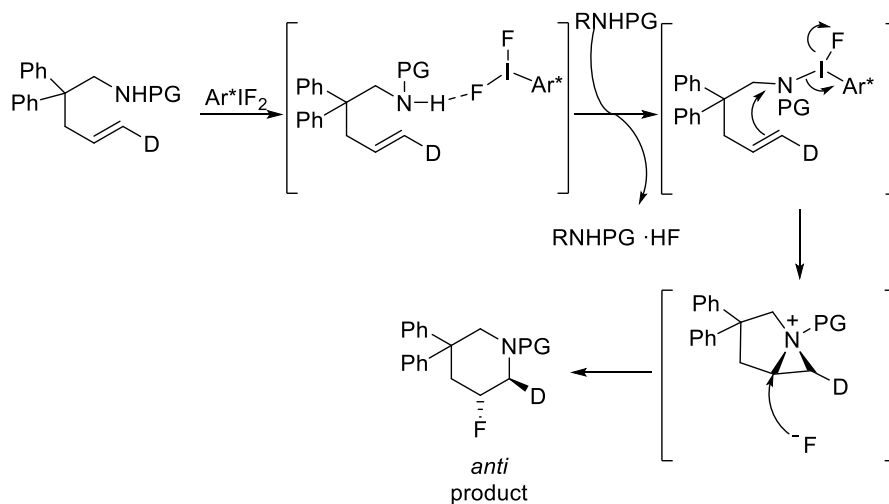


Figure 2.30 Enantioselective proposal for the synthesis of halo substituted piperidines developed by Nevado.

One year later, Shibata and Kita reported the catalytic version of this specific transformation using *p*-iodotoluene in catalytic amounts, HF-Pyr as fluorine source and *m*-CPBA as the terminal oxidant.⁷⁹ They also reported some results of an asymmetric variant using (*R*)-binaphthyl 2,2'-diiodide as a catalyst, although only low *ee* values were obtained.

⁷⁹ Suzuki, S.; Kamo, T.; Fukushi, K.; Hiramatsu, T.; Tokunaga, E.; Dohi, T.; Kita, Y.; Shibata, N. *Chem. Sci.* **2014**, *5*, 2754.

As a summary, over the last years, several strategies were designed for the synthesis of a wide variety of *N*-heterocycles using iodine(III)-reactivity. Some key steps are crucial for the successful formation of the final cyclic products.

2.2. Objective

As discussed at the outset, hypervalent iodine reagents represent versatile synthetic tools for a series of oxidative transformations. The intramolecular aminocyclization of alkenes is one example of the high relevance of this type of reagents. Based on the synthesis of indolines reported by Dominguez (Figure 2.23),⁷¹ in which a cationic nitrogen intermediate is generated by the action of PIFA and intramolecularly attacked by the alkene, we observed that this approach was not applied for the synthesis of indoles.

We thus envisioned a metal-free synthesis of indoles starting from 2-vinyl anilines, a substrate widely used in transition metal-catalyzed reactions that undergoes cyclization in the presence of a hypervalent iodine reagent (Figure 2.31).

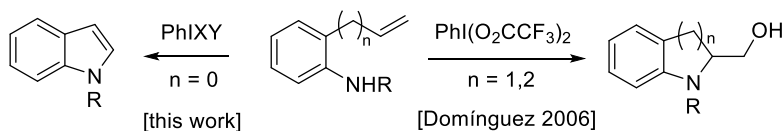


Figure 2.31 Iodine(III)-mediated intramolecular alkene amination.

2.3. Results and discussion

2.3.1 Optimization of reaction conditions

As described in Chapter 1, our group reported in 2013, the synthesis and the reactivity of a new hypervalent iodine reagent $\text{PhI}(\text{NTs})_2$ with defined I-N bonds. It was found that when this reagent reacted with *N*-tosylated 2-vinyl aniline, the corresponding diamination product was obtained in a 33% of yield. Surprisingly, when the reaction is carried out with PIFA, a clean cyclization takes place and the final indole was obtained in a 71% yield (Figure 2.32).

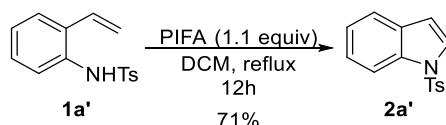


Figure 2.32 Previous result reported by our group.

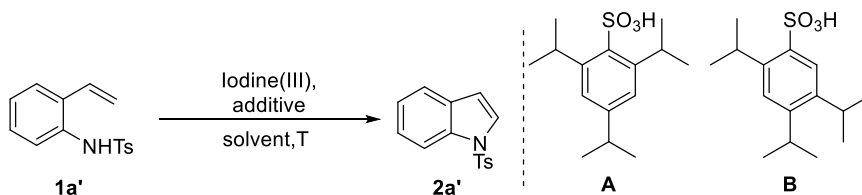
Based on this previous result, we decided to further explore the reactivity of this particular substrate for the iodine(III)-mediated intramolecular cyclization.

Despite repeated attempts, the previously obtained yield could not be reproduced. No indole formation was observed when the reaction was carried out with a freshly purchased sample of PIFA (Table 2.1, entry 1). We suspected that the PIFA source used for the initial experimentation contained undefined decomposition products. We tried to generate such compounds by addition of water (1 vol-%). Under these conditions, the final indole was indeed obtained, but the yield remained low (entry 2).

When the less reactive hypervalent iodine reagent PIDA is used, the yield increased to 67%, but when the temperature is decreased to room temperature, the yield dropped dramatically. In this case, the use of combinations with different Brønsted acids resulted in a beneficial effect increasing the yields at room temperature (entries 5 and 6). The use of the Koser reagent $\text{PhI}(\text{OH})(\text{OTs})$ ⁸⁰ (entries 7 and 8) and the *in situ* generation of derivatives from PhIO by the combination with two different sterically congested aryl

⁸⁰ a) Koser, G. F.; Wettach, R. H.; Troup, J. M.; Frenz, B. A. *J. Org. Chem.* **1976**, *41*, 3609; b) Yusubov, M. S.; Wirth, T. *Org. Lett.* **2005**, *7*, 519; c) Moriarty, R. M.; Vaid, R. K.; Koser, G. F. *Synlett* **1990**, 365.

sulfonic acids (A and B, entries 9 and 10, respectively) gave the final indole, but in low yield.

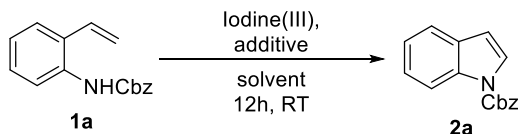


Entry	Iodine(III)	Additive	Solvent	t (h)	T (°C)	Yield (%) ^a
1	PIFA	-	DCM	24	40	<5
2	PIFA	H ₂ O	DCM	24	40	15
3	PIDA	-	DCM	12	40	67
4	PIDA	-	DCM	24	25	<5
5	PIDA	<i>p</i> -TsOH	DCM	12	25	25
6	PIDA	TfOH	DCM	12	25	14
7	PhI(OH)(OTs)	-	DCM	12	25	37
8	PhI(OH)(OTs)	-	DCM	12	40	30
9	PhIO	A	DCM	12	25	31
10	PhIO	B	DCM	12	25	34

^a: Isolated yield.

Table 2.1 Results obtained for the optimization of *N*-tosyl vinyl aniline.

Since all of these reactions starting from the *N*-tosylated 2-vinylaniline gave similar low yields, we decided to move to carbamate protecting groups. For this aim, the corresponding *N*-Cbz-protected 2-vinyl aniline was synthesized and tested in the cyclization reaction (Table 2.2).



Entry	Iodine(III)	Additive	Solvent	Yield (%) ^a
1	PIDA	-	DCM	<5
2	PIFA	-	DCM	14
3	PIDA	<i>p</i> -TsOH	DCM	31
4	PIDA	TfOH	DCM	13
5	PhI(OH)(OTs)	-	DCM	55
6	PhI(OH)(OTs)	-	CHCl ₃	64
7	PhIO	<i>p</i> -TsOH	CHCl ₃	64
8	PhIO	A	CHCl ₃	65
9	PhIO	B	CHCl ₃	92
10 ^b	PhIO	B	CHCl ₃	92

^a: Isolated yield.

^b: Reaction time of 1 h.

Table 2.2 Results obtained for the optimization of *N*-Cbz 2-vinyl aniline.

The use of PIDA (Table 2.2, entry 1), PIFA (entry 2) and combinations of the former with Brønsted acids (entries 3 and 4), as in the screening for the *N*-tosyl derivative, delivered the desired indole, but the yields remained low. However, when the Koser reagent was tested, the final product was formed in a 55% yield together with some unidentified side products (entry 5). This result was improved to 64% when chloroform was used as the solvent (entry 6). An *in situ* formation of the active reagent from iodosobenzene (PhIO) and 4-toluene sulfonic acid or 2,4,6-tris-isopropylbenzene sulfonic acid (A) gave the same result (entries 7 and 8). However, the use of 2,4,5-tris-isopropylbenzene sulfonic acid (TIPBSA, B) led to the formation of the desired indole in a 92% yield. For this optimum combination of PhIO and B, the reaction time could be lowered to 1 h without loss of yield (entry 10).

Under these reaction conditions, some other *N*-carbamoyl precursors such as the methyl carbamate and the Fmoc derivative were cyclized to the corresponding indole in

good yields (Figure 2.33). The benzoyl protection is also well tolerated, but due to the acidic reaction conditions the Boc group is beyond the scope of this cyclization.

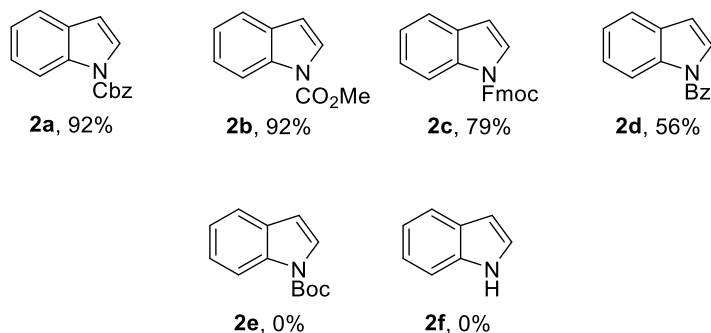
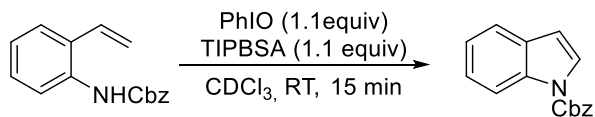


Figure 2.33 *N*-protected anilines tested under optimized reaction conditions.

2.3.2 Kinetic profile of the cyclization

During the optimization of the reaction conditions, an unprecedented high rate for this transformation was observed. To support this observation, a kinetic experiment was carried out.

Following the standard procedure, the starting material *N*-Cbz-protected 2-vinyl aniline (0.25 mmol) was dissolved in CDCl_3 (3 mL). PhIO (0.275 mmol) and 2,4,5-trisopropylbenzene sulfonic acid (TIPBSA) (0.275 mmol) were added. The progress of the reaction was monitored through integration of the respective ratio between starting material and product, which was calculated with an estimated 5% error margin from the resulting ^1H NMR spectra (Table 2.3, Figure 2.34).



Time (min)	Conversion (%)
0,5	8
1	55
2	85
3	92
4	95
5	97
7	98
10	100

Table 2.3 Data obtained from the integration of $^1\text{H-NMR}$ data during the course of the cyclization.

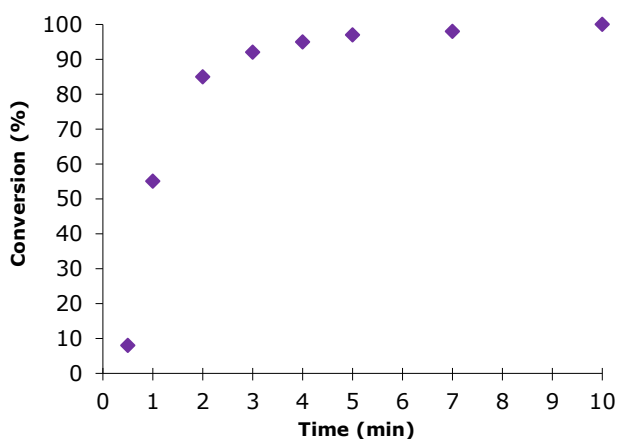
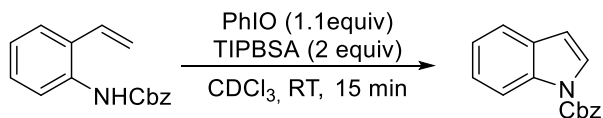


Figure 2.34 Kinetic profile for the formation of the indole under standard conditions.

As depicted, the result of the NMR study suggests that for the model substrate, oxidation to the corresponding indole is finished within ten minutes at room temperature, corroborating the observation by TLC during the course of the reaction.

In addition, the same NMR study was applied to study the effect of the acid. The experiment was performed following the standard procedure described above, but

increasing the amount of the aryl sulfonic acid TIPBSA (B) to 2 equivalents (Table 2.4, Figure 2.35).



Time (min)	Conversion (%)
0,33	52
0,5	64
1	81
2	92
4	97
5	100

Table 2.4 Data obtained from the integration of $^1\text{H-NMR}$ data during the course of the cyclization.

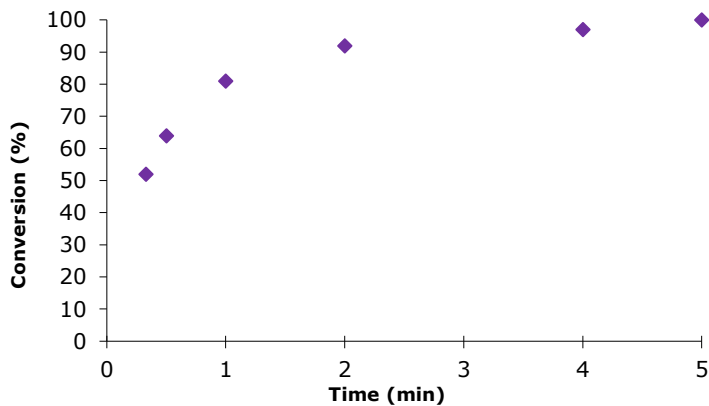


Figure 2.35 Kinetic profile for the formation of the indole under with 2 equivalents of acid.

The comparison between both graphs (Figure 2.34 and 2.35) by overlay revealed that an increase in the amount of acid accelerated the reaction, which was now complete within five minutes (Figure 2.36).

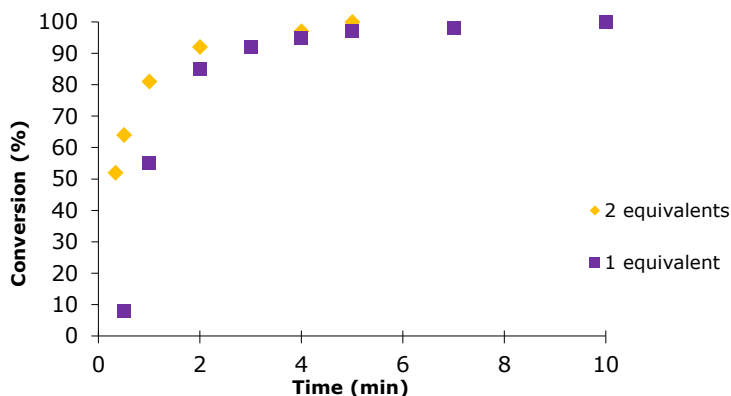


Figure 2.36 Effect of the amount of acid in the rate of the reaction.

2.3.3. Scope of the cyclization reaction

With the optimized conditions in hand, a series of different precursors were successfully cyclized to the corresponding indoles. First, a reaction on a 5 g-scale was developed and the model indole **2a** was obtained in a 78% of yield.

The general reaction conditions were found to be applicable for the synthesis of 5-substituted indoles (Figure 2.37). 5-Alkyl (**2g**) and halide (**2h-k**) substituents were tolerated.

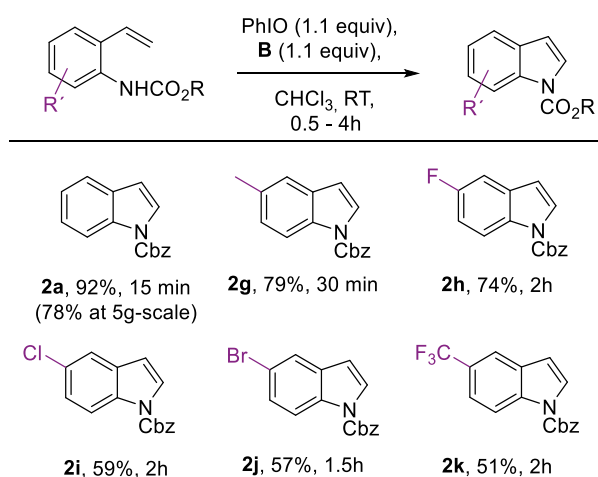


Figure 2.37 Examples of 5-substituted indoles with electron-donating and withdrawing groups.

Other 5-carbonyl substituted precursors cyclized readily into the corresponding indoles, including a formyl group (**2l**) that remains stable under the strong oxidation conditions. Derivatives with carbon substituents, such as phenyl and phenylacetylenyl could be oxidized efficiently to the correspondent indoles (**2p, q**) (Figure 2.38).

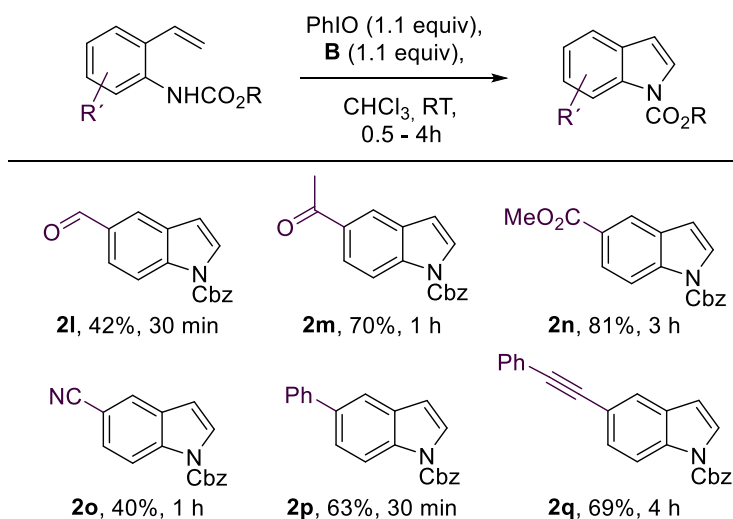


Figure 2.38 Examples of 5-substituted indoles with carbonyl and carbon substituents.

Under the optimized conditions, related 6-functionalized indoles **2r-w** were also generated. The correspondent indole derivatives with electron-donating substituents, such as methylated **2r** or methoxylated **2w**, and electron withdrawing groups as in **2u** were encountered in good to very good yields. This methodology also tolerates 5,6-disubstituted substrates (**2x, y**) demonstrating the high applicability of the present transformation that surpasses related ones from potentially competing metal-mediated processes (Figure 2.39).

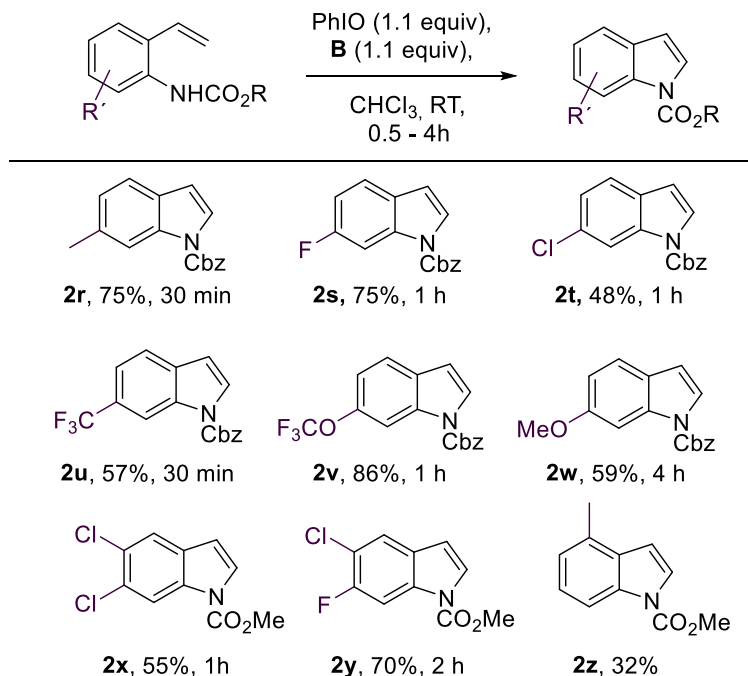


Figure 2.39 Examples of 6- and 5,6- substituted indoles with electron-donating and withdrawing groups.

Certain limitations were found during further exploration of the scope of this reaction. For the case of 4-methyl indole **2z**, the cyclization reaction with the combination of PhIO and TIPBSA was slow, probably due to the steric hindrance. When the reaction is carried out with a more reactive PIFA (1.1 equiv.) at 0 °C in chloroform, a significantly faster conversion is observed and the desired indole is obtained in a 32% yield in 24h.

Other substrates with different substituents were submitted with unsuccessful results (Figure 2.40). For example, a high electron-withdrawing substituent or a 5,7-disubstitution are less tolerated and the corresponding indoles were obtained in very low yields.

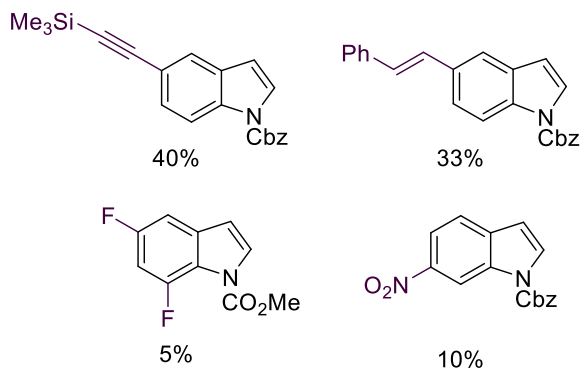
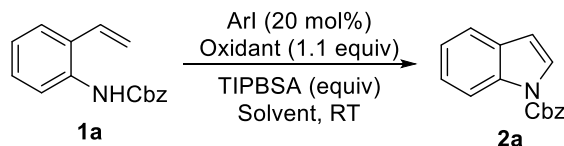


Figure 2.40 Less successful results under the optimized conditions.

2.3.4. Optimization of the catalytic version of the cyclization

In view of the successful results obtained for the stoichiometric cyclization reaction, we envisioned the development of a catalytic version of this oxidative transformation. We started to explore the potential of different oxidants in combination with phenyl iodine, where *m*-CPBA appears to be the best one for this transformation. It was observed that when equimolar amounts of acid with respect to the catalyst are used, the same yields are obtained as with the stoichiometric iodine(III) oxidants (Table 2.5).



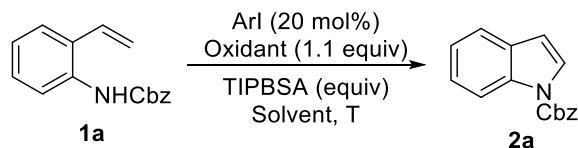
Entry	Arl	Oxidant	TIPBSA equiv.	Solvent	Conversion (%) ^a
1	PhI	H ₂ O ₂	0.2	CHCl ₃	0
2	PhI	Perchloric acid	0.2	CHCl ₃	13
3	PhI	Peracetic acid	0.2	CHCl ₃	10
4	PhI	Selectfluor	0.2	CHCl ₃	12
5	PhI	NFSI	0.2	CHCl ₃	13
6	PhI	Choramine-T	0.2	CHCl ₃	0
7	PhI	<i>m</i> -CPBA	0.2	CHCl ₃	100 (37%)
8	PhI	Perchloric acid	1	CHCl ₃	16
9	PhI	NaClO ₄	1	CHCl ₃	17
10 ^b	PhI	NaBO ₃	1	CHCl ₃	16
11	PhI	Selectfluor	1	CHCl ₃	22
12	PhI	Selectfluor	1	MeCN	11
13	PhI	Oxone ^b	1	MeCN/H ₂ O	25
14	PhI	<i>m</i> -CPBA	1	CHCl ₃	100 (44%)

^a: Isolated yield in brackets.

^b: NBu₄Cl was used as phase transfer reagent;

Table 2.5 First trials for the optimization of the catalytic version of the oxidative cyclization.

An extensive screening of the ideal catalyst was performed with different substituted aryl iodine candidates in combination with *m*-CPBA as the terminal oxidant (Table 2.6). The obtained results revealed that the more electron-rich 4-methoxy iodobenzene is the best catalyst choice for the present cyclization. It was noteworthy that when the reaction is carried out with a reduced amount of acid, longer reaction times are required, although no detrimental effect on the yield is observed.



Entry	Arl	Oxidant	TIPBSA equiv.	Solvent	T (°C)	Conversion (%) ^a
1	4-Me-PhI	<i>m</i> -CPBA	1	CHCl ₃	25	100 (49%)
2	3,5-Me-PhI	<i>m</i> -CPBA	1	CHCl ₃	25	100 (43%)
3	4-OMe-PhI	<i>m</i> -CPBA	1	CHCl ₃	25	100 (68%)
4	4-OMe-PhI	<i>m</i> -CPBA	0.3	CHCl ₃	25	100 (65%) ^b
5	4-OMe-PhI	<i>m</i> -CPBA	1	CHCl ₃	60	100 (49%)
6	4-OMe-PhI	<i>m</i> -CPBA	1	CHCl ₃	-10	100 (68%)
7	4-OMe-PhI	<i>m</i> -CPBA	1	CHCl ₃	-20	40
8	4-OMe-PhI	<i>m</i> -CPBA	1	CHCl ₃ /H ₂ O	25	100 (62%)

^a: Isolated yield in brackets.

^b: Reaction occurs significantly slower with less acid (6 hours with 0.3 equiv. vs. 30 min. with 1 equiv.)

Table 2.6 Screening of the catalyst for the oxidative cyclization.

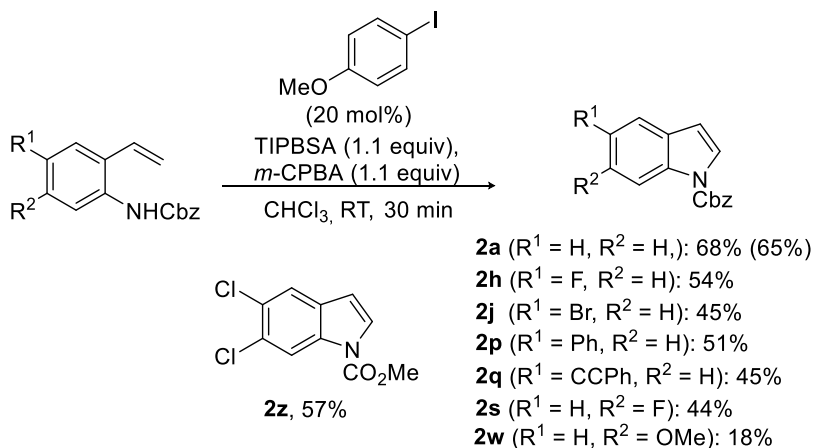


Figure 2.41 Scope of the catalytic indole synthesis.

With the best catalytic conditions, several precursors were converted into the corresponding indoles (Figure 2.41). Although the stoichiometric reaction showed a high productivity with a broad substrate scope, the obtained results questioned the efficiency of the catalytic version.

2.3.5. Mechanistic studies and final proposal

In order to elucidate the mechanism of the present oxidative cyclization reaction, the corresponding selectively deuterated starting materials were synthesized. When these compounds were submitted separately under the standard procedure, a partial migration of the deuterium marker was observed (Figure 2.42).

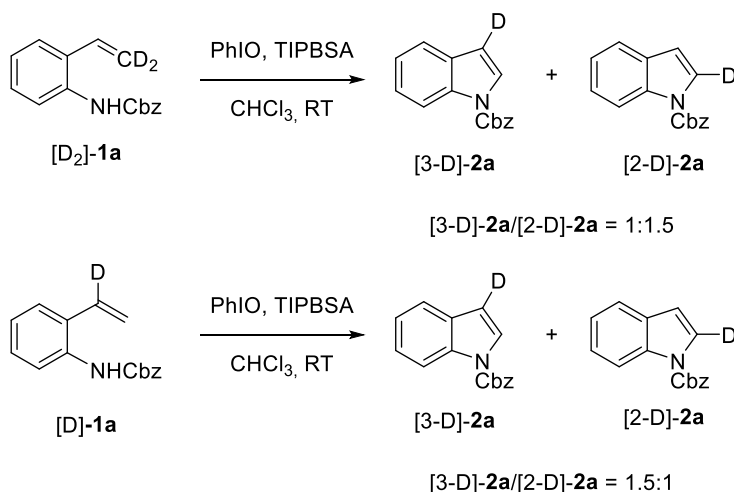


Figure 2.42 Control experiments using deuterium labelling.

In view of these observations, we decided to perform some experiments varying with the substitution in the hypervalent iodine reagent and in the aryl sulfonic acid (Figure 2.43). When a less sterically congested aryl sulfonic acid (2,4,6-trimethylbenzenesulfonic acid, TMBSA) is used, the deuterium engages more strongly toward the migration and a 1:1-ratio of products was observed. However, when the aryl moiety of the hypervalent iodine reagent is modified (ArIO, 2,4,6-trimethyliodosobenzene), no effect on the deuterium migration was observed.

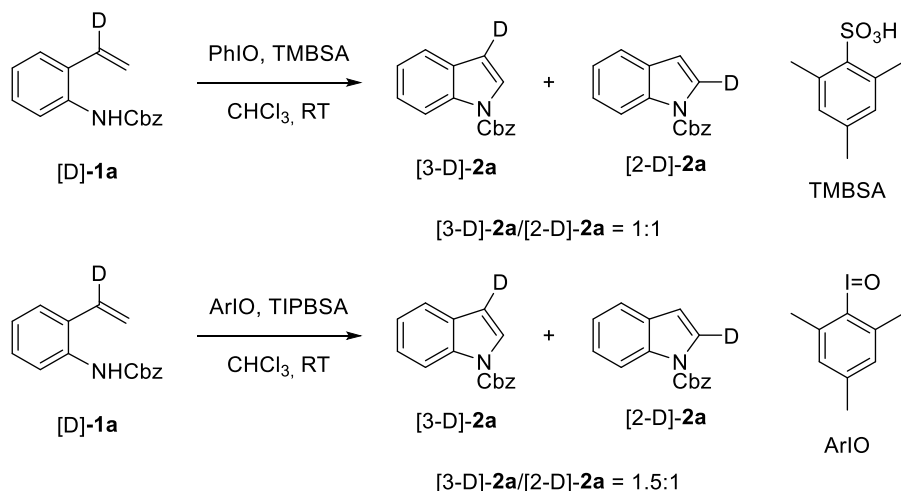


Figure 2.43 Control experiments with different substitution in the aryl moiety of the iodine(III)-reagent and sulfonic acid, respectively.

The corresponding competition experiment for the study of the kinetic isotopic effect was also performed (Figure 2.44). As for the standard cyclization procedure, a 1:1 mixture of both vinylcarbamates (5 equivalents) were dissolved in deuterated chloroform and stirred in a Pyrex tube. Then, PhIO (1.1 equivalents) and 2,4,5-tris-isopropylbenzenesulfonic acid (1.1 equivalents) were added. After work-up, the crude mixture was analyzed by ¹H NMR. Integration revealed a kinetic isotope effect of $k_H/k_D = 1.2$. This small value does not provide sufficient information on the mechanism of the cyclization.

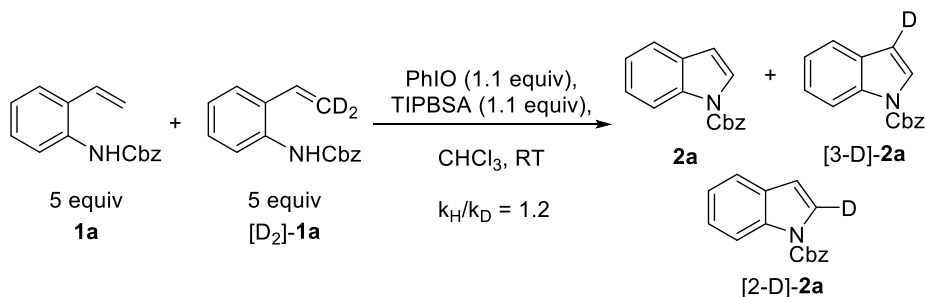


Figure 2.44 Kinetic isotopic effect experiment.

Taking into account all of these results, the mechanistic scenario is more complex than expected for this type of cyclization. We propose the following mechanism (Figure 2.45): the reaction started with the interaction between the modified Koser reagent generated *in situ* and the vinyl fragment of **1a**, leading to the iodonium ion intermediate **I** and then to the 1,2-iodooxygenated intermediate **II**. This route is in agreement with the proposal for the 1,2-dioxygenation reaction with related Koser reagents.⁸¹

Intermediate **II** is stabilized through the formation of a cyclopropyl phenonium ion **III**, well known in this type of oxidative transformations.⁸² This intermediate **III** receives stabilization through the amino group.

Now, two different pathways are feasible depending on the opening position at the spiro-cyclopropyl ring: a) the attack can take place at the methylene position resulting in the formation of 3-oxygenated indoline **IV**, which undergoes in a rapid aromatization to give the final indole, or b) the ring opening at the oxygenated carbon generates the 2-oxygenated indoline **V** and/or the iminium derivative **V'**. Again, elimination of the aryl sulfonic acid provides the final indole **2a**.

⁸¹ a) Koser, G. F.; Rebrovic, L.; Wettach, R. H. *J. Org. Chem.* **1981**, *46*, 4324; b) Zefirov, N. S.; Zhdankin, V. V.; Dan'kov, Y. V.; Sorokin, V. D.; Semerikov, V. N.; Koźmin, A. S.; Caple, R.; Berglund, B. A. *Tetrahedron Lett.* **1986**, *27*, 3971; c) Hirt, U. H.; Spingler, B.; Wirth, T. *J. Org. Chem.* **1998**, *63*, 7674; d) Wirth, T.; Hirt, U. H. *Tetrahedron: Asymmetry* **1997**, *k*, 23; e) Hirt, U. H.; Schuster, M. F. H.; French, A. N.; Wiest, O. G.; Wirth, T. *Eur. J. Org. Chem.* **2001**, 1569; f) Boye, A. C.; Meyer, D.; Ingison, C. K.; French, A. N.; Wirth, T. *Org. Lett.* **2003**, *5*, 2157; g) Kang, Y.-B.; Gade, L. H. *J. Am. Chem. Soc.* **2011**, *133*, 3658; h) Koser, G. F. *Top. Curr. Chem.* **2003**, *208*, 137.

⁸² Ulmer, A.; Brunner, C.; Arnold, A. M.; Pöthig, A.; Gulder, T. *Chem. Eur. J.* **2016**, *22*, 3660.

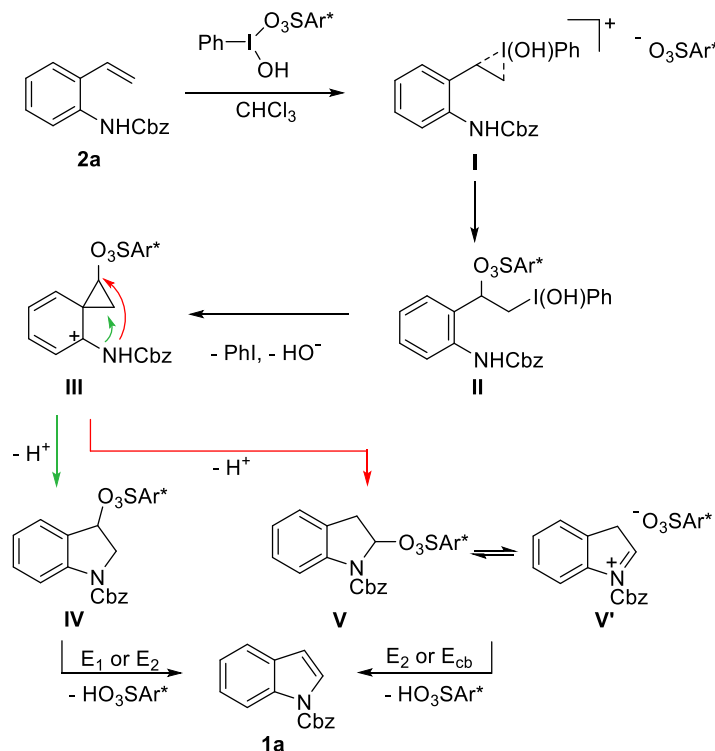


Figure 2.45 Mechanistic proposal for the indole formation.

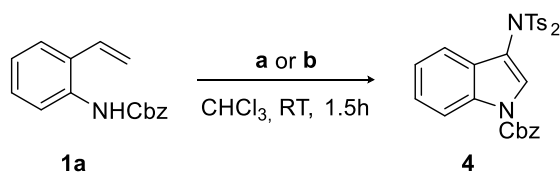
This mechanistic proposal is in agreement with the deuterium labelling experiments, observing some preference for the former pathway through the formation of intermediate **IV**, which is potentially due to steric reasons.

2.3.6. Development of a iodine(III)-mediated indole functionalization

In view that the cyclization reaction is almost completed within 10 minutes, we explored the possibility of a further functionalization combining two different iodine(III) reagents.

After several unsuccessful trials with different diaryliodonium salts, we decided to try our previously described aminating reagent, $\text{PhI}(\text{NTs})_2$. Following this idea, first we tested the amination of indole **2a** with different amounts of this reagent in different solvents and at different temperatures, to determine the best conditions to furnish the

final C3-aminated indole **4**. Once these conditions were found, model substrate **1a** was cyclized and then C3-selectively aminated to the final product **4** through a clean two-fold oxidative aminating process (Figure 2.46). The structure of the final product was confirmed by X-ray analysis.



- a:** TIPBSA (1.1 equiv), PhIO (1.1 equiv), PhI(NTs₂)₂ (1.1 equiv): 48%
b: TIPBSA (1.1 equiv), PhIO (2.2 equiv), HNTs₂ (1.1 equiv): 52%

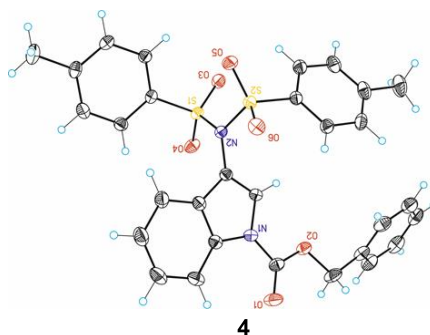


Figure 2.46 Sequential amination reaction with two different iodine(III) oxidants. X-ray crystal structure of **4**.

This result shows that the cyclization remains kinetically preferred over the amination process. The reaction could be also conducted with iodosobenzene as the sole oxidant by adding TIPBSA and bistosylimide for the two independent metal-free amination reactions. This observation demonstrates the robustness of the present indole formation and reveals the potential of its combination with other oxidation reactions.

2.4. Conclusions

We expand the approach for an iodine(III)-mediated intramolecular amination reaction to the indole synthesis.

A total of 21 different substrates were cyclized in the presence of a modified Koser reagent generated in situ by combination of iodosobenzene and a sterically congested 2,4,5-tris-isopropylbenzene sulfonic acid. A catalytic version of this oxidative cyclization was also developed using an electron-rich 4-methoxy iodobenzene as the catalyst in combination with *m*-CPBA as the terminal oxidant.

Several control experiments were performed in order to elucidate the reaction mechanism. It was found that the reaction goes first through the oxidation of the alkene that then is stabilized by the adjacent phenyl group in a neighbouring group participation forming the cyclopropyl phenonium ion key intermediate.

To demonstrate the applicability of the present metal-free cyclization reaction, we successfully designed two independent amination reactions in a one-pot process. The combination of two different hypervalent iodine reagents gives a selectively at position C3 aminated indole demonstrating the different synthetic possibilities of the present transformation.

2.5 Experimental part

General remarks: If not otherwise stated, all solvents, reagents and deuterated solvents were purchased from Aldrich, Alfa Aesar or TCI Europe. Column chromatography was performed with silica gel (Merck, type 60, 0.063-0.2 mm). NMR spectra were recorded on a Bruker Avance 400 MHz or 500 MHz spectrometer. All chemical shifts in NMR experiments are reported as ppm. The following calibration was used: CDCl_3 δ = 7.26 and 77.0 ppm. MS (ESI-LCMS) experiments were performed using an Agilent 1100 HPLC with a Bruker micro-TOF instrument (ESI). MS (ESI) and HRMS experiments were performed on a Kratos MS 50 within the service centers at ICIQ. IR spectra were measured on a Bruker Alpha instrument in the solid state.

Commercially available compounds were used as received. The following compounds were synthesized according to literature procedures: PhIO,⁸³ 2,4,5-tris-isopropylbenzenesulfonic acid,⁸⁴ 2,4,6-tris-isopropylbenzenesulfonic acid.⁸⁵ The spectral data of these compounds match the ones reported in the original literature.

Experimental procedures:

General procedure for synthesis of protected anilines (GP1): Compounds were synthesized following a previously described procedure.⁸⁶ A solution of the corresponding aniline (1 mmol) and pyridine (1.4 mmol) in ethyl acetate (3 mL) was treated dropwise with the corresponding chloroformate (1.2 mmol) at room temperature. After 2 hours, the suspension was washed successively with water, an aqueous solution of HCl (10%), a saturated aqueous solution of NaHCO₃ and a saturated aqueous solution of brine. The organic layer was dried over anhydrous Na₂SO₄, filtered and concentrated under reduced pressure. Compounds were purified by crystallization from hexane.

General procedure for synthesis of vinyl derivatives (GP2): Compounds were synthesized following a previously described procedure.⁸⁷ To a deoxygenated solution of the corresponding haloarene (1 mmol) in DME (4 mL) was added Pd(PPh₃)₄ (0.05 mmol), and the mixture was stirred at room temperature under argon atmosphere for 15 min. Potassium carbonate (1.2 mmol) in water (1.3 mL), and 2,4,6-trivinylcyclotriboroxane-pyridine complex (1.03 mmol) were added, and the reaction mixture was heated under reflux overnight. Then, water was added and the mixture was extracted with CH₂Cl₂ (3 x 20 mL). The organic layer was washed with water and a saturated aqueous solution of brine and dried over anhydrous Na₂SO₄. The solvent was removed under reduced pressure. The residue was purified by column chromatography (silica gel, *n*-hexane/ethyl acetate, 90/10, v/v).

⁸³ Saltzman, H.; Sharefkin, J. G. *Org. Synth.* **1973**, *5*, 658.

⁸⁴ a) Smith, L. I.; Cass, O.W. *J. Am. Chem. Soc.* **1932**, *54*, 1603; b) Cerfontain, H.; Koeberg-Telder, A.; C. Ris, C. *J. Chem. Soc., Perkin Trans. 2* **1977**, 720.

⁸⁵ Jautze, S.; Peters, R. *Angew. Chem. Int. Ed.* **2008**, *47*, 9284.

⁸⁶ Hennessy, E. J.; Buchwald, S. L. *J. Am. Chem. Soc.* **2003**, *125*, 12084.

⁸⁷ Kerins, F.; O'Shea, D. F. *J. Org. Chem.* **2002**, *67*, 4968.

General procedure for iodine(III)-mediated indole formation (GP3): PhIO (0.275 mmol) and 2,4,5-tris-iso-propylbenzenesulfonic acid (0.275 mmol) were added to a stirred solution of the corresponding starting material (0.250 mmol) in CHCl_3 (3 mL). The reaction was quenched with pyridine (0.275 mmol) and solvent was removed under reduced pressure. The crude reaction product was purified by column chromatography (neutral alumina, *n*-hexane/ethyl acetate, 98/2, v/v).

General procedure for iodine (III)-catalyzed indole formation (GP4): 4-Iodoanisole (0.055 mmol) and 2,4,5-tris-iso-propylbenzenesulfonic acid (0.275 mmol) were added to a stirred solution of the corresponding starting material (0.250 mmol) in CHCl_3 (3 mL). Then, 3-chloro perbenzoic acid (0.275 mmol) was added. The reaction was quenched with pyridine (0.550 mmol) and solvent was removed under reduced pressure. The crude reaction product was purified by column chromatography (neutral alumina, *n*-hexane/ethyl acetate, 98/2, v/v).

Synthesis and characterization of starting materials:

Synthesis of 2-vinyl aniline:

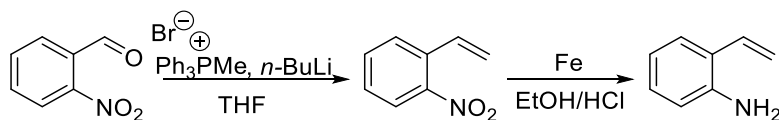
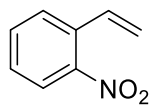


Figure 2.47 Synthesis of 2-vinyl aniline.

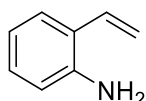
2-Nitrostyrene



To a solution of Ph_3PMeBr (11.82 g, 33.1 mmol) in THF (120 mL) was added *n*-BuLi (2M) in cyclohexane (16.4 mL) dropwise at 0 °C under argon. The reaction mixture was stirred at room temperature for 1 hour. Then, 2-nitrobenzaldehyde (5 g, 33.1 mmol) was added and the mixture was heated to 65 °C for 5 hours. The reaction was quenched by the addition of a saturated aqueous solution of NH_4Cl . The aqueous phase was extracted with CH_2Cl_2 (3 x 20 mL). The combined organic layers were dried over Na_2SO_4 and evaporated under reduced pressure. The obtained residue was purified by column chromatography (silica gel, *n*-

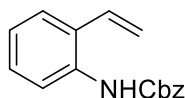
hexane/ethyl acetate, 90/10, v/v) to afford the title compound as yellow oil (7.61 g, 77% yield). The NMR spectra match the literature data.⁸⁸

2-Vinylaniline



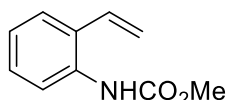
The compound was synthesized in 92% yield as brown oil following a literature procedure.⁸⁹ The NMR spectra match the literature data.⁸⁸

Benzyl (2-vinylphenyl)carbamate (1a)



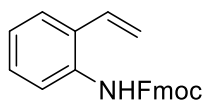
Following GP1, using benzyl chloroformate, benzyl (2-vinylphenyl)carbamate was isolated as a colorless solid in 65% yield. The NMR spectra match the literature data.⁹⁰

Methyl (2-vinylphenyl)carbamate (1b)



Following GP1, using methyl chloroformate, methyl (2-vinylphenyl)carbamate was isolated in 96% yield as a colorless oil. **¹H NMR (500 MHz, CDCl₃):** δ = 7.77 (s, 1H), 7.40 (dd, J = 7.7, 1.7 Hz, 1H), 7.30-7.28 (m, 1H), 7.11 (td, J = 7.5, 1.4 Hz, 1H), 6.81 (dd, J = 17.4, 11.0 Hz, 1H), 6.60 (brs, 1H), 5.66 (dd, J = 17.4, 1.3 Hz, 1H), 5.41 (dd, J = 11.0, 1.3 Hz, 1H), 3.78 (s, 3H). **¹³C NMR (101 MHz, CDCl₃):** δ = 154.4, 134.5, 132.1, 129.0, 128.6, 126.9, 124.5, 122.0, 118.1, 52.5. **HRMS (ESI-MS):** calcd for C₁₀H₁₁NNaO₂: 200.0682; found: 200.0674. **IR v (cm⁻¹):** 3199, 2910, 2905, 1715.

(9H-Fluoren-9-yl)methyl (2-vinylphenyl)carbamate (1c)



Following GP1, using Fmoc chloride and CH₂Cl₂ as solvent, (9H-fluoren-9-yl)methyl (2-vinylphenyl)carbamate was isolated as a white solid in 78% yield. **¹H NMR (400 MHz, CDCl₃):** δ = 7.79 (d, J = 7.6 Hz, 2H), 7.63-7.57 (m, 2H), 7.43 (t, J = 7.7 Hz, 3H), 7.35-7.28 (m, 4H), 7.16 (t, J = 7.6

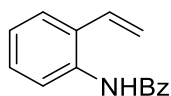
⁸⁸ Arisawa, M.; Fujii, Y.; Kato, H.; Fukuda, H.; Matsumoto, T.; Ito, M.; Abe, H.; Ito, Y.; Shuto, S. *Angew. Chem. Int. Ed.* **2013**, *52*, 1003.

⁸⁹ Gauthier, D.; Dodd, R. H.; Dauban, P. *Tetrahedron* **2009**, *65*, 8542.

⁹⁰ Arisawa, M.; Terada, M.; Takahashi, K.; Nakagawa, M.; Nishida, A. *J. Org. Chem.* **2006**, *71*, 4255.

Hz, 1H), 6.83 (dd, $J = 17.4, 11.0$ Hz, 1H), 6.62 (brs, 1H), 5.70 (d, $J = 17.4$ Hz, 1H), 5.44 (d, $J = 11.0$ Hz, 1H), 4.54 (dd, $J = 7.0, 1.9$ Hz, 2H), 4.29 (t, $J = 6.9$ Hz, 1H). $^{13}\text{C NMR}$ (126 MHz, CDCl_3): $\delta = 153.9, 143.8, 141.4, 134.3, 132.1, 128.6, 127.9, 127.8, 127.2, 127.1, 126.9, 125.2, 125.1, 120.1, 118.0, 67.1, 47.2$. HRMS (ESI-MS): calcd for $\text{C}_{23}\text{H}_{19}\text{NNaO}_2$: 364.1308; found: 364.1314. IR ν (cm^{-1}): 3288, 3008, 2926, 1715. m.p.: 111-112 °C.

N-(2-vinylphenyl)benzamide (1d)



2-Vinylaniline (500 mg, 4.20 mmol) and DMAP (615 mg, 5.04 mmol) were dissolved in CH_2Cl_2 (5 mL) and benzoyl chloride (0.58 mL, 5.04 mmol) was added dropwise. The reaction was stirred for 1 hour and quenched with an aqueous solution of HCl (10%). The mixture was washed with an aqueous solution of HCl (10%) and a saturated aqueous solution of brine. The organic layer was dried over anhydrous Na_2SO_4 , filtered and concentrated under vacuo. *N*-(2-vinylphenyl)benzamide was crystallised from hexane and isolated as a white solid in 89% yield. $^1\text{H NMR}$ (400 MHz, CDCl_3): $\delta = 7.98$ (d, $J = 8.3$ Hz, 1H), 7.92-7.83 (m, 2H), 7.59-7.53 (m, 1H), 7.51-7.44 (m, 3H), 7.32 (td, $J = 7.8, 1.6$ Hz, 1H), 7.19 (td, $J = 7.4, 1.0$ Hz, 1H), 6.86 (dd, $J = 17.5, 11.0$ Hz, 1H), 5.71 (dd, $J = 17.5, 1.3$ Hz, 1H), 5.45 (dd, $J = 11.1, 1.3$ Hz, 1H). $^{13}\text{C NMR}$ (101 MHz, CDCl_3): $\delta = 165.7, 134.7, 134.5, 132.3, 131.9, 130.7, 128.8, 128.6, 127.1, 127.1, 125.5, 123.6, 118.4$. HRMS (ESI-MS): calcd for $\text{C}_{15}\text{H}_{13}\text{NNaO}$: 246.0889; found: 246.0895. IR ν (cm^{-1}): 3286, 2901, 2905, 1713, 1680. m.p.: 156-158 °C.

Synthesis of Benzyl (4-methyl-2-vinylphenyl)carbamate (1g):

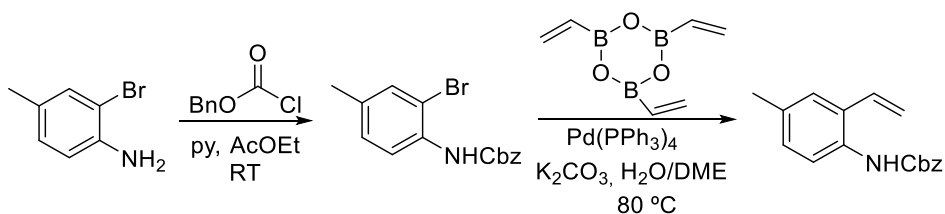
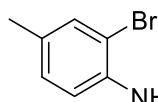


Figure 2.48 Synthesis of 1g.

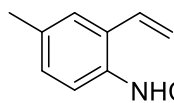
Benzyl (2-bromo-4-methylphenyl)carbamate



Following GP1, benzyl (2-bromo-4-methylphenyl)carbamate was isolated as a white solid in 99% yield. $^1\text{H NMR}$ (400 MHz, CDCl_3): $\delta = 8.01$ (d, $J = 8.4$ Hz, 1H), 7.48-7.31 (m, 6H), 7.17-7.07 (m, 2H), 5.22 (s, 2H), 2.29 (s, 3H). $^{13}\text{C NMR}$ (126 MHz, CDCl_3): $\delta = 153.2, 135.9, 134.4, 133.2,$

132.6, 129.0, 128.6, 128.4, 128.4, 120.2, 112.5, 67.2, 20.4. **HRMS (ESI-MS):** calcd for $C_{15}H_{14}BrNNaO_2$: 342.0100; found: 342.0103. **IR v (cm^{-1}):** 3283, 3033, 2918, 1694. **m.p.:** 76-78 °C

Benzyl (4-methyl-2-vinylphenyl)carbamate (1g)



Following GP2, benzyl (4-methyl-2-vinylphenyl)carbamate was isolated as a white solid in 74% yield. **1H NMR (400 MHz, $CDCl_3$):** δ = 7.65 (brs, 1H), 7.42-7.34 (m, 5H), 7.21 (s, 1H), 7.09 (dd, J = 8.2, 1.5 Hz, 1H), 6.77 (dd, J = 17.5, 11.0 Hz, 1H), 5.64 (dd, J = 17.4, 1.3 Hz, 1H), 5.36 (dd, J = 11.0, 1.3 Hz, 1H), 5.20 (s, 2H), 2.32 (s, 3H). **^{13}C NMR (126 MHz, $CDCl_3$):** δ = 154.0, 136.2, 132.6, 132.2, 131.9, 129.5, 129.3, 129.1, 128.6, 128.4, 128.3, 127.3, 117.6, 67.1, 20.9. **HRMS (ESI-MS):** calcd for $C_{17}H_{17}NNaO_2$: 290.1151; found: 290.1161. **IR v (cm^{-1}):** 3271, 1687, 1521. **m.p.:** 63-65 °C.

Synthesis of Benzyl (4-fluoro-2-vinylphenyl)carbamate (1h):

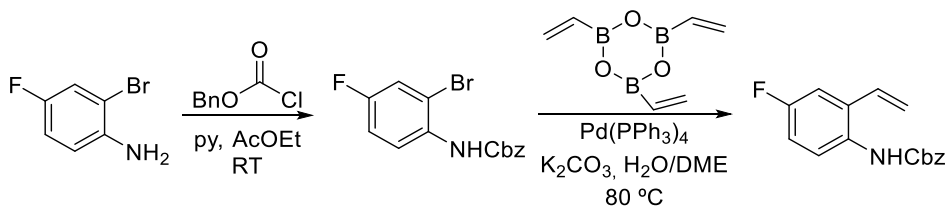
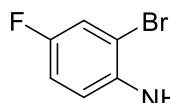
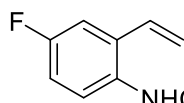


Figure 2.49 Synthesis of 1h.

Benzyl (2-bromo-4-fluorophenyl)carbamate



Following GP1, benzyl (2-bromo-4-fluorophenyl)carbamate was isolated as a white solid in 99% yield. **1H NMR (400 MHz, $CDCl_3$):** δ = 8.13-8.11 (m, 1H), 7.49-7.33 (m, 5H), 7.28 (dd, J = 7.8, 2.9 Hz, 1H), 7.11-6.98 (m, 2H), 5.22 (s, 2H). **^{13}C NMR (126 MHz, $CDCl_3$):** δ = 158.1 (d, $^1J_{C-F}$ = 250.2 Hz), 153.2, 135.7, 132.3, 132.2, 128.7, 128.5, 128.4, 121.4, 119.3 (d, $^2J_{C-F}$ = 24.8 Hz), 115.3 (d, $^2J_{C-F}$ = 22.0 Hz), 67.4. **^{19}F NMR (376 MHz, $CDCl_3$):** δ = -117.73. **HRMS (ESI-MS):** calcd for $C_{14}H_{10}BrFNO_2$: 321.9884; found: 321.9883. **IR v (cm^{-1}):** 3288, 3066, 3030, 2953, 1690. **m.p.:** 87-88 °C.

Benzyl (4-fluoro-2-vinylphenyl)carbamate (1h)

Following GP2, benzyl (4-fluoro-2-vinylphenyl)carbamate was isolated as a white solid in 78% yield. **¹H NMR (400 MHz, CDCl₃):** δ = 7.69 (s, 1H), 7.40-7.35 (m, 5H), 7.12 (dd, J = 9.4, 3.0 Hz, 1H), 7.01-6.95 (m, 1H), 6.75 (ddd, J = 17.5, 11.0, 1.4 Hz, 1H), 6.48 (brs, 1H), 5.67 (dd, J = 17.3, 1.0 Hz, 1H), 5.43 (dd, J = 11.0, 1.0 Hz, 1H), 5.20 (s, 2H). **¹³C NMR (126 MHz, CDCl₃):** δ = 159.9 (d, $^1J_{C-F}$ = 242.1 Hz) 154.1, 136.0, 131.2, 131.1, 130.3, 128.6, 128.4, 128.4, 124.6, 118.8, 115.2 (d, $^2J_{C-F}$ = 22.6 Hz), 113.0 (d, $^2J_{C-F}$ = 23.1 Hz) 67.3. **¹⁹F NMR (376 MHz, CDCl₃):** δ = -117.98. **HRMS (ESI-MS):** calcd for C₁₆H₁₄FNNaO₂: 294.0901; found: 294.0904. **IR v (cm⁻¹):** 3264, 1684, 1532. **m.p.:** 100-102 °C.

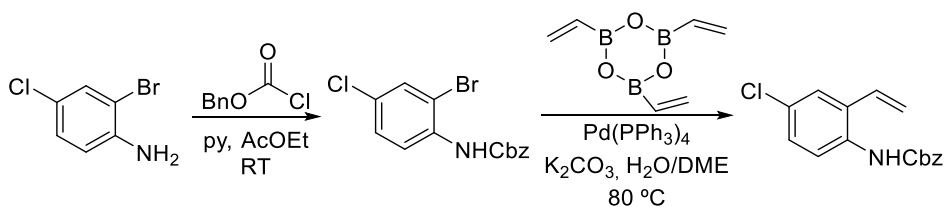
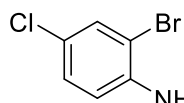
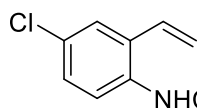
Synthesis of Benzyl (4-chloro-2-vinylphenyl)carbamate (1i):

Figure 2.50 Synthesis of 1i.

Benzyl (2-bromo-4-chlorophenyl)carbamate

Following GP1, benzyl (2-bromo-5-chlorophenyl)carbamate was isolated as a white solid in 69% yield. **¹H NMR (400 MHz, CDCl₃):** δ = 8.14 (d, J = 8.9 Hz, 1H), 7.52 (d, J = 2.4 Hz, 1H), 7.45-7.35 (m, 5H), 7.29 (dd, J = 8.9, 2.4 Hz, 1H), 7.15 (brs, 1H), 5.22 (s, 2H). **¹³C NMR (101 MHz, CDCl₃):** δ = 152.9, 135.6, 134.6, 131.7, 128.7, 128.6, 128.5, 128.5, 120.8, 112.6, 67.5. **HRMS (ESI-MS):** calcd for C₁₄H₁₁BrClNNaO₂: 361.9554; found 361.9554. **IR v (cm⁻¹):** 3314, 3071, 2948, 2896, 1747. **m.p.:** 100-102 °C.

Benzyl (4-chloro-2-vinylphenyl)carbamate (1i)

Following GP2, benzyl (4-chloro-2-vinylphenyl)carbamate was isolated as a white solid in 72% yield. **¹H NMR (300 MHz, CDCl₃):** δ = 7.79 (d, J = 8.7 Hz, 1H), 7.43-7.35 (m, 6H), 7.28-7.19 (m, 1H),

6.71 (dd, $J = 17.4, 11.0$ Hz, 1H), 6.57 (brs, 1H), 5.67 (dd, $J = 17.3, 1.1$ Hz, 1H), 5.45 (dd, $J = 11.1, 1.1$ Hz, 1H), 5.20 (s, 2H). ^{13}C NMR (101 MHz, CDCl_3): $\delta = 153.5, 135.8, 133.1, 130.9, 129.1, 128.7, 128.5, 128.5, 128.4, 128.3, 126.8, 119.5, 67.4$. HRMS (ESI-MS): calcd for $\text{C}_{16}\text{H}_{13}\text{ClNO}_2$: 286.0648; found: 286.0640. IR ν (cm^{-1}): 3281, 3065, 3033, 2951, 2897, 1685. m.p.: 111-112 °C.

Synthesis of Benzyl (4-bromo-2-vinylphenyl)carbamate (**1j**):

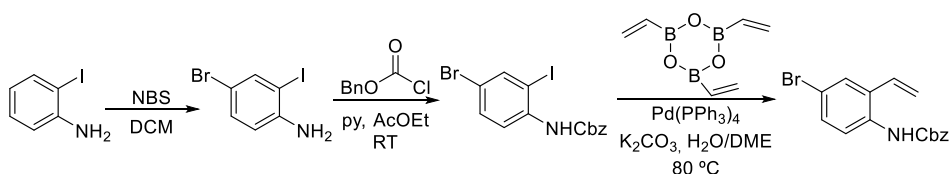
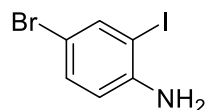


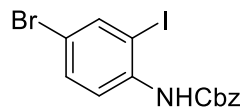
Figure 2.51 Synthesis of **1j**.

4-Bromo-2-iodoaniline



To a stirred solution of 2-iodoaniline (1932 mg, 8.82 mmol) in CH_2Cl_2 (10 mL), N-bromosuccinimide (1649 mg, 9.263 mmol) was added at 0 °C. After 16 hours, the reaction was quenched with water and extracted with CH_2Cl_2 (3x20mL). The combined organic layers were dried over Na_2SO_4 and solvent was removed under reduced pressure. The crude was purified by crystallization from hexane giving 2629 mg of the corresponding 4-bromo-2-iodoaniline as a purple solid in 99% yield. The NMR spectra match with the literature data.⁹¹ ^1H NMR (400 MHz, CDCl_3): $\delta = 7.73$ (d, $J = 2.2$ Hz, 1H), 7.22 (dd, $J = 8.5, 2.2$ Hz, 1H), 6.62 (d, $J = 8.5$ Hz, 1H), 4.10 (brs, 2H). ^{13}C NMR (101 MHz, CDCl_3): $\delta = 145.9, 140.3, 132.1, 115.5, 109.9, 84.0$.

Benzyl (4-bromo-2-iodophenyl)carbamate

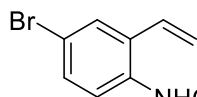


Following GP1, benzyl (4-bromo-2-iodophenyl)carbamate was isolated as a purple solid in quantitative yield. ^1H NMR (400 MHz, CDCl_3): $\delta = 7.99$ (d, $J = 8.9$ Hz, 1H), 7.88 (d, $J = 2.2$ Hz, 1H), 7.48-7.34 (m, 6H), 6.99 (brs, 1H), 5.22 (s, 2H). ^{13}C NMR (101 MHz, CDCl_3): $\delta = 153.0$,

⁹¹ Chrétien, M.; Zammattio, F.; Le Grogne, E.; Paris, M.; Cahingt, B.; Montavon, G.; Quintard, J.-P. *J. Org. Chem.* **2005**, *70*, 2870.

140.6, 137.6, 135.6, 132.2, 128.7, 128.6, 128.5, 121.1, 116.4, 77.2, 67.5. **HRMS (ESI-MS):** calcd for $C_{14}H_{10}BrINO_2$: 429.8945; found: 429.8931. **IR v (cm^{-1}):** 3298, 3059, 2944, 2895, 1683. **m.p.:** 130-131 °C.

Benzyl (4-bromo-2-vinylphenyl)carbamate (**1j**)



Following GP2, benzyl (4-bromo-2-vinylphenyl)carbamate was isolated as a white solid in 86% yield. **1H NMR (500 MHz, $CDCl_3$):** δ = 7.75 (brs, 1H), 7.50 (d, J = 2.3 Hz, 1H), 7.40-7.35 (m, 6H), 6.70 (dd, J = 17.3, 11.0 Hz, 1H), 6.59 (brs, 1H), 5.66 (dd, J = 17.3, 1.1 Hz, 1H), 5.45 (dd, J = 11.0, 1.1 Hz, 1H), 5.20 (s, 2H). **^{13}C NMR (126 MHz, $CDCl_3$):** δ = 153.4, 135.8, 133.6, 132.0, 131.4, 130.8, 129.7, 128.7, 128.6, 128.5, 128.4, 128.4, 119.7, 67.4. **HRMS (ESI-MS):** calcd for $C_{16}H_{13}BrNO_2$: 330.0135; found: 330.0140. **IR v (cm^{-1}):** 3282, 3062, 3032, 2950, 2924, 2897, 1683. **m.p.:** 120-121 °C.

Synthesis of Benzyl (4-(trifluoromethyl)-2-vinylphenyl)carbamate (**1k**):

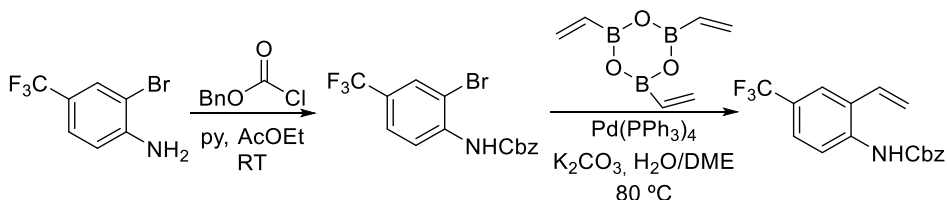
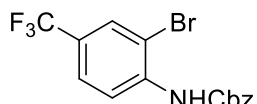


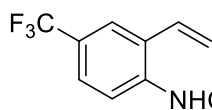
Figure 2.52 Synthesis of **1k**.

Benzyl (2-bromo-4-(trifluoromethyl)phenyl)carbamate



Following GP1, benzyl (2-bromo-4-(trifluoromethyl)phenyl)carbamate was isolated as a white solid in 40% yield. **1H NMR (400 MHz, $CDCl_3$):** δ = 8.36 (d, J = 8.7 Hz, 1H), 7.78 (d, J = 2.5 Hz, 1H), 7.57 (dd, J = 8.7, 2.4 Hz, 1H), 7.49-7.32 (m, 6H), 5.25 (s, 2H). **^{13}C NMR (101 MHz, $CDCl_3$):** δ = 152.7, 138.9, 135.4, 129.5 (q, $^3J_{C-F}$ = 3.8 Hz), 128.7, 128.7, 128.5, 126.1 (q, $^2J_{C-F}$ = 33.6 Hz), 125.6 (q, $^3J_{C-F}$ = 3.6 Hz), 123.2 (q, $^1J_{C-F}$ = 271.9 Hz), 119.4, 111.8, 67.8. **^{19}F NMR (376 MHz, $CDCl_3$):** δ = -62.18. **HRMS (ESI-MS):** calcd for $C_{15}H_{11}BrF_3NNaO_2$: 395.9831; found 395.9817. **IR v (cm^{-1}):** 3376, 3076, 3040, 1713. **m.p.:** 60-62 °C.

Benzyl (4-(trifluoromethyl)-2-vinylphenyl)carbamate (**1k**)



Following GP2, benzyl (4-(trifluoromethyl)-2-vinylphenyl)carbamate was isolated as a white solid in 66% yield. $^1\text{H NMR}$ (500 MHz, CDCl_3): δ = 8.11 (d, J = 8.5 Hz, 1H), 7.59 (s, 1H), 7.53 (dd, J = 8.7, 2.2 Hz, 1H), 7.45-7.34 (m, 5H), 6.82 (brs, 1H), 6.75 (dd, J = 17.4, 11.1 Hz, 1H), 5.71 (dd, J = 17.4, 1.0 Hz, 1H), 5.53 (dd, J = 11.1, 1.0 Hz, 1H), 5.23 (s, 2H). $^{13}\text{C NMR}$ (101 MHz, CDCl_3): δ = 153.1, 137.7, 135.6, 130.9, 128.7, 128.6, 128.5, 128.4, 126.0 (q, $^2J_{\text{C-F}}$ = 32.9 Hz), 125.5 (q, $^3J_{\text{C-F}}$ = 3.7 Hz), 124.1 (q, $^1J_{\text{C-F}}$ = 271.3 Hz), 124.4 (q, $^3J_{\text{C-F}}$ = 3.8 Hz), 120.6, 120.4, 67.6. $^{19}\text{F NMR}$ (376 MHz, CDCl_3): δ = -62.31. HRMS (ESI-MS): calcd for $\text{C}_{17}\text{H}_{14}\text{F}_3\text{NNaO}_2$: 344.0869; found 344.0876. IR (cm^{-1}): 3283, 3039, 2962, 2924, 1693. m.p.: 75-77 °C.

Synthesis of Benzyl (4-formyl-2-vinylphenyl)carbamate (**1l**) :

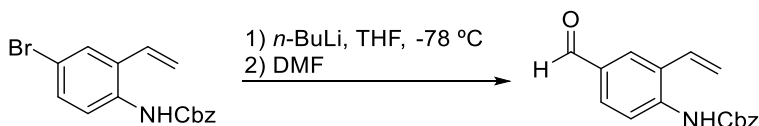
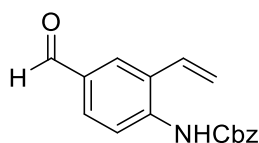


Figure 2.53 Synthesis of **1l**.

Benzyl (4-formyl-2-vinylphenyl)carbamate (**1l**)



To a deoxygenated solution of **1j** (300 mg, 0.904 mmol) in THF (10 mL), $n\text{-BuLi}$ (0.5 mL, 0.994 mmol) was added dropwise at -78 °C. After 30 minutes, DMF (0.08 mL, 0.994 mmol) was added dropwise at the same temperature, and the resulting reaction was stirred at room temperature until completion. The reaction was quenched with a saturated aqueous solution of NH_4Cl and extracted with Et_2O . The combined organic layers were dried over Na_2SO_4 and the solvent was removed. The crude was purified by column chromatography (silica gel, $n\text{-hexane}$ /ethyl acetate, 90/10, v/v) to obtain 100 mg (40% yield) of the title compound. $^1\text{H NMR}$ (400 MHz, CDCl_3): δ = 9.92 (s, 1H), 8.24 (d, J = 8.5 Hz, 1H), 7.86-7.84 (m, 1H), 7.80 (dd, J = 8.5, 2.0 Hz, 1H), 7.44-7.36 (m, 5H), 6.97 (brs, 1H), 6.76 (dd, J = 17.3, 11.0 Hz, 1H), 5.74 (dd, J = 17.3, 1.1 Hz, 1H), 5.55 (dd, J = 11.0, 1.1 Hz, 1H), 5.23 (s, 2H). $^{13}\text{C NMR}$ (101 MHz, CDCl_3): δ = 191.1, 152.8,

140.3, 135.5, 131.8, 130.9, 130.7, 128.9, 128.7, 128.7, 128.6, 128.4, 120.9, 119.5, 67.6.

HRMS (ESI-MS): calcd for $C_{17}H_{14}NO_3$: 280.0979; found: 280.0985. **IR ν (cm^{-1}):** 3234, 3035, 2922, 2840, 1733, 1671. **m.p.:** 84-85 °C.

Synthesis of Benzyl (4-acetyl-2-vinylphenyl)carbamate (**1m**):

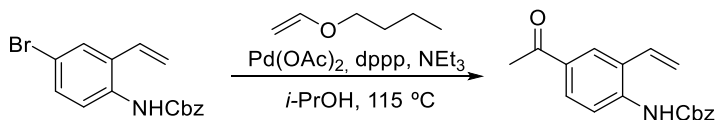
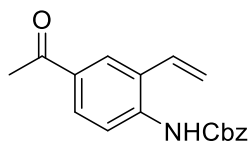


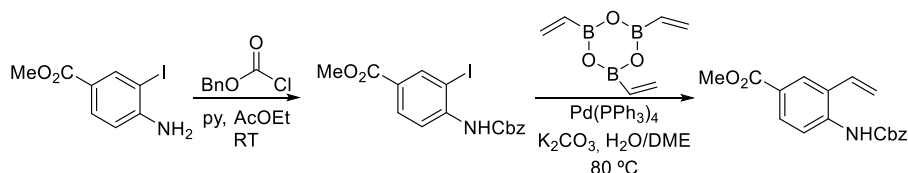
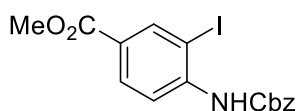
Figure 2.54 Synthesis of **1m**.

Benzyl (4-acetyl-2-vinylphenyl)carbamate (**1m**)



Benzyl (4-acetyl-2-vinylphenyl)carbamate was synthesized following a literature protocol.⁹² To a deoxygenated mixture of **1j** (300 mg, 0.906 mmol), $Pd(OAc)_2$ (8 mg, 0.036 mmol) and dppp (30 mg, 0.08 mmol) in *i*-PrOH (2 mL), Et_3N (0.31 mL, 2.267 mmol) and the corresponding olefin were sequentially added. The mixture was heated at 115 °C under argon until completion. The flask was then cooled to room temperature and an aqueous solution of HCl (5%) was added. The reaction was stirred for another 30 minutes. CH_2Cl_2 was added and the aqueous phase was extracted (2x10mL). The combined organic layers were washed with water and dried over Na_2SO_4 . Then solvent was removed and the crude was purified by column chromatography (silica gel, *n*-hexane/ethyl acetate, 90/10, v/v) to obtain 110 mg (41% yield) of the title compound. **1H NMR (500 MHz, $CDCl_3$):** δ = 8.11 (d, J = 8.6 Hz, 1H), 7.94 (d, J = 2.0 Hz, 1H), 7.86 (dd, J = 8.7, 1.6 Hz, 1H), 7.44-7.33 (m, 5H), 6.98 (brs, 1H), 6.76 (dd, J = 17.3, 11.0 Hz, 1H), 5.71 (dd, J = 17.3, 1.1 Hz, 1H), 5.51 (dd, J = 11.0, 1.1 Hz, 1H), 5.22 (s, 2H), 2.57 (s, 3H). **^{13}C NMR (126 MHz, $CDCl_3$):** δ = 197.0, 153.0, 139.1, 135.6, 132.5, 131.3, 129.1, 128.7, 128.6, 128.5, 128.1, 127.7, 120.3, 119.4, 67.5, 26.4. **HRMS (ESI-MS):** calcd for $C_{18}H_{16}NO_3$: 294.1136; found: 294.1136. **IR ν (cm^{-1}):** 3313, 2998, 1699, 1676. **m.p.:** 104-106 °C.

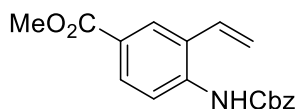
⁹² Hyder, Z.; Ruan, J.; Xiao, J. *Chem. Eur. J.* **2008**, *14*, 5555.

Synthesis of Methyl 4-(((benzyloxy)carbonyl)amino)-3-vinylbenzoate (1n):**Figure 2.55** Synthesis of **1n**.**Methyl 4-(((benzyloxy)carbonyl)amino)-3-iodobenzoate**

Following GP1, methyl 4-(((benzyloxy)carbonyl)amino)-3-iodobenzoate was isolated as a white solid in 99% yield.

¹H NMR (400 MHz, CDCl₃): δ = 8.44 (d, J = 1.9 Hz, 1H), 8.23 (d, J = 8.7 Hz, 1H), 8.00 (dd, J = 8.7, 1.9 Hz, 1H), 7.48-7.34

(m, 6H), 5.24 (s, 2H), 3.90 (s, 3H). **¹³C NMR (101 MHz, CDCl₃):** δ = 165.2, 152.8, 142.2, 140.4, 135.5, 130.9, 128.7, 128.6, 128.5, 126.3, 118.4, 87.1, 67.7, 52.2. **HRMS (ESI-MS):** calcd for C₁₆H₁₄INNaO₄: 433.9860; found: 433.9874. **IR v (cm⁻¹):** 3316, 2944, 1716, 1692. **m.p.:** 102-103 °C.

Methyl 4-(((benzyloxy)carbonyl)amino)-3-vinylbenzoate (1n)

Following GP2, methyl 4-(((benzyloxy)carbonyl)amino)-3-vinylbenzoate was isolated as a white solid in 81% yield.

¹H NMR (400 MHz, CDCl₃): δ = 8.09 (d, J = 8.5 Hz, 1H), 8.03 (d, J = 2.0 Hz, 1H), 7.95 (dd, J = 8.5, 2.0 Hz, 1H), 7.44-7.34 (m, 5H), 6.90 (brs, 1H), 6.75 (dd, J = 17.3, 11.0 Hz, 1H), 5.72 (dd, J = 17.3, 1.2 Hz, 1H), 5.50 (dd, J = 10.9, 1.1 Hz, 1H), 5.22 (s, 2H), 3.90 (s, 3H). **¹³C NMR (101 MHz, CDCl₃):** δ = 166.6, 153.0, 138.8, 135.6, 131.2, 130.1, 129.0, 128.7, 128.6, 128.5, 127.9, 125.2, 120.2, 119.5, 67.5, 52.0. **HRMS (ESI-MS):** calcd for C₁₈H₁₇NNaO₄: 334.1050; found: 334.1041. **IR v (cm⁻¹):** 3285, 2953, 1711, 1690. **m.p.:** 102-104 °C.

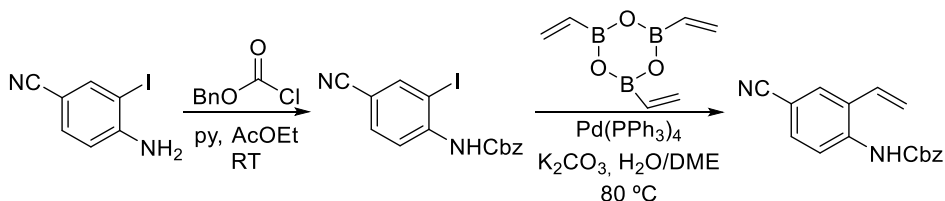
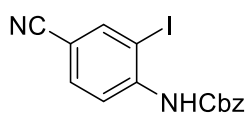
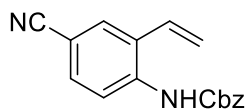
Synthesis of Benzyl (4-cyano-2-vinylphenyl)carbamate (1o):

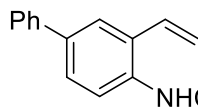
Figure 2.56 Synthesis of 1o.

Benzyl (4-cyano-2-iodophenyl)carbamate

Following GP1, benzyl (4-cyano-2-iodophenyl)carbamate was isolated as a non-separable mixture of protected and deprotected anilines. The crude mixture was therefore submitted directly to the next step.

Benzyl (4-cyano-2-vinylphenyl)carbamate (1o)

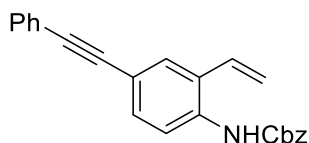
Following GP2, benzyl (4-cyano-2-vinylphenyl)carbamate was isolated as a pale yellow solid in 72% yield over two steps. ^1H NMR (400 MHz, CDCl_3): δ = 8.18 (d, J = 8.6 Hz, 1H), 7.59 (dd, J = 2.0, 0.6 Hz, 1H), 7.55 (dd, J = 8.6, 2.0 Hz, 1H), 7.46-7.33 (m, 5H), 6.90 (brs, 1H), 6.69 (dd, J = 17.3, 11.0 Hz, 1H), 5.69 (dd, J = 17.3, 1.0 Hz, 1H), 5.57 (dd, J = 11.0, 1.0 Hz, 1H), 5.22 (s, 2H). ^{13}C NMR (101 MHz, CDCl_3): δ = 152.8, 138.8, 135.4, 132.4, 131.4, 130.2, 128.7, 128.7, 128.6, 127.3, 121.6, 120.0, 118.8, 106.9, 67.7. HRMS (ESI-MS): calcd for $\text{C}_{17}\text{H}_{14}\text{N}_2\text{NaO}_2$: 301.0947; found: 301.0951. IR ν (cm^{-1}): 3292, 2228, 1692. m.p.: 96-98 °C.

Benzyl [3-vinyl-(1,1'-biphenyl)-4-yl]carbamate (1p)

Compound **1j** (331 mg, 1 mmol) and $\text{PdCl}_2(\text{PPh}_3)_2$ (35 mg, 0.05 mmol) were placed in a Schlenk flask under argon and DMF (5 mL) was added. Then K_2CO_3 (166 mg, 1.2 mmol) dissolved in water (1 mL) and phenyl boronic acid (147 mg, 1.2 mmol) were added subsequently. The mixture was stirred at 80 °C for 24 hours. The reaction was quenched with an aqueous solution of HCl (10%) and extracted with ethyl acetate (3x10 mL). The combined organic layers were dry over Na_2SO_4 and solvent was removed under vacuo. The crude was

purified by column chromatography (silica gel, *n*-hexane/ethyl acetate, 95/5, v/v). The corresponding benzyl [3-vinyl- (1,1'-biphenyl) -4-yl]carbamate was isolated as a white solid in 82% yield (271 mg). **¹H NMR (400 MHz, CDCl₃):** δ = 7.92 (s, 1H), 7.62-7.56 (m, 3H), 7.52 (dd, *J* = 8.5, 2.3 Hz, 1H), 7.47-7.31 (m, 8H), 6.84 (dd, *J* = 17.4, 11.0 Hz, 1H), 6.67 (brs, 1H), 5.73 (dd, *J* = 17.4, 1.3 Hz, 1H), 5.46 (dd, *J* = 11.0, 1.3 Hz, 1H), 5.23 (s, 2H). **¹³C NMR (126 MHz, CDCl₃):** δ = 153.7, 140.5, 137.4, 136.1, 133.9, 132.1, 128.8, 128.7, 128.5, 128.4, 127.3, 127.3, 127.0, 127.0, 126.8, 125.7, 118.6, 67.33 **HRMS (ESI-MS):** calcd for C₂₂H₁₉NNaO₂: 352.1308; found: 352.1306. **IR v (cm⁻¹):** 3296, 1695. **m.p.:** 137-138 °C.

Benzyl (4-(phenylethynyl)-2-vinylphenyl)carbamate (1q)



Compound **1j** (200mg, 0.602 mmol), PdCl₂(PPh₃)₂ (21 mg, 0.030 mmol), CuI (6 mg, 0.030 mmol) and PPh₃ (16 mg, 0.060 mmol) were placed in a flamed-dried and argon filled flask. After addition of toluene (1 mL) and *i*Pr₂NH (0.2 mL), the reaction was stirred for 5 minutes and the alkyne (0.08 mL, 0.723 mmol) was added. After 2 hours, the reaction was quenched with an aqueous solution of HCl (10%) and the mixture was extracted with CH₂Cl₂ (2x15mL). The combined organic layers were dried over Na₂SO₄ and solvent was removed. The crude was purified by column chromatography (silica gel, *n*-hexane/ethyl acetate, 95/5, v/v). The title compound was isolated as a white solid in 85% yield (181 mg). **¹H NMR (400 MHz, CDCl₃):** δ = 8.00-7.90 (m, 1H), 7.55-7.52 (m, 3H), 7.46 (dd, *J* = 8.4, 2.0 Hz, 1H), 7.44-7.32 (m, 8H), 6.79-6.69 (m, 2H), 5.70 (dd, *J* = 17.3, 1.2 Hz, 1H), 5.47 (dd, *J* = 11.0, 1.2 Hz, 1H), 5.22 (s, 2H). **¹³C NMR (126 MHz, CDCl₃):** δ = 153.3, 135.9, 134.7, 132.1, 131.8, 131.6, 131.3, 130.4, 128.7, 128.5, 128.4, 128.3, 128.2, 123.3, 120.7, 119.5, 118.9, 89.1, 89.0, 67.4. **HRMS (ESI-MS):** calcd for C₂₄H₁₉NNaO₂: 376.1308; found: 376.1310. **IR v (cm⁻¹):** 3285, 3060, 3029, 2946, 2894, 1954, 1687. **m.p.:** 133-134 °C.

Synthesis of Benzyl (5-methyl-2-vinylphenyl)carbamate (1r):

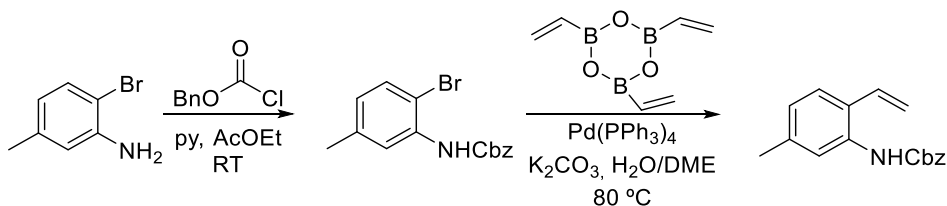
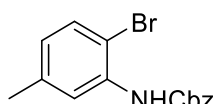


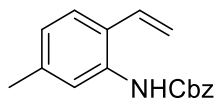
Figure 2.57 Synthesis of **1r**.

Benzyl (2-bromo-5-methylphenyl)carbamate



Following GP1, benzyl (2-bromo-5-methylphenyl)carbamate was isolated as a white solid in 92% yield. ¹H NMR (400 MHz, CDCl₃): δ = 8.01 (d, *J* = 2.2 Hz, 1H), 7.43-7.36 (m, 6H), 7.16 (brs, 1H), 6.75 (ddd, *J* = 8.2, 2.1, 0.8 Hz, 1H), 5.23 (s, 2H), 2.33 (s, 3H). ¹³C NMR (101 MHz, CDCl₃): δ = 153.1, 138.7, 135.9, 135.3, 131.9, 128.7, 128.5, 128.4, 125.3, 120.8, 109.3, 67.3, 21.3. HRMS (ESI-MS): calcd for C₁₅H₁₄BrNNaO₂: 342.0100; found: 342.0104. IR ν (cm⁻¹): 3288, 3032, 2972, 1695, 1580. m.p.: 112-113 °C.

Benzyl (5-methyl-2-vinylphenyl)carbamate (1r)



Following GP2, benzyl (5-methyl-2-vinylphenyl)carbamate was isolated as a white solid in 68% yield. ¹H NMR (400 MHz, CDCl₃): δ = 7.67 (s, 1H), 7.50-7.35 (m, 5H), 7.32 (d, *J* = 8.0 Hz, 1H), 6.96 (d, *J* = 7.9 Hz, 1H), 6.78 (dd, *J* = 17.4, 11.0 Hz, 1H), 6.69 (brs, 1H), 5.64 (dd, *J* = 17.4, 1.2 Hz, 1H), 5.36 (dd, *J* = 11.0, 0.8 Hz, 1H), 5.24 (s, 2H), 2.37 (s, 3H). ¹³C NMR (126 MHz, CDCl₃): δ = 153.8, 138.7, 136.2, 134.3, 131.9, 128.7, 128.6, 128.5, 128.4, 126.7, 125.5, 122.5, 117.2, 67.1, 21.4. HRMS (ESI-MS): calcd for C₁₇H₁₇NNaO₂: 290.1151; found: 290.1159. IR ν (cm⁻¹): 3290, 3030, 2973, 2918, 1687. m.p.: 121-122 °C.

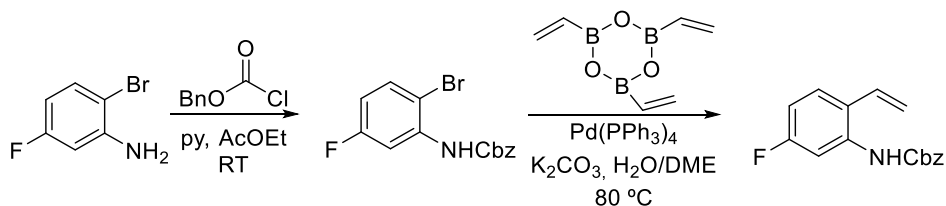
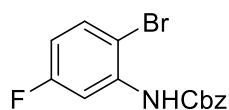
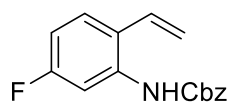
Synthesis of Benzyl (5-fluoro-2-vinylphenyl)carbamate (1s):

Figure 2.58 Synthesis of 1s.

Benzyl (2-bromo-5-fluorophenyl)carbamate

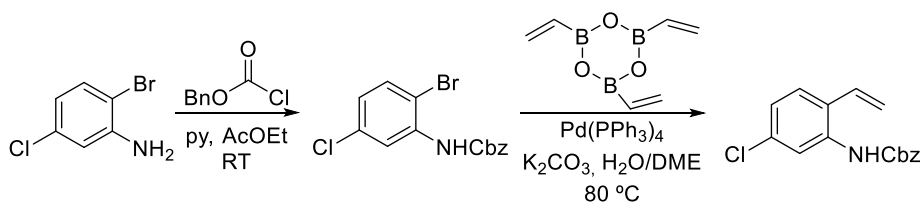
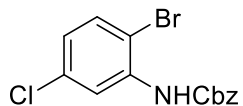
Following GP1, benzyl (2-bromo-5-fluorophenyl)carbamate was isolated as a white solid in 85% yield. $^1\text{H NMR}$ (400 MHz, CDCl_3):

$\delta = 8.05$ (dd, $J = 11.1, 3.0$ Hz, 1H), 7.50-7.34 (m, 6H), 7.25 (brs, 1H), 6.70 (ddd, $J = 8.8, 7.6, 3.0$ Hz, 1H), 5.24 (s, 2H). $^{13}\text{C NMR}$ (126 MHz, CDCl_3): $\delta = 162.4$ (d, $^1J_{\text{C-F}} = 245.4$ Hz) 152.7, 137.0 (d, $^3J_{\text{C-F}} = 12.0$ Hz), 135.5, 133.0 (d, $^3J_{\text{C-F}} = 9.3$ Hz), 128.7, 128.6, 128.5, 111.2 (d, $^2J_{\text{C-F}} = 23.2$ Hz), 107.5 (d, $^2J_{\text{C-F}} = 29.5$ Hz), 106.1 (d, $^4J_{\text{C-F}} = 3.4$ Hz), 67.6. $^{19}\text{F NMR}$ (376 MHz, CDCl_3): $\delta = -111.36$. HRMS (ESI-MS): calcd for $\text{C}_{14}\text{H}_{11}\text{BrFNNaO}_2$: 345.9849; found: 345.9839. IR ν (cm^{-1}): 3286, 3074, 3035, 1603, 1587. m.p.: 60-61 °C.

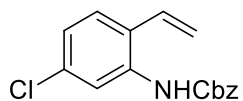
Benzyl (5-fluoro-2-vinylphenyl)carbamate (1s)

Following GP2, benzyl (5-fluoro-2-vinylphenyl)carbamate was isolated as a white solid in 87% yield. $^1\text{H NMR}$ (400 MHz, CDCl_3):

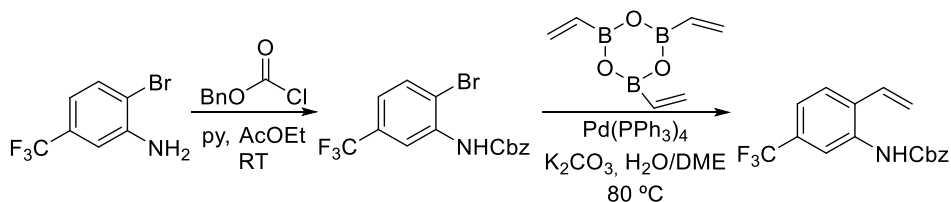
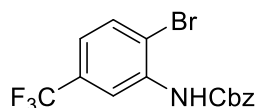
$\delta = 7.76$ (d, $J = 11.0$ Hz, 1H), 7.43-7.35 (m, 5H), 7.31-7.28 (m, 1H), 6.81-6.76 (m, 1H), 6.73 (brs, 1H), 6.72-6.66 (m, 1H), 5.59 (dd, $J = 17.4, 1.2$ Hz, 1H), 5.41 (dd, $J = 11.1, 1.2$ Hz, 1H), 5.21 (s, 2H). $^{13}\text{C NMR}$ (126 MHz, CDCl_3): $\delta = 162.7$ (d, $^1J_{\text{C-F}} = 245.7$ Hz), 153.1, 136.0 (d, $^3J_{\text{C-F}} = 11.4$ Hz), 135.8, 131.2, 128.7, 128.5, 128.5, 128.4, 128.4, 124.4, 118.7, 110.8 (d, $^2J_{\text{C-F}} = 20.1$ Hz), 67.4. $^{19}\text{F NMR}$ (376 MHz, CDCl_3): $\delta = -111.90$. HRMS (ESI-MS): calcd for $\text{C}_{16}\text{H}_{14}\text{FNNaO}_2$: 294.090; found: 294.0902. IR ν (cm^{-1}): 3277, 3079, 2982, 2957, 1686, 1627. m.p.: 111-112 °C.

Synthesis of Benzyl (5-chloro-2-vinylphenyl)carbamate (1t):**Figure 2.59** Synthesis of **1t**.**Benzyl (2-bromo-5-chlorophenyl)carbamate**

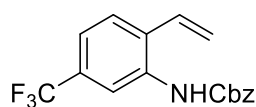
Following GP1, benzyl (2-bromo-5-chlorophenyl)carbamate was isolated as a white solid in 51% yield. **¹H NMR (400 MHz, CDCl₃):** δ = 8.28 (d, J = 2.5 Hz, 1H), 7.46-7.34 (m, 6H), 7.20 (brs, 1H), 6.92 (dd, J = 8.5, 2.5 Hz, 1H), 5.23 (s, 2H). **¹³C NMR (101 MHz, CDCl₃):** δ = 152.7, 136.7, 135.5, 134.4, 132.9, 128.7, 128.6, 128.5, 124.2, 120.0, 110.0, 67.6. **HRMS (ESI-MS):** calcd for C₁₄H₁₁BrClNNaO₂: 361.9554; found: 361.9561. **IR v (cm⁻¹):** 3295, 2922, 1693, 1572. **m.p.:** 120-122 °C.

Benzyl (5-chloro-2-vinylphenyl)carbamate (1t)

Following GP2, benzyl (5-chloro-2-vinylphenyl)carbamate was isolated as a white solid in 57% yield. **¹H NMR (400 MHz, CDCl₃):** δ = 7.97 (s, 1H), 7.44-7.35 (m, 5H), 7.28 (d, J = 8.3 Hz, 1H), 7.07 (dd, J = 8.3, 2.1 Hz, 1H), 6.74-6.67 (m, 2H), 5.64 (dd, J = 17.4, 1.2 Hz, 1H), 5.43 (dd, J = 11.0, 1.2 Hz, 1H), 5.22 (s, 2H). **¹³C NMR (126 MHz, CDCl₃):** δ = 153.3, 135.8, 135.5, 134.2, 131.1, 128.7, 128.5, 128.5, 128.3, 128.1, 124.3, 121.1, 119.0, 67.4. **HRMS (ESI-MS):** calcd for C₁₆H₁₄ClNNaO₂: 310.0605; found: 310.0609. **IR v (cm⁻¹):** 3288, 3066, 3029, 2955, 1686, 1567. **m.p.:** 130-131 °C.

Synthesis of Benzyl (5-(trifluoromethyl)-2-vinylphenyl)carbamate (1u):**Figure 2.60** Synthesis of **1u**.**Benzyl (2-bromo-5-(trifluoromethyl)phenyl)carbamate**

Following GP1, benzyl (2-bromo-5-(trifluoromethyl)phenyl)carbamate was isolated as a white solid in 60% yield. $^1\text{H NMR}$ (400 MHz, CDCl_3): δ = 8.54 (s, 1H), 7.63 (d, J = 8.3 Hz, 1H), 7.46-7.36 (m, 5H), 7.33 (brs, 1H), 7.19 (dd, J = 8.2, 1.9 Hz, 1H), 5.25 (s, 2H). $^{13}\text{C NMR}$ (126 MHz, CDCl_3): δ = 152.8, 136.5, 135.4, 132.8, 131.0 (q, $^2J_{\text{C-F}}$ = 33.0 Hz), 128.7, 128.6, 128.5, 123.6 (q, $^1J_{\text{C-F}}$ = 272.5 Hz), 120.6 (q, $^3J_{\text{C-F}}$ = 3.8 Hz), 116.8 (q, $^3J_{\text{C-F}}$ = 4.1 Hz), 115.6, 67.7. $^{19}\text{F NMR}$ (376 MHz, CDCl_3): δ = -62.99. **HRMS (ESI-MS)**: calcd for $\text{C}_{15}\text{H}_{11}\text{BrF}_3\text{NNaO}_2$: 395.9817; found: 395.9817. **IR v** (cm^{-1}): 3307, 1698, 1527. **m.p.**: 92-93 °C.

Benzyl (5-(trifluoromethyl)-2-vinylphenyl)carbamate (1u)

Following GP2, benzyl (5-(trifluoromethyl)-2-vinylphenyl)carbamate was isolated as a white solid in 87% yield. $^1\text{H NMR}$ (500 MHz, CDCl_3): δ = 8.23 (s, 1H), 7.55-7.30 (m, 7H), 6.80-6.74 (m, 2H), 5.73 (dd, J = 17.4, 1.1 Hz, 1H), 5.53 (dd, J = 11.1, 1.1 Hz, 1H), 5.23 (s, 2H). $^{13}\text{C NMR}$ (126 MHz, CDCl_3): δ = 153.3, 135.7, 135.0, 132.1, 131.0, 130.6 (q, $^2J_{\text{C-F}}$ = 32.6 Hz), 128.7, 128.6, 128.5, 127.6, 123.6 (q, $^1J_{\text{C-F}}$ = 272.3 Hz), 120.7, 120.6, 118.1, 67.5. $^{19}\text{F NMR}$ (376 MHz, CDCl_3): δ = -62.78. **HRMS (ESI-MS)**: calcd for $\text{C}_{17}\text{H}_{13}\text{F}_3\text{NO}_2$: 320.0904; found: 320.0909. **IR v** (cm^{-1}): 3279, 1693, 1530. **m.p.**: 107-108 °C.

Synthesis of Benzyl (5-(trifluoromethoxy)-2-vinylphenyl)carbamate (1v):

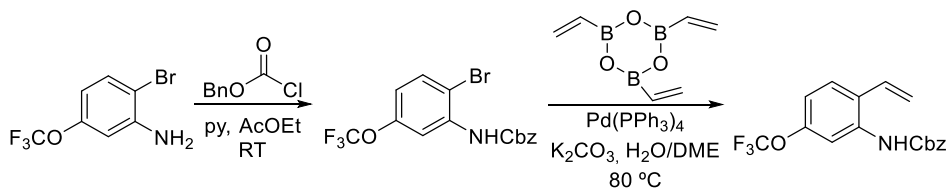
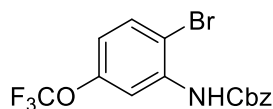


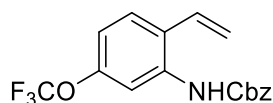
Figure 2.61 Synthesis of **1v**.

Benzyl (2-bromo-5-(trifluoromethoxy)phenyl)carbamate

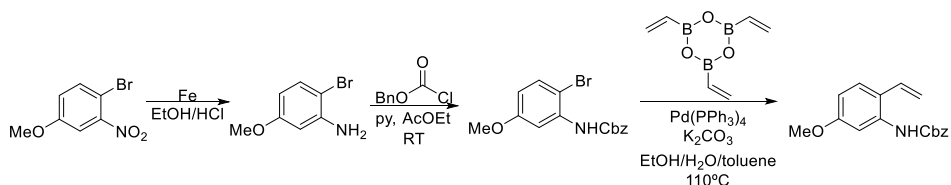
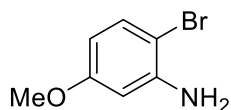


Following GP1, benzyl (2-bromo-5-(trifluoromethoxy)phenyl)carbamate was isolated as a white solid in 99% yield. ¹H NMR (500 MHz, CDCl₃): δ = 8.20 (d, *J* = 2.6 Hz, 1H), 7.52 (d, *J* = 8.8 Hz, 1H), 7.46-7.33 (m, 5H), 6.82 (d, *J* = 8.8, 1.6 Hz, 1H), 5.24 (s, 2H). ¹³C NMR (126 MHz, CDCl₃): δ = 152.7, 149.0 (q, ³*J*_{C-F} = 1.8 Hz), 137.1, 135.5, 132.9, 128.7, 128.6, 128.5, 120.3 (q, ¹*J*_{C-F} = 258.0 Hz), 116.3, 112.8, 109.5, 67.7. ¹⁹F NMR (376 MHz, CDCl₃): δ = -58.40. HRMS (ESI-MS): calcd for C₁₅H₁₁BrF₃NNaO₃: 411.9767; found: 411.9772. IR ν (cm⁻¹): 3334, 3036, 2957, 2895, 1704. m.p.: 66-67 °C.

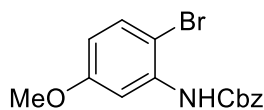
Benzyl (5-(trifluoromethoxy)-2-vinylphenyl)carbamate (1v)



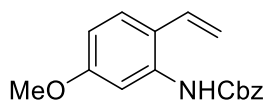
Following GP2, benzyl (5-(trifluoromethoxy)-2-vinylphenyl)carbamate was isolated as a white solid in 84% yield. ¹H NMR (400 MHz, CDCl₃): δ = 7.93 (s, 1H), 7.46-7.33 (m, 6H), 6.96 (ddd, *J* = 9.1, 2.7, 1.3 Hz, 1H), 6.79 (brs, 1H), 6.72 (dd, *J* = 17.4, 11.0 Hz, 1H), 5.65 (dd, *J* = 17.4, 1.0 Hz, 1H), 5.47 (dd, *J* = 11.0, 1.2 Hz, 1H), 5.23 (s, 2H). ¹³C NMR (101 MHz, CDCl₃): δ = 153.2, 149.1 (q, ³*J*_{C-F} = 1.9 Hz), 135.8, 135.7, 130.9, 128.7, 128.6, 128.5, 128.2, 127.1, 120.5 (q, ¹*J*_{C-F} = 257.4 Hz) 119.6, 116.2, 113.4, 67.5. ¹⁹F NMR (376 MHz, CDCl₃): δ = -58.13. HRMS (ESI-MS): calcd for C₁₇H₁₃F₃NO₃: 336.0853; found: 336.0860. IR ν (cm⁻¹): 3273, 1695, 1526. m.p.: 92-93 °C.

Synthesis of Benzyl (5-methoxy-2-vinylphenyl)carbamate (1w):**Figure 2.62** Synthesis of **1w**.**2-Bromo-5-methoxyaniline**

The compound was synthesized in 91% yield following the procedure described in the literature.⁸⁹ The NMR spectra match the literature data.⁸⁹

Benzyl (2-bromo-5-methoxyphenyl)carbamate

Following GP1, benzyl (2-bromo-5-methoxyphenyl)carbamate was isolated as a white solid in 63% yield. ¹H NMR (400 MHz, CDCl₃): δ = 7.87 (d, *J* = 2.8 Hz, 1H), 7.47-7.33 (m, 6H), 7.20 (brs, 1H), 6.52 (dd, *J* = 8.8, 3.0 Hz, 1H), 5.23 (s, 2H), 3.80 (s, 3H). ¹³C NMR (101 MHz, CDCl₃): δ = 159.7, 153.0, 136.5, 135.7, 132.4, 128.7, 128.5, 128.4, 111.0, 105.3, 102.7, 67.3, 55.6. HRMS (ESI-MS): calcd for C₁₅H₁₄BrNNaO₃: 358.0049; found: 358.0043. IR ν (cm⁻¹): 3298, 2941, 1700. m.p.: 70-73 °C.

Benzyl (5-methoxy-2-vinylphenyl)carbamate (1w)

Following GP2, benzyl (5-methoxy-2-vinylphenyl)carbamate was isolated as a white solid in 64% yield. ¹H NMR (500 MHz, CDCl₃): δ = 7.52 (s, 1H), 7.44-7.34 (m, 5H), 7.29 (d, *J* = 8.6 Hz, 1H), 6.74-6.63 (m, 3H), 5.55 (dd, *J* = 17.3, 1.3 Hz, 1H), 5.30 (dd, *J* = 10.9, 1.3 Hz, 1H), 5.21 (s, 2H), 3.81 (s, 3H). ¹³C NMR (126 MHz, CDCl₃): δ = 159.9, 153.5, 136.0, 135.6, 131.5, 128.6, 128.4, 128.4, 128.3, 127.9, 116.5, 115.7, 110.9, 67.2, 55.4. HRMS (ESI-MS): calcd for C₁₇H₁₇NNaO₃: 306.1101; found: 306.1106. IR ν (cm⁻¹): 3277, 3031, 2997, 2955, 2931, 2831, 1691. m.p.: 114-116 °C.

Synthesis of Methyl (4,5-dichloro-2-vinylphenyl)carbamate (**1x**):

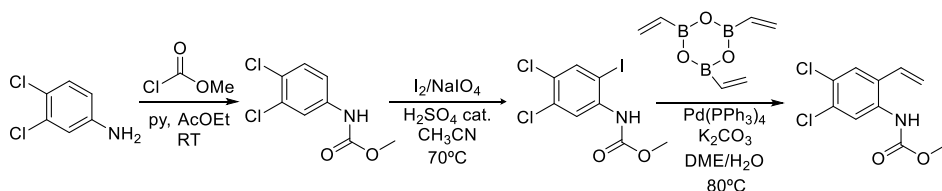
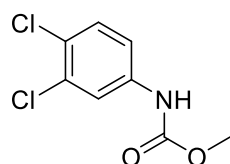


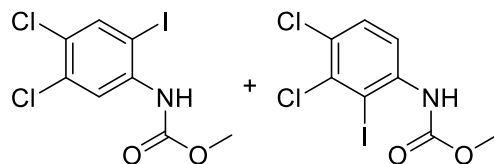
Figure 2.63 Synthesis of **1x**.

Methyl (3,4-dichlorophenyl)carbamate

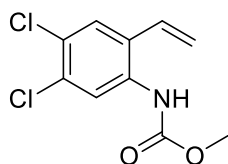


Following GP1, with the corresponding chloroformate, methyl (3,4-dichlorophenyl)carbamate was isolated as a white solid in 88% yield. $^1\text{H NMR}$ (500 MHz, CDCl_3): δ = 7.60 (d, J = 2.6 Hz, 1H), 7.35 (d, J = 8.7 Hz, 1H), 7.20 (dd, J = 8.8, 2.6 Hz, 1H), 6.65 (brs, 1H), 3.78 (s, 3H). $^{13}\text{C NMR}$ (126 MHz, CDCl_3): δ = 153.6, 137.4, 132.9, 130.5, 126.7, 120.3, 117.8, 52.6. **HRMS (ESI-MS)**: calcd for $\text{C}_8\text{H}_6\text{Cl}_2\text{NO}_2$: 217.9781; found: 217.9781. **IR v** (cm^{-1}): 3330, 3107, 3031, 2958, 1722, 1700, 1586. **m.p.**: 125-126 °C.

Methyl (4,5-dichloro-2-iodophenyl)carbamate



To a stirred solution of methyl (3,4-dichlorophenyl)carbamate (1.5 g, 6.82 mmol) in MeCN (15 mL) were added NaIO_4 (1.46 g, 6.82 mmol), I_2 (1.73 g, 6.82 mmol) and H_2SO_4 (0.36 μL , 0.68 mmol). The resulting solution was stirred during 2 days at room temperature. The reaction mixture was washed with water, saturated aqueous solution of $\text{Na}_2\text{S}_2\text{O}_3$ and saturated aqueous solution of brine. The organic layer was dried over magnesium sulfate and filtered. The solvent was removed under reduced pressure. The crude was purified by column chromatography (silicagel, *n*-hexane/ethyl acetate, 95/5, v/v) to obtain 0.76g (30% yield) of a mixture of a two iodinated compounds (1:0.08) as yellow solids. $^1\text{H NMR}$ (500 MHz, CDCl_3): δ = 8.25 (s, 1H), 7.80 (s, 1H), 6.92 (brs, 1H), 3.82 (s, 3H). $^{13}\text{C NMR}$ (101 MHz, CDCl_3): δ = 153.4, 138.9, 138.0, 133.6, 130.3, 127.4, 120.7, 85.2, 52.9. **HRMS (ESI-MS)**: calcd for $\text{C}_8\text{H}_5\text{Cl}_2\text{INO}_2$: 343.8748; found: 343.8747. **IR v** (cm^{-1}): 3326, 3101, 3000, 2949, 2832, 1699.

Methyl (4,5-dichloro-2-vinylphenyl)carbamate (1x)

Following GP2, methyl (4,5-dichloro-2-vinylphenyl)carbamate was isolated as a yellow solid in 46% yield. $^1\text{H NMR}$ (400 MHz, CDCl_3): δ = 7.98 (s, 1H), 7.40 (s, 1H), 6.72-6.54 (m, 2H), 5.65 (dd, J = 17.4, 0.9 Hz, 1H), 5.47 (dd, J = 11.0, 1.2 Hz, 1H), 3.77 (s, 3H). $^{13}\text{C NMR}$ (101 MHz, CDCl_3): δ = 153.9, 133.9, 132.0, 130.1, 129.0, 128.2, 127.7, 123.0, 119.9, 52.7. **HRMS (ESI-MS)**: calcd for $\text{C}_{10}\text{H}_8\text{Cl}_2\text{NO}_2$: 243.9938; found: 243.9939. **IR v** (cm^{-1}): 3237, 3009, 2956, 2846, 1711, 1690. **m.p.**: 117-118 °C.

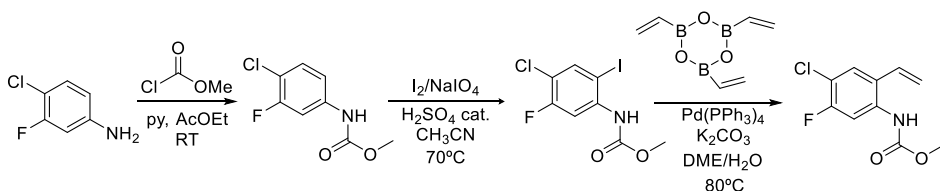
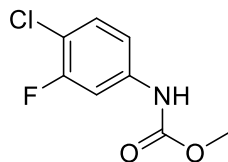
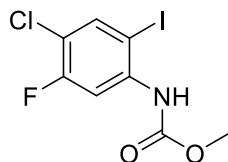
Synthesis of Methyl (4-chloro-5-fluoro-2-vinylphenyl)carbamate (1y):

Figure 2.64 Synthesis of 1y.

Methyl (4-chloro-3-fluorophenyl)carbamate

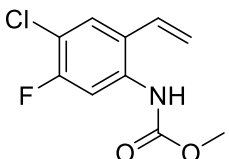
Following GP1, with the corresponding chloroformate, methyl (4-chloro-3-fluorophenyl)carbamate was isolated as a white solid in 95% yield. $^1\text{H NMR}$ (500 MHz, CDCl_3): δ = 7.48-7.40 (m, 1H), 7.31-7.23 (m, 1H), 7.02-6.96 (m, 1H), 6.84 (brs, 1H), 3.78 (s, 3H). $^{13}\text{C NMR}$ (101 MHz, CDCl_3): δ = 158.2 (d, $^1J_{\text{C-F}}$ = 247.1 Hz), 153.7, 138.0 (d, $^3J_{\text{C-F}}$ = 9.9 Hz), 130.5, 114.9 (d, $^2J_{\text{C-F}}$ = 18.0 Hz), 114.6, 107.2 (d, $^2J_{\text{C-F}}$ = 26.1 Hz), 52.6. $^{19}\text{F NMR}$ (376 MHz, CDCl_3): δ = -113.48. **HRMS (ESI-MS)**: calcd for $\text{C}_8\text{H}_6\text{ClFNO}_2$: 202.0077; found: 202.0072. **IR v** (cm^{-1}): 3355, 3100, 2994, 2956, 2850, 1742, 1708, 1609. **m.p.**: 115-117 °C.

Methyl (4-chloro-5-fluoro-2-iodophenyl)carbamate

This compound was synthesized following the procedure described for the methyl (4,5-dichloro-2-iodophenyl)carbamates. The product was isolated as a white solid in a 95% yield. $^1\text{H NMR}$ (500 MHz, CDCl_3): δ = 8.05 (d, J =

11.5 Hz, 1H), 7.75 (dd, $J = 7.7, 0.9$ Hz, 1H), 6.98 (brs, 1H), 3.82 (s, 3H). $^{13}\text{C NMR}$ (101 MHz, CDCl_3): $\delta = 158.5$ (d, $^1J_{\text{C-F}} = 248.6$ Hz), 153.4, 138.8, 138.5 (d, $^3J_{\text{C-F}} = 10.5$ Hz), 115.9 (d, $^2J_{\text{C-F}} = 19.0$ Hz), 107.9 (d, $^2J_{\text{C-F}} = 28.3$ Hz), 80.3, 52.9. $^{19}\text{F NMR}$ (376 MHz, CDCl_3): $\delta = -112.20$. **HRMS (APCI-MS)**: calcd for $\text{C}_8\text{H}_5\text{ClFINO}_2$: 327.9043; found: 327.9044. **IR v (cm^{-1})**: 3365, 3094, 3023, 2961, 2924, 2852, 1731, 1577. **m.p.**: 87-89 °C.

Methyl (4-chloro-5-fluoro-2-vinylphenyl)carbamate (**1y**)

 Following GP2, methyl (4-chloro-5-fluoro-2-vinylphenyl)carbamate was isolated as a white solid in a 68% yield. $^1\text{H NMR}$ (500 MHz, CDCl_3): $\delta = 7.82$ (m, 1H), 7.34 (d, $J = 7.9$ Hz, 1H), 6.72-6.57 (m, 2H), 5.61 (dd, $J = 17.4, 1.0$ Hz, 1H), 5.47 (dd, $J = 10.9, 1.0$ Hz, 1H), 3.79 (s, 3H). $^{13}\text{C NMR}$ (101 MHz, CDCl_3): $\delta = 157.5$ (d, $^1J_{\text{C-F}} = 248.1$ Hz), 153.7, 134.5 (d, $^3J_{\text{C-F}} = 10.0$ Hz), 130.1, 128.5, 125.6, 119.6, 115.7 (d, $^2J_{\text{C-F}} = 18.4$ Hz), 109.1 (d, $^2J_{\text{C-F}} = 26.9$ Hz), 52.7. $^{19}\text{F NMR}$ (376 MHz, CDCl_3): $\delta = -114.14$. **HRMS (ESI-MS)**: calcd for $\text{C}_{10}\text{H}_9\text{ClFINNaO}_2$: 252.0198; found: 252.0197. **IR v (cm^{-1})**: 3239, 3108, 3052, 3012, 2958, 2850, 1869, 1713, 1693. **m.p.**: 76-77 °C.

Synthesis of Methyl (3-methyl-2-vinylphenyl)carbamate (**1z**):

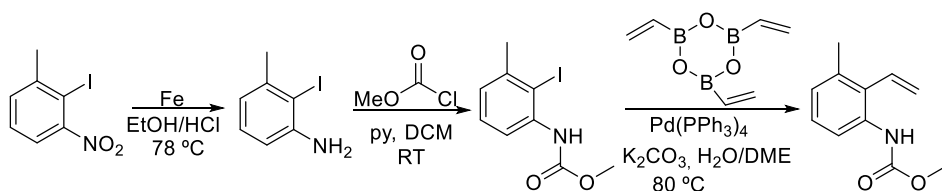
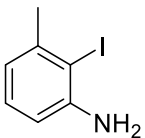
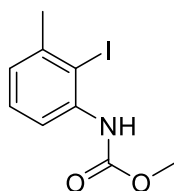


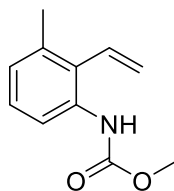
Figure 2.65 Synthesis of **1z**.

2-Iodo-3-methylaniline

 The compound was synthesized in 85% yield as a brown solid, following the procedure described in the literature.⁸⁹ $^1\text{H NMR}$ (500 MHz, CDCl_3): $\delta = 7.02$ (td, $J = 7.6, 1.5$ Hz, 1H), 6.65 (d, $J = 7.3$ Hz, 1H), 6.58 (d, $J = 7.9$ Hz, 1H), 4.18 (brs, 2H), 2.43 (s, 3H). $^{13}\text{C NMR}$ (126 MHz, CDCl_3): $\delta = 147.1, 142.4, 128.5, 119.6, 111.9, 91.5, 29.3$. **HRMS (ESI-MS)**: calcd for $\text{C}_7\text{H}_9\text{IN}$: 233.9774; found: 233.9772. **IR v (cm^{-1})**: 3393, 3295, 3188. **m.p.**: 43-44 °C.

Methyl (2-iodo-3-methylphenyl)carbamate

Following GP1, with the corresponding chloroformate, methyl (2-iodo-3-methylphenyl)carbamate was isolated as colorless solid in 77% yield. $^1\text{H NMR}$ (400 MHz, CDCl_3): δ = 7.83 (d, J = 8.2 Hz, 1H), 7.22 (t, J = 7.8 Hz, 1H), 7.13 (brs, 1H), 7.01-6.96 (m, 1H), 3.80 (s, 3H), 2.47 (s, 3H). $^{13}\text{C NMR}$ (101 MHz, CDCl_3): δ = 154.0, 142.3, 138.5, 128.6, 124.9, 117.7, 96.7, 52.5, 29.7. **HRMS (ESI-MS)**: calcd for $\text{C}_9\text{H}_{10}\text{INNaO}_2$: 313.9648; found: 313.9656. **IR ν (cm^{-1})**: 3433, 3387, 3004, 2948, 1720. **m.p.**: 78-80 °C.

Methyl (3-methyl-2-vinylphenyl)carbamate (1z)

Following GP2, methyl (3-methyl-2-vinylphenyl)carbamate was isolated as yellow oil in 44% yield. $^1\text{H NMR}$ (400 MHz, CDCl_3): δ = 7.90 (d, J = 8.4 Hz, 1H), 7.17 (t, J = 7.9 Hz, 1H), 6.99 (brs, 1H), 6.92 (dd, J = 6.6, 0.9 Hz, 1H), 6.61 (dd, J = 18.1, 11.4 Hz, 1H), 5.70 (dd, J = 11.5, 1.8 Hz, 1H), 5.41 (dd, J = 18.1, 1.9 Hz, 1H), 3.76 (s, 3H), 2.25 (s, 3H). $^{13}\text{C NMR}$ (126 MHz, CDCl_3): δ = 154.0, 136.4, 134.8, 132.8, 127.7, 127.6, 124.8, 121.8, 117.0, 52.2, 20.5. **HRMS (ESI-MS)**: calcd for $\text{C}_{11}\text{H}_{14}\text{NO}_2$: 192.1019; found: 192.1022. **IR ν (cm^{-1})**: 3419, 2951, 1734.

Characterization of indole products: The NMR spectra of benzyl 1*H*-indole-1-carboxylate **2a**,⁹⁰ 1-(methoxycarbonyl)indole **2b**,⁹³ (9*H*-fluoren-9-yl)methyl 1*H*-indole-1-carboxylate **2c**,⁹⁴ *N*-benzoylindole **2d**,⁹⁵ *tert*-butyl 1*H*-indole-1-carboxylate **2e**⁹⁶ and 1-tosyl-1*H*-indole,⁹⁶ match the literature data.

Gram scale-synthesis of indole 2a

The cyclization of the model compound was carried out on a 5gram-scale. PhIO (4.8g, 21.74 mmol) and 2,4,5-tris-*iso*-propylbenzenesulfonic acid (6.2 g, 21.74 mmol) were added to a stirred solution of the starting material **1a** (5 g, 19.8 mmol) in CHCl_3 (240 mL). After 30 minutes, solvent was directly removed under reduced pressure. The crude was dissolved in dichloromethane and the solid was filtered off. The crude was adsorbed on

⁹³ Shieh, W.-C.; Dell, S.; Bach, A.; Repic, O.; Blacklock, T. J. *J. Org. Chem.* **2003**, *68*, 1954.

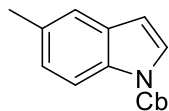
⁹⁴ Hsu, H.-C.; Hou, D.-R. *Tetrahedron Lett.* **2009**, *50*, 7169.

⁹⁵ Kirchberg, S.; Fröhlich, R.; Studer, A. *Angew. Chem. Int. Ed.* **2009**, *48*, 4235.

⁹⁶ Kim, J.; Kim, H.; Chang, S. *Org. Lett.* **2012**, *14*, 3924.

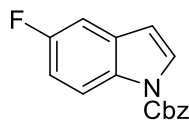
silica gel and purified by column chromatography (silica gel, *n*-hexane/ethyl acetate, 98/2, v/v) to obtain 3.89 g of indole **2a** as a colorless oil in 78% yield.

Benzyl 5-methyl-1*H*-indole-1-carboxylate (**2g**)



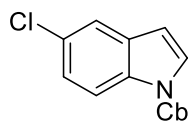
Following GP3, benzyl 5-methyl-1*H*-indole-1-carboxylate was isolated as a white solid in 79% yield. $^1\text{H NMR}$ (400 MHz, CDCl_3): δ = 8.05 (s, 1H), 7.60 (d, J = 2.7 Hz, 1H), 7.50-7.35 (m, 6H), 7.14 (d, J = 8.5 Hz, 1H), 6.53 (dd, J = 3.8, 1.2 Hz, 1H), 5.45 (s, 2H), 2.44 (s, 3H). $^{13}\text{C NMR}$ (101 MHz, CDCl_3): δ = 135.2, 132.5, 130.8, 128.8, 128.7, 128.6, 128.4, 128.3, 125.9, 125.6, 120.9, 114.8, 108.0, 68.6, 21.3. **HRMS (ESI-MS)**: calcd for $\text{C}_{17}\text{H}_{15}\text{NNaO}_2$: 288.0995; found: 288.0997. **IR** ν (cm^{-1}): 2922, 1719, 1393. **m.p.**: 44-46 °C.

Benzyl 5-fluoro-1*H*-indole-1-carboxylate (**2h**)

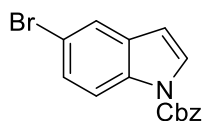


Following GP3, benzyl 5-fluoro-1*H*-indole-1-carboxylate was isolated as a solid in 74% yield. $^1\text{H NMR}$ (400 MHz, CDCl_3): δ = 8.13 (s, 1H), 7.67 (d, J = 3.8 Hz, 1H), 7.49 (dd, J = 8.0, 1.8 Hz, 2H), 7.46-7.38 (m, 3H), 7.22 (dd, J = 8.8, 2.6 Hz, 1H), 7.05 (td, J = 9.1, 2.6 Hz, 1H), 6.55 (dd, J = 3.8, 0.7 Hz, 1H), 5.45 (s, 2H). $^{13}\text{C NMR}$ (126 MHz, CDCl_3): δ = 159.4 (d, $^1J_{\text{C-F}}$ = 239.3 Hz), 150.7, 135.0, 131.6, 131.4 (d, $^3J_{\text{C-F}}$ = 10.3 Hz), 128.8, 128.5, 127.1, 116.1 (d, $^3J_{\text{C-F}}$ = 9.2 Hz), 112.3 (d, $^2J_{\text{C-F}}$ = 25.1 Hz), 107.9, 107.9, 106.5 (d, $^2J_{\text{C-F}}$ = 23.9 Hz), 68.7. $^{19}\text{F NMR}$ (376 MHz, CDCl_3): δ = -120.67. **HRMS (ESI-MS)**: calcd for $\text{C}_{16}\text{H}_{13}\text{FNO}_2$: 294.0925; found: 294.0914. **m.p.**: 50-51 °C.

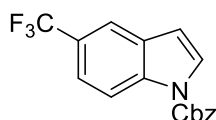
Benzyl 5-chloro-1*H*-indole-1-carboxylate (**2i**)



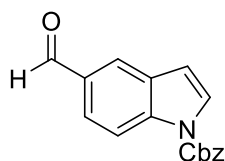
Following GP3, benzyl 5-chloro-1*H*-indole-1-carboxylate was isolated as a solid in 59% yield. $^1\text{H NMR}$ (500 MHz, CDCl_3): δ = 8.10 (d, J = 8.2 Hz, 1H), 7.65 (d, J = 3.8 Hz, 1H), 7.53 (d, J = 2.1 Hz, 1H), 7.51-7.38 (m, 5H), 7.27 (dd, J = 8.9, 2.2 Hz, 1H), 6.53 (dd, J = 3.8, 0.8 Hz, 1H), 5.45 (s, 2H). $^{13}\text{C NMR}$ (126 MHz, CDCl_3): δ = 150.6, 134.9, 133.6, 131.7, 128.9, 128.8, 128.7, 128.5, 126.8, 124.7, 120.6, 116.2, 107.5, 69.0. **HRMS (ESI-MS)**: calcd for $\text{C}_{16}\text{H}_{13}\text{ClNO}_2$: 286.0629; found: 286.0617. **IR** ν (cm^{-1}): 3149, 3110, 3068, 3038, 2962, 1731. **m.p.**: 67-69 °C.

Benzyl 5-bromo-1*H*-indole-1-carboxylate (2j)

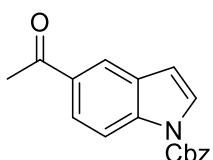
Following GP3, benzyl 5-bromo-1*H*-indole-1-carboxylate was isolated as a solid in 57% yield. $^1\text{H NMR}$ (500 MHz, CDCl_3): δ = 8.06 (d, J = 7.1 Hz, 1H), 7.69 (d, J = 1.9 Hz, 1H), 7.63 (d, J = 3.8 Hz, 1H), 7.50-7.47 (m, 2H), 7.45-7.38 (m, 4H), 6.53 (dd, J = 3.8, 0.8 Hz, 1H), 5.45 (s, 2H). $^{13}\text{C NMR}$ (126 MHz, CDCl_3): δ = 150.6, 134.8, 134.0, 132.2, 128.9, 128.8, 128.5, 127.4, 126.7, 123.7, 116.6, 116.4, 107.4, 69.0. **HRMS (ESI-MS)**: calcd for $\text{C}_{16}\text{H}_{12}\text{BrNNaO}_2$: 351.9944; found: 351.9930. **IR v** (cm^{-1}): 3038, 1728. **m.p.**: 73-74 °C.

Benzyl 5-(trifluoromethyl)-1*H*-indole-1-carboxylate (2k)

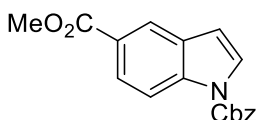
Following GP3, benzyl 5-(trifluoromethyl)-1*H*-indole-1-carboxylate was isolated as a solid in 51% yield. $^1\text{H NMR}$ (400 MHz, CDCl_3): δ = 8.29 (d, J = 8.7 Hz, 1H), 7.85 (s, 1H), 7.73 (d, J = 3.8 Hz, 1H), 7.57 (dd, J = 8.7, 1.8 Hz, 1H), 7.54-7.35 (m, 5H), 6.67 (d, J = 3.7 Hz, 1H), 5.48 (s, 2H). $^{13}\text{C NMR}$ (101 MHz, CDCl_3): δ = 150.5, 136.8, 134.7, 130.2, 128.9, 128.8, 128.6, 127.2, 125.5 (q, $^2J_{\text{C-F}}$ = 32.3 Hz), 124.7 (d, $^1J_{\text{C-F}}$ = 269.6 Hz), 121.3 (q, $^3J_{\text{C-F}}$ = 3.6 Hz), 118.4 (q, $^3J_{\text{C-F}}$ = 4.1 Hz), 115.5, 108.2, 69.2. $^{19}\text{F NMR}$ (376 MHz, CDCl_3): δ = -61.21. **HRMS (ESI-MS)**: calcd for $\text{C}_{17}\text{H}_{13}\text{F}_3\text{NO}_2$: 320.0893; found: 320.0886. **IR v** (cm^{-1}): 2965, 1736. **m.p.**: 69-71 °C.

Benzyl 5-formyl-1*H*-indole-1-carboxylate (2l)

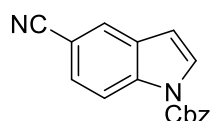
Following GP3, benzyl 5-formyl-1*H*-indole-1-carboxylate was isolated as a solid in 42% yield. $^1\text{H NMR}$ (400 MHz, CDCl_3): δ = 10.06 (s, 1H), 8.33 (d, J = 8.6 Hz, 1H), 8.10 (s, 1H), 7.86 (dt, J = 8.7, 1.2 Hz, 1H), 7.73 (d, J = 3.7 Hz, 1H), 7.51-7.40 (m, 2H), 7.45-7.39 (m, 3H), 6.71 (d, J = 3.3 Hz, 1H), 5.48 (s, 2H). $^{13}\text{C NMR}$ (101 MHz, CDCl_3): δ = 192.0, 150.5, 138.8, 134.6, 132.1, 130.7, 129.0, 128.9, 128.6, 127.3, 125.6, 124.1, 115.7, 108.7, 69.3. **HRMS (ESI-MS)**: calcd for $\text{C}_{17}\text{H}_{13}\text{NNaO}_3$: 302.0788; found: 302.0787. **IR v** (cm^{-1}): 3140, 2989, 2924, 1738, 1684. **m.p.**: 70-71 °C.

Benzyl 5-acetyl-1*H*-indole-1-carboxylate (2m)

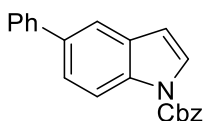
Following GP3, benzyl 5-acetyl-1*H*-indole-1-carboxylate was isolated as a solid in 70% yield. **¹H NMR (400 MHz, CDCl₃):** δ = 8.23 (d, J = 8.8 Hz, 1H), 8.20 (d, J = 1.7 Hz, 1H), 7.95 (dd, J = 8.7, 1.8 Hz, 1H), 7.69 (d, J = 3.8 Hz, 1H), 7.49 (dd, J = 7.9, 1.8 Hz, 2H), 7.48-7.39 (m, 3H), 6.68 (dd, J = 3.8, 0.7 Hz, 1H), 5.47 (s, 2H), 2.66 (s, 3H). **¹³C NMR (101 MHz, CDCl₃):** δ = 197.8, 150.6, 137.9, 134.7, 132.6, 130.4, 128.9, 128.8, 128.6, 127.0, 124.8, 122.1, 115.0, 108.8, 69.1, 26.7. **HRMS (ESI-MS):** calcd for C₁₈H₁₆NO₃: 294.1125; found: 294.1114. **IR ν (cm⁻¹):** 3163, 2955, 1720, 1669. **m.p.:** 68-69 °C

1-Benzyl 5-methyl 1*H*-indole-1,5-dicarboxylate (2n)

Following GP3, 1-benzyl 5-methyl 1*H*-indole-1,5-dicarboxylate was isolated as a solid in 81% yield. **¹H NMR (400 MHz, CDCl₃):** δ = 8.29 (d, J = 1.2 Hz, 1H), 8.22 (d, J = 8.5 Hz, 1H), 8.02 (dd, J = 8.8, 1.7 Hz, 1H), 7.68 (d, J = 3.7 Hz, 1H), 7.49 (dd, J = 7.9, 1.7 Hz, 2H), 7.47-7.36 (m, 3H), 6.66 (d, J = 3.8 Hz, 1H), 5.47 (s, 2H), 3.94 (s, 3H). **¹³C NMR (101 MHz, CDCl₃):** δ = 167.4, 150.6, 137.9, 134.8, 130.3, 128.9, 128.8, 128.6, 126.8, 125.9, 125.1, 123.3, 114.9, 108.6, 69.1, 52.1. **HRMS (ESI-MS):** calcd for C₁₈H₁₅NNaO₄: 332.0893; found: 332.0898. **IR ν (cm⁻¹):** 2987, 1746, 1708. **m.p.:** 86-87 °C.

Benzyl 5-cyano-1*H*-indole-1-carboxylate (2o)

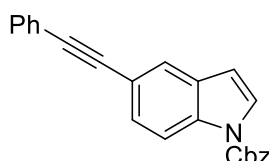
Following GP3, benzyl 5-cyano-1*H*-indole-1-carboxylate was isolated as a pale yellow solid in 40% yield. **¹H NMR (400 MHz, CDCl₃):** δ = 8.28 (d, J = 7.8 Hz, 1H), 7.89 (d, J = 1.7 Hz, 1H), 7.74 (d, J = 3.8 Hz, 1H), 7.60-7.53 (m, 1H), 7.49 (dd, J = 7.8, 1.9 Hz, 2H), 7.46-7.40 (m, 3H), 6.65 (dd, J = 3.7, 0.8 Hz, 1H), 5.48 (s, 2H). **¹³C NMR (101 MHz, CDCl₃):** δ = 150.3, 137.1, 134.5, 130.5, 129.0, 128.9, 128.7, 127.7, 125.8, 119.6, 116.1, 116.0, 107.8, 106.6, 69.4. **HRMS (ESI-MS):** calcd for C₁₇H₁₂N₂NaO₂: 299.0791; found: 299.0805. **IR ν (cm⁻¹):** 3150, 3118, 2961, 2924, 2222, 1741. **m.p.:** 86-88 °C.

Benzyl 5-phenyl-1*H*-indole-1-carboxylate (2p)

Following GP3, benzyl 5-phenyl-1*H*-indole-1-carboxylate was isolated as a solid in 63% yield. **¹H NMR (400 MHz, CDCl₃):** δ = 8.25 (d, J = 8.4 Hz, 1H), 7.78 (s, 1H), 7.71-7.63 (m, 3H), 7.58 (dt, J = 8.8, 1.7 Hz, 1H), 7.55-7.49 (m, 2H), 7.49-7.33 (m, 6H), 6.66 (d, J = 3.7 Hz, 1H), 5.49 (s, 2H). **¹³C**

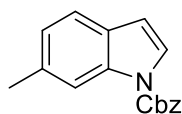
NMR (101 MHz, CDCl₃): δ = 150.9, 141.5, 136.5, 135.1, 134.7, 131.1, 128.8, 128.8, 128.7, 128.5, 127.4, 126.9, 126.1, 124.1, 119.5, 115.4, 108.5, 68.8. **HRMS (ESI-MS):** calcd for C₂₂H₁₇NNaO₂: 350.1151; found: 350.1150. **IR v (cm⁻¹):** 3033, 2958, 2925, 1737. **m.p.:** 82-84 °C.

Benzyl 5-(phenylethynyl)-1H-indole-1-carboxylate (2q)



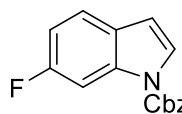
Following GP3, benzyl 5-(phenylethynyl)-1H-indole-1-carboxylate was isolated as a solid in 69% yield. **¹H NMR (400 MHz, CDCl₃):** δ = 8.17 (d, J = 8.2 Hz, 1H), 7.76 (dd, J = 1.4, 0.8 Hz, 1H), 7.66 (d, J = 3.8 Hz, 1H), 7.55 (dd, J = 7.9, 1.6 Hz, 2H), 7.50 (dt, J = 7.8, 1.8 Hz, 2H), 7.46-7.39 (m, 2H), 7.39-7.30 (m, 5H), 6.59 (dd, J = 3.8, 0.8 Hz, 1H), 5.47 (s, 2H). **¹³C NMR (101 MHz, CDCl₃):** δ = 150.7, 134.9, 134.8, 131.6, 130.5, 128.8, 128.8, 128.5, 128.3, 128.1, 128.1, 126.4, 124.5, 123.5, 117.9, 115.2, 108.0, 89.9, 88.3, 68.9. **HRMS (ESI-MS):** calcd for C₂₄H₁₇NNaO₂: 374.1151; found: 374.1147. **IR v (cm⁻¹):** 3038, 2924, 2208, 1731. **m.p.:** 129-130 °C.

Benzyl 6-methyl-1H-indole-1-carboxylate (2r)

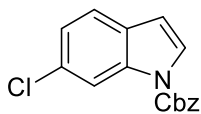


Following GP3, benzyl 6-methyl-1H-indole-1-carboxylate was isolated as a solid in 75% yield. **¹H NMR (400 MHz, CDCl₃):** δ = 8.06 (s, 1H), 7.56 (d, J = 3.7 Hz, 1H), 7.50 (d, J = 7.2 Hz, 2H), 7.47-7.37 (m, 4H), 7.09 (d, J = 7.9 Hz, 1H), 6.55 (d, J = 3.7 Hz, 1H), 5.46 (s, 2H), 2.49 (s, 3H). **¹³C NMR (126 MHz, CDCl₃):** δ = 150.9, 135.7, 135.2, 134.6, 128.8, 128.7, 128.4, 128.2, 124.9, 124.5, 120.6, 115.4, 108.1, 68.6, 21.9. **HRMS (ESI-MS):** calcd for C₁₇H₁₅NNaO₂: 288.0995; found: 290.1000. **IR v (cm⁻¹):** 2921, 1729. **m.p.:** 66-67 °C.

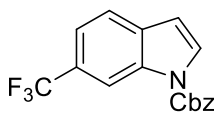
Benzyl 6-fluoro-1H-indole-1-carboxylate (2s)



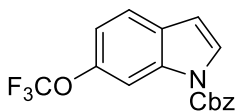
Following GP3, benzyl 6-fluoro-1H-indole-1-carboxylate was isolated as a white solid in 75% yield. **¹H NMR (500 MHz, CDCl₃):** δ = 7.93 (d, J = 8.8 Hz, 1H), 7.61 (d, J = 3.8 Hz, 1H), 7.53-7.37 (m, 6H), 7.01 (td, J = 8.9, 2.4 Hz, 1H), 6.56 (dd, J = 3.9, 0.8 Hz, 1H), 5.46 (s, 2H). **¹³C NMR (126 MHz, CDCl₃):** δ = 161.0 (d, $^1J_{C-F}$ = 240.4 Hz), 150.6, 135.5 (d, $^3J_{C-F}$ = 14.3 Hz), 134.9, 128.8, 128.8, 128.5, 126.7, 125.8, 121.6 (d, $^3J_{C-F}$ = 10.0 Hz), 111.3 (d, $^2J_{C-F}$ = 24.2 Hz), 107.9, 102.6 (d, $^2J_{C-F}$ = 28.6 Hz), 68.9. **¹⁹F NMR (376 MHz, CDCl₃):** δ = -117.13. **HRMS (ESI-MS):** calcd for C₁₆H₁₃FNO₂: 270.0925; found: 270.0925. **IR v (cm⁻¹):** 2959, 1735. **m.p.:** 50-51 °C.

Benzyl 6-chloro-1H-indole-1-carboxylate (2t)

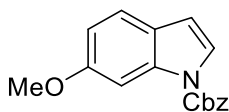
Following GP3, benzyl 6-chloro-1H-indole-1-carboxylate was isolated as a solid in 48% yield. $^1\text{H NMR}$ (500 MHz, CDCl_3): δ = 8.24 (s, 1H), 7.61 (d, J = 3.8 Hz, 1H), 7.51-7.38 (m, 6H), 7.23 (dd, J = 8.4, 1.9 Hz, 1H), 6.56 (dd, J = 3.8, 0.8 Hz, 1H), 5.46 (s, 2H). $^{13}\text{C NMR}$ (126 MHz, CDCl_3): δ = 150.5, 135.6, 134.9, 130.5, 128.9, 128.9, 128.8, 128.5, 126.1, 123.7, 121.7, 115.5, 107.9, 69.0. **HRMS (ESI-MS)**: calcd for $\text{C}_{16}\text{H}_{13}\text{ClNNaO}_2$: 308.0449; found: 308.0453. **IR v** (cm^{-1}): 2958, 1729. **m.p.**: 59-60 °C

Benzyl 6-(trifluoromethyl)-1H-indole-1-carboxylate (2u)

Following GP3, benzyl 6-(trifluoromethyl)-1H-indole-1-carboxylate was isolated as a white solid in 57% yield. $^1\text{H NMR}$ (400 MHz, CDCl_3): δ = 8.53 (s, 1H), 7.76 (d, J = 3.7 Hz, 1H), 7.65 (dd, J = 8.2, 1.0 Hz, 1H), 7.52-7.49 (m, 3H), 7.44-7.41 (m, 3H), 6.65 (dd, J = 3.8, 0.8 Hz, 1H), 5.49 (s, 2H). $^{13}\text{C NMR}$ (101 MHz, CDCl_3): δ = 150.5, 134.7, 133.0, 128.9, 128.8, 128.6, 128.3, 128.0, 126.6 (q, $^2J_{\text{C-F}}$ = 32.2 Hz), 124.8 (q, $^1J_{\text{C-F}}$ = 271.7 Hz), 121.3, 119.8 (q, $^3J_{\text{C-F}}$ = 3.6 Hz), 112.8 (q, $^3J_{\text{C-F}}$ = 3.6 Hz), 107.8, 69.2. $^{19}\text{F NMR}$ (376 MHz, CDCl_3): δ = -61.16. **HRMS (ESI-MS)**: calcd for $\text{C}_{17}\text{H}_{12}\text{F}_3\text{NNaO}_2$: 342.0712; found: 342.0713. **IR v** (cm^{-1}): 2924, 1738, 1446. **m.p.**: 48-49 °C.

Benzyl 6-(trifluoromethoxy)-1H-indole-1-carboxylate (2v)

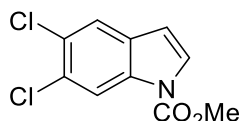
Following GP3, benzyl 6-(trifluoromethoxy)-1H-indole-1-carboxylate was isolated as a colorless oil in 86% yield. $^1\text{H NMR}$ (400 MHz, CDCl_3): δ = 8.18 (s, 1H), 7.70 (d, J = 3.8 Hz, 1H), 7.49 (dd, J = 8.0, 1.8 Hz, 2H), 7.48-7.37 (m, 4H), 7.29-7.14 (m, 1H), 6.60 (dd, J = 3.6, 0.8 Hz, 1H), 5.47 (s, 2H). $^{13}\text{C NMR}$ (101 MHz, CDCl_3): δ = 150.6, 145.2, 145.1, 134.8, 133.5, 131.2, 128.9, 128.8, 128.5, 127.3, 120.7 (q, $^1J_{\text{C-F}}$ = 256.4 Hz), 118.0, 116.0, 113.4, 107.9, 69.0. $^{19}\text{F NMR}$ (376 MHz, CDCl_3): δ = -58.16. **HRMS (ESI-MS)**: calcd for $\text{C}_{17}\text{H}_{12}\text{F}_3\text{NO}_3$: 335.0769; found: 335.0770. **IR v** (cm^{-1}): 3036, 2963, 1737.

Benzyl 6-methoxy-1H-indole-1-carboxylate (2w)

Following GP3, benzyl 6-methoxy-1H-indole-1-carboxylate was isolated as a solid in 59% yield. $^1\text{H NMR}$ (400 MHz, CDCl_3): δ = 7.77 (s, 1H), 7.56-7.36 (m, 7H), 6.88 (dd, J = 8.6, 2.4 Hz, 1H), 6.52 (dd, J = 3.7, 0.8 Hz, 1H), 5.45 (s, 2H), 3.83 (s, 3H). $^{13}\text{C NMR}$ (126 MHz, CDCl_3): δ = 157.9,

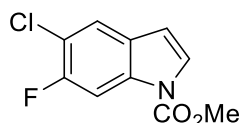
150.9, 136.3, 135.1, 128.8, 128.7, 128.4, 124.2, 124.1, 121.4, 112.4, 108.1, 99.3, 68.6, 55.6. **HRMS (ESI-MS):** calcd for $C_{17}H_{15}NNaO_3$: 304.0944; found: 304.0946. **IR ν (cm^{-1}):** 2995, 2837, 1728. **m.p.:** 59-61 °C.

Methyl 5,6-dichloro-1*H*-indole-1-carboxylate (**2x**)



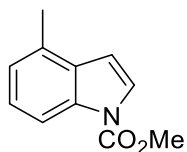
Following GP3, methyl 5,6-dichloro-1*H*-indole-1-carboxylate was isolated as a white solid in 55% yield. **1H NMR (400 MHz, $CDCl_3$):** δ = 8.29 (s, 1H), 7.62 (s, 1H), 7.60 (d, J = 3.8 Hz, 1H), 6.51 (dd, J = 3.8, 0.8 Hz, 1H), 4.05 (s, 3H). **^{13}C NMR (101 MHz, $CDCl_3$):** δ = 150.9, 137.5, 133.8, 130.0, 128.5, 127.2, 121.9, 116.8, 107.1, 54.2. **HRMS (APCI-MS):** calcd for $C_{10}H_8Cl_2NO_2$: 243.9927; found: 243.9923. **IR ν (cm^{-1}):** 3146, 3114, 2961, 2855, 1739, 1649. **m.p.:** 102-103 °C.

Methyl 5-chloro-6-fluoro-1*H*-indole-1-carboxylate (**2y**)



Following GP3, methyl 5-chloro-6-fluoro-1*H*-indole-1-carboxylate was isolated as a white solid in 72% yield. **1H NMR (500 MHz, $CDCl_3$):** δ = 8.02-7.93 (m, 1H), 7.62-7.59 (m, 1H), 7.55 (d, J = 7.2 Hz, 1H), 6.52 (d, J = 3.7 Hz, 1H), 4.05 (s, 3H). **^{13}C NMR (101 MHz, $CDCl_3$):** δ = 155.8 (d, $^1J_{C-F}$ = 243.2 Hz), 151.0, 133.6 (d, $^3J_{C-F}$ = 9.1 Hz), 127.0, 126.7, 121.7, 116.7 (d, $^2J_{C-F}$ = 20.0 Hz), 107.1, 103.6 (d, $^2J_{C-F}$ = 28.5 Hz), 54.1. **^{19}F NMR (376 MHz, $CDCl_3$):** δ = -118.66. **HRMS (APCI-MS):** calcd for $C_{10}H_8ClFNO_2$: 228.0217; found: 228.0217. **IR ν (cm^{-1}):** 3168, 3129, 3107, 3016, 2963, 2856, 1989, 1809, 1728, 1633. **m.p.:** 78-79 °C.

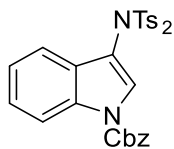
Methyl 4-methyl-1*H*-indole-1-carboxylate (**2z**)



[Bis(trifluoroacetoxy)iodo]benzene (0.275 mmol) were added to a stirring solution of methyl (3-methyl-2-vinylphenyl)carbamate (0.250 mmol) in $CHCl_3$ (3 mL) at 0 °C and stirred during 24 hours. The solvent was removed under reduced pressure. The crude was purified by column chromatography (neutral alumina, *n*-hexane/ethyl acetate, 98/2, v/v). The product was obtained as a colorless oil in a 32% of yield. **1H NMR (500 MHz, $CDCl_3$):** δ = 8.05 (d, J = 8.4 Hz, 1H), 7.63 (d, J = 3.8 Hz, 1H), 7.31-7.24 (m, 1H), 7.13-7.04 (m, 1H), 6.67 (d, J = 3.8 Hz, 1H), 4.07 (s, 3H), 2.56 (s, 3H). **^{13}C NMR (126 MHz, $CDCl_3$):** δ = 151.6, 135.0, 130.4, 130.1, 124.9, 124.5, 123.4, 112.6, 106.5, 53.7, 18.5. **HRMS (APCI-**

MS): calcd for $C_{11}H_{12}NO_2$: 190.0863; found: 190.0859. **IR ν (cm^{-1}):** 2955, 2922, 2855, 1737, 1600.

Benzyl 3-(4-methyl-*N*-tosylphenylsulfonamido)-1*H*-indole-1-carboxylate (**4**)



Procedure a: PhIO (121 mg, 0.55 mmol), 2,4,5-tris-isopropylbenzene sulfonic acid (156 mg, 0.55 mmol) and PhI(NTs₂)₂ (469 mg, 0.55 mmol) were added to a stirring solution of the starting material **1a** (126 mg, 0.50 mmol) in CHCl₃ (5 mL). After one hour, the solvent was removed under reduced pressure. The crude was purified by column chromatography (silica gel, *n*-hexane/ethyl acetate, 95/5, v/v) to afford the title compound **4** as a white foam in a 48% yield. **Procedure b:** PhIO (121 mg, 0.55 mmol), 2,4,5-tris-isopropylbenzene sulfonic acid (78 mg, 0.275 mmol) and HNTs₂ (179 mg, 0.55 mmol) were added to a stirring solution of the starting material **1a** (63 mg, 0.250 mmol) in CHCl₃ (3 mL). After one hour, the solvent was removed under reduced pressure. The crude was purified by column chromatography (silica gel, *n*-hexane/ethyl acetate, 95/5, v/v) to afford the title compound **4** as a white foam in a 52% yield. **¹H NMR (400 MHz, CDCl₃):** δ = 8.16 (d, *J* = 8.4 Hz, 1H), 7.85 (d, *J* = 8.3 Hz, 4H), 7.50 (s, 1H), 7.49-7.40 (m, 5H), 7.32-7.28 (m, 5H), 7.12 (ddd, *J* = 8.0, 7.3, 1.0 Hz, 1H), 7.00 (dd, *J* = 7.8, 1.0 Hz, 1H), 5.45 (s, 2H), 2.45 (s, 6H). **¹³C NMR (101 MHz, CDCl₃):** δ = 150.3, 145.2, 136.3, 134.6, 134.2, 129.6, 129.0, 128.8, 128.7, 128.6, 127.9, 127.2, 125.5, 123.7, 119.2, 116.4, 115.3, 69.3, 21.7. **HRMS (ESI-MS):** calcd for C₃₀H₂₆N₂NaO₆S₂: 597.1124; found: 597.1137. **IR ν (cm^{-1}):** 3035, 1745, 1596, 1494, 1452. **m.p.:** 169-171°C.

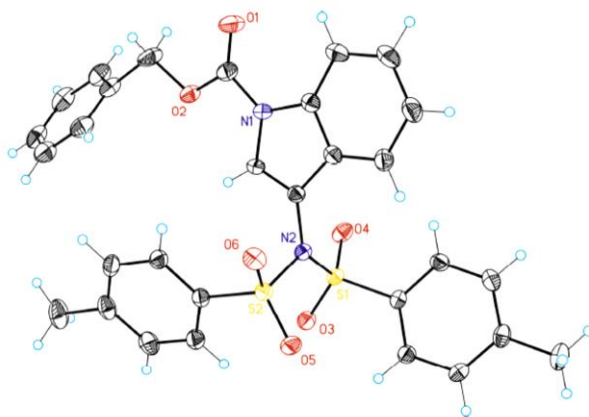


Table 2.7 Crystal data and structure refinement for compound **4**.

Identification code	CCDC 987831
Empirical formula	C ₃₀ H ₂₆ N ₂ O ₆ S ₂
Formula weight	574.65
Temperature	100(2) K
Wavelength	0.71073 Å
Crystal system	Triclinic
Space group	P-1
Unit cell dimensions	a = 10.5643(6)Å α = 113.543(2)°. b = 11.1061(7)Å β = 91.704(2)°. c = 12.5681(8)Å γ = 92.030(2)°.
Volume	1349.45(14) Å ³
Z	2
Density (calculated)	1.414 Mg/m ³
Absorption coefficient	0.246 mm ⁻¹
F(000)	600
Crystal size	0.30 x 0.30 x 0.20 mm ³
Theta range for data collection	1.769 to 30.146°.
Index ranges	-13<=h<=14, -14<=k<=15, -17<=l<=17
Reflections collected	15642
Independent reflections	6851[R(int) = 0.0254]
Completeness to theta =30.146°	86.0%
Absorption correction	Empirical
Max. and min. transmission	0.952 and 0.882
Refinement method	Full-matrix least-squares on F ²
Data / restraints / parameters	6851/ 0/ 363
Goodness-of-fit on F ²	1.076
Final R indices [I>2sigma(I)]	R1 = 0.0402, wR2 = 0.1033
R indices (all data)	R1 = 0.0499, wR2 = 0.1101
Largest diff. peak and hole	0.756 and -0.548 e.Å ⁻³

Control experiments on potential palladium participation:

In order to verify that the reported indole synthesis does not involve the participation of any palladium traces that might be present as contamination resulting from the previous Suzuki coupling, compound **1a** was synthesized within a sequence that is rigorously free of transition metals. Compound **1a** was then tested in a potential palladium-catalyzed oxidative cyclization in the presence of iodobenzene (Figure 2.66). Different palladium sources employed for synthesis of other substrates **1** were tested, which include both palladium(0) as well as palladium(II) precursors. Hence, for tetrakis(triphenylphosphino)palladium(0) and tris(dibenzylideneacetone)-dipalladium(0) as well as for bis(triphenylphosphino) palladium dichloride and palladium diacetate, respectively. Even in the presence of a loading as high as 20 mol% of [Pd] (PdCl₂(PPh₃)₂, Pd(OAc)₂, Pd[(PPh₃)₃]₄, Pd₂(dba)₃) no indole formation was detected in any case and starting material was recovered. As a result, participation of any traces of palladium residues is ruled out to be involved in the present indole formation.

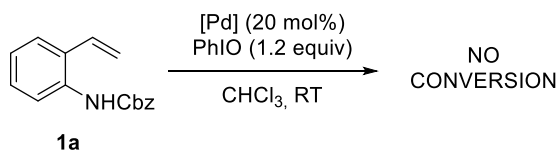
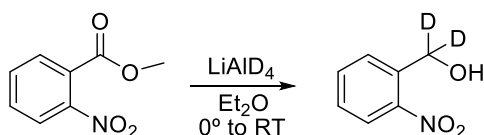


Figure 2.66 Reaction scheme for the control experiments with different palladium sources.

Synthesis and characterization of deuterated starting materials:

(2-Nitrophenyl)methanol-d₂

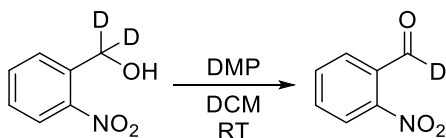


In a flame-dried schlenk flask, starting material (1.57 g, 8.67 mmol) was placed under argon, and dissolved in ether (26 mL). The solution was cooled to 0 °C and

LiAlD₄ (0.28 g, 6.76 mmol) was added portionwise and stirred overnight at room temperature. Then, cold water was added dropwise and the aqueous phase was extracted with ether (3x30mL). The combined organic layers were washed with a saturated aqueous solution of brine and dried over MgSO₄. Solvent was removed under reduced pressure. The product was obtained as an orange solid in 93% yield in pure form and no further purification was required. ¹H NMR (400 MHz, CDCl₃): δ = 8.10 (dd, *J* = 8.2, 1.3 Hz, 1H), 7.74 (dd, *J* = 7.6, 1.7 Hz, 1H), 7.68 (td, *J* = 7.5, 1.3 Hz, 1H), 7.48 (ddd, *J* = 8.2,

7.3, 1.6 Hz, 1H). ^{13}C NMR (126 MHz, CDCl_3): δ = 147.6, 136.7, 134.1, 129.9, 128.5, 125.0, 61.8 (m).

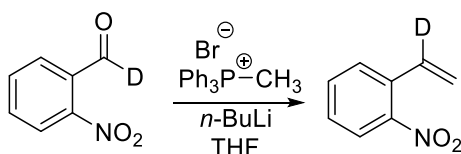
2-Nitrobenzaldehyde- d_1



The starting material (1.1g, 7.1 mmol) was dissolved in dry dichloromethane (26 mL), and Dess-Martin periodane (3.61g, 8.5 mmol) was added. The reaction was stirred

for 2 hours at room temperature. The reaction was washed with an aqueous solution of $\text{Na}_2\text{S}_2\text{O}_3$ (10%) and a saturated aqueous solution of NaHCO_3 (1:1), dried over MgSO_4 . The solvent was removed under reduced pressure. The residue was purified by column chromatography (silica gel, *n*-hexane/ethyl acetate, 95/5, v/v) to obtain 0.8 g of a brown solid in 73% yield. ^1H NMR (500 MHz, CDCl_3): δ = 8.10 (dd, J = 8.0, 1.4 Hz, 1H), 7.95-7.91 (m, 1H), 7.82-7.72 (m, 2H). ^{13}C NMR (75 MHz, CDCl_3): δ = 187.8 (t), 149.6, 134.1, 133.7, 131.3, 129.6, 124.5.

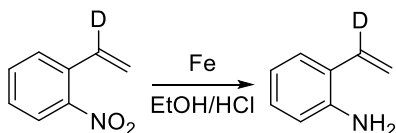
2-Nitrostyrene- d_1



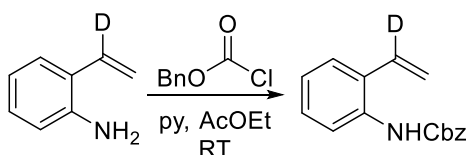
The 2-nitrostyrene deuteride was synthesized following the procedure described for the 2-nitrostyrene in a 76% of yield. ^1H NMR (500 MHz, CDCl_3): δ =

7.92 (dd, J = 8.2, 1.3 Hz, 1H), 7.66-7.54 (m, 2H), 7.41 (ddd, J = 8.6, 7.3, 1.5 Hz, 1H), 5.77-5.71 (m, 1H), 5.50-5.46 (m, 1H). ^{13}C NMR (126 MHz, CDCl_3): δ = 147.8, 133.2, 133.1, 132.1 (t), 128.4, 128.3, 124.4, 118.8.

2-Vinyl- d_1 -aniline

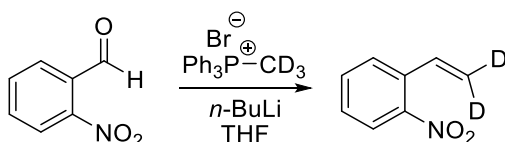


The compound was synthesized following the procedure described in literature.⁸⁹ The crude was submitted to the next step without further purification.

Benzyl (2-vinyl-d₁-phenyl)carbamate

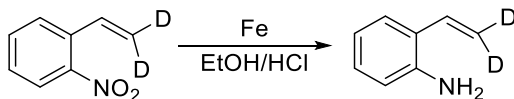
Following GP1, benzyl (2-vinyl-d₁-phenyl)carbamate was isolated as a colorless solid in 29% yield in both steps.

¹H NMR (300 MHz, CDCl₃): δ = 7.82 (d, J = 8.1 Hz, 1H), 7.49-7.28 (m, 7H), 7.11 (td, J = 7.5, 1.3 Hz, 1H), 6.62 (brs, 1H), 5.66-5.64 (m, 1H), 5.41-5.39 (m, 1H), 5.21 (s, 2H). **¹³C NMR (126 MHz, CDCl₃):** δ = 153.7, 136.0, 134.5, 131.7 (t), 128.6, 128.6, 128.4, 127.0, 124.5, 121.8, 118.1, 67.2.

2-Nitrostyrene-d₂

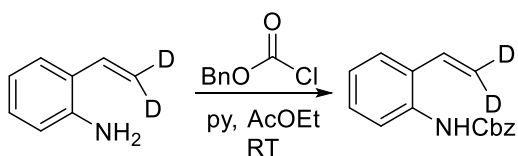
The 2-nitrostyrene deuteride was synthesized following the procedure described for the 2-nitrostyrene in a 53% yield. **¹H NMR (500 MHz, CDCl₃):**

δ = 7.92 (dd, J = 8.2, 1.3 Hz, 1H), 7.64-7.55 (m, 2H), 7.43-7.38 (m, 1H), 7.16 (s, 1H). **¹³C NMR (126 MHz, CDCl₃):** δ = 147.9, 133.3, 133.1, 132.3, 128.5, 128.3, 124.4, 118.4 (m).

2-Vinyl-d₂-aniline

The compound was synthesized in 80% yield as a brown oil following the procedure described in the

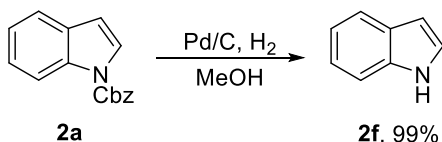
literature.⁸⁹ The NMR spectra match the literature data.⁹⁷

Benzyl (2-vinyl-d₂-phenyl)carbamate

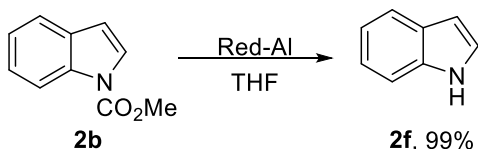
Following GP1, benzyl (2-vinyl-d₂-phenyl)carbamate was isolated as a colorless solid in 42% yield. **¹H NMR (400 MHz, CDCl₃):** δ = 7.83 (s, 1H),

7.46-7.33 (m, 6H), 7.33-7.24 (m, 1H), 7.11 (td, J = 7.6, 1.4 Hz, 1H), 6.78 (s, 1H), 6.62 (brs, 1H), 5.21 (2H, s). **¹³C NMR (126 MHz, CDCl₃):** δ = 153.7, 136.1, 134.5, 131.9, 128.6, 128.6, 128.4, 127.0, 124.5, 121.8, 117.8 (m), 67.2.

⁹⁷ Ye, K. Y.; He, H.; Liu, W. B.; Dai, L. X.; Helmchen, G.; You, S. L. *J. Am. Chem. Soc.* **2011**, *133*, 19006.

Deprotection of carbamate to free indole:

The protected indole **2a** (251 mg, 1 mmol) was dissolved in MeOH (5 mL), palladium on carbon (5% Pd) was added and the reaction was stirred for 2 hours under a H₂ atmosphere. Then, the reaction was diluted with CH₂Cl₂ and filtered through a short Celite® pad. Deprotected indole **2f** was isolated as a colorless oil in 99% (117 mg) and NMR spectra matched with the reported data.⁹⁰



The protected indole **2a** (50 mg, 0.286 mmol) was placed under argon atmosphere and dissolved in THF (1 mL). Then Red-Al® (0.17 mL, 0.571 mmol) was added dropwise at 0 °C. After 2 hours, cool water was added dropwise at 0 °C. Then, the reaction was extracted with CH₂Cl₂ (3x10mL), the combined organic layers were dried over Na₂SO₄ and solvent was removed. The crude was purified by column chromatography (silica gel, *n*-hexane/ethyl acetate, 95/5, v/v). Deprotected indole **2f** was isolated as a colourless oil in quantitative yield (99%, 33 mg) and NMR spectra matched with the reported data.⁹⁰

UNIVERSITAT ROVIRA I VIRGILI

NEW APPLICATIONS OF IODINE(III) REACTIVITY: SYNTHESIS AND FUNCTIONALIZATION OF HETEROCYCLES

Laura Fra Fernández

Chapter 3

Indole Synthesis through Sequential Electrophilic N–H/C–H Bond activation Using Iodine(III) Reactivity

3.1 Introduction

In Chapter 2, we focused in the synthesis of indoles through the interaction between an alkene and a nitrogen. For this end, we selected 2-vinyl anilines as the appropriate substrate to access to 2,3-unsubstituted indole core that can subsequently be further functionalized.

As the complementary synthesis of 2,3-functionalized indoles has certain limitations, we proposed another approach based in the interaction between an alkyne and an aniline to achieve the synthesis of 2,3-diarylated indoles. This synthetic approach has been widely applied using transition metals, although it would be interesting to apply it to a metal-free alternative.

3.1.1 Transition metal-catalyzed cyclization of alkynes and anilines

The introduction of transition metal reagents for the cyclization of alkynes and anilines for indole synthesis was first reported by Castro in the 1960s. They proposed a copper-mediated indoles synthesis by employing copper(I) acetylides and *o*-iodoaniline.⁹⁸

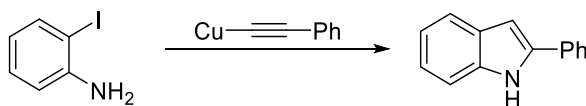


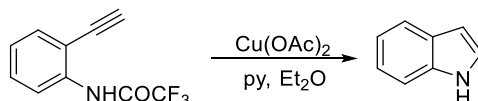
Figure 3.1 Castro proposal for the synthesis of 2-phenyl indole.

⁹⁸ a) Castro, C. E.; Stevens, R. D. *J. Org. Chem.* **1963**, *28*, 2163; b) Castro, C. E.; Gaughan, E. J.; Owsley, D. C. *J. Org. Chem.* **1966**, *31*, 4071.

They discovered that the reaction is controlled by the solvent. When pyridine was used instead of DMF, the tolane product was obtained. This coupling product could be cyclized to the corresponding indole derivative using cuprous iodide and DMF.

Copper-catalyzed cyclizations have been widely explored for the synthesis of indoles. In 1995, Saulnier described the intramolecular cyclization of 2-ethynyl trifluoroacetanilide into the free indole using 3.2 equivalents of copper acetate, $\text{Cu}(\text{OAc})_2$ (Figure 3.2 a).⁹⁹ Later, Barluenga reported a synthetic strategy, in which first an *ortho*-iodination of substituted anilines takes place, followed by a palladium-catalyzed coupling with a silylated acetylene of the resulting iodinated amines.¹⁰⁰ The strategy terminates with the cyclization of the *o*-alkynyl anilines with copper iodide to the unprotected indole (Figure 3.2 b).

a) Saulnier, 1995.



b) Barluenga, 1996.

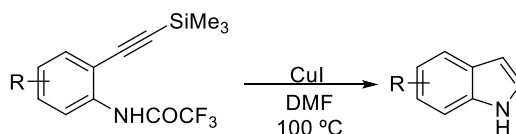


Figure 3.2 Copper-mediated indole formation.

The same approach was developed by Sakamoto, but in this case they applied a methodology that they previously reported,¹⁰¹ in which the cyclization reaction of the

⁹⁹ Saulnier, M. G.; Frennesson, D. B.; Deshpande, M. S.; Vyas, D. M. *Tetrahedron Lett.* **1995**, *36*, 7841.

¹⁰⁰ Ezquerro, J.; Pedregal, C.; Lamas, C.; Barluenga, J.; Pérez, M.; García-Martin, M. A.; González, J. M. *J. Org. Chem.* **1996**, *61*, 5804.

¹⁰¹ a) Sakamoto, T.; Kondo, Y.; Yamanaka, H. *Heterocycles* **1986**, *24*, 31; b) Sakamoto, T.; Kondo, Y.; Iwashita, S.; Yamanaka, H. *Chem. Pharm. Bull.* **1987**, *35*, 1823; c) Sakamoto, T.; Kondo, Y.; Iwashita, S.; Nagano, T.; Yamanaka, H. *Chem. Pharm. Bull.* **1988**, *36*, 1305; d) Kondo, Y.; Kojima, S.; Sakamoto, T. *Heterocycles* **1996**, *43*, 2741.

corresponding *o*-alkynyl anilines is mediated by potassium *tert*-butoxide.¹⁰² This methodology was improved introducing Cu(OAc)₂ as the catalyst for this type of cyclization reactions (Figure 3.3).¹⁰³

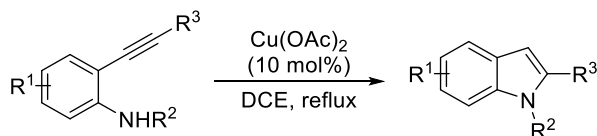
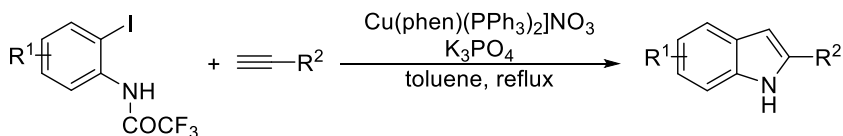


Figure 3.3 Copper-catalyzed cyclization reaction proposed by Sakamoto.

In 2003, Cacchi reported a domino copper-catalyzed coupling/cyclization process, in which 2-iodotrifluoroacetanilides are successfully converted into the corresponding 2-aryl and 2-heteroaryl indoles (Figure 3.4 a).¹⁰⁴ Later, Ma applied this approach for the development of a CuI/L-proline-catalyzed coupling between 2-bromotrifluoroacetanilides and alkynes followed by a CuI-catalyzed cyclization (Figure 3.4 b).¹⁰⁵

a) Cacchi, 2003.



b) Ma, 2007.

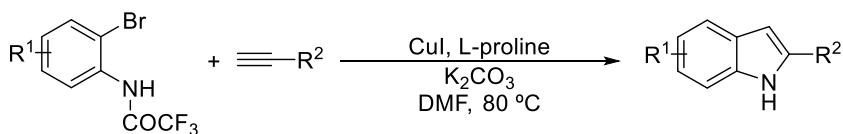


Figure 3.4 Domino copper-catalyzed coupling/cyclization reaction for indole synthesis.

¹⁰² Kondo, Y.; Kojima, S.; Sakamoto, T. *J. Org. Chem.* **1997**, *62*, 6507.

¹⁰³ a) Hiroya, K.; Itoh, S.; Ozawa, M.; Kanamori, Y.; Sakamoto, T. *Tetrahedron Lett.* **2002**, *43*, 1277;

b) Hiroya, K.; Itoh, S.; Sakamoto, T. *J. Org. Chem.* **2004**, *69*, 1126.

¹⁰⁴ Cacchi, S.; Fabrizi, G.; Parisi, L. M. *Org. Lett.* **2003**, *5*, 3843.

¹⁰⁵ Liu, F.; Ma, D. *J. Org. Chem.* **2007**, *72*, 4844.

Other transition metals were used for the cyclization reaction towards the indole formation, too. Palladium has been fruitfully chosen as the catalyst for the heteroannulation reaction between *o*-iodoanilines and alkynes. It was Larock, in 1991, who reported the synthesis of indoles through a one pot Pd-catalyzed coupling of 2-iodoanilines and internal alkynes.¹⁰⁶ Later, the same authors discovered that the addition of a ligand did not significantly improve the yield (Figure 3.5).¹⁰⁷ The reaction tolerates a wide variety of disubstituted alkynes as coupling partners and is highly regioselective, although high temperatures, excess of base and a full equivalent of lithium chloride are needed for reproducibility.

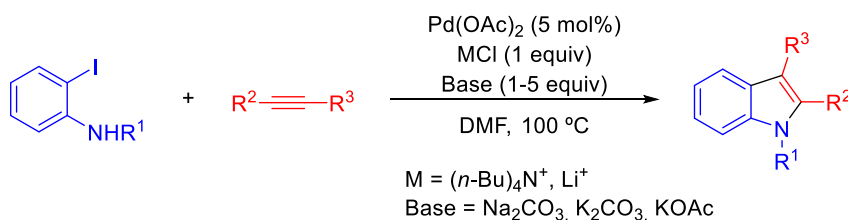


Figure 3.5 Larock synthesis of indoles.

Inspired by Larock's work, Senanayake explored the possibility of replacing the iodoanilines with the much cheaper 2-bromo or 2-chloro derivatives. They found that the addition of a phosphine-ferrocene complex (1,1'-bis(*di-tert*-butylphosphino)ferrocene) afforded the desired indole derivatives in good yields (Figure 3.6).¹⁰⁸ Later, this methodology was expanded to the use of 2-alkynylpyridines as the coupling partner by a slight modification of the reaction conditions.¹⁰⁹

¹⁰⁶ Larock, R. C.; Yum, E. K. *J. Am. Chem. Soc.* **1991**, *113*, 6689.

¹⁰⁷ Larock, R. C.; Yum, E. K.; Refvik, M. D. *J. Org. Chem.* **1998**, *63*, 7652.

¹⁰⁸ Shen, M.; Li, G.; Lu, B. Z.; Hossain, A.; Roschangar, F.; Farina, V.; Senanayake, C. H. *Org. Lett.* **2004**, *6*, 4129.

¹⁰⁹ Roschangar, F.; Liu, J.; Estanove, E.; Dufour, M.; Rodriguez, S.; Farina, V.; Hickey, E.; Hossain, A.; Jones, P.-J.; Lee, H.; Lu, B. Z.; Varsolona, R.; Schröder, J.; Beaulieu, P.; Gillard, J.; Senanayake, C. H. *Tetrahedron Lett.* **2008**, *49*, 363.

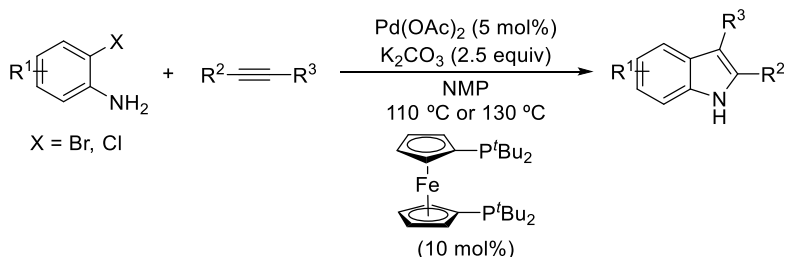


Figure 3.6 Senanayake proposal for the synthesis of indoles from 2-chloro and 2-bromo anilines.

The cyclization of 2-haloanilides to 2,3-substituted indoles was extensively explored by Ackermann. In 2004, they reported a one-pot synthesis of indoles based on a titanium-catalyzed hydroamination reaction of alkynes with 2-chloroaniline followed by 5-*endo* Heck cyclization reaction using a sterically hindered carbene precursor (Figure 3.7). The reaction proceeded with some regioselectivity, and the 2-alkyl-3-arylated indole was obtained as the major regioisomer.¹¹⁰

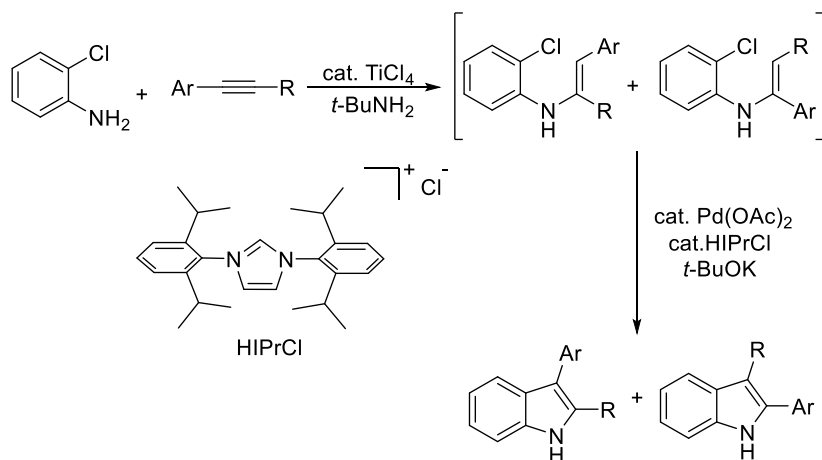


Figure 3.7 Synthetic route proposed by Ackermann for the synthesis of indoles.

After these results, they focused in the development of hydroamination methodologies based on late transition-metal catalysts for indole synthesis. In 2006, they presented a one-pot synthesis of 2- or 2,3-substituted indoles in which the 2-chloroanilino enamine was generated through a regioselective ruthenium-catalyzed

¹¹⁰ a) Ackermann, L.; Kaspar, L. T.; Gschrei, C. J. *Chem. Commun.* **2004**, 6, 2824; b) Ackermann, L.; Sandmann, R.; Villar, A.; Kaspar, L. T. *Tetrahedron* **2008**, 64, 769.

hydroamination reaction, and cyclized *via* a palladium-catalyzed intramolecular Heck reaction.¹¹¹

In 2012, they reported a completely different methodology, the first ruthenium-catalyzed oxidative annulation of alkynes using simple anilines as starting materials (Figure 3.8).¹¹² The reaction takes place in the presence of a cationic ruthenium(II) complex in water through the reversible formation of six-membered ruthenacycles as key intermediates. The 2-pyrimidyl protecting group acts as a directing group and is easily removed. This methodology was later improved using the successful *N*-2-pyrimidyl anilines and a nickel catalyst in combination with a phosphine based ligand in the absence of metal salts as oxidants.¹¹³

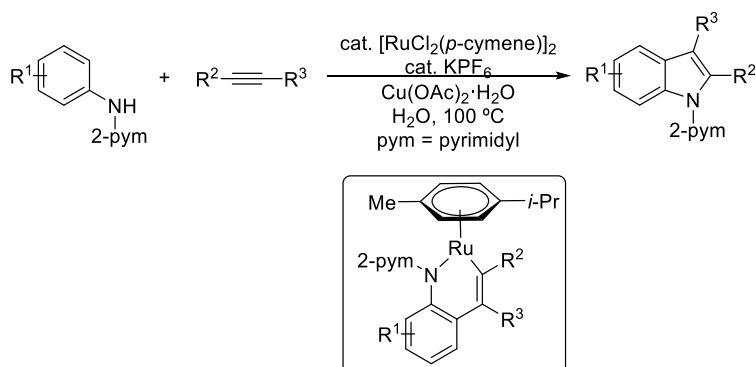


Figure 3.8 First ruthenium-catalyzed oxidative cyclization of *N*-protected anilines in water.

Protected anilines were widely used as substrates for transition metal-catalyzed oxidative annulations. For example, Lu reported in 2011 a palladium-catalyzed C-H bond activation of electron-rich anilines and subsequent insertion of the alkyne (Figure 3.9).¹¹⁴

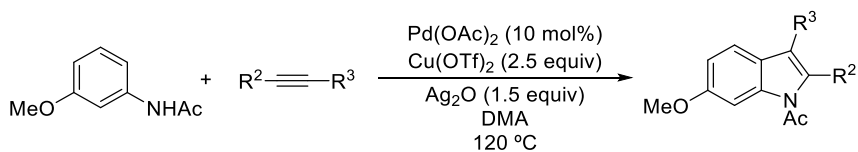


Figure 3.9 Lu's approach for the synthesis of indoles catalyzed by palladium.

¹¹¹ Ackermann, L.; Althammer, A. *Synlett* **2006**, 3125.

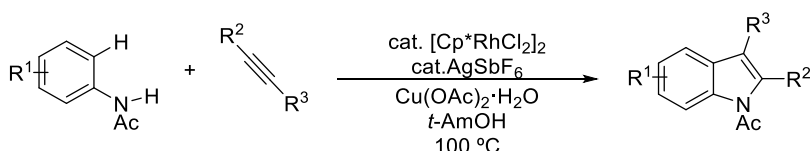
¹¹² Ackermann, L.; Lygin, A. V. *Org. Lett.* **2012**, *14*, 764.

¹¹³ Song, W.; Ackermann, L. *Chem. Commun.* **2013**, *49*, 6638.

¹¹⁴ Zhou, F.; Han, X.; Lu, X. *Tetrahedron Lett.* **2011**, *52*, 4681.

Other transition metals, such as rhodium, were used as a catalyst for this type of transformation. It was Fagnou, in 2008, who observed the formation of the 2,3-disubstituted indoles in the presence of a Rh(III)-catalyst (Figure 3.10 a).¹¹⁵ This synthetic approach has several limitations such high reaction temperatures, limited alkyne scope and the presence of a metal oxidant, among others. In order to solve all these disadvantages, they developed a new methodology introducing a dicationic analogue rhodium-catalyst and the use of molecular oxygen as the terminal oxidant (Figure 3.10 b).¹¹⁶

a) Fagnou, 2008.



b) Fagnou, 2010.

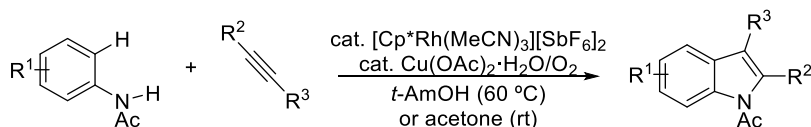


Figure 3.10 Rhodium-catalyzed oxidative coupling of acetanilides and alkynes for indole synthesis.

The same approach was used by Li in 2010. They reported a rhodium-catalyzed oxidative coupling of *N*-2-pyrimidyl anilines with internal alkynes furnishing the corresponding *N*-pyridyl-substituted indole (Figure 3.11).¹¹⁷ In order to improve this methodology, they developed a palladium-catalyzed intermolecular cyclization using the same substrates. This synthetic approach solved the disadvantages of the Rh(III)-catalyzed version in terms of both cost of the catalyst and substrate scope.¹¹⁸

¹¹⁵ Stuart, D.; Bertrand-Laperle, M.; Burgess, K. M. N.; Fagnou, K. *J. Am. Chem. Soc.* **2008**, *130*, 16474.

¹¹⁶ Stuart, D.; Alsabeh, P.; Kuhn, M.; Fagnou, K. *J. Am. Chem. Soc.* **2010**, *132*, 18326.

¹¹⁷ Chen, J.; Song, G.; Pan, C.-L.; Li, X. *Org. Lett.* **2010**, *12*, 5426.

¹¹⁸ Chen, J.; Pang, Q.; Sun, Y.; Li, X. *J. Org. Chem.* **2011**, *76*, 3523.

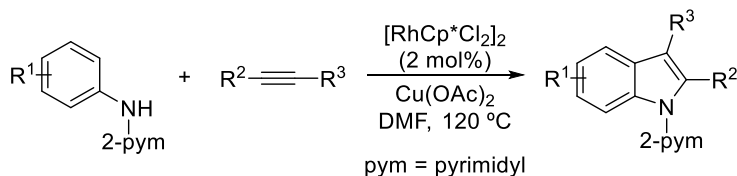


Figure 3.11 Li's proposal for the synthesis of 2,3-disubstituted indoles.

Unprotected commercial anilines were used as substrates in these rhodium-catalyzed oxidative couplings. In 2014, Huang reported the formation of a range of 2,3-disubstituted indoles using a Rh/O₂ catalytic system proving the ability of molecular oxygen to oxidize the Rh(I) to Rh(III) species in the presence of an appropriate acid (Figure 3.12).¹¹⁹

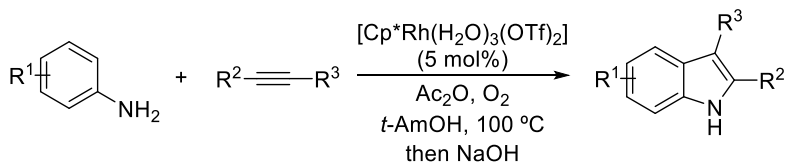


Figure 3.12 Oxidative annulation of anilines and alkynes reported by Huang.

At the same time, Tanaka published the oxidative coupling of anilides with internal alkynes at room temperature under air using a dinuclear electron-deficient (η^5 -cyclopentadienyl)rhodium(III) complex (Figure 3.13).¹²⁰ In addition to indoles, this methodology was also applied for the synthesis of pyrroles.

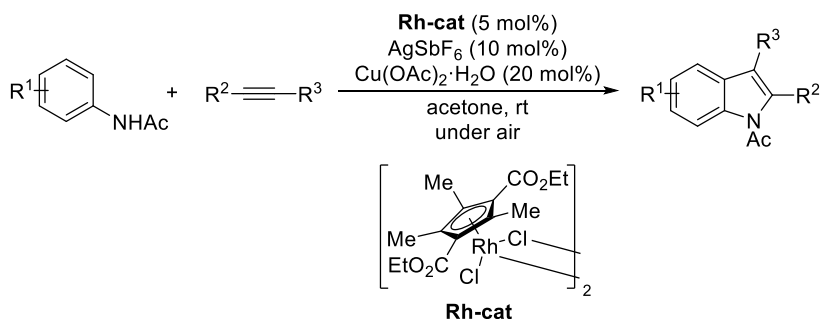


Figure 3.13 Coupling between anilides and alkynes using a dinuclear rhodium(III) complex.

¹¹⁹ Zhang, G.; Yu, H.; Qin, G.; Huang, H. *Chem. Commun.* **2014**, 50, 4331.

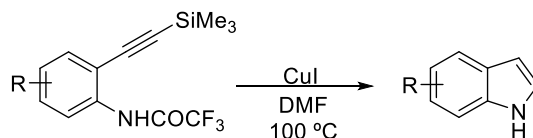
¹²⁰ Hoshino, Y.; Shibata, Y.; Tanaka, K. *Adv. Synth. Catal.* **2014**, 356, 1577.

Most of these transition metal-catalyzed transformations present certain limitations such as high temperatures, use of inert conditions, presence of oxidants, among others. A metal-free approach would be convenient in order to overcome these main disadvantages.

3.1.2 Hypervalent iodine-mediated intramolecular oxidative C(sp)-N bond formation

After reporting their copper-mediated intramolecular oxidative annulation of *o*-((trimethylsilyl)ethynyl)aniline derivatives,¹⁰⁰ Barluenga discovered that a related cyclization could be mediated by the iodinating reagent bis(pyridine)iodonium(I) tetrafluoroborate, IPy₂BF₄ (Figure 3.14 b).¹²¹ This metal-free process is believed to proceed through the interaction between the electrophilic iodine and the alkyne moiety. Subsequently, this activated acetylene intermediate is attacked by the nucleophilic nitrogen to give the *N*-protected 3-iodo indoles.

a) Cu-mediated



b) I(III)-mediated

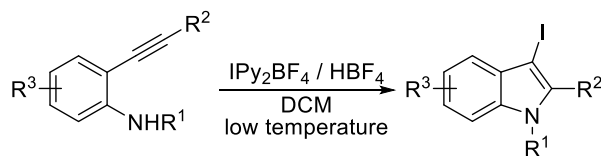


Figure 3.14 Barluenga's proposals for the synthesis of indoles.

¹²¹ Barluenga, J.; Trincado, M.; Rubio, E.; González, J. M. *Angew. Chem. Int. Ed.* **2003**, *42*, 2406.

This synthetic plan was also proposed by Kita for the formation of β -hydroxy ketones from alkynes in the presence of PIFA (Figure 3.15).¹²² They proposed that the reaction starts with the coordination of the hypervalent iodine reagent to the terminal alkyne, which acidifies the C—H bond and ultimately promotes the deprotonation. Then, an intermolecular nucleophilic attack by a molecule of water affords the correspondent β -hydroxy ketone.

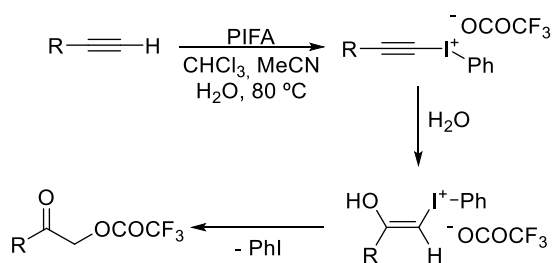


Figure 3.15 Iodine(III)-mediated formation of β -hydroxy ketones.

Based on this approach, the synthesis of *N*-based heterocycles could be achieved using an internal nitrogen for the nucleophilic attack. Depending on the substrate, two different pathways could be feasible: either the electrophilic iodine is coordinated to the alkyne (Figure 3.16 a) as proposed by Kita,¹²² or the nitrogen is formally oxidized and attacked intramolecularly by the alkynyl moiety (Figure 3.16 b).

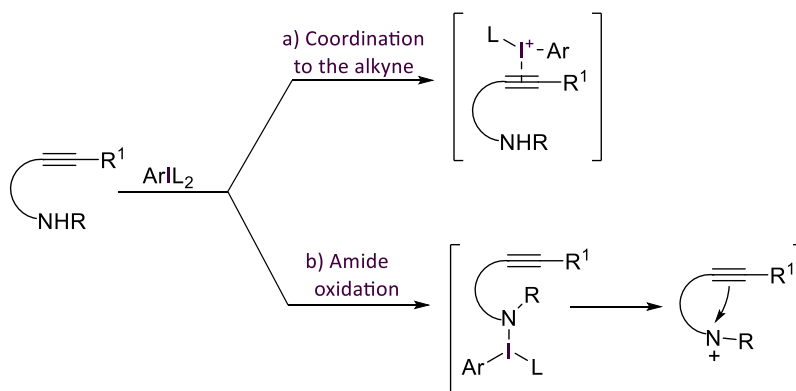


Figure 3.16 Synthetic routes for the formation of nitrogen-containing heterocycles.

¹²² Tamura, Y.; Yakura, T.; Haruta, J.-I.; Kita, Y. *Tetrahedron Lett.* **1985**, *26*, 3837.

As had been described in Chapter 2, Dominguez developed an entire methodology for the synthesis of heterocycles based on the use of PIFA for the amide oxidation and subsequently attack of a double bond. This results together with the reactivity described above, lead to the development of a new synthetic access to *N*-based heterocycles. In 2005, Dominguez proposed the synthesis of 5-substituted pyrrolidinones through the formation of an acylnitrenium ion generated by the action of PIFA, which is attacked by the triple bond (Figure 3.17).¹²³

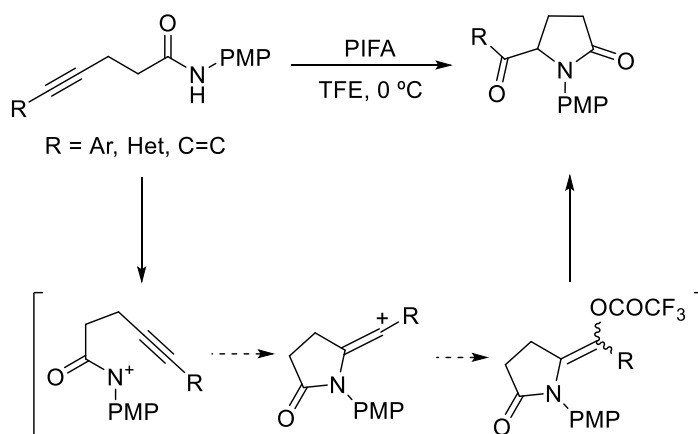


Figure 3.17 Dominguez's proposal for the synthesis of pyrrolidinones mediated by PIFA.

Two years later, they extended this methodology to the use of *N*-substituted alkynylamides that cyclized in presence of PIFA affording the corresponding pyrrolidinones.¹²⁴ This fact suggests that the hypervalent iodine reagent can also activate the alkyne toward the intramolecular nucleophilic attack of the amide moiety (Figure 3.16 a). This proposal was verified for the cyclization of alkynylcarboxylic acids with PIFA leading to the formation of the corresponding furanones.

To summarize, convenient iodine(III) compounds can be reagents of choice to promote the formation of *N*-heterocycles under mild conditions overcoming some of the disadvantages encountered in related transition metal mediated versions.

¹²³ Serna, S.; Tellitu, I.; Domínguez, E.; Moreno, I.; SanMartín, R. *Org. Lett.* **2005**, *7*, 3073.

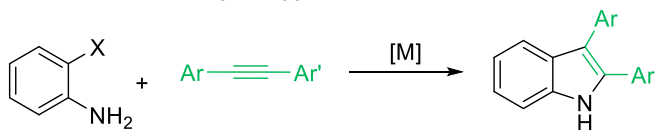
¹²⁴ Tellitu, I.; Serna, S.; Herrero, M. T.; Moreno, I.; Domínguez, E.; SanMartín, R. *J. Org. Chem.* **2007**, *72*, 1526.

3.2. Objective

The synthesis of indoles has been an active field of research over the last years. In Chapter 2, we proposed a metal-free oxidative approach using iodine(III) reactivity for the intramolecular cyclization of 2-vinyl anilines. This methodology allows unprecedented access to the 2,3-unsubstituted indole core. The latter can be further functionalized demonstrating the robustness of this reaction and its synthetic possibilities as a result of its combination with other oxidation processes.

As had been described previously, transition metal-catalysis has been widely used for the synthesis of 2,3-substituted indole derivatives (Figure 3.18 a), but we decided to go further and explore the reactivity of hypervalent iodine reagents for such a transformation. This choice could be more appropriate when considering the terms of purity for its application in the areas of biological and medicinal chemistry. For this aim, we explored this synthetic challenge from the perspective of an iodine(III)-mediated intramolecular cyclization reaction using a removable tether (Figure 3.18 b).

a) Transition metal-catalyzed approach.



b) Intramolecular (tethered) approach.

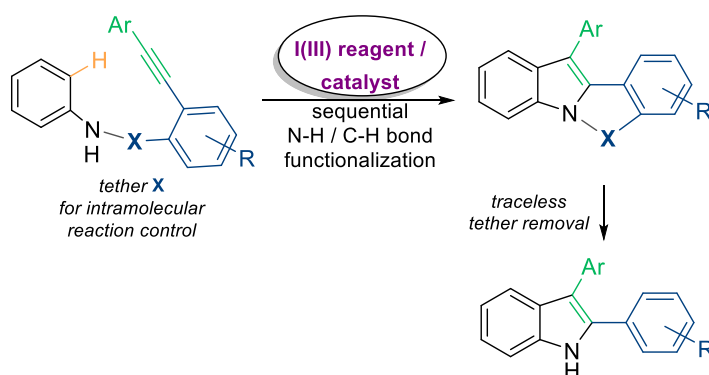


Figure 3.18 Our approach towards the formation of the 2,3-diarylated indole core.

To achieve the indole core, the hypervalent iodine reagent should be able to promote the required sequential N-H and C-H bond activation at the aniline component for a formal oxidative [3+2] cycloaddition with the acetylene. Then, traceless removal of the tether group would generate the 2,3-diarylated indole with complete selectivity regarding the position of the aryl group.

Such an approach is reminiscent of the pioneering work by Mascareñas¹²⁵ on transition metal promoted cyclization reactions of multicomponent building blocks.¹²⁶ They reported a Rh-catalyzed cycloaddition of *N*-alkynylbenzamides for the synthesis of interesting polycyclic isoquinolones or indolizinones. However, cyclization of anilides was not successful under the conditions used in the intramolecular reaction. So, we anticipate that iodine(III)-reactivity can be the key for the accomplishment of the intramolecular cyclization towards the indole core.

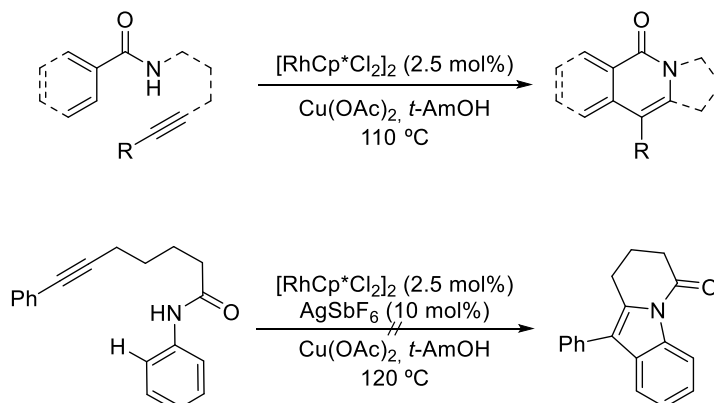


Figure 3.19 Rh-catalyzed cyclization of *N*-alkynylbenzamides proposed by Mascareñas.

¹²⁵ Quiñones, N.; Seoane, A.; García-Fandiño, R.; Mascareñas, J. L.; Gulías, M. *Chem. Sci.* **2013**, *4*, 2874.

¹²⁶ a) Guimond, N.; Gouliaras, C.; Fagnou, K. *J. Am. Chem. Soc.* **2010**, *132*, 6908; b) Guimond, N.; Gorelsky, S. I.; Fagnou, K. *J. Am. Chem. Soc.* **2011**, *133*, 6449; c) Ackermann, L.; Fenner, S. *Org. Lett.* **2011**, *13*, 6548; d) Ackermann, L.; Lygin, A. V.; Hofmann, N. *Angew. Chem. Int. Ed.* **2011**, *50*, 6379.

3.3. Results and discussion

Our first attempts for the achievement of the 2,3-substituted indole core focused on the same approach that had used in the transition metal-catalyzed version (Figure 3.20).

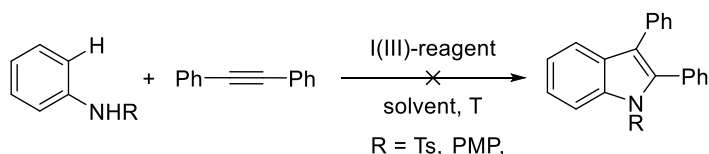


Figure 3.20 Iodine(III)-based approach for the 2,3-diphenyl indole derivatives.

To accomplish this challenge, different iodine(III)-based oxidants such as PIFA, PIDA, Koser reagent, iodosobenzene and their combination with trifluoroacetic acid, *p*-toluene sulfonic acid or our previously arylsulfonic acid, TIPBSA were tested but in most of the cases, the *N*-protected aniline remains unreactive. However, when PIFA was used to promote the intermolecular cyclization, due to the high reactivity of this reagent, no remaining starting material or the desired indole were observed. At that point, some factors were tested: the temperature was decreased to 0, -10, -20 or even -30 °C, the change of the solvent (CHCl₃, DCM, HFIP, TFE, MeCN) or the reaction time without any further improvement.

After all these unsuccessful results, we envisioned an intramolecular cyclization using a sulfonyl group as a tether¹²⁷ for the reaction control that can be easily removed, affording the final indole with regioselectivity concerning the three aryl groups positioning.

3.3.1 Modular synthesis of starting materials

One of the conceptual advantages of this method is the synthetic route performed for the preparation of the starting materials. The chosen modular composition allows

¹²⁷ a) Evans, P.; McCabe, T.; Morgan, B. S.; Reau, S. *Org. Lett.* **2005**, *7*, 43; b) Evans, P. *J. Org. Chem.* **2007**, *72*, 1830; c) Geoghegan, K; Evans, P. *J. Org. Chem.* **2013**, *78*, 3410.

for the concise modification of the substitution pattern of the three aryl groups that participate in the final cyclization reaction (Figure 3.21).

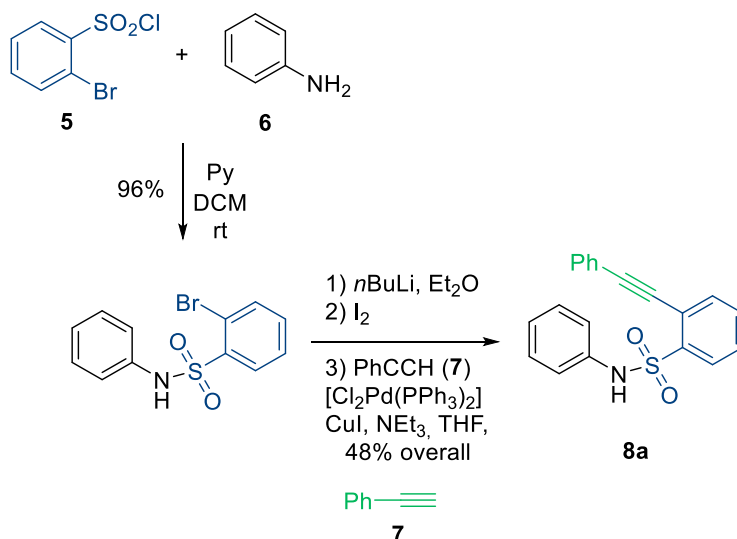
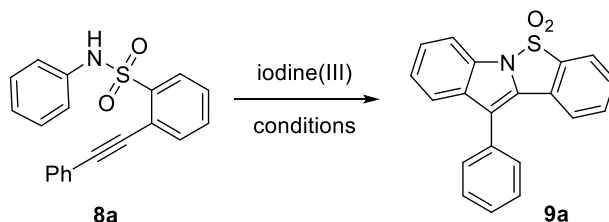


Figure 3.21 Example of the synthetic scheme for the preparation of the starting materials.

For the synthesis of the model substrate **8a**, commercial available 2-bromobenzene sulfonyl chloride **5** is condensed with aniline **6**, followed by a bromine/iodine exchange give the iodinated intermediate needed for the final Sonogashira coupling step with acetylene **7**. With this strategy, different functionalized derivatives of **8a** can be easily prepared choosing the appropriate substituted derivatives of **5**, **6**, and/or **7**.

3.3.2 Optimization of the reaction conditions

With the model substrate **8a** in hand, we explored the reactivity using stoichiometric amounts of different hypervalent iodine(III) reagents (Table 3.1).



Entry	Iodine(III)	Solvent	T (°C)	t	Yield (%) ^a
1	PIFA	DCM	25	10min	57
2	PIFA	DCM	0	6h	78
3	PIFA	DCM	-15	10h	64
4	PIDA	DCM	25	12h	<10 ^b
5	PIDA	HFIP	25	45min	85

^a: Isolated yield after purification. ^b: Based on the analysis of the crude mixture by ¹H-NMR spectroscopy.

Table 3.1 Table of the first trials using stoichiometric amounts of iodine(III) reagents.

The first experiment was carried out using PIFA (entry 1) at room temperature. Surprisingly, already after 10 minutes the expected product **9a** was readily observed by NMR control and further isolated in a 57% yield. Overlap of the aromatic signals in the ¹H NMR spectrum of the purified product made an immediate confirmation difficult, and the structure was unambiguously confirmed by X-ray analysis (Figure 3.22).

when hexafluoroisopropanol (HFIP) was used as the solvent, complete conversion was observed within 45 minutes and the cyclized product was obtained in an excellent 85% yield (entry 5). The best conditions (entries 2 and 5) were applied subsequently in the exploration of the substrate scope.

With these promising results for the stoichiometric version of the reaction, we decided to explore the possibility of the development of an iodine-based catalytic system. For this aim, experiments were carried out in the High Throughput Experimentation (HTE) Unit at ICIQ testing different conditions and explorative analyses by UPLC of all the crude samples taken from the reaction mixture.

Different iodine(I) compounds were tested (Figure 3.23). After trying commercially available iodobenzene and its derivatives (**10**, **11**), we tested the diiodo derivatives 1,2-diiodobenzene **12** and 2,2'-diiodobiphenyl **13**. According to the analyses of the product samples, best results were obtained with the latter diiodo compounds.

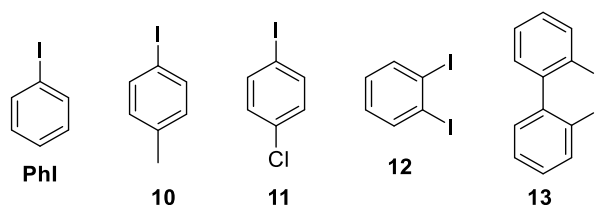
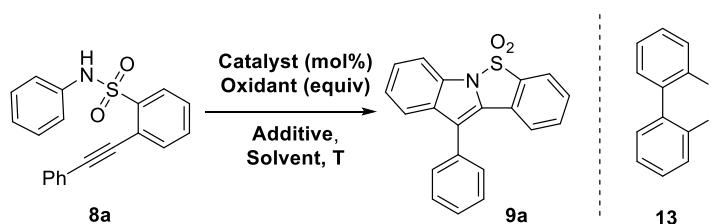


Figure 3.23 Possible iodine(I)-catalyst precursors tested in the HTE Unit.

All these catalyst were combined with three different oxidants, *m*-CPBA, AcOOH and TBHP in many solvents, such DCE, HFIP or TFE at room temperature. The effect of the addition of Lewis acids (TMSOTf, BF₃·OEt₂, TFA) and water were also tested.

The analyses of all the results provided by this experimentation led the way to find the needed clues for the development of the catalytic version of this cyclization reaction. The best conditions founded were then reproduced on mmol scale in the laboratory and adjusted to accomplish the best result. For this purpose, more than one hundred experiments were carried out following the positive results obtained on smaller scale. A summary of the optimization for the catalytic version of this transformation is summarized below (Table 3.2).



Entry	Catalyst (mol%)	Oxidant (equiv)	Additive	Solvent	T	Yield (%) ^a
1	PhI (20)	AcOOH (1.1)	-	HFIP	RT	33
2	PhI (20)	AcOOH (1.1)	AcOH	HFIP	RT	38
3	13 (20)	AcOOH (2.2)	-	HFIP	RT	64
4	13 (20)	<i>m</i> -CPBA (2.2)	TMSOTf	DCE	RT	35
5	13 (20)	<i>m</i> -CPBA (2.2)	TMSOTf	DCE	0	32
6	13 (10)	AcOOH (2.2)	-	HFIP	RT	47
7	13 (10)	AcOOH (2.0)	-	HFIP	RT	40
8	13 (10)	AcOOH (1.8)	-	HFIP	RT	40
9	13 (10)	AcOOH (1.6)	-	HFIP	RT	52
10	13 (10)	AcOOH (1.4)	-	HFIP	RT	51
11	13 (5)	AcOOH (2.2)	-	HFIP	RT	35
12	13 (5)	AcOOH (1.8)	-	HFIP	RT	45
13	13 (5)	AcOOH (1.5)	-	HFIP	RT	50
14	13 (5)	AcOOH (1.1)	-	HFIP	RT	62
15	13 (5)	AcOOH (0.95)	-	HFIP	RT	65
16	13 (10)	AcOOH (0.95)	-	HFIP	RT	55

^a: Isolated yield after purification.

Table 3.2 Results obtained with catalyst precursor **13**.

After observing that the diiodo-based catalysts showed higher activity, catalyst **13** was first explored together with commercial iodobenzene. The latter is oxidized by peracetic acid giving the final product in a 33% yield (entry 1). The addition of acetic acid slightly increased the yield (38%, entry 2). When the same catalytic amount of catalyst **13** is tested with 2.2 equivalents of the same oxidant, the yield increased to 64% (entry 3) confirming the activity that we observed on small scale. On this scale, we also

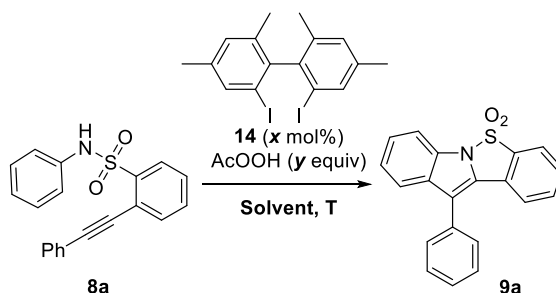
obtained some good results with *m*-CPBA in combination with TMSOTf, but no further increase was later observed (entries 4 and 5). Coming back to the choice of peracetic acid as the terminal oxidant, the catalyst loading was decreased to 10 mol% (entry 6). Under these conditions, the yield decreased. However, it is noteworthy that if the amount of oxidant was decreased, the isolated yield increased (entries 7, 8, 9 and 10).

After this observation, the catalyst loading was decreased to 5 mol% (entry 11). Once again, the best results were obtained when the amount of oxidant was decreased (entries 12, 13 and 14), giving the best result when it was employed as limiting agent (entry 15). Surprisingly, an increased catalyst loading of 10 mol% did not improve the latter result (entry 16). The best result obtained under the conditions described in entry 15 was to be applied later for the substrate scope.

We next decided to vary the electronics in the aryl rings of the catalyst by using Kita's catalyst **14** (Table 3.3).¹²⁸ When the best conditions discovered for catalyst **13**, the cyclized product was obtained in low yield (44%, entry 1). Increasing catalyst loading, at the first moment, decreased the yield (35%, entry 2); but, when 20 mol% of catalyst **14** was employed, the yield slightly increased to 50% (entry 3). If the amount of oxidant is increased, 57% of the desired product was isolated (entry 4).

After observing that upon increasing the amount of oxidant the yield dropped (entry 5), we decided to add the oxidant sequentially in two portions. With this protocol, 20 mol% of catalyst **14** was used, and the cyclized product was isolated in 61% yield (entry 6). In order to avoid the observed degradation, we tried to combine two solvents (entry 7) and the oxidant addition at 0 °C increasing the yield to 78% (entry 9). Larger amounts of the oxidant did not show good results (entries 10 and 11), neither did diminished amounts of catalyst (entries 12 and 13). Different solvent mixtures from dichloroethane and hexafluoroisopropanol were tried without any beneficial effect (entries 14, 15, 16 and 17). With all of these results in hand, the conditions described in entry 9 were selected for application in the investigation on substrate scope.

¹²⁸ Dohi, T.; Takenaga, N.; Fukushima, K.; Uchiyama, T.; Kato, D.; Motoo, S.; Fujioka, H.; Kita, Y. *Chem. Commun.* **2010**, *46*, 7697.



Entry	x (mol%)	y (equiv)	Solvent	T	Yield (%) ^a
1	5	0.095	HFIP	RT	44
2	10	0.095	HFIP	RT	35
3	20	0.095	HFIP	RT	50
4	10	1.1	HFIP	RT	57
5	10	2	HFIP	RT	39
6 ^b	20	1.5	HFIP	RT	61
7 ^b	20	1.5	HFIP:DCE (1:1)	RT	59
8 ^b	20	1.5	HFIP:DCE (1:1)	0-RT	69
9 ^b	20	1.8	HFIP:DCE (1:1)	0-RT	78
10 ^b	20	2	HFIP:DCE (1:1)	0-RT	63
11 ^b	20	2.2	HFIP:DCE (1:1)	0-RT	53
12 ^b	15	1.8	HFIP:DCE (1:1)	0-RT	71
13 ^b	15	2	HFIP:DCE (1:1)	0-RT	75
14 ^b	20	1.8	HFIP:DCE (2:1)	0-RT	64
15 ^b	20	1.8	HFIP:DCE (3:1)	0-RT	53
16 ^b	20	1.8	HFIP:DCE (1:3)	0-RT	61
17 ^b	20	2	HFIP:DCE (1:3)	0-RT	60

^a: Isolated yield after purification. ^b: Sequential addition of the oxidant in two portions (second after 15 min reaction time). In some cases, the addition is at 0 °C.

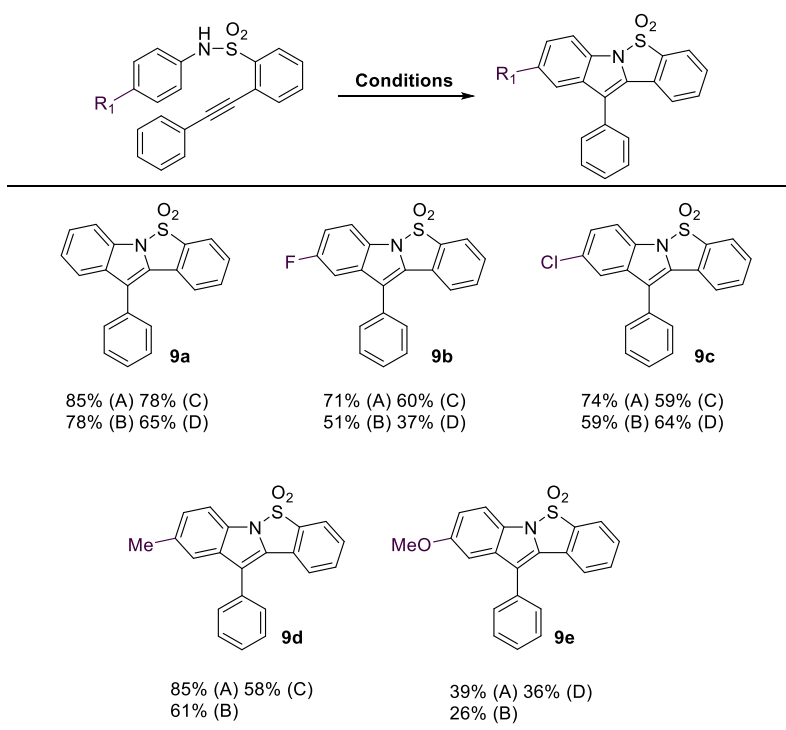
Table 3.3 Results obtained when catalyst **14** is used.

In summary, we identified four different protocols, two stoichiometric and two catalytic ones, which anticipate the versatility of this cyclization.

3.3.3 Scope for the cyclization reaction

After an extensive screening for the optimization of the reaction, 18 substrates with different substitution pattern at all three arene rings were successfully cyclized to the correspondent products conducting the reactions under the developed protocols.

Some derivatives with different substituents in *para* position of the aniline ring were transformed into the correspondent cyclized products. Halogen (**9b**, **c**) and electron-donating (**9d**, **e**) substituted products were isolated in good yields under both the stoichiometric and the catalytic conditions (Figure 3.24).



(A): starting sulfonamide **8** (0.1 mmol), PIDA (0.15 mmol) in HFIP (1 mL) at RT.

(B): starting sulfonamide **8** (0.085 mmol), PIFA (0.094 mmol) in DCM (1 mL) at 0 °C.

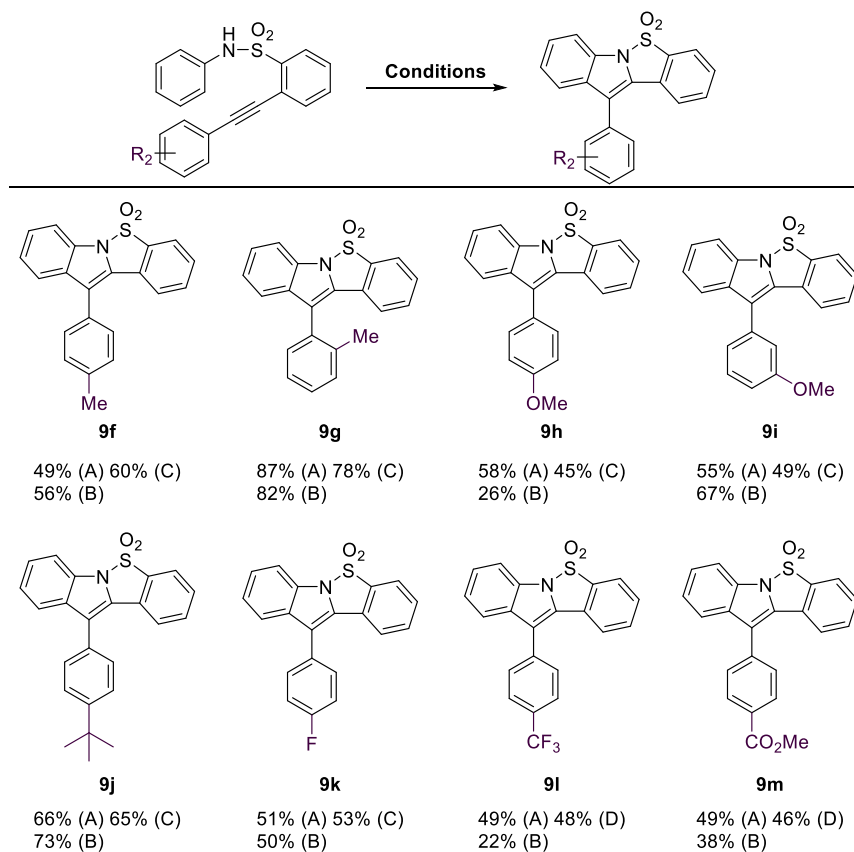
(C): starting sulfonamide **8** (0.1 mmol), **14** (20 mol%), AcOOH (0.18 mmol) in HFIP/DCE (1/1, v/v, 1 mL) from 0 °C to RT.

(D): starting sulfonamide **8** (0.1 mmol), **13** (5 mol%), AcOOH (0.095 mmol) in HFIP (1 mL) at RT.

Figure 3.24 Scope for different substituents at the *para* position of the aniline arene ring.

The present transformation also tolerates several functional groups in different positions in the acetylene aryl moiety (Figure 3.25). Electron-donating substituents as in

derivatives **9f-j** and electron-withdrawing ones in **9k-m** were successfully converted into the corresponding cyclized products in good to excellent yields.



(A): starting sulfonamide **8** (0.1 mmol), PIDA (0.15 mmol) in HFIP (1 mL) at RT.
 (B): starting sulfonamide **8** (0.085 mmol), PIFA (0.094 mmol) in DCM (1 mL) at 0 °C.
 (C): starting sulfonamide **8** (0.1 mmol), **14** (20 mol%), AcOOH (0.18 mmol) in HFIP/DCE (1/1, v/v, 1 mL) from 0 °C to RT.
 (D): starting sulfonamide **8** (0.1 mmol), **13** (5 mol%), AcOOH (0.095 mmol) in HFIP (1 mL) at RT.

Figure 3.25 Scope for different substituents at the arene ring of the acetylene moiety.

Di- and tri-substituted aryl rings as in **9n, o** and different aromatic rings at the acetylene residue as in **9q, r** were also found to be fully compatible with the different reaction conditions (Figure 3.26). Substitution at the aryl ring of the sulfonyl tether group is tolerated as well (product **9p**).

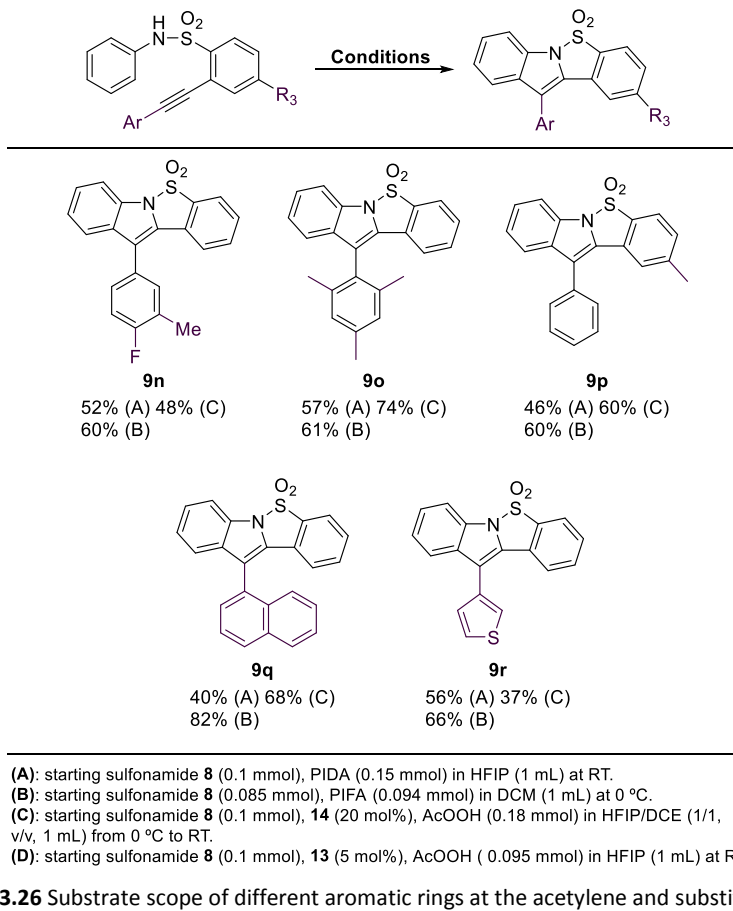


Figure 3.26 Substrate scope of different aromatic rings at the acetylene and substituted aryl sulfonyl tether derivative.

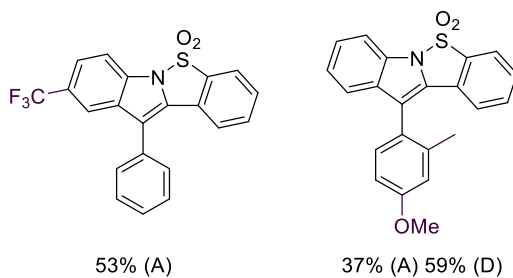


Figure 3.27 Less successful substrates under the different reaction conditions.

A total of 18 examples with different substitution pattern at the three different arene rings demonstrate the capacity of the present transformation to become a general route in the arsenal of indole syntheses. However, as with all methodology, some of the substituted derivatives are beyond the general scope and thus provide lower yields, if any (Figure 3.27).

3.3.4. Mechanistic studies and final proposal

As in Chapter 2, to clarify the mechanism of the present cyclization reaction, we designed the following kinetic competition experiment (Figure 3.28). The deuterated compound **8g-d₅** labelled at the aniline aryl ring together with the corresponding derivative **8g** were submitted under the standard procedure A. No kinetic isotope effect was observed ($k_H/k_D = 1.0$).

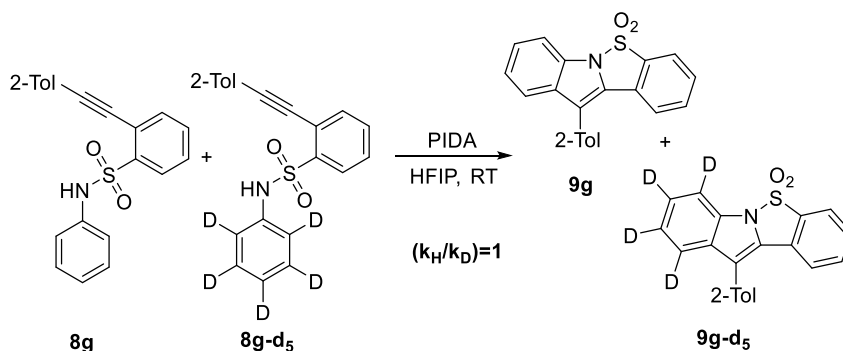


Figure 3.28 Kinetic competition experiment under standard procedure A.

In order to obtain additional information about the mechanism of the present transformation, a Hammett correlation experiment was carried out with the correspondingly substituted amides **8f**, **j**, **k**, **l** in competition with the model substrate **8a** under standard procedure A used previously (Figure 3.29).

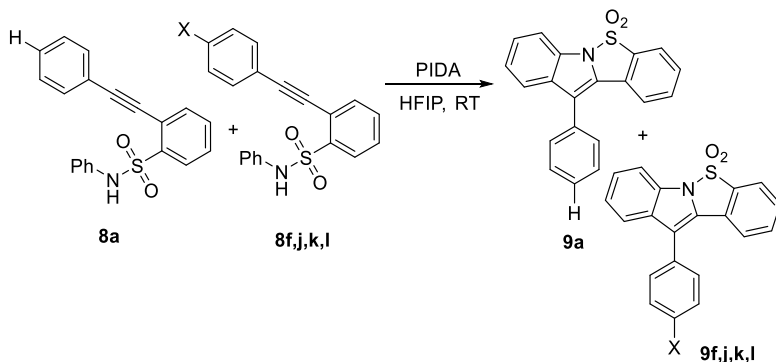


Figure 3.29 Reaction scheme for the Hammett correlation experiment.

For each independent run, the ratio of the two products was calculated employing GC chromatography (Figure 3.30). For the case of entry 5, for the correct integration, a correction factor calculated had to be introduced using mesitylene as a standard using the same analytical technique. A ρ -value of -0.35 was obtained after analysis of the Hammett plot.

Entry	X	$\log(k_X/k_H)$	Hammett constant σ_{p-X}
1	CF ₃	-0,1919469	0,54
2	F	-0,0194416	0,062
3	H	0	0
4	<i>t</i> -Bu	0,07786149	-0,197
5	Me	0,04320055	-0,17

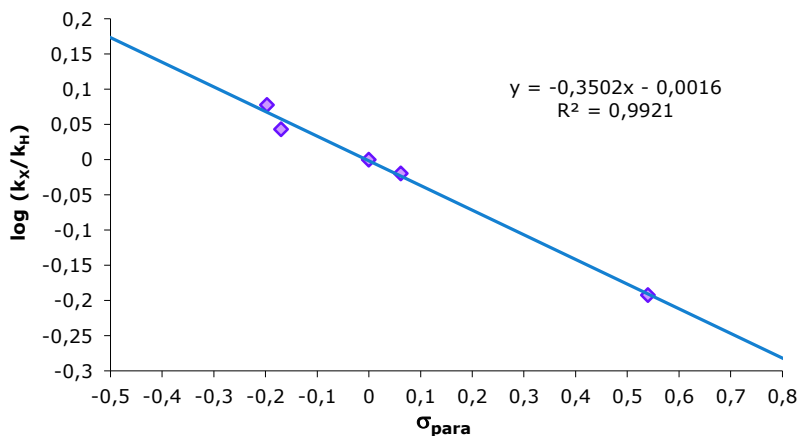


Figure 3.30 Data from the Hammett correlation.

Evaluating the results obtained through these two competition experiments, we propose the following mechanistic context (Figure 3.31). As already described in Figure 3.16, we propose that the reaction starts with the interaction between the hypervalent iodine reagent and the substrate **8**, most probably through the formation of a discrete I-N bond. The heterolytic cleavage of this bond generates an electrophilic nitrogen¹²⁹ (**VI**) that is subsequently attacked by the acetylene moiety through a 5-exo-dig cyclization. This intermediary vinylic cation **VII** undergoes further cyclization by nucleophilic attack of the aromatic ring of the aniline (**VIII**).¹³⁰ Rearomatization to the final product **9** is accomplished upon loss of a proton. This step is comparably fast as demonstrated by the kinetic competition experiment between **8g** and **8g-d₅**, which provided no observable kinetic isotope effect ($k_H/k_D = 1.0$). The ρ -value of -0.35 from Hammett correlation using electronic information at the remote aryl group of the tolane core indicates that the slow step of the overall reaction belongs to one of the electrophilic cyclization events at stages **VI** or **VII**.

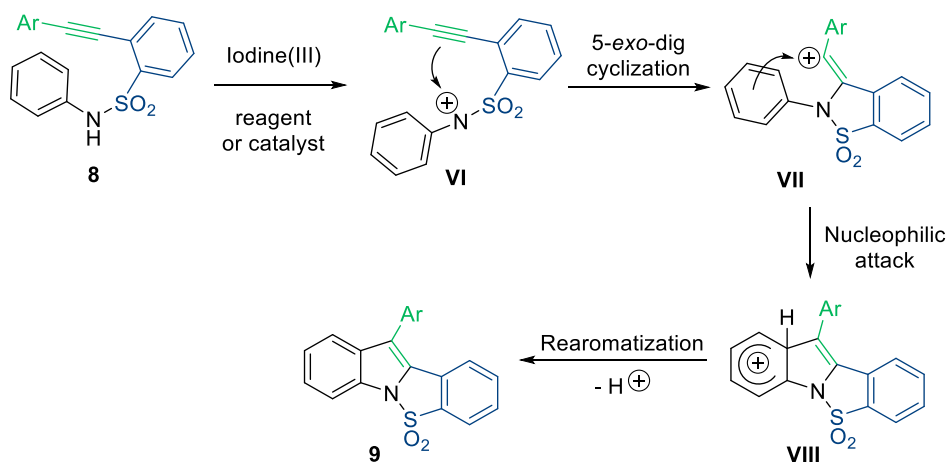


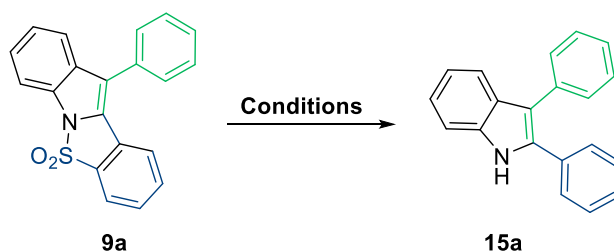
Figure 3.31 Mechanistic proposal based on control experiments.

¹²⁹ Antonchick, A. P.; Samanta, R.; Kulikov, K.; Lategahn, J. *Angew. Chem. Int. Ed.* **2011**, *50*, 8605.

¹³⁰ Ito, M.; H. Kubo, H.; I. Itani, I.; Morimoto, K.; Dohi, T.; Kita, Y. *J. Am. Chem. Soc.* **2013**, *135*, 14078.

3.3.5. Removal of tether and isolation of final indole.

To complete this new methodology toward indole synthesis, the sulfonyl tether used for the reaction control should be removed tracelessly in the final step. For this aim, some experiments were carried out with different methodologies derived from literature precedence (Table 3.4), although the obtained yields were at best unsatisfactory.



Entry	Conditions	Yield (%) ^a
1	Mg (5 equiv), MeOH:THF, RT	19
2	Mg (5 equiv), EtOH, RT	-
3	Mg (3 equiv), MeOH:THF, RT	25
4	Mg (2 equiv), MeOH:THF, RT	33
5	Mg (1.5 equiv), MeOH:THF, RT	22
6	Mg (350 equiv), NH ₄ Cl (0.3 equiv) MeOH:THF, RT	-
7	TBAF, THF, 65 °C	-
8	K ₂ CO ₃ , MeOH reflux	-
9	10% aq. NaOH, EtOH:DMSO, 50 °C	-
10	KOH (22 equiv), MeOH, 70 °C	-
11	KOH (33 equiv), MeOH, 65 °C	-

^a: Isolated yield after purification.

Table 3.4 Unsuccessful results obtained during the optimization of the tether removal.

After this evaluation, we decided to focus in the use of a magnesium-based procedure. We found that treatment of the cyclization products **9** with titanium tetraisopropoxide, elemental magnesium and TMSCl afforded the desired free 2,3-diarylated indoles in very good yields as demonstrated for the four derivatives **15a**, **f**, **k**, **l** (Figure 3.32).

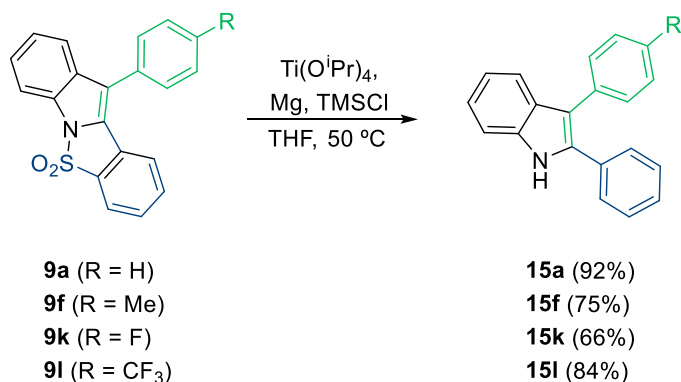


Figure 3.32 Successful tether removal procedure for preparation of 2,3-diarylated free indoles.

3.4. Conclusions

We have presented a new methodology for the construction of the indole core, which complements the synthesis presented in Chapter 2. We have successfully developed an iodine(III)-mediated or catalyzed formation of indoles through a new sequential N-H/C-H oxidation reaction. After an extensively screening of the conditions, we propose four different protocols for the cyclization reaction.

A total of 18 derivatives with different substitution pattern were fruitfully cyclized under stoichiometric amounts of a preformed iodine(III) reagents and under iodine(III) catalysis.

Some kinetic competition experiments, such as deuterium labelling or Hammett correlation were carried out in order to elucidate the reaction mechanism. This experiments support our mechanistic proposal.

Finally, we confirmed that the sulfonyl tether that was installed for reaction control, can be readily removed in a traceless manner to provide regioselective access to 2,3-diarylated indoles.

3.5. Experimental part

General remarks: All solvents, reagents and all deuterated solvents were purchased from Aldrich and TCI commercial suppliers. Column chromatography was performed with silica gel (Merck, type 60, 0.063-0.2 mm). NMR spectra were recorded on a Bruker Avance 400 MHz or 500 MHz spectrometer, respectively. All chemical shifts in NMR experiments were reported as ppm downfield from TMS. The following calibrations were used: CDCl_3 $\delta = 7.26$ and 77.16 ppm. MS (ESI-LCMS) experiments were performed using an Agilent 1100 HPLC with a Bruker micro-TOF instrument (ESI). MS (EI) and HRMS experiments were performed on a Kratos MS 50 within the service centres at ICIQ. IR spectra were taken in a Bruker Alpha instrument in the solid state. The following compounds were commercially available and used as received: 2-bromobenzenesulfonyl chloride, aniline, *p*-anisidine, 4-fluoroaniline, *p*-toluidine, 4-

chloroaniline, aniline-*d*₆, phenylacetylene, 4-ethynylanisole, 4-*tert*-butylphenylacetylene, 4-ethynyltoluene, 1-ethynyl-4-fluorobenzene, 4-ethynyl- α,α,α -trifluorotoluene, methyl 4-ethynylbenzoate, 2-ethynyltoluene, 3-ethynylanisole, 4-ethynyl-1-fluoro-2-methylbenzene, 2-ethynyl-1,3,5-trimethylbenzene, 1-ethynyl-naphthalene, 3-ethynylthiophene, pyridine, iodine, *n*-butyllithium solution (2M in cyclohexanes), dichlorobis(triphenylphosphine)palladium(II), triethylamine, cuprous iodide, (diacetoxyiodo)benzene, [bis(trifluoroacetoxy)iodo]benzene, peracetic acid solution (36-40 wt. % in acetic acid), magnesium, titanium (IV) tetraisopropoxide and trimethylsilyl chloride. The following compounds were synthesized according to literature procedures: 2,2'-diiodo-1,1'-biphenyl and 2,2'-diiodo-4,4',6,6'-tetramethyl-1,1'-biphenyl.¹³¹ The spectral data of these compounds match the ones reported in the original literature.¹³¹

General procedure for the synthesis of starting materials (GP5):

Sulfonamide starting materials **8** were synthesized following a three-step procedure as outlined below (Figure 3.33).

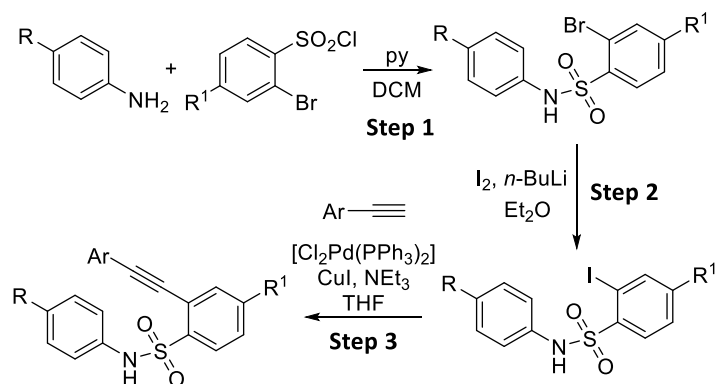


Figure 3.33 Synthetic scheme for precursor's synthesis.

Step 1. To a solution of the corresponding aniline (1 mmol) in DCM (2 mL) were added the corresponding benzenesulfonyl chloride (1.1 mmol) and pyridine (3 mmol). The mixture was stirred at room temperature overnight. Then, water was added and the mixture was extracted with DCM (3 x 15 mL). The combined organic layers were washed

¹³¹ Dohi, T.; Kato, D.; Hyodo, R.; Yamashita, D.; Shiro, M.; Kita, Y. *Angew. Chem. Int. Ed.* **2011**, *50*, 3784.

with an aqueous solution of HCl (10%), a saturated aqueous solution of NaHCO₃ and a saturated aqueous solution of brine, and dried over anhydrous Na₂SO₄. The solvent was removed under reduced pressure. Compounds were purified by crystallisation from chloroform and hexane.

Step 2. The solid obtained in the previous step (1 mmol) was dissolved in Et₂O (4.5 mL) and cooled to -78 °C. Then, *n*-butyllithium (2M solution in cyclohexanes, 16.4 mL) was added dropwise under argon. After stirring at room temperature for two hours, molecular iodine (1.2 mmol) was added and the reaction mixture was stirred overnight. The reaction was quenched with a saturated aqueous solution of Na₂S₂O₃ and extracted with Et₂O (3 x 20 mL). The combined organic layers were dried over anhydrous Na₂SO₄. The solvent was removed under reduced pressure. The obtained crude product was submitted to the next step directly.

Step 3. To a deoxygenated solution of the corresponding iodinated sulfonamide (1 mmol), Cl₂Pd(PPh₃)₂ (0.05 mmol) and CuI (0.10 mmol) in THF (3.6 mL), the corresponding acetylene (1.2 mmol) and NEt₃ (1.2 mmol) were added directly. The reaction mixture was stirred at room temperature overnight. Then, a saturated aqueous solution of NH₄Cl was added and the mixture was extracted with DCM (3 x 15 mL). The combined organic layers were dried over anhydrous Na₂SO₄ and the solvent was removed under reduced pressure. The residue was purified by column chromatography (silica gel, *n*-hexane/ethyl acetate, 90/10, v/v) to give the pure product **8**.

General procedures for the cyclization reactions:

General procedure for the stoichiometric cyclization with (diacetoxyiodo)benzene (PIDA) (GP6): In a Pyrex tube, the corresponding starting material (0.1 mmol) was dissolved in HFIP (1 mL) and (diacetoxyiodo)benzene (PIDA, 0.15 mmol) was added to the solution. The reaction was monitored by TLC chromatography. When the reaction was finished, the solvent was removed under reduced pressure and the residue was purified by column chromatography (silica gel, *n*-hexane/ethyl acetate, 95/5, v/v).

General procedure for the stoichiometric cyclization with [bis(trifluoroacetoxy)iodo]benzene (PIFA) (GP7): A solution of the corresponding starting material (0.085 mmol) in DCM (1 mL) was cooled to 0 °C and

[bis(trifluoroacetoxy)iodo]benzene (PIFA, 0.094 mmol) was added. The reaction was monitored by TLC chromatography. Then, the solvent was removed under reduced pressure and the residue was purified by column chromatography (silica gel, *n*-hexane/ethyl acetate, 95/5, v/v).

General procedure for the iodine (III)-catalyzed cyclization with 2,2'-diiodo-4,4',6,6'-tetramethyl-1,1'-biphenyl (GP8): A solution of the corresponding starting material (0.1 mmol) and 2,2'-diiodo-4,4',6,6'-tetramethyl-1,1'-biphenyl (0.02 mmol) in a mixture of DCE and HFIP (1/1, v/v, 1 mL) was cooled to 0 °C. Then, peracetic acid (0.18 mmol, 36-40 wt. % solution in acetic acid) was added in 2 equal portions (second portion was added after 15 min). The reaction mixture was stirred at 0 °C for 30 minutes and was allowed to reach room temperature. The reaction was monitored by TLC chromatography. Once the reaction was finished, the solvent was removed under reduced pressure and the product was purified by column chromatography (silica gel, *n*-hexane/ethyl acetate, 95/5, v/v).

General procedure for the iodine (III)-catalyzed cyclization with 2,2'-diiodo-1,1'-biphenyl (GP9): A pyrex tube is charged with the corresponding starting sulfonamide (0.1 mmol), 2,2'-diiodo-1,1'-biphenyl (5 mol%) in HFIP (1 mL) and peracetic acid (0.095 mmol, 36-40 wt. % solution in acetic acid) was added at room temperature. The reaction was monitored by TLC chromatography. Once the reaction was finished, the solvent was removed under reduced pressure and the product was purified by column chromatography (silica gel, *n*-hexane/ethyl acetate, 95/5, v/v).

Procedures for kinetic competition experiments:

Kinetic isotopic effect: KIE experiment was carried out following the general procedure (GP6) with 5 equivalents of substrate **8g** and 5 equivalents of substrate **8g-d₅** (Figure 3.34).

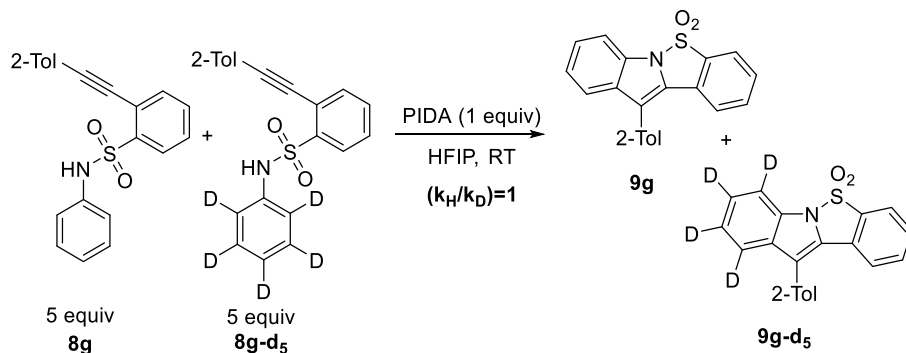


Figure 3.34 Reaction scheme for KIE experiment.

Hammett correlation studies: A Pyrex tube equipped with a stirrer bar is charged with *N*-phenyl-2-(phenylethynyl)benzenesulfonamide **8a** (5 equiv, 0.1 mmol) and the corresponding substituted sulfonamide **8f,j,k,l** (5 equiv, 0.1 mmol), dissolved in HFIP (2 mL) and (diacetoxyiodo)benzene (PIDA, 1.0 equiv, 0.01 mmol) was added to the solution. The solution was stirred at 25 °C (Figure 3.35).

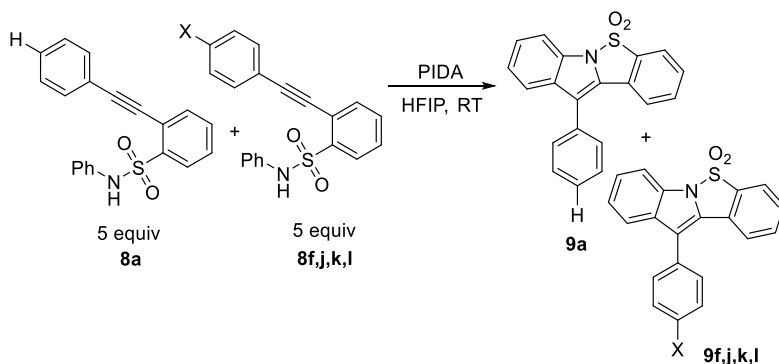


Figure 3.35 Reaction scheme for Hammett correlation studies.

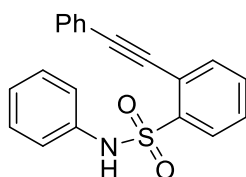
Deprotection and isolation of free indoles (GP10): The N-S bond was cleaved following a previously reported procedure.¹³² A heat-dried Schlenk was charged with the corresponding cyclic sulfonamide (1 equiv, 0.3 mmol), Mg (5 equiv, 1.5 mmol) and THF (1.5 mL). Then, Ti(O^{*i*}Pr)₄ (1 equiv, 0.3 mmol) and TMSCl (1.5 equiv, 0.45 mmol) were added. The reaction was stirred at 50 °C. After 12 hours, 0.12 ml of a 3M aqueous

¹³² Shohji, N.; Kawaji, T.; Okamoto, S. *Org. Lett.* **2011**, *13*, 2626.

solution of NaOH, 4.5 mL of Et₂O, 0.3 g of NaF and 0.3 g of Celite[®] were sequentially added at room temperature. After being stirred for 30 min, the mixture was filtered through Celite[®]. To the resulting filtrate, a 3M aqueous solution of NaOH was added and the mixture was extracted with Et₂O (3 x 15 mL). The combined organic layers were washed with a 3M aqueous solution of NaOH (3 x 15 mL), dried over MgSO₄, filtered and concentrated. The residue was purified by column chromatography (silica gel, *n*-hexane/ethyl acetate, 98/2, v/v).

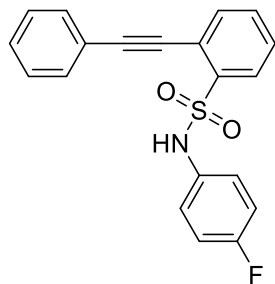
Data for the starting materials 8:

***N*-Phenyl-2-(phenylethynyl)benzenesulfonamide (8a)**

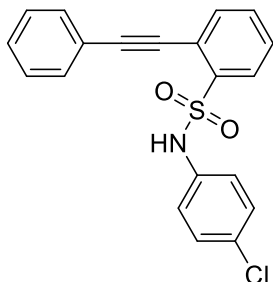


Synthesized following GP5. Brown solid, 95%. ¹H NMR (400 MHz, CDCl₃): δ = 7.94 (dd, *J* = 7.9, 1.3 Hz, 1H), 7.69-7.65 (m, 3H), 7.49 (td, *J* = 7.6, 1.4 Hz, 1H), 7.48-7.41 (m, 3H), 7.36 (td, *J* = 7.8, 1.3 Hz, 1H), 7.22-7.16 (m, 3H), 7.14-7.10 (m, 2H), 7.09-7.04 (m, 1H). ¹³C NMR (101 MHz, CDCl₃): δ = 139.9, 136.3, 134.2, 132.6, 131.9, 130.0, 129.8, 129.4, 128.9, 128.5, 125.8, 122.2, 121.9, 121.0, 98.0, 86.3. HRMS (ESI-MS): calcd for C₂₀H₁₆NO₂S: 334.0896; found: 334.0897. IR ν (cm⁻¹): 3278, 3070, 3048, 2957, 2873, 2212, 1597. m.p.: 103-104 °C.

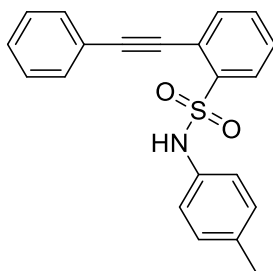
***N*-(4-Fluorophenyl)-2-(phenylethynyl)benzenesulfonamide (8b)**



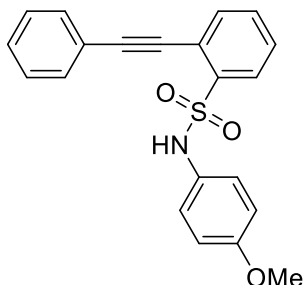
Synthesized following GP5. Brown oil, 70%. ¹H NMR (500 MHz, CDCl₃): δ = 7.88 (dd, *J* = 8.0, 1.3 Hz, 1H), 7.72-7.64 (m, 3H), 7.51 (td, *J* = 7.6, 1.3 Hz, 1H), 7.45-7.42 (m, 3H), 7.36 (td, *J* = 7.7, 1.4 Hz, 1H), 7.15-7.07 (m, 3H), 6.92-6.85 (m, 2H). ¹³C NMR (126 MHz, CDCl₃): δ = 160.9 (d, *J*_{C-F} = 245.7 Hz), 139.6, 134.2, 132.7, 132.1 (d, *J*_{C-F} = 3.1 Hz), 131.9, 130.0, 129.9, 128.9, 128.6, 125.1 (d, *J*_{C-F} = 8.4 Hz), 121.7, 120.9, 116.2 (d, *J*_{C-F} = 22.9 Hz), 98.2, 86.2. ¹⁹F NMR (376 MHz, CDCl₃): δ = -115.90. HRMS (ESI-MS): calcd for C₂₀H₁₄FNNaO₂S: 374.0621; found: 374.0617. IR ν (cm⁻¹): 3327, 3276, 3062, 3033, 2955, 2928, 2215, 1598.

***N*-(4-Chlorophenyl)-2-(phenylethynyl)benzenesulfonamide (8c)**

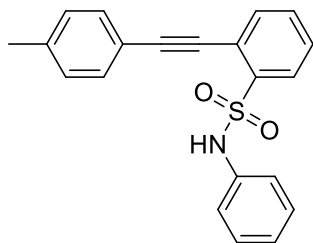
Synthesized following GP5. Brown oil, 92%. $^1\text{H NMR}$ (400 MHz, CDCl_3): δ = 7.92 (dd, J = 8.0, 1.3 Hz, 1H), 7.70-7.64 (m, 3H), 7.52 (td, J = 7.6, 1.3 Hz, 1H), 7.47-7.42 (m, 3H), 7.38 (td, J = 7.8, 1.3 Hz, 1H), 7.18-7.12 (m, 3H), 7.08-7.03 (m, 2H). $^{13}\text{C NMR}$ (101 MHz, CDCl_3): δ = 139.5, 134.8, 134.2, 132.8, 131.9, 131.5, 130.0, 129.9, 129.5, 129.0, 128.7, 123.6, 121.7, 120.9, 98.2, 86.1. HRMS (ESI-MS): calcd for $\text{C}_{20}\text{H}_{13}\text{ClNO}_2\text{S}$: 366.0361; found: 366.0357. IR ν (cm^{-1}): 3273, 3059, 2959, 2926, 2215, 1717, 1597.

***N*-(4-tolyl)-2-(phenylethynyl)benzenesulfonamide (8d)**

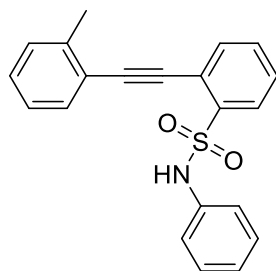
Synthesized following GP5. Brown solid, 99%. $^1\text{H NMR}$ (500 MHz, CDCl_3): δ = 7.91 (dd, J = 7.9, 1.3 Hz, 1H), 7.70-7.64 (m, 3H), 7.49 (td, J = 7.6, 1.3 Hz, 1H), 7.46-7.40 (m, 3H), 7.35 (td, J = 7.8, 1.3 Hz, 1H), 7.10 (bs, 1H), 7.02-6.97 (m, 4H), 2.22 (s, 3H). $^{13}\text{C NMR}$ (126 MHz, CDCl_3): δ = 140.0, 135.9, 134.1, 133.5, 132.5, 131.9, 130.0, 129.9, 129.8, 128.9, 128.5, 122.8, 121.9, 120.9, 98.0, 86.3, 21.0. HRMS (ESI-MS): calcd for $\text{C}_{21}\text{H}_{17}\text{NNO}_2\text{S}$: 370.0872; found: 370.0862. IR ν (cm^{-1}): 3347, 3071, 3040, 2922, 2854, 2218, 1979, 1948, 1908, 1609. m.p.: 101-103 °C.

***N*-(4-Methoxyphenyl)-2-(phenylethynyl)benzenesulfonamide (8e)**

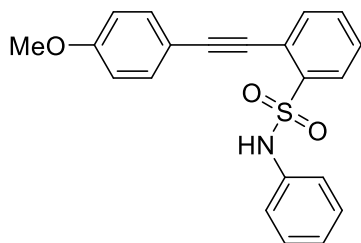
Synthesized following GP5. Brown oil, 73%. $^1\text{H NMR}$ (500 MHz, CDCl_3): δ = 7.86 (ddd, J = 7.9, 1.3, 0.5 Hz, 1H), 7.70 (ddd, J = 7.6, 1.3, 0.5 Hz, 1H), 7.67-7.64 (m, 2H), 7.50 (td, J = 7.6, 1.3 Hz, 1H), 7.44-7.42 (m, 3H), 7.34 (td, J = 7.8, 1.3 Hz, 1H), 7.08-7.02 (m, 3H), 6.73-6.68 (m, 2H), 3.70 (s, 3H). $^{13}\text{C NMR}$ (126 MHz, CDCl_3): δ = 158.2, 140.0, 134.1, 132.5, 131.9, 130.0, 129.8, 128.9, 128.7, 128.6, 125.6, 121.9, 120.9, 114.5, 98.1, 86.3, 55.5. HRMS (ESI-MS): calcd for $\text{C}_{21}\text{H}_{17}\text{NNO}_3\text{S}$: 386.0821; found: 386.0822. IR ν (cm^{-1}): 3278, 3060, 2954, 2932, 2836, 2215, 1736, 1597.

***N*-Phenyl-2-(*p*-tolylethynyl)benzenesulfonamide (8f)**

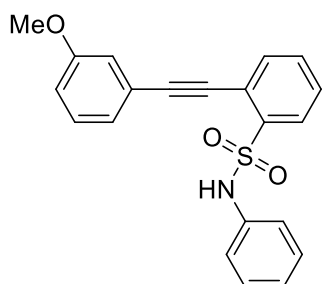
Synthesized following GP5. Brown oil, 83%. $^1\text{H NMR}$ (400 MHz, CDCl_3): δ = 7.93 (dd, J = 8.0, 1.3 Hz, 1H), 7.66 (dd, J = 7.7, 1.3 Hz, 1H), 7.56 (d, J = 8.1 Hz, 2H), 7.48 (td, J = 7.6, 1.3 Hz, 1H), 7.34 (td, J = 7.7, 1.3 Hz, 1H), 7.25 (d, J = 7.8 Hz, 2H), 7.20-7.16 (m, 3H), 7.15-7.08 (m, 2H), 7.10-7.01 (m, 1H), 2.41 (s, 3H). $^{13}\text{C NMR}$ (101 MHz, CDCl_3): δ = 140.3, 139.7, 136.3, 134.1, 132.6, 131.8, 130.0, 129.7, 129.4, 128.3, 125.8, 122.2, 121.1, 118.8, 98.4, 85.8, 21.8. HRMS (ESI-MS): calcd for $\text{C}_{21}\text{H}_{17}\text{NNaO}_2\text{S}$: 370.0872; found: 370.0865. IR ν (cm^{-1}): 3327, 3029, 2920, 2858, 2213, 1738, 1599.

***N*-Phenyl-2-(*o*-tolylethynyl)benzenesulfonamide (8g)**

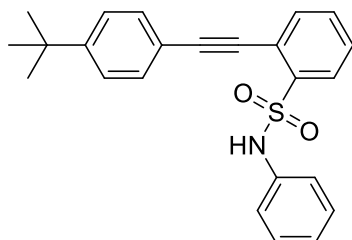
Synthesized following GP5. Brown oil, quantitative. $^1\text{H NMR}$ (400 MHz, CDCl_3): δ = 7.94 (dd, J = 7.9, 1.3 Hz, 1H), 7.69 (dd, J = 7.7, 1.3 Hz, 1H), 7.66-7.61 (m, 1H), 7.49 (td, J = 7.6, 1.4 Hz, 1H), 7.40-7.27 (m, 4H), 7.24-7.15 (m, 3H), 7.15-7.01 (m, 3H), 2.62 (s, 3H). $^{13}\text{C NMR}$ (101 MHz, CDCl_3): δ = 140.9, 139.5, 136.3, 134.4, 132.6, 132.5, 130.1, 129.9, 129.8, 129.4, 128.5, 126.1, 125.8, 122.2, 121.7, 121.2, 97.2, 89.7, 21.1. HRMS (ESI-MS): calcd for $\text{C}_{21}\text{H}_{17}\text{NNaO}_2\text{S}$: 370.0872; found: 370.0876. IR ν (cm^{-1}): 3267, 3061, 3021, 2921, 2211, 1718, 1598.

2-((4-Methoxyphenyl)ethynyl)-*N*-phenylbenzenesulfonamide (8h)

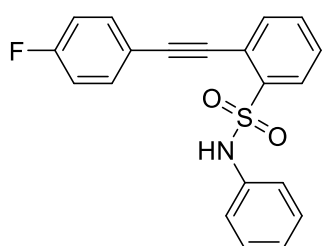
Synthesized following GP5. Brown solid, 86%. $^1\text{H NMR}$ (500 MHz, CDCl_3): δ = 7.92 (dd, J = 8.1, 1.4 Hz, 1H), 7.66-7.57 (m, 3H), 7.47 (td, J = 7.6, 1.3 Hz, 1H), 7.32 (td, J = 7.7, 1.3 Hz, 1H), 7.23-7.15 (m, 3H), 7.14-7.09 (m, 2H), 7.09-7.03 (m, 1H), 6.98-6.90 (m, 2H), 3.86 (s, 3H). $^{13}\text{C NMR}$ (101 MHz, CDCl_3): δ = 160.8, 139.5, 136.3, 133.9, 133.5, 132.6, 129.9, 129.3, 128.1, 125.8, 122.2, 121.3, 114.6, 113.8, 98.4, 85.2, 55.6. HRMS (ESI-MS): calcd for $\text{C}_{21}\text{H}_{17}\text{NNaO}_3\text{S}$: 386.0821; found: 386.0805. IR ν (cm^{-1}): 3282, 3072, 3037, 3010, 2961, 2931, 2832, 2206, 1602. m.p.: 109-111 °C.

2-((3-Methoxyphenyl)ethynyl)-*N*-phenylbenzenesulfonamide (8i)

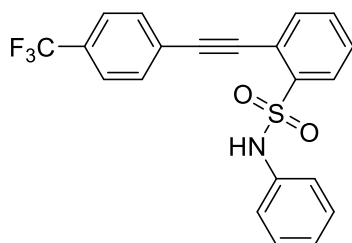
Synthesized following GP5. Brown solid, 70%. $^1\text{H NMR}$ (400 MHz, CDCl_3): δ = 7.94 (dd, J = 8.0, 1.3 Hz, 1H), 7.67 (dd, J = 7.7, 1.3 Hz, 1H), 7.49 (td, J = 7.6, 1.3 Hz, 1H), 7.38-7.31 (m, 2H), 7.30-7.23 (m, 1H), 7.22-7.15 (m, 4H), 7.14-7.09 (m, 2H), 7.09-7.03 (m, 1H), 7.00 (ddd, J = 8.3, 2.7, 1.1 Hz, 1H), 3.86 (s, 3H). $^{13}\text{C NMR}$ (126 MHz, CDCl_3): δ = 159.8, 139.9, 136.2, 134.2, 132.6, 130.0, 130.0, 129.4, 128.6, 125.8, 124.4, 122.8, 122.2, 120.8, 116.3, 116.6, 97.9, 86.0, 55.6. **HRMS (ESI-MS)**: calcd for $\text{C}_{21}\text{H}_{15}\text{NNaO}_3\text{S}$: 384.0665; found: 384.0664. **IR v (cm^{-1})**: 3241, 3069, 2998, 2952, 2935, 2829, 2209, 1596. **m.p.**: 71-73 °C.

2-((4-(*tert*-Butyl)phenyl)ethynyl)-*N*-phenylbenzenesulfonamide (8j)

Synthesized following GP5. Brown solid, 80%. $^1\text{H NMR}$ (400 MHz, CDCl_3): δ = 7.93 (dd, J = 8.0, 1.5 Hz, 1H), 7.66 (dd, J = 7.7, 1.3 Hz, 1H), 7.64-7.59 (m, 2H), 7.52-7.43 (m, 3H), 7.34 (td, J = 7.8, 1.3 Hz, 1H), 7.24-7.14 (m, 3H), 7.16-7.09 (m, 2H), 7.09-7.03 (m, 1H), 1.36 (s, 9H). $^{13}\text{C NMR}$ (101 MHz, CDCl_3): δ = 153.3, 139.8, 136.3, 134.1, 132.6, 131.7, 129.9, 129.3, 128.3, 126.0, 125.8, 122.2, 121.1, 118.8, 98.4, 85.7, 35.1, 31.3. **HRMS (ESI-MS)**: calcd for $\text{C}_{24}\text{H}_{24}\text{NO}_2\text{S}$: 390.1522; found: 390.1523. **IR v (cm^{-1})**: 3362, 3089, 3064, 3035, 2961, 2902, 2867, 2214, 1737, 1600. **m.p.**: 121-123 °C.

2-((4-Fluorophenyl)ethynyl)-*N*-phenylbenzenesulfonamide (8k)

Synthesized following GP5. Brown solid, 61%. $^1\text{H NMR}$ (400 MHz, CDCl_3): δ = 7.93 (dd, J = 7.9, 1.3 Hz, 1H), 7.69-7.63 (m, 3H), 7.49 (td, J = 7.6, 1.3 Hz, 1H), 7.35 (td, J = 7.8, 1.3 Hz, 1H), 7.22-7.05 (m, 8H). $^{13}\text{C NMR}$ (101 MHz, CDCl_3): δ = 163.4 (d, $J_{\text{C-F}}$ = 251.9 Hz), 139.8, 136.2, 134.1, 134.0 (d, $J_{\text{C-F}}$ = 8.6 Hz), 132.6, 130.0, 129.4, 128.6, 125.9, 122.3, 120.8, 118.0 (d, $J_{\text{C-F}}$ = 3.6 Hz), 116.3 (d, $J_{\text{C-F}}$ = 22.3 Hz), 96.9, 86.0. $^{19}\text{F NMR}$ (376 MHz, CDCl_3): δ = -108.45. **HRMS (ESI-MS)**: calcd for $\text{C}_{20}\text{H}_{13}\text{FNO}_2\text{S}$: 350.0657; found: 350.0655. **IR v (cm^{-1})**: 3354, 3104, 3048, 2922, 2854, 2220, 1942, 1892, 1717, 1599. **m.p.**: 101-103 °C.

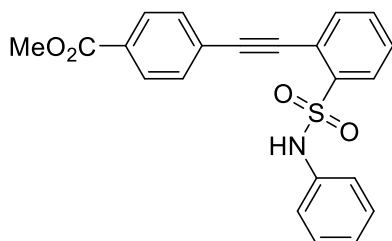
***N*-Phenyl-2-((4-(trifluoromethyl)phenyl)ethynyl)benzenesulfonamide (8l)**

Synthesized following GP5. Brown solid, 88%. ^1H

NMR (400 MHz, CDCl_3): δ = 7.95 (dd, J = 7.9, 1.3 Hz, 1H), 7.77 (d, J = 8.2 Hz, 2H), 7.72-7.66 (m, 3H), 7.52 (td, J = 7.6, 1.3 Hz, 1H), 7.40 (td, J = 7.8, 1.4 Hz, 1H), 7.23-7.14 (m, 2H), 7.12-7.06 (m, 3H), 7.03 (bs, 1H).

^{13}C **NMR (101 MHz, CDCl_3):** δ = 140.1, 136.1, 133.4,

132.7, 132.2, 131.4 (q, $J_{\text{C-F}}$ = 33.0 Hz), 130.1, 129.4, 129.1, 125.9, 125.8 (q, $J_{\text{C-F}}$ = 3.8 Hz), 123.9 (q, $J_{\text{C-F}}$ = 272.4 Hz), 122.2, 121.8, 120.3, 96.1, 88.3. ^{19}F **NMR (376 MHz, CDCl_3):** δ = -63.04. **HRMS (ESI-MS):** calcd for $\text{C}_{21}\text{H}_{15}\text{F}_3\text{NO}_2\text{S}$: 402.0770; found: 402.0769. **IR ν (cm^{-1}):** 3263, 3219, 3094, 3065, 2957, 2924, 2853, 1613. **m.p.:** 116-118 °C.

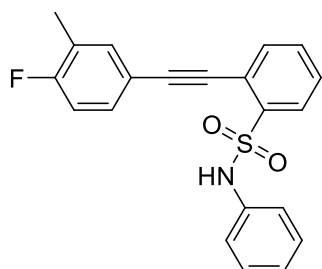
Methyl 4-((2-(*N*-phenylsulfamoyl)phenyl)ethynyl)benzoate (8m)

Synthesized following GP5. Yellow solid, 71%. ^1H

NMR (400 MHz, CDCl_3): δ = 8.12-8.07 (m, 2H), 7.95 (dd, J = 7.9, 1.3 Hz, 1H), 7.74-7.67 (m, 3H), 7.51 (td, J = 7.6, 1.4 Hz, 1H), 7.39 (td, J = 7.7, 1.4 Hz, 1H), 7.22-7.16 (m, 2H), 7.12-7.06 (m, 4H), 3.95 (s, 3H). ^{13}C **NMR (101 MHz, CDCl_3):** δ =

166.4, 140.0, 136.1, 134.4, 132.7, 131.8, 130.8, 130.1, 130.0, 129.4, 129.0, 126.4, 125.9,

122.2, 120.4, 96.8, 88.7, 52.5. **HRMS (ESI-MS):** calcd for $\text{C}_{22}\text{H}_{18}\text{NO}_4\text{S}$: 392.0951; found: 392.0947. **IR ν (cm^{-1}):** 3285, 3020, 2950, 2850, 1694, 1603. **m.p.:** 166-168 °C.

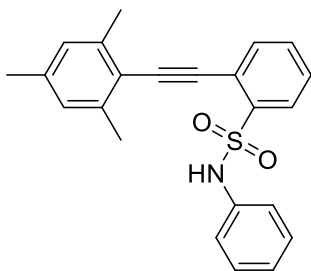
2-((4-Fluoro-3-methylphenyl)ethynyl)-*N*-phenylbenzenesulfonamide (8n)

Synthesized following GP5. Brown oil, 63%. ^1H **NMR**

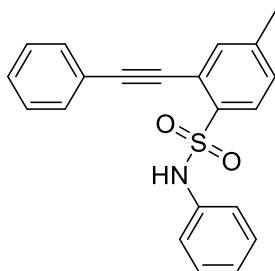
(500 MHz, CDCl_3): δ = 7.92 (dd, J = 8.0, 1.2 Hz, 1H), 7.65 (dd, J = 7.6, 1.3 Hz, 1H), 7.53-7.45 (m, 3H), 7.35 (td, J = 7.8, 1.3 Hz, 1H), 7.21-7.17 (m, 2H), 7.14 (bs, 1H), 7.12-7.04 (m, 4H), 2.32 (d, J = 2.0 Hz, 3H). ^{13}C **NMR (126 MHz, CDCl_3):** δ = 162.1 (d, $J_{\text{C-F}}$ = 250.6 Hz), 139.7, 136.2, 135.1

(d, $J_{\text{C-F}}$ = 5.8 Hz), 134.1, 132.6, 131.3 (d, $J_{\text{C-F}}$ = 8.5 Hz),

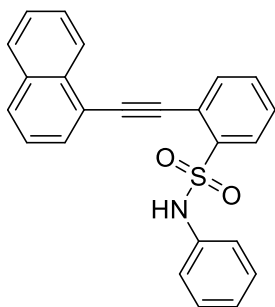
130.0, 129.4, 128.5, 126.1 (d, $J_{\text{C-F}}$ = 18.3 Hz), 125.6, 122.3, 120.9, 117.6 (d, $J_{\text{C-F}}$ = 3.9 Hz), 115.9 (d, $J_{\text{C-F}}$ = 23.3 Hz), 97.3, 85.6, 14.6 (d, $J_{\text{C-F}}$ = 3.4 Hz). ^{19}F **NMR (376 MHz, CDCl_3):** δ = -112.90. **HRMS (ESI-MS):** calcd for $\text{C}_{21}\text{H}_{16}\text{FNNaO}_2\text{S}$: 388.0778; found: 388.0774. **IR ν (cm^{-1}):** 3277, 3058, 2956, 2926, 2210, 1736, 1598.

2-(Mesitylethynyl)-*N*-phenylbenzenesulfonamide (8o)

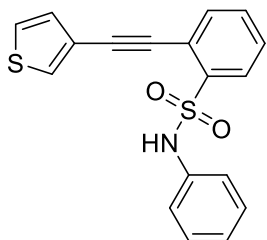
Synthesized following GP5. Brown oil, quantitative. $^1\text{H NMR}$ (500 MHz, CDCl_3): δ = 7.92 (dd, J = 8.0, 1.3 Hz, 1H), 7.68 (dd, J = 7.8, 1.3 Hz, 1H), 7.48 (td, J = 7.6, 1.3 Hz, 1H), 7.34 (td, J = 7.7, 1.3 Hz, 1H), 7.29 (bs, 1H), 7.22-7.14 (m, 2H), 7.13-7.09 (m, 2H), 7.06 (ddt, J = 7.8, 6.8, 1.3 Hz, 1H), 6.96 (s, 2H), 2.58 (s, 6H), 2.33 (s, 3H). $^{13}\text{C NMR}$ (126 MHz, CDCl_3): δ = 141.1, 139.7, 139.0, 136.4, 134.5, 132.6, 129.9, 129.4, 128.2, 128.2, 125.8, 122.3, 121.7, 118.7, 96.7, 93.4, 21.6, 21.4. **HRMS (ESI-MS)**: calcd for $\text{C}_{23}\text{H}_{21}\text{NNaO}_2\text{S}$: 398.1185; found: 398.1171. **IR v (cm^{-1})**: 3328, 3017, 2946, 2916, 2854, 2201, 1735, 1599.

4-Methyl-*N*-phenyl-2-(phenylethynyl)benzenesulfonamide (8p)

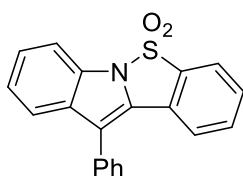
Synthesized following GP5. Brown oil, 89%. $^1\text{H NMR}$ (500 MHz, CDCl_3): δ = 7.82 (d, J = 8.1 Hz, 1H), 7.69-7.63 (m, 2H), 7.48 (dd, J = 1.2, 0.6 Hz, 1H), 7.47-7.41 (m, 3H), 7.22-7.08 (m, 6H), 7.06 (m, 1H), 2.36 (s, 3H). $^{13}\text{C NMR}$ (126 MHz, CDCl_3): δ = 143.5, 137.0, 136.4, 134.7, 131.9, 130.1, 129.7, 129.4, 129.3, 128.9, 125.7, 122.1, 122.0, 120.7, 97.4, 86.4, 21.3. **HRMS (ESI-MS)**: calcd for $\text{C}_{21}\text{H}_{17}\text{NNaO}_2\text{S}$: 370.0872; found: 370.0870. **IR v (cm^{-1})**: 3354, 3047, 2960, 2924, 2854, 2205, 1738, 1595.

2-(Naphthalen-1-ylethynyl)-*N*-phenylbenzenesulfonamide (8q)

Synthesized following GP5. Brown solid, 95%. $^1\text{H NMR}$ (500 MHz, CDCl_3): δ = 8.59 (dd, J = 8.4, 1.0 Hz, 1H), 7.99 (ddd, J = 7.9, 1.3, 0.5 Hz, 1H), 7.96 (dt, J = 8.3, 1.0 Hz, 1H), 7.92 (dd, J = 7.2, 1.1 Hz, 2H), 7.83-7.77 (m, 1H), 7.71-7.68 (m, 1H), 7.61-7.58 (m, 1H), 7.56-7.52 (m, 2H), 7.41-7.38 (m, 1H), 7.23 (bs, 1H), 7.19-7.14 (m, 2H), 7.11-7.08 (m, 2H), 7.07-7.03 (m, 1H). $^{13}\text{C NMR}$ (126 MHz, CDCl_3): δ = 139.7, 136.2, 134.5, 133.5, 133.4, 132.7, 131.5, 130.4, 130.1, 129.4, 128.7, 128.6, 127.8, 127.1, 126.2, 125.7, 125.5, 122.1, 121.1, 119.5, 96.5, 90.6. **HRMS (ESI-MS)**: calcd for $\text{C}_{24}\text{H}_{18}\text{NO}_2\text{S}$: 384.1053; found: 384.1044. **IR v (cm^{-1})**: 3281, 3057, 2205, 1601. **m.p.**: 104-106 °C.

***N*-Phenyl-2-(thiophen-3-ylethynyl)benzenesulfonamide (8r)**

Synthesized following GP5. Brown oil, 94%. $^1\text{H NMR}$ (500 MHz, CDCl_3): δ = 7.93 (dd, J = 8.0, 1.3 Hz, 1H), 7.73 (dd, J = 3.0, 1.2 Hz, 1H), 7.65 (dd, J = 7.7, 1.3 Hz, 1H), 7.48 (td, J = 7.6, 1.3 Hz, 1H), 7.40 (dd, J = 5.0, 3.0 Hz, 1H), 7.37-7.30 (m, 2H), 7.20-7.16 (m, 3H), 7.13-7.10 (m, 2H), 7.09-7.04 (m, 1H). $^{13}\text{C NMR}$ (126 MHz, CDCl_3): δ = 139.8, 136.2, 134.1, 132.6, 130.6, 130.0, 129.7, 129.4, 128.5, 126.4, 125.8, 122.2, 120.9, 120.9, 93.4, 85.9. HRMS (ESI-MS): calcd for $\text{C}_{18}\text{H}_{13}\text{NNaO}_2\text{S}_2$: 362.0280; found: 362.0294. IR ν (cm^{-1}): 3286, 3110, 2962, 2926, 2203, 1599.

Data for the final indoles 9:**11-Phenylbenzo[4,5]isothiazolo[2,3- σ]indole 5,5-dioxide (9a)**

Pale yellow solid. Synthesized following GP6, 85%; GP7, 78% and GP8, 78%. $^1\text{H NMR}$ (500 MHz, CDCl_3): δ = 7.85-7.83 (m, 1H), 7.78 (d, J = 8.1 Hz, 1H), 7.69-7.65 (m, 1H), 7.65-7.62 (m, 2H), 7.62-7.54 (m, 3H), 7.54-7.40 (m, 4H), 7.31-7.24 (m, 1H). $^{13}\text{C NMR}$ (126 MHz, CDCl_3): δ = 138.3, 134.0, 133.2, 132.7, 131.8, 129.7, 129.3, 129.2, 128.7, 128.6, 128.0, 126.5, 123.7, 122.7, 122.4, 121.6, 118.8, 112.0. HRMS (ESI-MS): calcd for $\text{C}_{20}\text{H}_{13}\text{NNaO}_2\text{S}$: 354.0559; found: 354.0556. IR ν (cm^{-1}): 3062, 2927, 2853, 1594. m.p.: 150-152 °C.

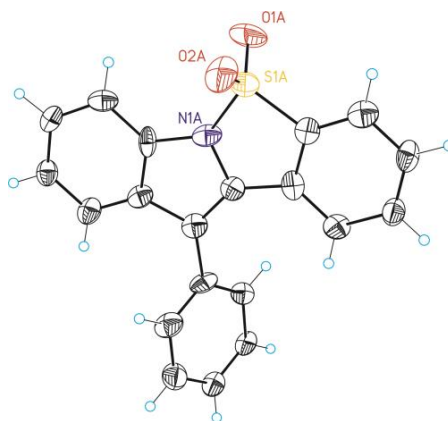
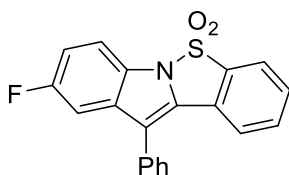
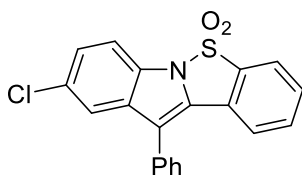


Table 3.5 Crystal data and structure refinement for compound **9a**.

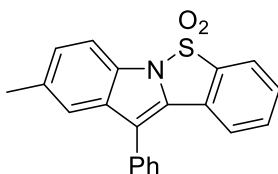
Identification code	CCDC 1441257
Empirical formula	C ₂₀ H ₁₃ N O ₂ S
Formula weight	331.37
Temperature	100(2) K
Wavelength	0.71073 Å
Crystal system	Triclinic
Space group	P1
Unit cell dimensions	a = 10.0031(10)Å α = 82.031(4)°. b = 10.6770(12)Å β = 74.074(3)°. c = 16.7246(16)Å γ = 63.597(4)°.
Volume	1538.2(3) Å ³
Z	4
Density (calculated)	1.431 Mg/m ³
Absorption coefficient	0.222 mm ⁻¹
F(000)	688
Crystal size	0.12 x 0.04 x 0.02 mm ³
Theta range for data collection	1.266 to 25.132°.
Index ranges	-11<=h<=11, -10<=k<=12, 19<=l<=19
Reflections collected	21935
Independent reflections	8807[R(int) = 0.0452]
Completeness to theta =25.132°	93.2%
Absorption correction	Empirical
Max. and min. transmission	0.996 and 0.855
Refinement method	Full-matrix least-squares on F ²
Data / restraints / parameters	8807/ 840/ 1081
Goodness-of-fit on F ²	1.024
Final R indices [I>2sigma(I)]	R1 = 0.0661, wR2 = 0.1473
R indices (all data)	R1 = 0.0920, wR2 = 0.1612
Flack parameter	x = 0.09(4)
Largest diff. peak and hole	1.357 and -0.484 e. Å ⁻³

9-Fluoro-11-phenylbenzo[4,5]isothiazolo[2,3-*a*]indole 5,5-dioxide (9b)

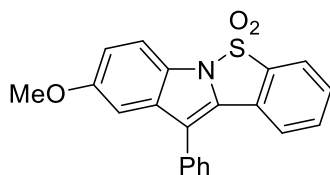
Pale yellow solid. Synthesized following GP6, 71%; GP7, 51% and GP8, 60%. $^1\text{H NMR}$ (500 MHz, CDCl_3): δ = 7.87-7.82 (m, 1H), 7.73-7.65 (m, 2H), 7.64-7.45 (m, 7H), 7.29-7.21 (m, 1H), 7.16 (td, J = 8.9, 2.5 Hz, 1H). $^{13}\text{C NMR}$ (126 MHz, CDCl_3): δ = 160.1 (d, $J_{\text{C-F}}$ = 240.9 Hz), 138.2, 134.2, 134.1, 131.3, 130.3, 129.6, 129.6, 129.4, 129.0, 128.9, 127.8, 122.8, 122.6, 118.6 (d, $J_{\text{C-F}}$ = 4.5 Hz), 114.7 (d, $J_{\text{C-F}}$ = 26.3 Hz), 112.9 (d, $J_{\text{C-F}}$ = 9.5 Hz), 107.3 (d, $J_{\text{C-F}}$ = 24.9 Hz). $^{19}\text{F NMR}$ (376 MHz, CDCl_3): δ = -118.79. HRMS (ESI-MS): calcd for $\text{C}_{20}\text{H}_{12}\text{FNNaO}_2\text{S}$: 372.0465; found: 372.0459. IR ν (cm^{-1}): 3241, 3099, 3071, 2960, 2924, 2852, 1715, 1575. m.p.: 135-137 °C.

9-Chloro-11-phenylbenzo[4,5]isothiazolo[2,3-*a*]indole 5,5-dioxide (9c)

White solid. Synthesized following GP6, 74%; GP7, 59%, GP8, 59% and GP9, 64%. $^1\text{H NMR}$ (500 MHz, CDCl_3): δ = 7.87-7.83 (m, 1H), 7.71-7.64 (m, 2H), 7.64-7.46 (m, 8H), 7.39 (dd, J = 8.6, 2.0 Hz, 1H). $^{13}\text{C NMR}$ (126 MHz, CDCl_3): δ = 138.2, 134.3, 134.2, 131.1, 130.9, 129.9, 129.7, 129.7, 129.6, 129.4, 128.9, 127.6, 126.7, 122.8, 122.6, 121.2, 118.0, 112.9. HRMS (ESI-MS): calcd for $\text{C}_{20}\text{H}_{12}\text{ClNNaO}_2\text{S}$: 388.0169; found: 388.0160. IR ν (cm^{-1}): 3058, 3027, 2956, 2921, 2851, 1726, 1595. m.p.: 166-168 °C.

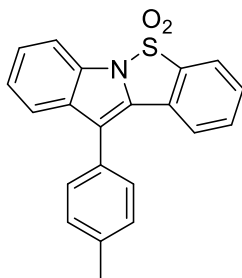
9-Methyl-11-phenylbenzo[4,5]isothiazolo[2,3-*a*]indole 5,5-dioxide (9d)

White solid. Synthesized following GP6, 85%; GP7, 61% and GP8, 58%. $^1\text{H NMR}$ (400 MHz, CDCl_3): δ = 7.83 (dd, J = 7.8, 1.3 Hz, 1H), 7.69-7.59 (m, 4H), 7.62-7.53 (m, 2H), 7.54-7.40 (m, 3H), 7.39-7.34 (m, 1H), 7.26-7.24 (m, 1H), 2.43 (s, 3H). $^{13}\text{C NMR}$ (101 MHz, CDCl_3): δ = 138.3, 133.9, 133.5, 133.4, 131.9, 130.9, 129.7, 129.2, 129.1, 128.9, 128.6, 128.2, 127.9, 122.7, 122.3, 121.3, 118.6, 111.6, 21.6. HRMS (ESI-MS): calcd for $\text{C}_{21}\text{H}_{15}\text{NNaO}_2\text{S}$: 368.0716; found: 368.0702. IR ν (cm^{-1}): 3052, 2960, 2920, 2854, 1608, 1593. m.p.: 169-171 °C.

9-Methoxy-11-phenylbenzo[4,5]isothiazolo[2,3-*a*]indole 5,5-dioxide (9e)

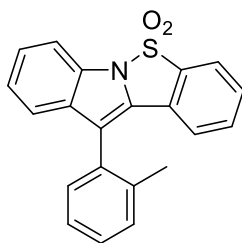
White solid. Synthesized following GP6, 39%; GP7, 26% and GP8, 36%. $^1\text{H NMR}$ (500 MHz, CDCl_3): δ = 7.85-7.80 (m, 1H), 7.66 (dd, J = 8.8, 0.6 Hz, 1H), 7.64-7.61 (m, 3H), 7.60-7.56 (m, 2H), 7.53-7.42 (m, 3H), 7.05 (dd, J = 8.8, 2.5 Hz, 1H), 7.01 (dd, J = 2.6, 0.6 Hz, 1H), 3.81 (s, 3H).

$^{13}\text{C NMR}$ (126 MHz, CDCl_3): δ = 157.0, 138.3, 134.1, 134.0, 131.9, 129.7, 129.5, 129.3, 129.2, 128.6, 128.1, 127.5, 122.7, 122.3, 118.7, 115.8, 112.7, 103.9, 56.0. **HRMS (ESI-MS)**: calcd for $\text{C}_{21}\text{H}_{16}\text{NO}_3\text{S}$: 362.0845; found: 362.0835. **IR ν (cm^{-1})**: 3059, 2959, 2924, 2853, 1726, 1594. **m.p.**: 202-204 °C.

11-(*p*-Tolyl)benzo[4,5]isothiazolo[2,3-*a*]indole 5,5-dioxide (9f)

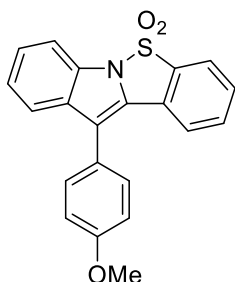
Pale yellow solid. Synthesized following GP6, 49%; GP7, 56% and GP8, 60%. $^1\text{H NMR}$ (400 MHz, CDCl_3): δ = 7.86-7.81 (m, 1H), 7.77 (dt, J = 8.1, 0.9 Hz, 1H), 7.71-7.68 (m, 1H), 7.59 (dt, J = 8.1, 0.9 Hz, 1H), 7.54-7.36 (m, 7H), 7.30-7.23 (m, 1H), 2.49 (s, 3H). $^{13}\text{C NMR}$ (101 MHz, CDCl_3): δ = 138.6, 138.3, 134.0, 133.3, 132.7, 130.0, 129.6, 129.2, 128.7, 128.6, 128.2, 126.5, 123.7, 122.7, 122.5, 121.6, 118.9, 112.0, 21.6. **HRMS (ESI-MS)**: calcd

for $\text{C}_{21}\text{H}_{15}\text{NNaO}_2\text{S}$: 368.0716; found: 368.0718. **IR ν (cm^{-1})**: 3064, 3027, 2957, 2922, 2853, 1593. **m.p.**: 198-199 °C.

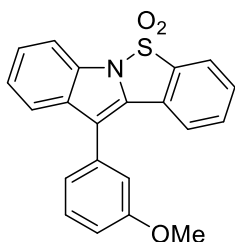
11-(*o*-Tolyl)benzo[4,5]isothiazolo[2,3-*a*]indole 5,5-dioxide (9g)

Pale yellow solid. Synthesized following GP6, 87%; GP7, 82%, 78%. $^1\text{H NMR}$ (500 MHz, CDCl_3): δ = 7.85-7.82 (m, 1H), 7.79 (d, J = 8.2 Hz, 1H), 7.47-7.39 (m, 6H), 7.36-7.31 (m, 2H), 7.24 (ddd, J = 8.1, 7.2, 1.0 Hz, 1H), 7.17-7.15 (m, 1H), 2.24 (s, 3H). $^{13}\text{C NMR}$ (126 MHz, CDCl_3): δ = 138.4, 137.7, 134.1, 133.6, 132.6,

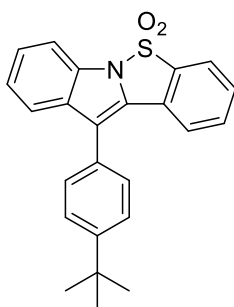
130.9, 130.8, 130.7, 129.2, 129.1, 129.0, 128.0, 126.4, 123.6, 122.7, 122.6, 121.8, 117.6, 112.0, 20.2. **HRMS (ESI-MS)**: calcd for $\text{C}_{21}\text{H}_{15}\text{NNaO}_2\text{S}$: 368.0716; found: 368.0721. **IR ν (cm^{-1})**: 3059, 3019, 2956, 2923, 2853, 1720, 1595. **m.p.**: 121-123 °C.

11-(4-Methoxyphenyl)benzo[4,5]isothiazolo[2,3-*a*]indole 5,5-dioxide (9h)

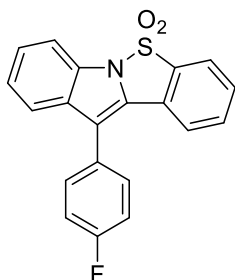
White solid. Synthesised following GP6, 58%; GP7, 26% and GP8, 45%. $^1\text{H NMR}$ (400 MHz, CDCl_3): δ = 7.83 (ddd, J = 7.6, 1.4, 0.7 Hz, 1H), 7.76 (dt, J = 8.2, 0.9 Hz, 1H), 7.67 (ddd, J = 7.8, 1.3, 0.7 Hz, 1H), 7.61-7.37 (m, 6H), 7.31-7.22 (m, 1H), 7.12-7.07 (m, 2H), 3.92 (s, 3H). $^{13}\text{C NMR}$ (101 MHz, CDCl_3): δ = 159.9, 138.3, 134.0, 133.4, 132.7, 130.9, 129.1, 128.5, 128.2, 126.5, 123.8, 123.7, 122.8, 122.4, 121.6, 118.7, 114.7, 112.0, 55.6. **HRMS (ESI-MS)**: calcd for $\text{C}_{21}\text{H}_{16}\text{NO}_3\text{S}$: 362.0845; found: 362.0859. **IR v** (cm^{-1}): 3054, 3013, 2956, 2925, 2854, 2839, 1725, 1595. **m.p.**: 165-167 °C.

11-(3-Methoxyphenyl)benzo[4,5]isothiazolo[2,3-*a*]indole 5,5-dioxide (9i)

White solid. Synthesized following GP6, 55%; GP7, 67% and GP8, 49%. $^1\text{H NMR}$ (400 MHz, CDCl_3): δ = 7.84 (ddd, J = 7.5, 1.4, 0.7 Hz, 1H), 7.77 (dt, J = 8.2, 0.8 Hz, 1H), 7.73 (ddd, J = 7.9, 1.2, 0.7 Hz, 1H), 7.62-7.60 (m, 1H), 7.54-7.40 (m, 4H), 7.32-7.23 (m, 1H), 7.22 (ddd, J = 7.5, 1.6, 1.0 Hz, 1H), 7.17-7.16 (m, 1H), 7.05-7.02 (m, 1H), 3.88 (s, 3H). $^{13}\text{C NMR}$ (101 MHz, CDCl_3): δ = 160.2, 138.3, 134.0, 133.1, 133.1, 132.6, 130.3, 129.3, 128.8, 128.0, 126.5, 123.8, 122.8, 122.6, 122.1, 121.6, 118.7, 115.2, 114.2, 112.0, 55.6. **HRMS (ESI-MS)**: calcd for $\text{C}_{21}\text{H}_{15}\text{NNaO}_3\text{S}$: 384.0665; found: 384.0664. **IR v** (cm^{-1}): 3066, 3012, 2956, 2928, 2836, 1722, 1594. **m.p.**: 140-142 °C.

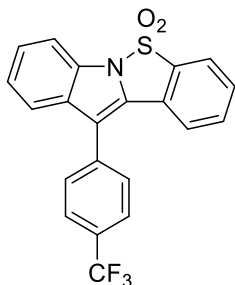
11-(4-(*tert*-Butyl)phenyl)benzo[4,5]isothiazolo[2,3-*a*]indole 5,5-dioxide (9j)

White solid. Synthesized following GP6, 66%; GP7, 73% and GP8, 65%. $^1\text{H NMR}$ (400 MHz, CDCl_3): δ = 7.83 (ddd, J = 7.7, 1.3, 0.7 Hz, 1H), 7.82-7.71 (m, 2H), 7.66-7.59 (m, 1H), 7.62-7.38 (m, 7H), 7.28-7.24 (m, 1H), 1.43 (s, 9H). $^{13}\text{C NMR}$ (101 MHz, CDCl_3): δ = 151.7, 138.2, 134.0, 133.3, 132.7, 129.3, 129.2, 128.6, 128.5, 128.1, 126.4, 126.1, 123.6, 122.7, 122.5, 121.8, 118.9, 111.9, 35.0, 31.5. **HRMS (ESI-MS)**: calcd for $\text{C}_{24}\text{H}_{21}\text{NNaO}_2\text{S}$: 410.1185; found: 410.1181. **IR v** (cm^{-1}): 3067, 2961, 2866, 1596. **m.p.**: 202-204 °C.

11-(4-Fluorophenyl)benzo[4,5]isothiazolo[2,3- σ]indole 5,5-dioxide (9k)

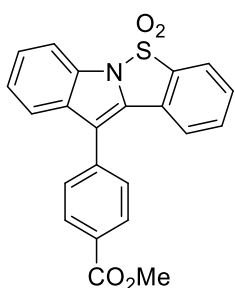
White solid. Synthesized following GP6, 51%; GP7, 50% and GP8, 53%. $^1\text{H NMR}$ (400 MHz, CDCl_3): δ = 7.87-7.83 (m, 1H), 7.78 (dt, J = 8.2, 0.8 Hz, 1H), 7.65-7.56 (m, 3H), 7.58-7.39 (m, 4H), 7.32-7.23 (m, 3H). $^{13}\text{C NMR}$ (126 MHz, CDCl_3): δ = 162.8 (d, $J_{\text{C-F}}$ = 248.5 Hz), 138.3, 134.1, 133.1, 132.6, 131.5 (d, $J_{\text{C-F}}$ = 8.1 Hz), 129.4, 128.8, 127.9, 127.7 (d, $J_{\text{C-F}}$ = 3.3 Hz), 126.6, 123.8, 122.9, 122.3, 121.3, 117.6, 116.4 (d, $J_{\text{C-F}}$ = 21.6 Hz), 112.0. $^{19}\text{F NMR}$ (376 MHz, CDCl_3): δ = -112.67. **HRMS (ESI-MS)**: calcd for $\text{C}_{20}\text{H}_{12}\text{FNNaO}_2\text{S}$: 372.0465; found: 372.0469. **IR ν (cm^{-1})**: 3047, 2924, 2854, 1720, 1594.

m.p.: 195-196 °C.

11-(4-(Trifluoromethyl)phenyl)benzo[4,5]isothiazolo[2,3- σ]indole 5,5-dioxide (9l)

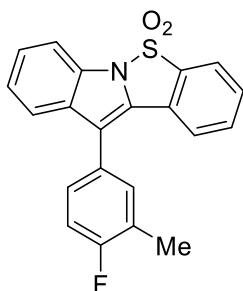
Pale yellow solid. Synthesized following GP6, 49%; GP7, 22% and GP9, 48%. $^1\text{H NMR}$ (400 MHz, CDCl_3): δ = 7.88-7.75 (m, 6H), 7.64-7.61 (m, 1H), 7.57-7.43 (m, 4H), 7.34-7.25 (m, 1H). $^{13}\text{C NMR}$ (101 MHz, CDCl_3): δ = 138.4, 135.8, 134.2, 132.7, 132.6, 130.7 (q, $J_{\text{C-F}}$ = 32.7 Hz), 130.1, 129.7, 129.1, 127.6, 126.8, 126.3 (q, $J_{\text{C-F}}$ = 3.7 Hz), 124.2 (q, $J_{\text{C-F}}$ = 272.4 Hz), 124.0, 123.0, 122.3, 121.2, 117.0, 112.1. $^{19}\text{F NMR}$ (376 MHz, CDCl_3): δ = -62.68.

HRMS (ESI-MS): calcd for $\text{C}_{21}\text{H}_{12}\text{F}_3\text{NNaO}_2\text{S}$: 422.0433; found: 422.0425. **IR ν (cm^{-1})**: 3072, 2961, 2924, 2853, 1725, 1618, 1597. **m.p.**: 226-228 °C.

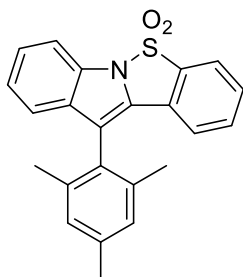
Methyl 4-(5,5-dioxidobenzo[4,5]isothiazolo[2,3- σ]indol-11-yl)benzoate (9m)

White solid. Synthesized following GP6, 49%; GP7, 38% and GP9, 46%. $^1\text{H NMR}$ (400 MHz, CDCl_3): δ = 8.26 (d, J = 8.3 Hz, 2H), 7.92-7.83 (m, 1H), 7.80 (dd, J = 8.3, 0.9 Hz, 1H), 7.75 (d, J = 8.2 Hz, 2H), 7.69-7.65 (m, 1H), 7.64-7.40 (m, 4H), 7.36-7.28 (m, 1H), 4.01 (s, 3H). $^{13}\text{C NMR}$ (101 MHz, CDCl_3): δ = 166.8, 138.3, 136.7, 134.2, 132.6, 132.6, 130.5, 130.3, 129.8, 129.6, 129.1, 127.7, 126.7, 124.0, 122.9, 122.4, 121.3, 117.6, 112.1, 52.5. **HRMS (ESI-MS)**: calcd for $\text{C}_{22}\text{H}_{15}\text{NNaO}_4\text{S}$: 412.0614; found: 412.0599.

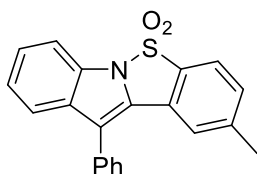
IR ν (cm^{-1}): 3059, 2958, 2926, 2854, 1717, 1607, 1594. **m.p.**: 209-211 °C.

11-(4-Fluoro-3-methylphenyl)benzo[4,5]isothiazolo[2,3-*a*]indole 5,5-dioxide (9n)

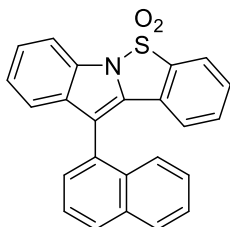
Pale yellow solid. Synthesized following GP6, 52%; GP7, 60% and GP8, 48%. $^1\text{H NMR}$ (400 MHz, CDCl_3): δ = 7.84 (ddd, J = 7.6, 1.1, 0.6 Hz, 1H), 7.77 (dt, J = 8.1, 0.9 Hz, 1H), 7.64-7.60 (m, 1H), 7.57-7.39 (m, 6H), 7.31-7.24 (m, 1H), 7.24-7.16 (m, 1H), 2.39 (d, J = 2.0 Hz, 3H). $^{13}\text{C NMR}$ (126 MHz, CDCl_3): δ = 161.5 (d, $J_{\text{C-F}}$ = 247.2 Hz), 138.3, 134.1, 133.2, 132.7 (d, $J_{\text{C-F}}$ = 5.3 Hz), 132.6, 129.3, 128.7, 128.7 (d, $J_{\text{C-F}}$ = 8.1 Hz), 128.0, 127.4 (d, $J_{\text{C-F}}$ = 3.7 Hz), 126.6, 126.0 (d, $J_{\text{C-F}}$ = 17.7 Hz), 123.8, 122.8, 122.3, 121.4, 117.9, 116.0 (d, $J_{\text{C-F}}$ = 22.7 Hz), 112.0, 14.8 (d, $J_{\text{C-F}}$ = 3.5 Hz). $^{19}\text{F NMR}$ (376 MHz, CDCl_3): δ = -117.05. **HRMS (ESI-MS)**: calcd for $\text{C}_{21}\text{H}_{14}\text{FNNaO}_2\text{S}$: 386.0621; found: 386.0610. **IR v** (cm^{-1}): 3065, 2957, 2924, 2854, 1724, 1595. **m.p.**: 178-180 °C.

11-Mesitylbenzo[4,5]isothiazolo[2,3-*a*]indole 5,5-dioxide (9o)

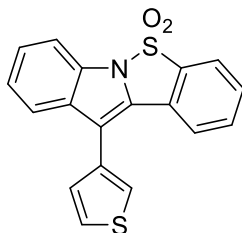
White solid. Synthesized following GP6, 57%; GP7, 61% and GP8, 74%. $^1\text{H NMR}$ (400 MHz, CDCl_3): δ = 7.85-7.81 (m, 1H), 7.79 (dt, J = 8.2, 0.9 Hz, 1H), 7.49-7.37 (m, 3H), 7.24-7.19 (m, 2H), 7.05 (s, 2H), 7.02-6.98 (m, 1H), 2.41 (s, 3H), 2.06 (s, 6H). $^{13}\text{C NMR}$ (101 MHz, CDCl_3): δ = 138.3, 137.9, 134.3, 133.3, 132.9, 129.2, 129.0, 128.8, 128.1, 126.9, 126.3, 123.6, 122.6, 122.3, 121.7, 116.5, 112.1, 21.4, 20.4. **HRMS (ESI-MS)**: calcd for $\text{C}_{23}\text{H}_{19}\text{NNaO}_2\text{S}$: 396.1029; found: 396.1030. **IR v** (cm^{-1}): 3056, 2920, 2851, 1728, 1602, 1592. **m.p.**: 240-241 °C.

2-Methyl-11-phenylbenzo[4,5]isothiazolo[2,3-*a*]indole 5,5-dioxide (9p)

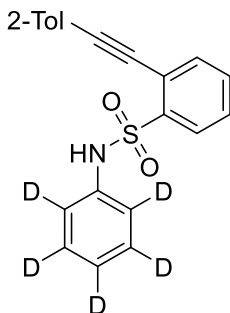
Pale yellow oil. Synthesized following GP6, 46%; GP7, 60% and GP8, 60%. $^1\text{H NMR}$ (400 MHz, CDCl_3): δ = 7.77 (dt, J = 8.1, 0.9 Hz, 1H), 7.72 (d, J = 8.0 Hz, 1H), 7.70-7.36 (m, 8H), 7.32-7.20 (m, 2H), 2.36 (s, 3H). $^{13}\text{C NMR}$ (101 MHz, CDCl_3): δ = 145.1, 135.6, 133.2, 132.6, 131.9, 130.2, 129.7, 129.2, 128.8, 128.6, 128.2, 126.4, 123.6, 122.7, 122.5, 121.5, 118.5, 111.9, 22.1. **HRMS (ESI-MS)**: calcd for $\text{C}_{21}\text{H}_{15}\text{NNaO}_2\text{S}$: 368.0716; found: 368.0718. **IR v** (cm^{-1}): 3071, 3027, 2957, 2923, 2855, 1725, 1598.

11-(Naphthalen-1-yl)benzo[4,5]isothiazolo[2,3-*a*]indole 5,5-dioxide (9q)

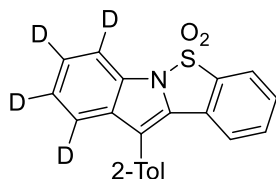
White solid. Synthesized following GP6, 40%; GP7, 82% and GP8, 68%. $^1\text{H NMR}$ (500 MHz, CDCl_3): δ = 8.04-7.99 (m, 2H), 7.86-7.79 (m, 3H), 7.70-7.62 (m, 2H), 7.58-7.54 (m, 1H), 7.48-7.38 (m, 3H), 7.35-7.29 (m, 2H), 7.21 (ddd, J = 8.1, 7.2, 1.0 Hz, 1H), 6.94-6.92 (m, 1H). $^{13}\text{C NMR}$ (126 MHz, CDCl_3): δ = 138.4, 134.2, 134.1, 134.0, 132.6, 132.0, 130.0, 129.3, 129.2, 129.0, 128.7, 128.5, 127.8, 126.9, 126.6, 126.5, 126.0, 125.8, 123.7, 123.2, 122.6, 122.1, 116.3, 112.0. **HRMS (ESI-MS)**: calcd for $\text{C}_{24}\text{H}_{15}\text{NNaO}_2\text{S}$: 404.0716; found: 404.0715. **IR v** (cm^{-1}): 3055, 2960, 2925, 2853, 1722, 1595. **m.p.**: 85-86 °C.

11-(Thiophen-3-yl)benzo[4,5]isothiazolo[2,3-*a*]indole 5,5-dioxide (9r)

Colorless oil. Synthesized following GP6, 56%; GP7, 66% and GP8, 37%. $^1\text{H NMR}$ (400 MHz, CDCl_3): δ = 7.86-7.83 (m, 1H), 7.82-7.73 (m, 2H), 7.62 (dt, J = 8.0, 0.9 Hz, 1H), 7.59-7.56 (m, 2H), 7.54 (dd, J = 7.8, 1.2 Hz, 1H), 7.49 (dd, J = 7.6, 1.1 Hz, 1H), 7.46-7.37 (m, 2H), 7.33-7.24 (m, 1H). $^{13}\text{C NMR}$ (101 MHz, CDCl_3): δ = 138.2, 134.1, 133.2, 132.6, 131.7, 129.3, 128.9, 128.6, 128.0, 126.9, 126.6, 124.7, 123.7, 122.8, 122.6, 121.6, 113.6, 112.0. **HRMS (ESI-MS)**: calcd for $\text{C}_{18}\text{H}_{11}\text{NNaO}_2\text{S}_2$: 360.0123; found: 360.0119. **IR v** (cm^{-1}): 3102, 2956, 2925, 2856, 1719, 1594.

Data for the deuterated compounds:***N*-Phenyl-*d*₅-2-(*o*-tolylethynyl)benzenesulfonamide (8g-*d*₅)**

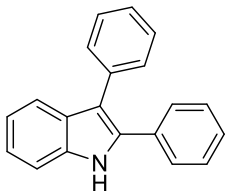
Synthesized following GP5 as a brown oil in 87% yield
 $^1\text{H NMR}$ (500 MHz, CDCl_3): δ = 7.94 (dd, J = 7.9, 1.3 Hz, 1H), 7.71-7.61 (m, 2H), 7.49 (td, J = 7.6, 1.4 Hz, 1H), 7.42-7.24 (m, 4H), 7.22 (bs, 1H), 2.63 (s, 3H). $^{13}\text{C NMR}$ (126 MHz, CDCl_3): δ = 140.9, 139.5, 136.1, 135.4 (m), 134.4, 132.6, 132.5, 130.1, 129.9, 129.8, 128.9 (m), 128.5, 126.1, 121.8 (m), 121.7, 121.2, 97.2, 89.8, 21.0.

11-(o-Tolyl)benzo[4,5]isothiazolo[2,3-a]indole-d₄ 5,5-dioxide (9g-d₅)

Synthesized following GP6 as a pale yellow oil in 80% yield.

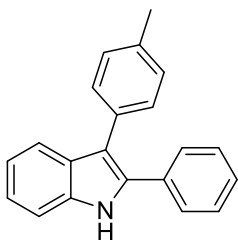
¹H NMR (500 MHz, CDCl₃): δ = 7.86-7.82 (m, 1H), 7.48-7.33 (m, 6H), 7.18-7.14 (m, 1H), 2.24 (s, 3H). ¹³C NMR (126 MHz, CDCl₃): δ = 138.4, 137.7, 134.1, 133.5, 132.5, 130.9, 130.8, 130.7, 129.2, 129.1, 128.9, 128.0, 126.4, 125.9 (m), 123.1

(m), 122.7, 122.6, 121.5 (m), 117.6, 111.6 (m), 20.2.

Data for the free indoles 15:**2,3-Diphenyl-1H-indole (15a)**

Synthesized following GP10 as a white solid in 92% yield. The NMR spectra match the literature data.¹³³ ¹H NMR (500 MHz, CDCl₃): δ = 8.22 (bs, 1H), 7.71 (d, *J* = 8.0 Hz, 1H), 7.49-7.41 (m, 5H), 7.40 (t, *J* = 7.6 Hz, 2H), 7.38-7.23 (m, 5H), 7.21-7.14 (m, 1H).

¹³C NMR (126 MHz, CDCl₃): δ = 136.0, 135.2, 134.2, 132.8, 130.3, 128.9, 128.8, 128.7, 128.3, 127.8, 126.4, 122.8, 120.6, 119.8, 115.2, 111.0.

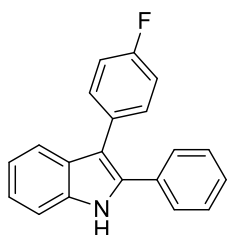
2-Phenyl-3-(p-tolyl)-1H-indole (15f)

Synthesized following GP10 as a white solid in a 75% yield. The NMR spectra match the literature data.¹³⁴ ¹H NMR (500 MHz, CDCl₃): δ = 8.20 (bs, 1H), 7.73 (d, *J* = 7.9 Hz, 1H), 7.49-7.19 (m, 12H), 2.44 (s, 3H). ¹³C NMR (126 MHz, CDCl₃): δ = 136.0, 135.9, 134.0, 132.9, 132.1, 130.1, 129.4, 129.0, 128.8, 128.2, 127.7,

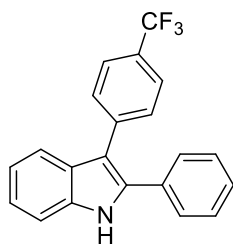
122.7, 120.4, 119.9, 115.1, 111.0, 21.4.

¹³³ Zhao, D.; Shi, Z.; Glorius, F. *Angew. Chem. Int. Ed.* **2013**, *52*, 12426.

¹³⁴ Arcadi, A.; Cacchi, S.; Fabrizi, G.; Goggiamani, A.; Iazzetti, A.; Marinelli, F. *Org. Biomol. Chem.* **2013**, *11*, 545.

3-(4-Fluorophenyl)-2-phenyl-1H-indole (15k)

Synthesized following GP10 as a white solid in a 66% yield. The NMR spectra match the literature data.¹³⁵ **¹H NMR (500 MHz, CDCl₃):** δ = 8.27 (bs, 1H), 7.63 (d, J = 8.0 Hz, 1H), 7.46-7.32 (m, 8H), 7.30-7.21 (m, 1H), 7.19-7.15 (m, 1H), 7.11-7.05 (m, 2H). **¹³C NMR (126 MHz, CDCl₃):** δ = 161.7 (d, J_{C-F} = 244.9 Hz), 135.9, 134.3, 132.6, 131.7 (d, J_{C-F} = 7.8 Hz), 131.1 (d, J_{C-F} = 3.4 Hz), 128.9, 128.8, 128.3, 127.9, 122.9, 120.6, 119.5, 115.6 (d, J_{C-F} = 21.2 Hz), 114.1, 111.1. **¹⁹F NMR (376 MHz, CDCl₃):** δ = -116.47.

2-Phenyl-3-(4-(trifluoromethyl)phenyl)-1H-indole (15l)

Synthesized following GP10 as a yellow solid in 84% yield. The NMR spectra match the literature data.¹³⁶ **¹H NMR (500 MHz, CDCl₃):** δ = 8.31 (bs, 1H), 7.68 (dd, J = 7.9, 1.2 Hz, 1H), 7.62 (d, J = 8.1 Hz, 2H), 7.55 (d, J = 8.1 Hz, 2H), 7.46 (d, J = 8.1 Hz, 1H), 7.45-7.31 (m, 5H), 7.33-7.24 (m, 1H), 7.24-7.15 (m, 1H). **¹³C NMR (126 MHz, CDCl₃):** δ = 139.2, 136.1, 135.1, 132.3, 130.3, 129.0, 128.5, 128.3, 128.2 (d, J_{C-F} = 33.0 Hz), 126.2, 125.6 (q, J_{C-F} = 3.8 Hz), 124.6 (d, J_{C-F} = 271.9 Hz), 123.2, 121.0, 119.4, 113.7, 111.2. **¹⁹F NMR (376 MHz, CDCl₃):** δ = -62.34

¹³⁵ Fang, Y.-Q.; Lautens, M. J. *Org. Chem.* **2008**, *73*, 538.

¹³⁶ Wang, X.; Gribkov, D. V.; Sames, D. J. *Org. Chem.* **2007**, *72*, 1476.

Chapter 4

Enantioselective 4-Hydroxylation of Phenols under Chiral Organoiodine(I/III) Catalysis

4.1 Introduction

In Chapters 2 and 3, we have presented two different but complementary indole syntheses based on iodine(III) reactivity. The unique reactivity characteristics of the involved iodine(III) reagents inspired the development of asymmetric transformations induced by chiral hypervalent iodine species (Figure 4.1). The exploration of this comparatively new area started with the pioneering report on the enantioselective oxidation of sulfides to sulfoxides (Figure 4.1 a),¹³⁷ but other transformations such as oxygenation of ketones (Figure 4.1 b),^{24,25} alkene difunctionalization (Figure 4.1 c),^{19-21,26-28} and oxidative dearomatization of phenols (Figure 4.1 d) were developed over the last years.

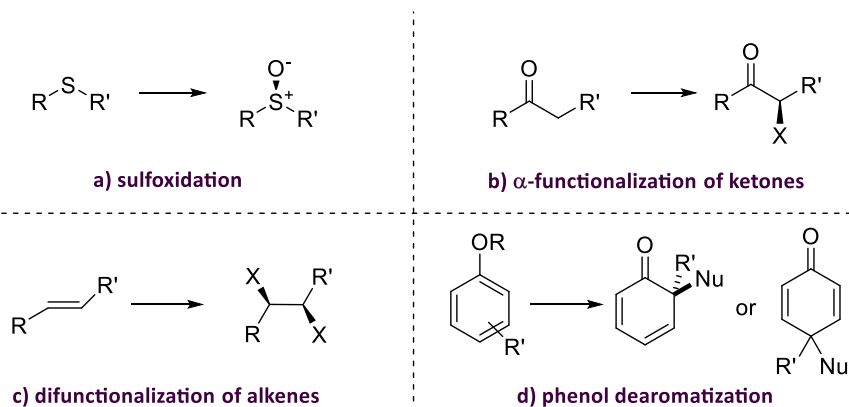


Figure 4.1 Chiral iodine-mediated asymmetric transformations.

¹³⁷ a) Imamoto, T.; Koto, H. *Chem. Lett.* **1986**, 967; b) Altermann, S. M.; Schafer, S.; Wirth, T. *Tetrahedron* **2010**, *66*, 5902; c) Ladziata, U.; Carlson, J.; Zhdkankin, V. V. *Tetrahedron Lett.* **2006**, *47*, 6301.

Influenced by this interesting area of unique reactivity, we decided to add to the field and explore the reactivity of chiral iodine(III) catalysts in different transformations: 2,3-diacetoxylation of indoles, Kita spirolactamization and 4-hydroxylation of phenols. Therefore, stereoselective alkene dioxygenation and phenol oxidative dearomatization will be further introduced throughout this last chapter.

4.1.1 Chiral alkene dioxygenation reaction

One of the most interesting difunctionalization reactions is the stereoselective dioxygenation of alkenes. In 1933, Prévost reported a one-pot transformation of alkenes into *trans* 1,2-diols through a silver-mediated oxidation reaction followed by reduction or hydrolysis of the correspondent 1,2-dicarboxylate intermediates (Figure 4.2).¹³⁸

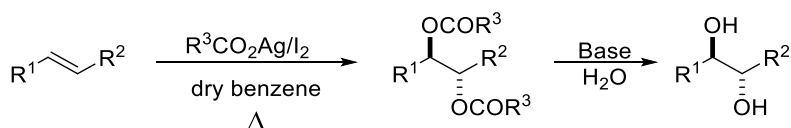


Figure 4.2 *Trans*-dihydroxylation of olefins proposed by Prévost.

A few years later, Woodward modified this protocol by the treatment of olefins with iodine and silver acetate in wet acetic acid. Under these conditions and in striking contrast to the Prévost reaction, *cis*-glycols are formed selectively (Figure 4.3).¹³⁹

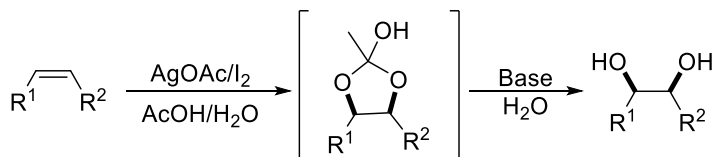


Figure 4.3 Woodward modification to prepare *cis*-diols.

¹³⁸ a) Prévost, C. *Compt. Rend.* **1933**, 196, 1129; b) Prévost, C. *Compt. Rend.* **1933**, 197, 1661; c) Prévost, C.; Lutz, B. *Compt. Rend.* **1933**, 198, 2264.

¹³⁹ Woodward, R. B.; Brucher, F. V. *J. Am. Chem. Soc.* **1958**, 80, 209.

Based on previous exploration on the formation of *cis*-diols using osmium tetroxide,¹⁴⁰ the main goal in this field was achieved by Sharpless. At the beginning of the 1980's, they reported the first asymmetric dihydroxylation reaction of olefins in the presence of stoichiometric osmium tetroxide and dihydroquinine acetate, a chiral tertiary amine ligand that belongs to the family of *Cinchona* alkaloids.¹⁴¹

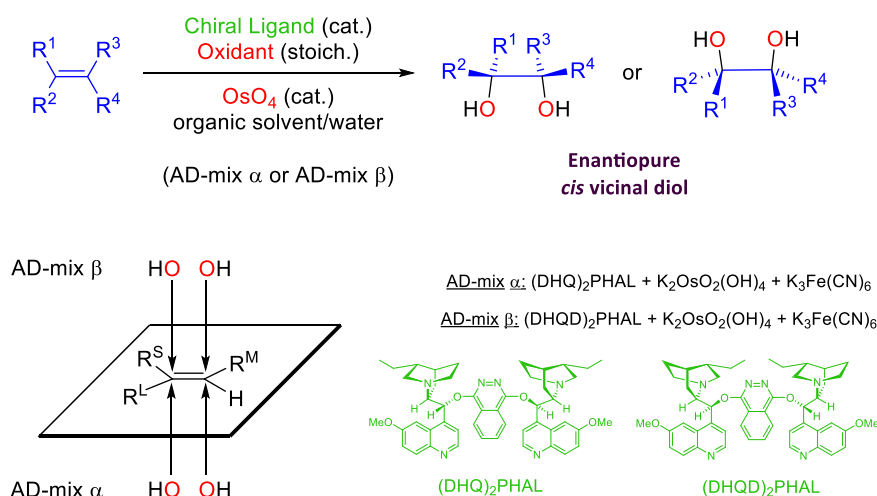


Figure 4.4 Sharpless reaction scheme and empirical face selection model.

Later, the introduction of NMO as a cooxidant enabled the use of diminished amounts of both osmium tetroxide and chiral amine.¹⁴² However, with this catalytic methodology, the enantiomeric excesses of the diol products were initially lower than those produced by the stoichiometric reaction. This problem was initially solved by the slow addition of the olefin.¹⁴³ Finally, the discovery of potassium ferricyanide¹⁴⁴ as a

¹⁴⁰ a) Criegee, R. *Justus Liebigs Ann. Chem.* **1938**, 522, 75; b) Criegee, R.; Marchand, B.; Wannowius, H. *Justus Liebigs Ann. Chem.* **1942**, 550, 99; c) Kolb, H. C.; VanNieuwenhze, M. S.; Sharpless, K. B. *Chem. Rev.* **1994**, 94, 2483; d) Noe, M. C.; Letavic, M. A.; Snow, S. L.; McCombie, S. W. *Org. React.* **2005**, 66, 109.

¹⁴¹ Hentges, S. G.; Sharpless, K. B. *J. Am. Chem. Soc.* **1980**, 102, 4263.

¹⁴² Jacobsen, E. N.; Markó, I.; Muneal, W. S.; Schroder, G.; Sharpless, K. B. *J. Am. Chem. Soc.* **1988**, 110, 1968.

¹⁴³ a) Wai, J. S. M.; Markó, I.; Svendsen, J. S.; Finn, M. G.; Jacobsen, E. N.; Sharpless, K. B. *J. Am. Chem. Soc.* **1989**, 111, 1123; b) Lohray, B. B.; Kalantar, T. H.; Kim, B. M.; Park, C. Y.; Shibata, T.; Wai, J. S. M.; Sharpless, K. B. *Tetrahedron Lett.* **1989**, 30, 2041.

¹⁴⁴ Kwong, H.-L.; Sorato, C.; Ogino, Y.; Chen, H.; Sharpless, K. B. *Tetrahedron Lett.* **1990**, 31, 2999.

stoichiometric reoxidant and its combination with $K_2OsO_2(OH)_4$ as a nonvolatile osmium together with the development of an enzyme-like binding pocket, the phthalazine ligand in the "dimeric" *Cinchona* alkaloid,¹⁴⁵ $(DHQ)_2PHAL$ and $(DHQD)_2PHAL$, lead to the preparation of a pre-mix containing all reagents, which is commercially available under the name of "AD-mix" (Figure 4.4).¹⁴⁶ The development of the Sharpless AD reaction constitutes one of the most impressive achievements in homogeneous catalysis; it was recognized with the Nobel Prize in 2001.

Chiral hypervalent iodine reagents can also mediate this type of oxidative transformations. In 1997, Wirth reported the first example of asymmetric oxidation of styrene using stoichiometric chiral iodine(III) reagent, in which the final ditosyloxyated product showed an enantiomeric excess up to 21%.¹⁴⁷ In order to improve this result, they introduced some modifications in the chiral hypervalent iodine reagent triggering finally an enantiomeric excess of up to 65% (Figure 4.5).¹⁴⁸ This chiral iodine(III) reagent displays a T-shaped structure and it can be considered as a chirally modified Koser reagent. The chiral 1-arylalkyl ether engages in chelation to the iodine center to provide a more rigid stereochemical environment at the iodine.

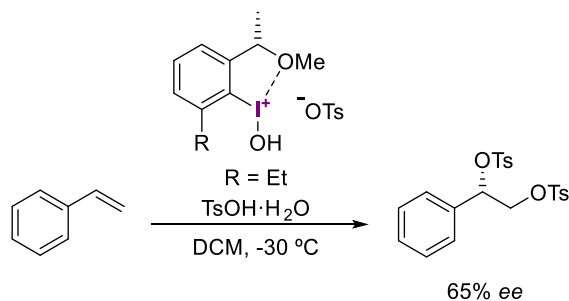


Figure 4.5 Enantioselective dihydroxylation of styrene proposed by Wirth.

¹⁴⁵ Sharpless, K. B.; Amberg, W.; Beller, M.; Chen, H.; Hartung, J.; Kawanami, Y.; Liibben, D.; Manoury, E.; Ogino, Y.; Shibata, T.; Ukita, T. *J. Org. Chem.* **1991**, *56*, 4585.

¹⁴⁶ a) Hartung, J.; Jeong, K.-S.; Kwong, H.-L.; Morikawa, K.; Wang, Z.-M.; Xu, D.; Zhang, X.-L. *J. Org. Chem.* **1992**, *57*, 2768; b) Amberg, W.; Bennani, Y. L.; Chadha, R. K.; Crispino, G. A.; Davis, W. D.; Hartung, J.; Jeong, K.-S.; Ogino, Y.; Shibata, T.; Sharpless, K. B. *J. Org. Chem.* **1993**, *58*, 844.

¹⁴⁷ Wirth, T.; Hirt, U. H. *Tetrahedron: Asymmetry* **1997**, *8*, 23.

¹⁴⁸ a) Hirt, U. H.; Spingler, B.; Wirth, T. *J. Org. Chem.* **1998**, *63*, 7674; b) Hirt, U. H.; Schuster, M. F. H.; Frenh, A. N.; Wiest, O. G.; Wirth, T. *Eur. J. Org. Chem.* **2001**, 1569.

Later, based on their previous results on chiral iodine(III)-mediated transformations,¹⁴⁹ Fujita reported an improved protocol for the enantioselective diacetoxylation reaction. Depending on the reaction conditions, the transformation can proceed with *syn* selectivity in a Woodward-type fashion. On the contrary, high *anti* selectivity can be accomplished following the Prévost mechanism. Using the two respective sets of conditions, they selectively obtained either the *syn* or *anti* products with enantioselectivities up to 96% for both cases (Figure 4.6).¹⁵⁰ The reaction is initiated by face selection of the alkene through the coordination to the chiral iodine(III) reagent.

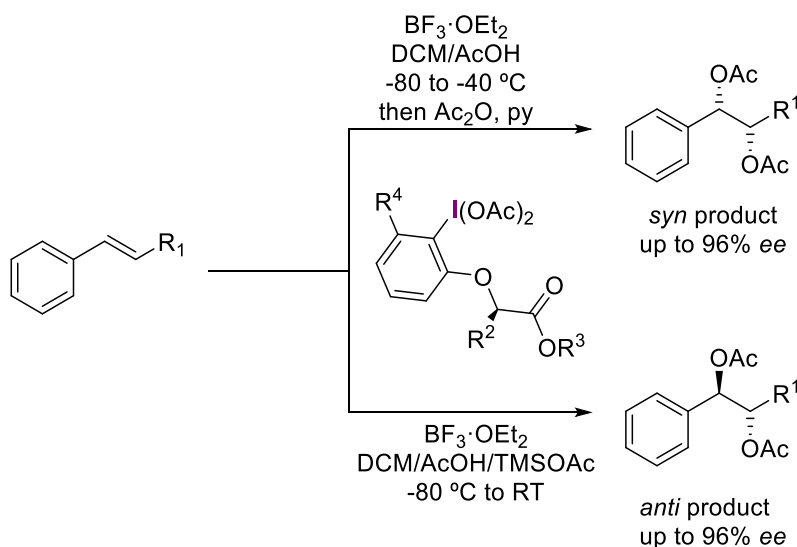


Figure 4.6 Enantioselective Prévost and Woodward reactions reported by Fujita.

This feature is highly important demonstrating that the chiral induction generated from a non-racemic hypervalent iodine reagent can compete with the enantiomeric excesses that are usually encountered from the osmium-catalyzed asymmetric dihydroxylation of styrene.

¹⁴⁹ a) Fujita, M.; Okuno, S.; Lee, H. J.; Sugimura, T.; Okuyama, T. *Tetrahedron Lett.* **2007**, *48*, 8691; b) Fujita, M.; Ookubo, Y.; Sugimura, T. *Tetrahedron Lett.* **2009**, *50*, 1298; c) Fujita, M.; Yoshida, Y.; Miyata, K.; Wakisaka, A.; Sugimura, T. *Angew. Chem. Int. Ed.* **2010**, *49*, 7068.

¹⁵⁰ Fujita, M.; Wakita, M.; Sugimura, T. *Chem. Commun.* **2011**, *47*, 3983.

The main drawback of these methodologies is the requirement of stoichiometric amounts of the chiral iodine(III) reagent. Therefore, our group has contributed to this field developing the first catalytic enantioselective diacetoxylation of styrenes using a chiral iodine(I) catalyst precursor **16** and peracetic acid as terminal oxidant (Figure 4.7).¹⁵¹ A total of 24 styrenes were converted into the corresponding diacetoxyated derivatives in an enantioselective and chemoselective manner, in good yields and with high enantioselectivities up to 94% *ee*.

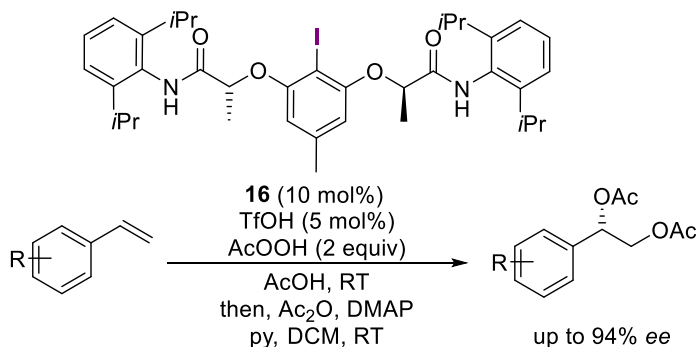


Figure 4.7 First catalytic enantioselective diacetoxylation of styrenes based on chiral iodine(III) reactivity.

By X-ray analysis, we could probe the decisive hydrogen bonding interaction between the amide NH groups and the acetoxy groups at the central iodine for the correspondent diacetoxy derivative **16a** (Figure 4.8 top). The main aspect of this observation resides in the creation of a supramolecular helical chirality around the iodine atom (Figure 4.8 bottom).¹⁵² Due to this effective interaction, the supramolecular arrangement induced by the lactamide chains is the cause of the observed high enantioselective induction in the diacetoxylation reaction.

¹⁵¹ Haubenreisser, S.; Wöste, T. H.; Martínez, C.; Ishihara, K.; Muñiz, K. *Angew. Chem. Int. Ed.* **2016**, *55*, 413.

¹⁵² a) Desiraju, G. R. *Angew. Chem. Int. Ed.* **2011**, *50*, 52; b) Lehn, J. N. *Supramolecular Chemistry. Concepts and Perspectives*; Wiley-VCH: Weinheim, **1995**; c) *Hydrogen Bonded Supramolecular Structures*; Li, Z.; Wu L.-Z., Ed.; Springer: Berlin, **2015**.

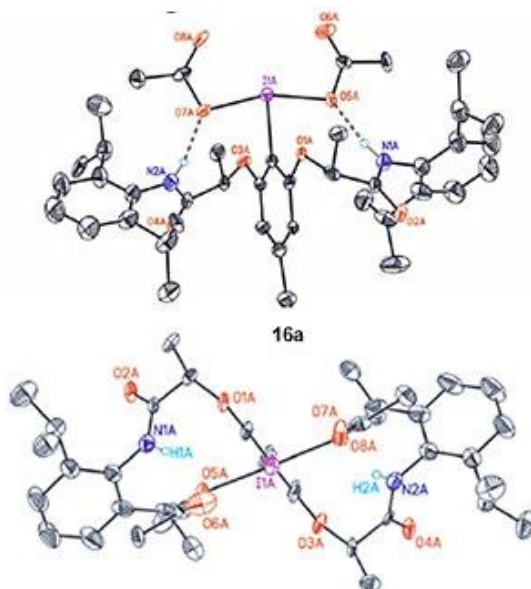


Figure 4.8 Intramolecular hydrogen bonding confirmed by X-Ray analysis.

We also explored the use of the parent diesters as a chiral catalyst for this transformation (Figure 4.9).¹⁵³ The 1-adamantyl derivative appears to be the most efficient derivative to promote the diacetoxylation reaction in the presence of Selectfluor as terminal oxidant and a Lewis acid, TMSOTf. The reaction conditions are general for a wide range of styrenes and can be extended to cinnamic alcohols, which represent internal alkenes.

¹⁵³ Wöste, T. H.; Muñiz, K. *Synthesis* **2016**, *48*, 816.

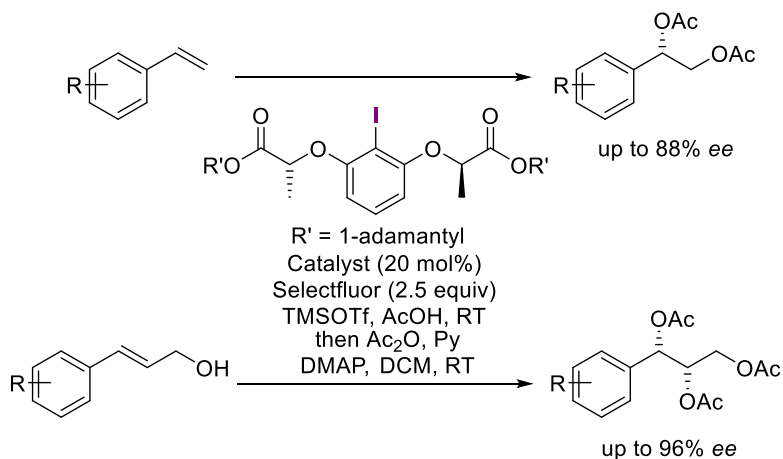


Figure 4.9 Diacetylation reaction catalyzed by a chiral 1-adamantyl diester derivative.

As it was described, chiral hypervalent reagents can be the appropriate alternative to the transition metal-mediated diacetylation reaction. This type of benign reagents reacts under mild conditions and provides the best chiral environment for enantioselection control.

4.1.2 Chiral phenol dearomatization reaction

The hypervalent iodine-mediated dearomatization of phenols is a well-known and highly useful reaction. This reaction can be conducted for a wide variety of phenols and thus shows a synthetically interesting scope. The underlying strategy is based on the readily accessible coordination of the iodine(III) to the OH group of the substrate. After this ligand exchange step, oxocyclopentadienyl cations are formed as intermediates that can be attacked by a suitable nucleophile in an overall process that constitutes an umpolung of the inherent phenol reactivity (Figure 4.10). Alternatively, simultaneous addition of the nucleophile to the coordinated phenolate has been suggested as the reaction mechanism.

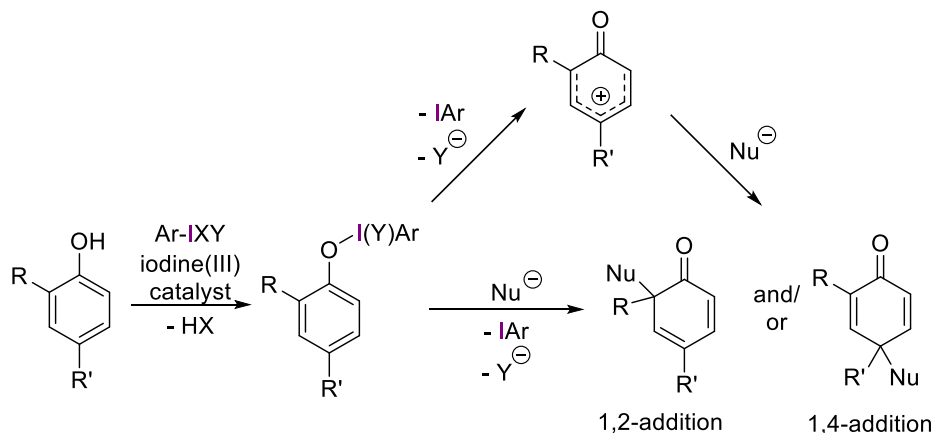


Figure 4.10 Commonly proposed mechanisms for the asymmetric iodine(III)-mediated dearomatization of phenols.

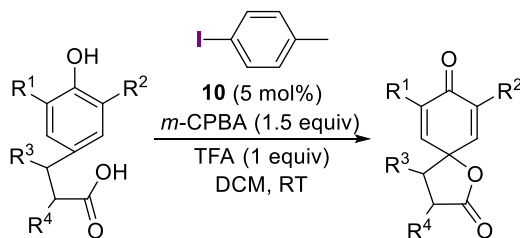
These two-electron oxidations that involve the addition of a nucleophile to the aromatic ring of the phenol, result in the formation of either 1,2- or 1,4-addition products. Both inter- and intramolecular nucleophilic attacks are possible with a sort of different nucleophiles. These mostly constitute heteroatom-based nucleophiles such as carboxylic acids, alcohols and amides, among others.

The intramolecular dearomatization of phenols is generally known as the Kita oxidation, in which the nucleophile is preinstalled in the starting phenol derivative. In 2005, they reported a catalytic intramolecular spirocyclization using iodine(III)-catalysis with *m*-CPBA as a terminal oxidant (Figure 4.11 a).¹⁵⁴ This methodology was further extended to a spirocyclization reaction by switching the solvent to a more polar and acidic one such as trifluoroethanol (Figure 4.11 b).¹⁵⁵ Later, they found that using diiodine-based biaryl catalyst **14**, peracetic acid is capable of acting as a terminal oxidant in this transformation.¹²⁸

¹⁵⁴ Dohi, T.; Maruyama, A.; Yoshimura, M.; Morimoto, K.; Tohma, H.; Kita, Y. *Angew. Chem. Int. Ed.* **2005**, *44*, 6193.

¹⁵⁵ Dohi, T.; Maruyama, A.; Minamitsuji, Y.; Takenaga, N.; Kita, Y. *Chem. Commun.* **2007**, 1224.

a) Catalytic spirolactonization



b) Catalytic spirolactamization.

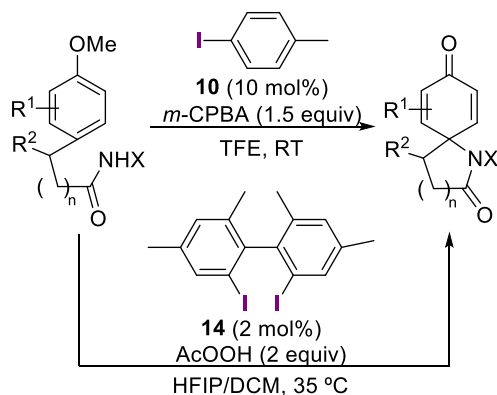


Figure 4.11 Examples for organocatalytic spirocyclization through phenol dearomatization reported by Kita.

The major breakthrough in this area was the development of a chiral hypervalent iodine-catalyzed Kita spirocyclization reaction. In 2008, they reported such a transformation starting from naphthols using a conformationally rigid, chiral iodine(III) reagent based on a 1,1'-spirobiindane backbone, **17**. Due to the creation of this chiral environment, spirolactones were obtained with high enantioselectivity up to 86% *ee* (Figure 4.12, top).¹⁵⁶ This result was further improved introducing *ortho* substituents to each iodine atom in the catalyst, **18b** (Figure 4.12, bottom).¹⁵⁷

¹⁵⁶ Dohi, T.; Maruyama, A.; Takenaga, N.; Senami, K.; Minamitsuji, Y.; Fujioka, H.; Caemmerer, S. B.; Kita, Y. *Angew. Chem., Int. Ed.* **2008**, *47*, 3787.

¹⁵⁷ Dohi, T.; Takenaga, N.; Nakae, T.; Toyoda, Y.; Yamasaki, M.; Shiro, M.; Fujioka, H.; Maruyama, A.; Kita, Y. *J. Am. Chem. Soc.* **2013**, *135*, 4558.

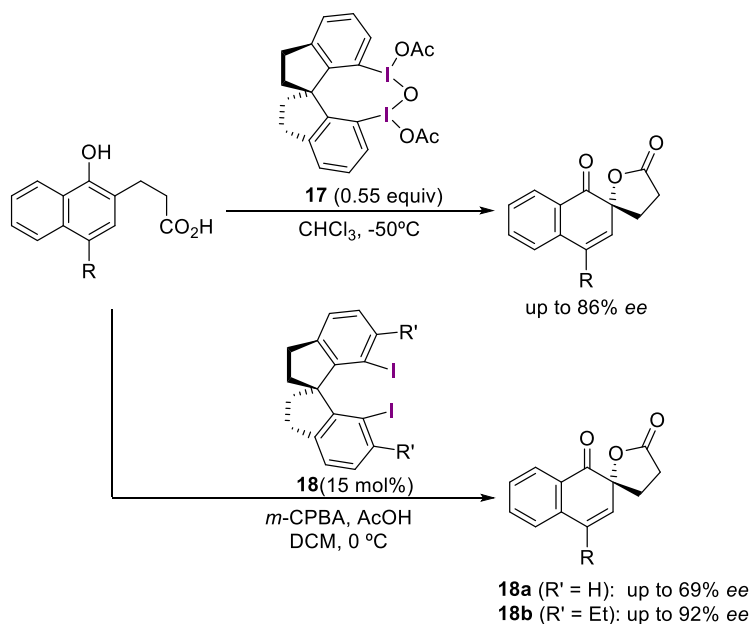


Figure 4.12 Kita enantioselective spirocyclization of naphthols.

A completely different catalyst design was proposed by Ishihara and Uyanik (Figure 4.13).¹⁵⁸ The successful combination of a conformationally flexible catalyst **19** and $m\text{-CPBA}$, afforded the correspondent lactones with high enantioselectivity due to the C_2 -symmetric chirality generated around the iodine atom, as in the previously described asymmetric diacetoxylation of styrenes.¹⁵¹

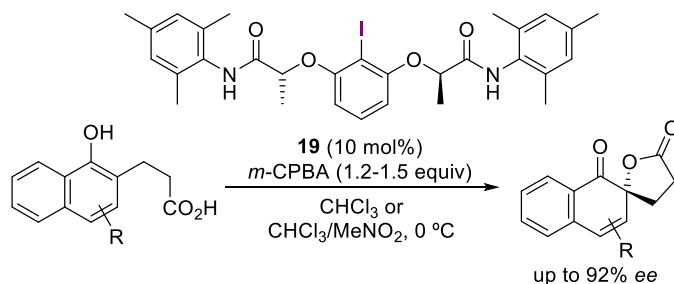


Figure 4.13 Asymmetric Kita oxidative spirocyclization designed by Ishihara and Uyanik.

¹⁵⁸ Uyanik, M.; Yasui, T.; Ishihara, K. *Angew. Chem. Int. Ed.* **2010**, *49*, 2175; b) Uyanik, M.; Yasui, T.; Ishihara, K. *Tetrahedron* **2010**, *66*, 5841.

Following this catalyst approach, they developed a methodology for an enantioselective catalytic oxidative dearomatization of simple phenol derivatives (Figure 4.14).¹⁵⁹ The cyclohexanodienone spiro lactones can be further trapped with dienophiles in a Diels-Alder reaction. A beneficial effect in the dearomatization reaction was observed when different alcohols were added to the reaction. Regarding the catalyst, good selectivity was observed with aryl iodide **19**, although low yields were obtained. Introducing some changes at the chiral arms, catalyst **20** provided the desired spiro lactones with high enantioselectivity.

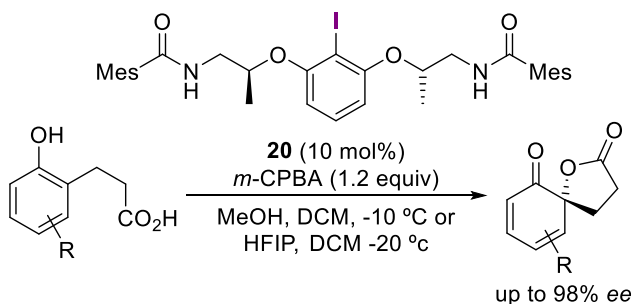


Figure 4.14 Ishihara and Uyanik's intramolecular oxidative dearomatization of phenols.

All these methodologies required preinstallation of the suitable nucleophile in the substrate. However, hypervalent iodine reagents can oxidize phenols to quinones and promote the addition reaction with external nucleophiles. A seminal work by Yakura and Konishi,¹⁶⁰ in which they reported the synthesis of *p*-quinols by catalytic oxidation of *p*-aryl phenols led the way to the use of catalytic amounts of iodine(III) reagents.

Although 1,4-addition to the deconjugated product is preferred, the achievement of an asymmetric intermolecular version of this transformation was not explored further. Usually, enantioselective 1,2- and 1,4-addition to the deconjugated product from intermolecular asymmetric oxidation of phenols can be also achieved through iodine(III) reactivity (Figure 4.10).

¹⁵⁹ Uyanik, M.; Yasui, T.; Ishihara, K. *Angew. Chem. Int. Ed.* **2013**, *52*, 9215.

¹⁶⁰ a) Yakura, T. *Synlett* **2007**, 765; b) Yakura, T.; Tian, Y.; Yamauchi, Y.; Omoto, M.; Konishi, T. *Chem. Pharm. Bull.* **2009**, *57*, 252.

In 2009, Quideau reported the hydroxylative dearomatization of 2-methyl naphthol to the corresponding 1,2-addition product (Figure 4.15).¹⁶¹ When catalytic amounts of aryl iodide **21** were used, the excess of oxidant promoted a subsequent diastereoselective epoxidation of the remaining double bond.

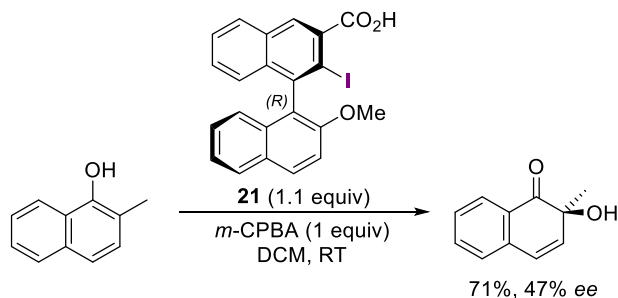


Figure 4.15 Quideau proposal for the hydroxylation at 2-position.

Recently, the same group improved this result by using substoichiometric amounts of a chiral iodosyl derivative **22** (Figure 4.16).¹⁶² This reagent arises from a selective *in situ* DMDO-mediated oxidation of the corresponding chiral diiodo biphenyl precursor. Under these conditions, the *o*-quinol is obtained with high enantioselectivity of up to 73% *ee*.

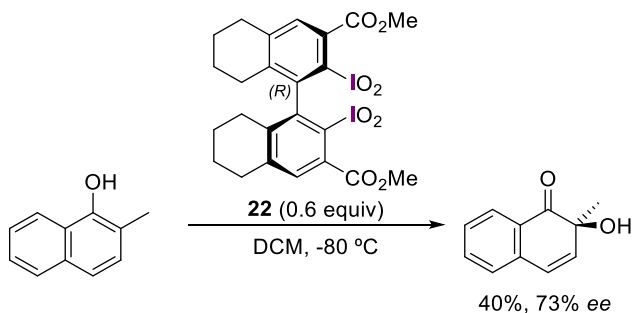


Figure 4.16 Asymmetric phenol dearomatization promoted by chiral biphenylic iodane.

¹⁶¹ Quideau, S.; Lyvynec, G.; Marguerit, M.; Bathany, K.; Ozanne-Beaudenon, A.; Buffeteau, T.; Cavagnat, D.; Chénéde, A. *Angew. Chem. Int. Ed.* **2009**, *48*, 4605.

¹⁶² Bosset, C.; Coffinier, R.; Peixoto, P. A.; El Assal, M.; Miqueu, K.; Sotiropoulos, J.-M.; Pouységu, L.; Quideau, S. *Angew. Chem. Int. Ed.* **2014**, *53*, 9860.

In 2014, Harned presented the first enantioselective synthesis of 2,5-cyclohexanodiones catalyzed by a chiral aryliodide (Figure 4.17).¹⁶³ A new catalyst **23** was developed for the enantiocontrol in the nucleophilic attack by water. The corresponding 4-hydroxylated products were obtained with good enantioselectivity although yields remained low.

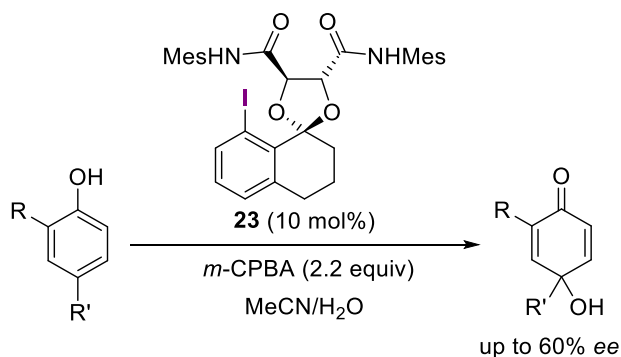


Figure 4.17 Harned's asymmetric dearomatization to 4-hydroxylated cyclohexanodiones.

In conclusion, enantioselective dearomatization of naphthols and phenols could be achieved using iodine(III)-catalysis. Different catalyst designs were proposed for enantiocontrol in the addition step of both an internal or an external nucleophile. Although, the intramolecular attack proceeds with high enantioselectivity, the related intermolecular version is still a challenge in the area of iodine(III)-catalysis.

¹⁶³ Volp, K.; Harned, A. M. *Chem. Commun.* **2013**, 49, 3001.

4.2. Objective

The development of chiral versions of hypervalent iodine reagents and catalysts has drawn particular attention in recent years. However, some hypervalent iodine-mediated transformations remain to be a challenge in the field of enantioselective catalysis.

Inspired by a work by Lei¹⁶⁴ in which diacetoxylyated indoles could be obtained with high diastereoselectivity using PIDA (Figure 4.18), we decided to try our catalytic system previously described for the diacetoxylation of styrenes **16** in such a transformation (Figure 4.19, top).

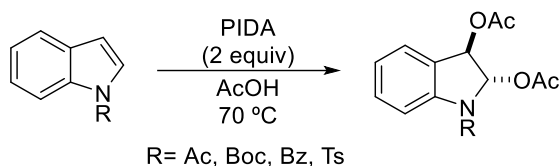


Figure 4.18 Iodine(III)-mediated *trans*-diacetoxylation of indoles developed by Lei.

One of the most known transformation in the field of asymmetric iodine(III)-catalysis is the dearomatization of phenols. The intramolecular version of this transformation known as Kita's oxidation has been widely explored and high enantioselectivities were achieved. In contrast, a few methodologies for the related intermolecular version have been reported.¹⁶¹⁻¹⁶³ Therefore, we envisioned the use of our chiral catalyst **16** and derivatives for the development of an intermolecular asymmetric dearomatization of phenols (Figure 4.19, bottom).

¹⁶⁴ Liu, Q.; Zhao, Q. Y.; Liu, J.; Wu, P.; Yi, H.; Lei, A. *Chem. Commun.* **2012**, *48*, 3239.

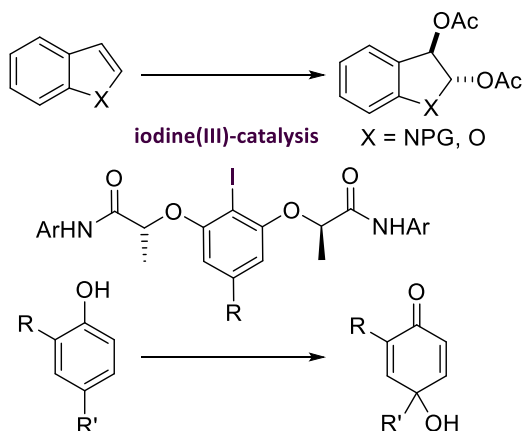


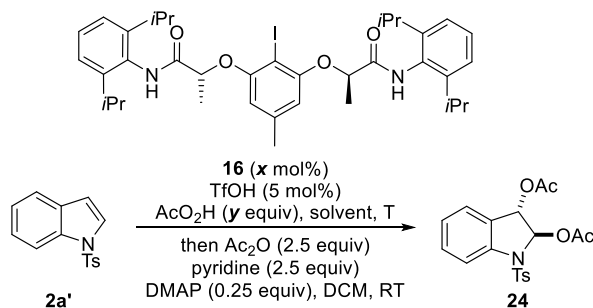
Figure 4.19 Synthetic scheme for asymmetric hypervalent iodine-catalyzed transformations.

4.3. Results and discussion

4.3.1 Optimization of the reaction conditions

We focused in the investigation of the activity of our chiral aryl iodide catalyst **16** and its possible derivatives in different transformations. For this aim, we started to explore its reactivity in the diacetoxylation of heterocycles. Benzofurane and *N*-tosylated indol were chosen as model substrates for this transformation.

Taking into account that indoles can be diacetoxyated under stoichiometric amounts of an iodine(III)-reagent¹⁶⁴ we decided to start to explore this substrate with our previously described chiral catalyst **16** (Table 4.1).¹⁵¹



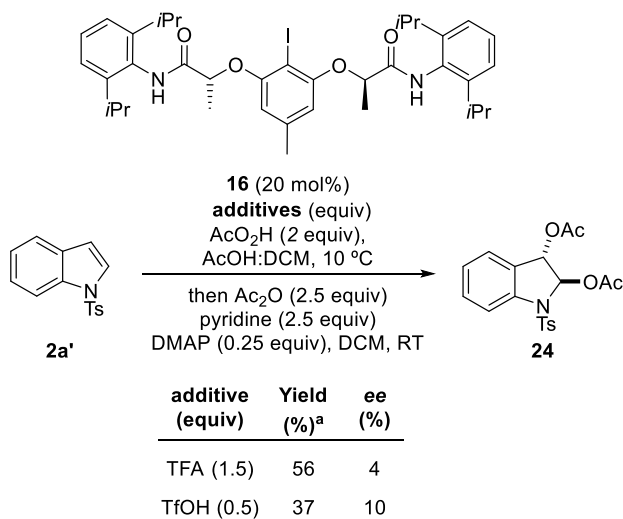
Entry	<i>x</i> equiv catalyst	<i>y</i> equiv oxidant	Solvent	T (°C)	Yield (%) ^a	ee (%)
1 ^b	0.1	2	AcOH	RT	<25 ^c	-
2	0.2	2	AcOH	RT	60	0
3	0.2	2	AcOH:DCM	10	88	<5
4 ^d	0.2	2	AcOH:DCM	10	87	12
5	0.2	2	AcOH:MeNO ₂	10	71	4
6	0.2	4	AcOH:DCM	10	83	8
7	0.2	2	AcOH:DCM	0	81	<5
8	0.2	4	AcOH:DCM	0	81	8

^a: Isolated yield after purification. ^b: Addition of substrate **2a'** dissolved in AcOH by syringe pump (see ref. 151) ^c: Based on crude reaction mixture. ^d: TMSOTf is used instead TfOH.

Table 4.1 First attempts for the enantioselective iodine(III)-diacetoxylation of indoles.

The first attempt applying our previously reported conditions for enantioselective diacetoxylation of styrenes results unsuccessful for this special substrate and less than 25% of the final product was observed by ¹H-NMR analysis of the crude reaction mixture (entry 1). The reaction appears to be slow under conditions with syringe pump addition of the substrate. When the reaction is performed by addition of the substrate in a single portion, 60% of the diacetoxylation indolin **24** was isolated, but no enantioselectivity was observed (entry 2). At this point, we performed the reaction at low temperature. For this aim, an additional solvent is needed to maintain solubility due to the melting point of the acetic acid. When the reaction was carried out at 10 °C, increased yields are obtained although no enantioinduction is observed (entries 3 and 4). Changes on the solvent mixture, increased amounts of oxidant or further decreased in the temperature did not improve the selectivity (entries 5, 6, 7 and 8). However, high diastereoselectivity was observed and only *trans*-diacetoxylation indolin was obtained.

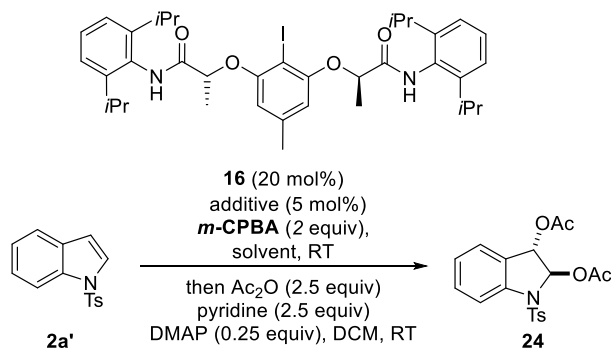
When other acids are used such trifluoroacetic acid, TFA and triflic acid, TfOH, the yield decreased and no beneficial effect in the selectivity was observed (Table 4.2).



^a: Isolated yield after purification.

Table 4.2 Results obtained with different acids.

After these unsuccessful results with respect to enantioselectivity, we explore the use of other oxidants such as *m*-CPBA (Table 4.3). When the diacetylation reaction is carried out applying the best conditions from the peracetic acid runs, no further improvement regarding enantiocontrol was observed, although the final indolin can be afforded in a 90% yield (entry 3).

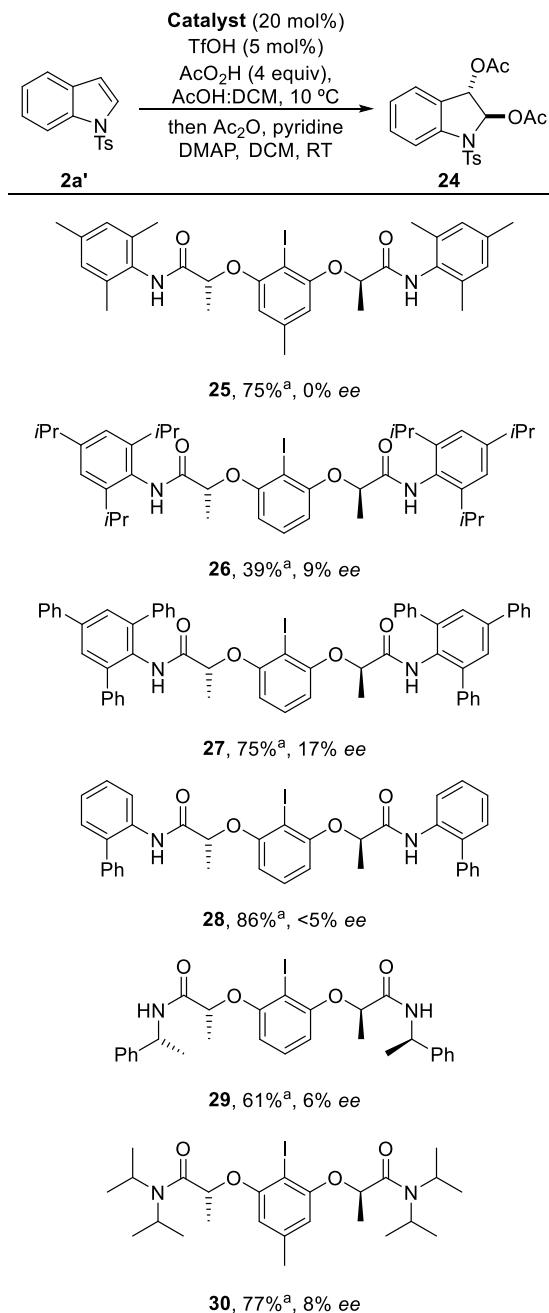


Entry	additive	solvent	Yield (%) ^a	ee (%)
1	-	AcOH	69	0
2	TfOH	AcOH	68	12
3	TMSOTf	AcOH	90	6
4	-	AcOH:DCM	64	0

^a: Isolated yield after purification.

Table 4.3 Screening of conditions using *m*-CPBA as terminal oxidant.

In order to increase the enantiocontrol in this transformation, different chiral catalysts derivatives were prepared and tested in the diacetoxylation reaction (Figure 4.20). First, catalysts **25**, **26**, **27** and **28** with different substitution pattern of the aryl in the amide group were synthesized, but no positive effect in enantioselectivity was observed. When anilines are replaced by chiral aliphatic amines, catalyst **29**, enantioinduction did not improve, neither using secondary amines as in catalyst **30**, which had previously been used successfully in the asymmetric diamination of styrenes.²⁶

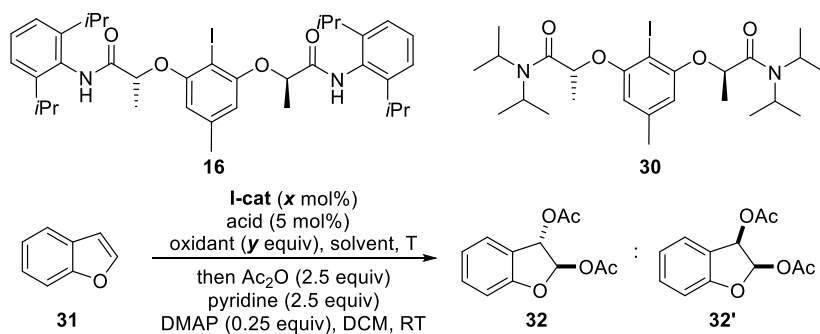


^a: Isolated yields after purification.

Figure 4.20 Screening of catalysts with different aryl substitution pattern in the amide group.

At this point, we decided to try other heterocycles such benzofurane as a substrate for the diacetoxylation reaction. The final diacetoxyated benzofurane has been not reported previously in the literature, so the enantioselective synthesis of such a product represents an interesting undertaking.

First attempts were carried out with two different catalysts **16** and **30** at room temperature (Table 4.4). The main difference of these two catalysts is the possibility of the amide NH group to interact to through hydrogen bonding for chiral induction for the former catalyst. When catalyst **16** was tested using our previous diacetoxylation conditions, the final diacetoxyated product was isolated in a 30% yield but without any chiral induction (entry 1). The use of catalyst **29** did not improve the enantioselectivity and the isolated yield dropped dramatically (entries 2 and 3). No final product was observed when this catalyst was combined with other acid such TMSOTf (entry 4). Coming back to catalyst **16** that showed better reactivity, other oxidant such *m*-CPBA was tested. Under these conditions, the yield slightly increased but no enantioselectivity was observed.



Entry	I-cat	x (equiv)	oxidant	y (equiv)	acid	solvent	T (°C)	32:32'	Yield (%) ^a	ee (%)
1	16	0.1	AcOOH	2	TfOH	AcOH	RT	1:0.22	30	0
2	29	0.1	AcOOH	2	TfOH	AcOH	RT	1:0.21	15	0
3	29	0.2	AcOOH	2	TfOH	AcOH	RT	1:0.18	12	0
4	29	0.2	AcOOH	2	TMSOTf	AcOH	RT	-	-	-
5	16	0.2	<i>m</i> -CPBA	2	TMSOTf	AcOH	RT	1:0.2	33	0
6	16	0.2	<i>m</i> -CPBA	2	TfOH	AcOH	RT	1:0.28	40	2

^a: Isolated yield after purification.

Table 4.4 First attempts at room temperature for diacetoxylation of benzofurane.

By ^1H NMR analysis, we observed that the reaction is reasonably diastereoselective and *trans*-2,3-diacetoxyated dihydrobenzofurane was mainly observed (Figure 4.21).

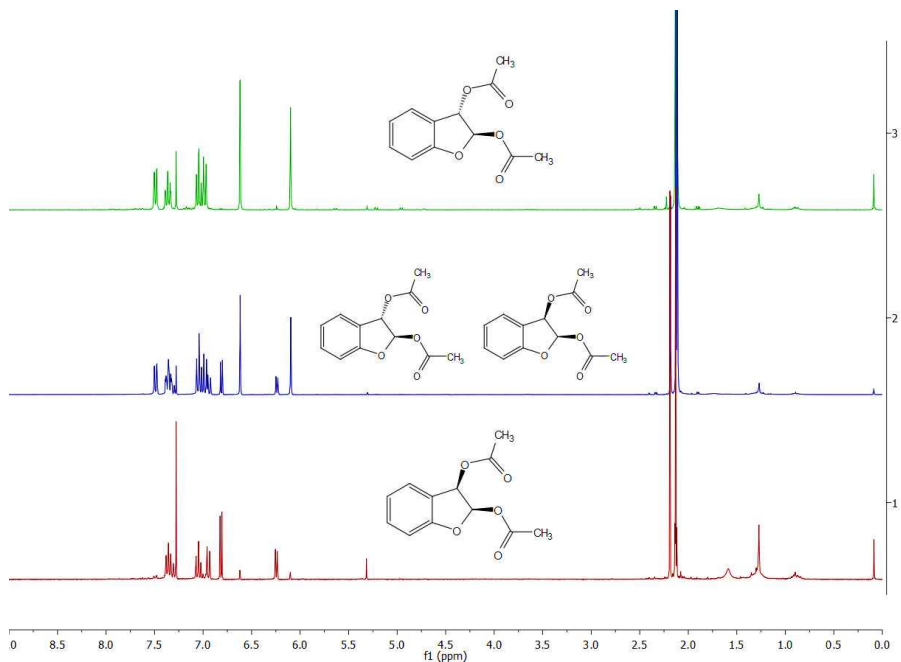
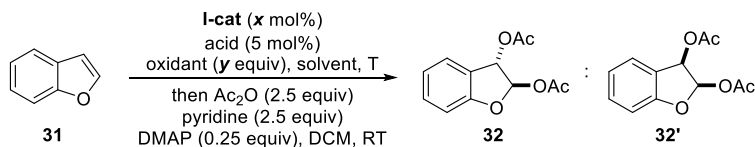


Figure 4.21 ^1H -NMR spectra of the diastomeric mixture and both diastomers separately.

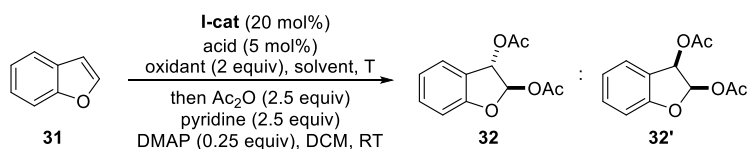
After these unsuccessful results, the reaction temperature was decreased (Table 4.5). At these temperatures, as for the indole diacetoxylation, the solvent mixture was changed and DCM was added. When the reaction was carried out with catalyst **16** at 10 $^{\circ}\text{C}$, a slightly increase in enantioselectivity was observed but remain low (entries 1, 2 and 3). At this temperature, catalyst **30** was not effective and the final diacetoxyated product was not observed (entries 4, 5 and 6). Further decrease of the reaction temperature didn't improve the enantioselectivity and the reaction appears to be slower, decreasing the isolated yield of the desired product (entry 7). However, when increased amounts of the catalyst were added, the reaction proceeded with high diastereoselectivity (entry 8).



Entry	I-cat	x (equiv)	oxidant	y (equiv)	acid	solvent ^a	T (°C)	32:32'	Yield (%) ^b	ee (%)
1	16	0.1	AcOOH	1.5	TfOH	AcOH:DCM	10	1:0.23	34	0
2	16	0.2	AcOOH	2	TfOH	AcOH:DCM	10	1:0.17	28	12
3	16	0.2	AcOOH	2	TMSOTf	AcOH:DCM	10	1:0.16	38	6
4	30	0.1	AcOOH	2	TfOH	AcOH:DCM	10	-	-	-
5	30	0.1	AcOOH	2	TMSOTf	AcOH:DCM	10	-	-	-
6	30	0.2	AcOOH	2	TfOH	AcOH:DCM	10	-	-	-
7	16	0.1	AcOOH	2	TfOH	AcOH:DCM	0	1:0.22	<10	5
8	16	0.2	AcOOH	2	TMSOTf	AcOH:DCM	0	1:0	11	14

^a: Reaction carried out in a solvent mixture AcOH/DCM, 2/1, v/v. ^b: Isolated yield after purification.

Table 4.5 Results obtained lowering the temperature to 0 and 10 °C.



Entry	I-cat	oxidant	acid	solvent	T (°C)	32:32'	Yield (%) ^a	ee (%)
1	16	AcOOH	TMSOTf	AcOH:DCM (1:1)	-10	1:0.17	13	16
2	16	<i>m</i> -CPBA	TMSOTf	AcOH:DCM (1:1)	-10	-	-	-
3	16	<i>m</i> -CPBA	TfOH	AcOH:DCM (1:1)	-10	-	-	-
4	16	<i>m</i> -CPBA	TfOH	AcOH:DCM (1:2)	-10	1:0.16	18	0
5	16	<i>m</i> -CPBA	TfOH	HFIP:DCM (1:2)	-10	1:0.15	17	4
6	16	AcOOH	TfOH	HFIP:DCM (1:2)	-10	-	-	-
7	16	<i>m</i> -CPBA	TfOH	HFIP:DCM (1:1)	-10	1:0.17	24	4
8	16	<i>m</i> -CPBA	TMSOTf	HFIP:DCM (1:1)	-10	1:0.17	24	4
9	16	<i>m</i> -CPBA	TfOH	HFIP:DCM (2:1)	-10	1:0.18	18	0

^a: Isolated yield after purification.

Table 4.6 Results obtained for the diacetoxylation of benzofuran at -10 °C.

At low temperatures such $-10\text{ }^{\circ}\text{C}$, no improvement neither in yield or in enantioselectivity was observed (Table 4.6).

With these failed results for the enantioselective diacetoxylation reaction, a tentative mechanistic rationalization was undertaken (Figure 4.22). The final diacetoxylation indole **24** can racemize throughout the reaction or after its completion. This would proceed through a sequence of an acetoxy elimination triggered by the lone pair at the nitrogen and subsequent formation of a Woodward-type dioxolonium intermediate.¹³⁹ Finally, nucleophilic attack at the benzylic position provides the opposite enantiomer.

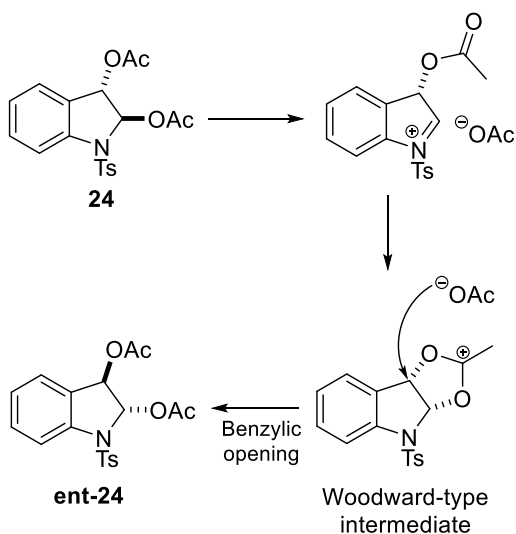
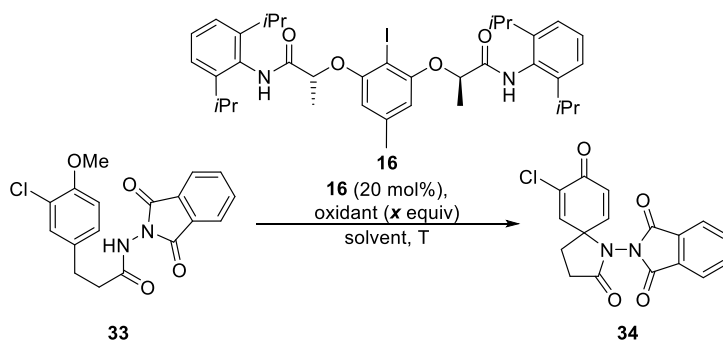


Figure 4.22 Proposal for the racemization observed during the optimization of the indole diacetoxylation.

In a subsequent investigation, we decided to explore the activity of our chiral catalysts in the Kita oxidation.¹⁵⁴⁻¹⁵⁹ As there is no precedent in literature, we decided to focus in the development of an enantioselective spiro lactamization reaction through phenol dearomatization (Table 4.7).

One of the problems found during the optimization of the reaction conditions was the purification by column chromatography due to the similar polarity of the substrate

33 and the final product **34**. Therefore, we focused in find the best conditions to achieve full conversion to the final lactam **34**. After an extensive screening of conditions, we found that catalyst **16** in the presence of either peracetic acid or *m*-CPBA in a fluorinated solvent, afforded the final lactam **34** in good yields but no enantioinduction was observed, even when lowering the temperature.

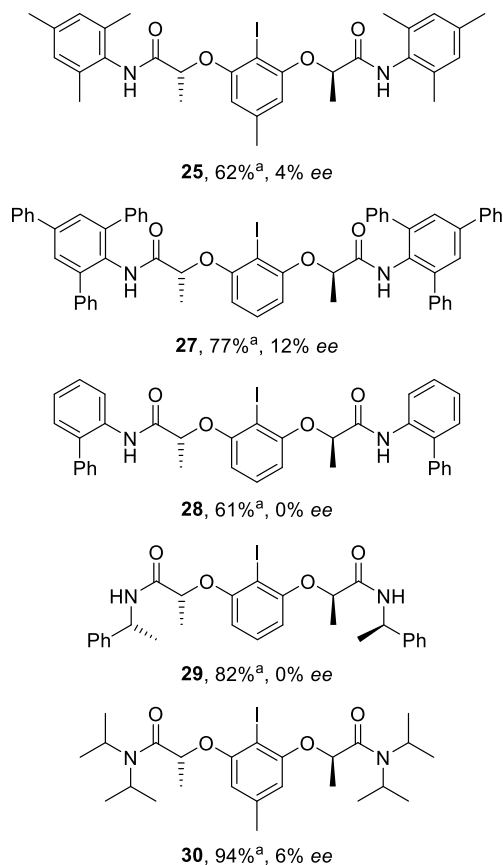
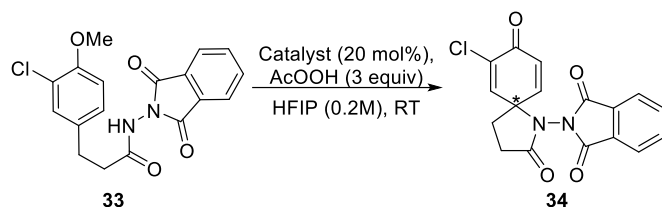


Entry	oxidant	x (equiv)	solvent	T (°C)	Yield (%) ^a	ee (%)
1 ^b	AcOOH	3	HFIP	RT	41	0
2	AcOOH	3	HFIP	RT	69	0
3	AcOOH	5	HFIP	RT	61	0
4	AcOOH	3	HFIP	10	57	0
5	AcOOH	5	HFIP	10	62	0
6	<i>m</i> -CPBA	5	TFE	RT	75	0

^a: Isolated yield after purification. ^b: Reaction at low concentration (0.1M).

Table 4.7 Summary of the results obtained for the optimization of chiral Kita oxidation.

Since no enantioselection was observed with catalyst **16**, a catalyst screening was performed (Figure 4.23). For this aim, we have chosen the conditions described in entry 2 together with various catalyst with different substituents at the amide group. Low enantioselectivity was observed with all of them; however, with catalyst **30** the final product was obtained in a 94% yield.



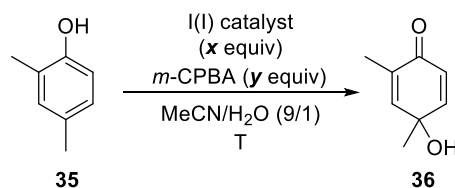
^a: Isolated yields after purification.

Figure 4.23 Catalyst screening for the optimization of chiral Kita oxidation.

As for the diacetoxylation reaction, almost no enantioselection was observed throughout the optimization of the reaction conditions. Best results were obtained with catalysts that contain bulkier groups at the aryl of the amide group, such as **27**. We can conclude that the catalyst design should be improved and adapted to generate the adequate chiral pocket needed for enantioinduction.

We selected commercial available 2,4-dimethyl phenol **35** as the model substrate. Initial experiments were carried out at room temperature using a mixture of solvents, MeCN and water, already used for this transformation (Table 4.8). When 10 mol% of iodine(I) **16** as catalyst source is combined with 2.2 equivalents of *m*-CPBA as terminal oxidant at room temperature the dearomatized product **36** was afforded in 33% isolated yield and with 26% *ee* (entry 1). Increase in the catalyst loading led to the formation of the final product **36** in a 76% of isolated yield, while the *ee* remained unchanged (entry 2).

If we modified the catalyst changing the electronics and the sterics of the aryl moiety directly bonded to the iodine as in catalyst **16'**, the yield dramatically dropped but a slightly increase in the enantiomeric excess was observed (32% *ee*, entry 3). This result represents the highest enantiomeric excess obtained so far for this substrate.¹⁶³ Increasing the catalyst loading, the isolated yield of the dearomatized product increased as well, although the enantioselectivity did not improve (entries 4 and 5). When a phenyl group was introduced into the *ortho* position of the aryl amide, catalyst **28**, no further improvement was observed (entry 6).



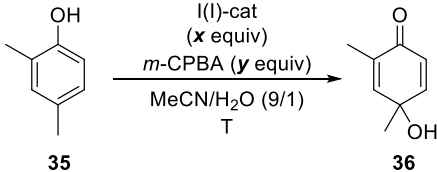
Entry	I(I)cat	x (equiv)	y (equiv)	T (°C)	Yield (%) ^a	ee (%)
1	16	0.1	2.2	RT	33	26
2	16	0.15	2.2	RT	76	28
3	16'	0.1	2.2	RT	27	32
4	16'	0.15	2.2	RT	51	30
5	16'	0.2	2.2	RT	62	28
6	28	0.1	2.2	RT	53	25

^a: Isolated yield after purification.

Table 4.8 Results for the optimization of hydroxylation of phenols at room temperature.

Observing these results, we explored the effect of the temperature in the enantiocontrol with the three different catalysts (Table 4.9).

When the reaction took place at 0 °C, the enantioselectivity increased for all three catalysts (entries 1-3). In these conditions, catalyst **28** was less effective than the others. At a reaction temperature of -5 °C, catalyst **16** showed significantly better results than its derivative **16'** (entries 4 and 9). Modifying the amount of oxidant (entries 5 and 6), the catalyst loading (entry 7) or adding the oxidant in two portions (entry 8) didn't affect the reaction outcome. Further decrease in the temperature caused a drop in yield although no effect in enantioselectivity was observed (entries 10 and 11).

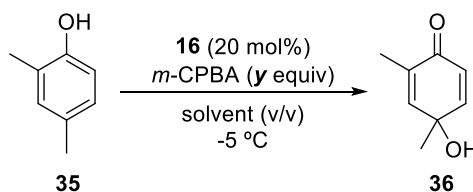


Entry	I(I)-cat	x (equiv)	y (equiv)	T (°C)	Yield (%) ^a	ee (%)
1	16	0.1	2.2	0	44	44
2	16'	0.1	2.2	0	49	45
3	28	0.1	2.2	0	45	38
4	16	0.1	2.2	-5	96	50
5	16	0.1	3	-5	87	48
6	16	0.1	1.5	-5	90	48
7	16	0.15	2.2	-5	98	50
8 ^b	16	0.1	2.2	-5	97	48
9	16'	0.1	2.2	-5	54	50
10	16'	0.1	2.2	-10	58	48
11	16	0.1	2.2	-10	54	50

^a: Isolated yield after purification. ^b: The oxidant was added in two portions.

Table 4.9 Results obtained for the dearomatization reaction lowering the temperature.

With conditions described in entry 4, several solvent mixtures were tested (Table 4.10). Different concentrations (entries 1 and 2) or different ratio of MeCN and water (entries 3 and 4) did not improve the previous results. Related results were obtained when water is combined with other solvents such MeNO₂ or THF (entries 5 and 6). The introduction of fluorinated solvents in the apparently most efficient solvent mixture (MeCN/H₂O) increased significantly the isolated yield of the dearomatized product **36** (entries 7-11). In these conditions, combination with trifluoroethanol and addition of 1.8 equivalents of terminal oxidant generated the *p*-quinol derivative **36** in a 94% yield and 46% *ee* (entry 10).



Entry	<i>y</i> (equiv)	solvent	v/v	Yield (%) ^a	<i>ee</i> (%)
1 ^b	2.2	MeCN/H ₂ O	9/1	80	48
2 ^c	2.2	MeCN/H ₂ O	9/1	69	46
3	2.2	MeCN/H ₂ O	2/1	52	46
4	2.2	MeCN/H ₂ O	4/1	67	48
5	2.2	MeNO ₂ /H ₂ O	9/1	65	10
6	2.2	THF/H ₂ O	9/1	25	28
7	2.2	MeCN/HFIP/H ₂ O	8/1/1	79	42
8	2.2	MeCN/TFE/H ₂ O	8/1/1	84	44
9	1.5	MeCN/TFE/H ₂ O	8/1/1	92	46
10	1.8	MeCN/TFE/H ₂ O	8/1/1	94	46
11	2.2	MeCN/TFE/H ₂ O	4.5/4.5/1	45	36

^a: isolated yield after purification. ^b: reaction at low concentration (0.08M). ^c: reaction at high concentration (0.25M).

Table 4.10 Optimization of the solvent mixture.

4.3.2 Scope of the enantioselective 4-hydroxylation of phenols

Based on the results obtained in the optimization of this transformation, two methods were selected concerning yield and enantioselectivity. Considering that catalyst **16** offered the best combination of this factors, 10 mol% of catalyst loading was used in both methods together with different amounts of oxidant: 1.8 equivalents in Method B or 2.2 equivalents in Method A at -5 °C reaction temperature. Under these two conditions, we explore the scope of the 4-hydroxylation of a range of phenols (Figure 4.26).

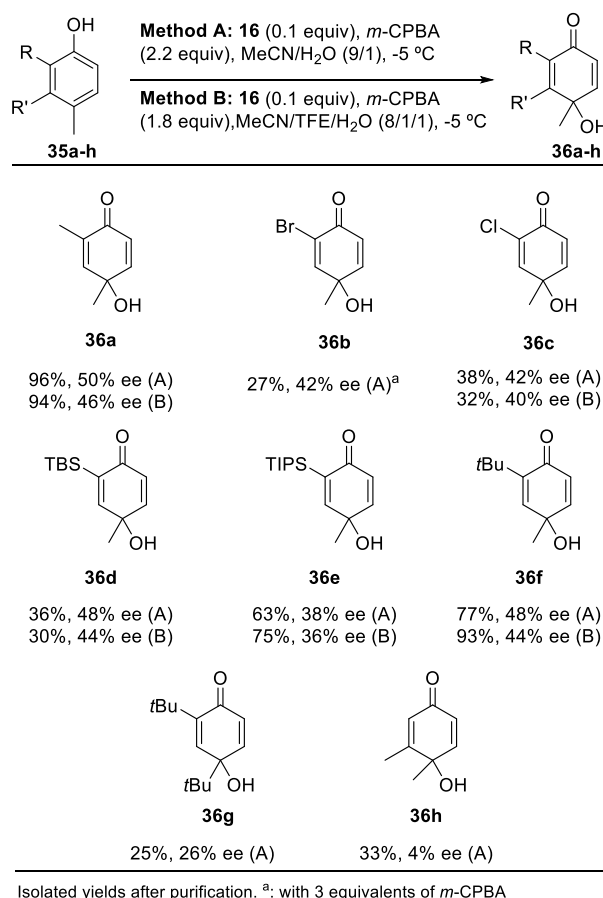


Figure 4.26 Scope of the iodine(III)-catalyzed enantioselective phenol dearomatization reaction.

Reasonable enantioselective induction was observed for 2,4-disubstituted phenols (**36a-f**). Different results were obtained depending on the substituents placed at the phenol ring. The individual steric size of the 2-substituent did not affect the enantioselectivities as was demonstrated by compound **36a** with a methyl group substituent and compound **36b** with a bulkier *tert*-butyl group. But when the latter bulky substituent is placed in *para*-position, the reaction rate dramatically decreased and only under conditions A, a moderate yield of 25% of **36g** could be obtained. Related result was observed for the 3,4-disubstituted phenol **35h**, which provided the corresponding quinol **36h** in 33% yield and almost no enantioselectivity, 4% *ee*.

With these results, we can conclude that catalyst **16** tolerates 2,4-disubstituted phenols (**36a-f**) with variable substituent size in 2-position but small alkyl substituents at *para* position.

4.3.3 Mechanistic proposal

Observing the effect of the substitution in the phenol aryl ring, we proposed the following mechanism (Figure 4.27). The catalytic cycle starts with the oxidation of the iodine(I)-catalyst to the active iodine(III) species **IX**. This catalyst state is in concordance with the identified corresponding diacetate involved in the diacetoxylation reaction of styrenes. Next, cationic iodine(III) **X** is generated by dissociation of one 3-chlorobenzoate ligand. Coordination of the iodine(III) to the phenol creates the required chiral pocket, based on the steric requirements, as it was observed for the substituents in 2-, 3-, and 4-positions of the phenol ring discussed before. At this stage, an environment for an efficient differentiation of the prochiral faces of the phenol ring is performed directing the attack by the water nucleophile within an arrangement **XI**, in agreement with a recent report by Ishihara on related catalyst control through hydrogen bonding in intramolecular 1,2- and 1,4- dearomatization reactions.¹⁶⁵ Once the C-O bond is formed, the corresponding enantioenriched *p*-quinol derivative **36a** is released together with a molecule of 3-chlorobenzoic acid closing the catalytic cycle with the regeneration of the initial iodine(I) catalyst **16**.

¹⁶⁵ Uyanik, M.; Sasakura, N.; Mizuno, M.; Ishihara, K. *ACS Catal.* **2017**, *7*, 872.

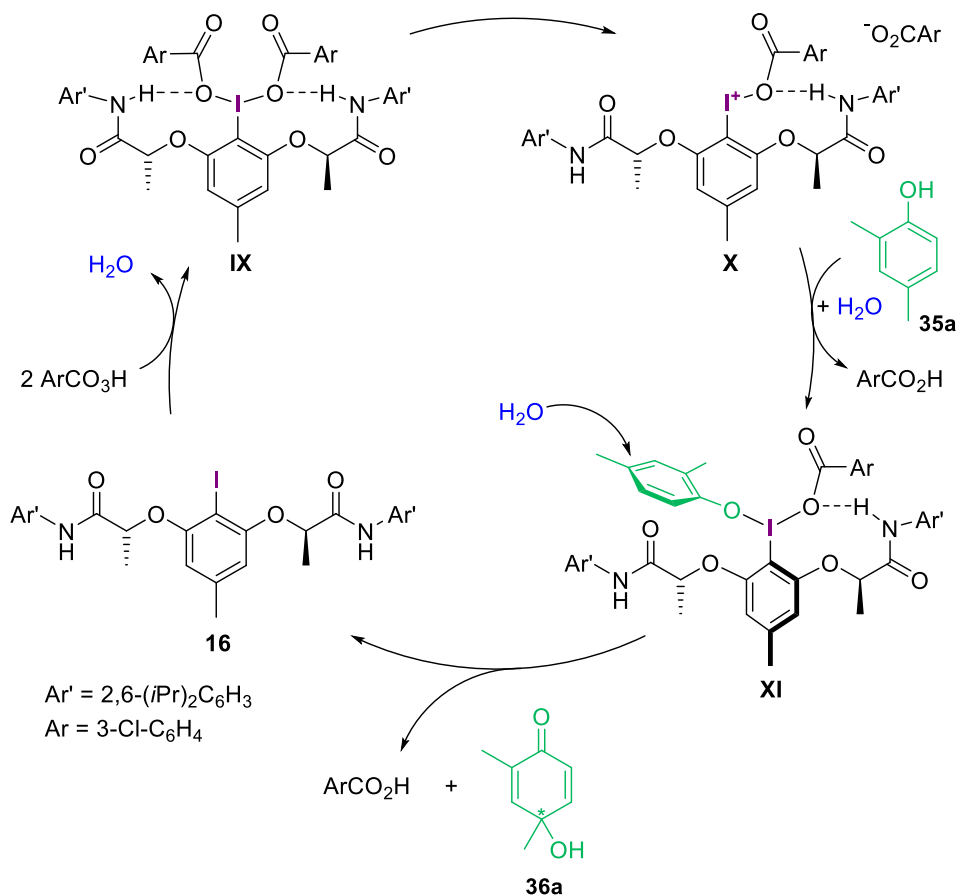


Figure 4.27 Catalytic cycle proposed for the enantioselective 4-hydroxylation of phenols.

4.3.4 Iodine(I/III)-catalyzed dearomatization of anilines

Dearomatization of anilines can be achieved by oxidation with hypervalent iodine(V) reagents such as IBX. One example was reported in 2005 by Quideau, in which a substituted

aniline is oxidized to the corresponding *o*-quinol imine with low selectivity (Figure 4.28).¹⁶⁶

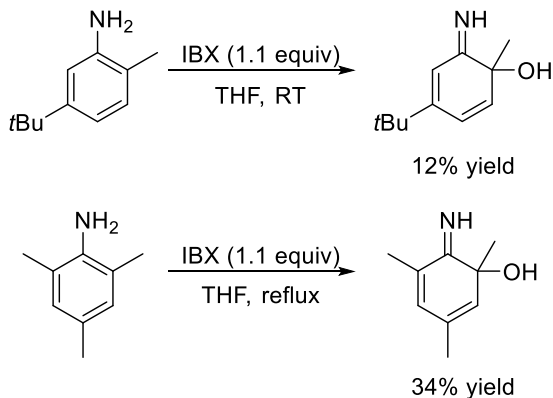


Figure 4.28 Examples for iodine(V)-mediated 2-hydroxylation reaction through aniline dearomatization.

We envisioned extending the scope of our 4-hydroxylation process to tosylated aniline **37** due to the comparable acidity of the N-H and the phenol OH in **35** (Figure 4.29). Under our standard conditions, we could isolate the final imine **38** in a completely chemoselective manner, improving the previous reported results. Enantiomeric excesses obtained for this substrate are similar to the related compound **36b**, demonstrating that our optimized conditions can be extended from phenols to *N*-tosyl anilines.

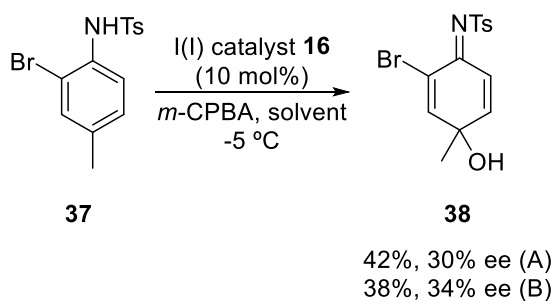


Figure 4.29 Enantioselective 4-hydroxylation of tosylated anilines under iodine(I/III)-catalysis.

¹⁶⁶ Quideau, S.; Pouységu, L.; Ozanne, A; Gagnepain, J. *Molecules* **2005**, *10*, 201.

4.4. Conclusions

After an extensive search of the best transformation to test our previously reported chiral catalyst **16** and its derivatives, we present a second methodology for an enantioselective dearomatization of phenols under intermolecular reaction control.

A total of 8 different substituted phenols were successfully converted into the correspondent 4-hydroxylated products through two different protocols in an enantioselective manner. This feature probes the efficiency of our method compare to the previous reported.

Based on the results obtained from the exploration of the scope of the reaction, we propose a mechanistic context derived from the sterics' requirements for enantioinduction of the needed chiral pocket.

Finally, our 4-hydroxylation process was successfully extended to the dearomatization of tosylated anilines, which exemplifies the exciting possibilities that this method offers.

4.5. Experimental part

General remarks: All solvents, reagents and all deuterated solvents were purchased from Aldrich and Acros. Column chromatography was performed with silica gel (Merck, type 60, 0.063-0.20 mm). NMR spectra were recorded on a Bruker Avance 300 MHz, 400 MHz or 500 MHz spectrometer, respectively. All chemical shifts in NMR experiments are reported in ppm downfield from TMS. The following calibrations were used: CDCl₃ δ = 7.26 and 77.16 ppm; DMSO-d₆ δ = 2.50 and 39.52 ppm. MS (ESILCMS) experiments were performed using an Agilent 1100 HPLC with a Bruker micro-TOF instrument (ESI). Unless otherwise stated, a Supelco C8 (5 cm x 4.6 mm, 5 μ m particles) column was used with a linear elution gradient from 100% H₂O (0.5% HCO₂H) to 100% MeCN in 13 min at a flow rate of 0.5 mL/min. MS (EI) and HRMS experiments were performed on a Kratos MS 50 within the service departments at ICIQ. Melting points were determined with a Buchi Melting Point B-540 apparatus. IR spectra were taken with a Bruker Alpha instrument in the solid state. Specific optical rotation values were measured with a Polarimeter

JascoP1030 equipped with a 100 mm cell. HPLC measurements were carried out on a ACQUITY UPLC® system (Waters) UltraPerformance Convergence Chromatography™ (UPC2™) equipped with a detector ACQUITY UPLC PDA (Photodiode Array detector). The respective chiral stationary phase and exact conditions are specified for each individual compound within the compound characterization section.

The following compounds were commercially available and used as received 2,4-Dimethylphenol (**35a**), 2-Bromo-4-methylphenol (**35b**), 2-Chloro-4-methylphenol (**35c**), 2-(*tert*-Butyl)-4-methylphenol (**35f**), 2,4-Di-*tert*-butylphenol (**35g**), 3,4-Dimethylphenol (**35h**). 2-(*tert*-Butyldimethylsilyl)-4-methylphenol (**35d**), 4-Methyl-2-(triisopropylsilyl)phenol (**35e**) were synthesized according to a literature protocol.¹⁶³ *N*-(2-Bromo-4-methylphenyl)-4-methylbenzenesulfonamide (**37**) was synthesized according to a literature protocol.¹⁶⁷ Products **36a,b,c,d,e,h** were reported previously.¹⁶³

General procedures:

Method A for enantioselective hydroxylation (GP11): Into a Pyrex tube equipped with a stir bar was placed the respective phenol (0.2 mmol, 1 equiv), the chiral iodine(I)-compound (0.02 mmol, 10 mol%) in a mixture of acetonitrile/H₂O (0.16 M, 9:1). Last was added *m*-CPBA (0.44 mmol, 2.2 equiv) and the mixture was stirred until completion. Then, the reaction was quenched with a saturated aqueous solution of NaHCO₃ (4 mL) and a saturated aqueous solution of Na₂S₂O₃ (4 mL). The mixture was extracted with CH₂Cl₂ (3x 10 mL) and the combined organic phases were dried over Na₂SO₄, filtered and concentrated under reduced pressure. The residue was purified by flash column chromatography (silica gel, *n*-hexane/ethyl acetate, 85/15, v/v) to afford the desired quinol, which was submitted to HPLC analysis.

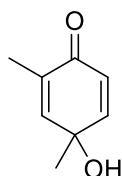
Method B for enantioselective hydroxylation (GP12): Into a Pyrex tube equipped with a stir bar was placed the respective phenol (0.2 mmol, 1 equiv), the chiral iodine(I)-compound (0.02 mmol, 10 mol%) in a mixture of acetonitrile/trifluoroethanol/H₂O (0.16 M, 8:1:1). Then, *m*-CPBA (0.36 mmol, 1.8 equiv) was added. and the mixture was stirred until completion. After such time, the reaction was quenched with a saturated aqueous solution of NaHCO₃ (4 mL) and a saturated aqueous solution of Na₂S₂O₃ (4 mL). The

¹⁶⁷ Song, H.; Liu, Y.; Liu, Y.; Wang, Q. *Org. Lett.* **2014**, *16*, 3240.

layers were separated and the aqueous phase was extracted with CH_2Cl_2 (3x 10 mL). The combined organic layers were dried over Na_2SO_4 , filtered and the solvent was removed under reduced pressure. The crude product was purified by flash column chromatography (silica gel, *n*-hexane/ethyl acetate, 85/15, v/v) to afford the desired quinol, which was submitted to HPLC analysis.

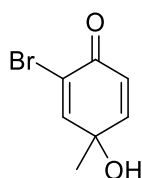
Data for the final products 36:

4-Hydroxy-2,4-dimethylcyclohexa-2,5-dienone (36a)



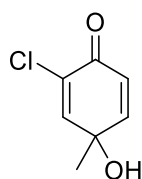
Yield: 26.5 mg (96%, Method A), 26 mg (94%, Method B); 50% *ee* (Method A), 46% *ee* (Method B) [HPLC (IA, CO_2 /*i*-PrOH, 95:5, 1500 psi, 3 mL/min): t_R = 1.80 (minor), 2.33 min (major)].

2-Bromo-4-hydroxy-4-methylcyclohexa-2,5-dienone (36b)

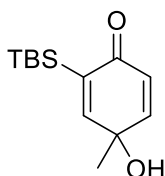


Yield: 11 mg (27%, Method A); 42% *ee* (Method A) [HPLC (IA, CO_2 /MeOH, 90:10, 1500 psi, 3 mL/min) t_R = 1.56 (major), 1.88 min (minor)].

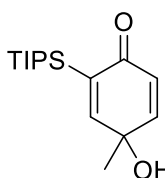
2-Chloro-4-hydroxy-4-methylcyclohexa-2,5-dienone (36c)



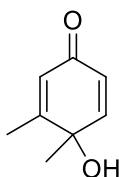
Yield: 12 mg (38%, Method A), 10 mg (32%, Method B); 42% *ee* (Method A), 40% *ee* (Method B) [HPLC (IA, CO_2 /EtOH, 90:10, 1500 psi, 3 mL/min): t_R = 1.38 (major), 1.93 min (minor)].

2-(tert-Butyldimethylsilyl)-4-hydroxy-4-methylcyclohexa-2,5-dienone (36d)

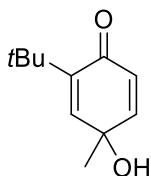
Yield: 17 mg (36%, Method A), 14.1 mg (30%, Method B); 48% *ee* (Method A), 44% *ee* (Method B) [HPLC (IC, CO₂/MeOH, 98:2, 1500 psi, 3 mL/min): *t_R* = 2.90 (minor), 4.90 min (major)].

4-Hydroxy-4-methyl-2-(triisopropylsilyl)cyclohexa-2,5-dienone (36e)

Yield: 35 mg (63%, Method A), 42.2 mg (75%, Method B); 38% *ee* (Method A), 36% *ee* (Method B); [HPLC (IC, CO₂/*i*-PrOH, 90:10, 1500 psi, 3 mL/min); *t_R* = 2.89 (minor), 3.62 min (major)].

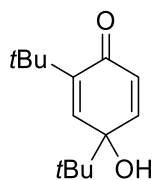
4-Hydroxy-3,4-dimethylcyclohexa-2,5-dienone (36h)

Yield: 9 mg (33%, Method A); 4% *ee* (Method A) [HPLC (IA, CO₂/*i*-PrOH, 95:5, 1500 psi, 3 mL/min): *t_R* = 3.33 (minor), 3.77 min (major)].

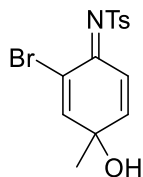
2-tert-Butyl-4-hydroxy-4-methylcyclohexa-2,5-dienone (36f)

Yellow solid; yield: 28 mg (77%, Method A), 33.5 mg (93%, Method B); 48% *ee* (Method A), 44% *ee* (Method B) [HPLC (IE, CO₂/MeOH = 98:2, 2000 psi, 3 mL/min): *t_R* = 2.10 (minor), 3.35 min (major)]. ¹H NMR (300 MHz, CDCl₃): δ = 6.75 (dd, *J* = 9.8, 3.0 Hz, 1 H), 6.63 (d, *J* = 3.0 Hz, 1 H), 5.98 (d, *J* = 9.8 Hz, 1 H), 2.67 (br s, 1 H), 1.42 (s, 3 H), 1.18 (s, 9 H). ¹³C

NMR (75 MHz, CDCl₃): δ = 185.8, 150.0, 146.0, 144.2, 128.8, 67.8, 34.4, 29.2, 27.4. HRMS (ESI-MS): calcd for C₁₁H₁₅O₂: 179.1078; found: 179.1080. IR ν (cm⁻¹): 3368, 2993, 2952, 2868, 1663, 1615, 1487, 1457, 1386, 1366, 1264, 1138, 1121, 1052, 1012, 935, 902, 866, 843. mp: 92–94 °C

2,4-Di-*tert*-butyl-4-hydroxycyclohexa-2,5-dienone (36g)

Yellow solid; yield: 11 mg (25%, Method A); 26% *ee* (Method A) [HPLC (IC, CO₂/*i*-PrOH, 90:10, 1500 psi, 3 mL/min): *t_R* = 0.96 (minor), 1.67 min (major)]. **¹H NMR (500 MHz, CDCl₃):** δ = 6.83 (dd, *J* = 10.1, 3.1 Hz, 1 H), 6.72 (d, *J* = 3.1 Hz, 1 H), 6.10 (d, *J* = 10.1 Hz, 1 H), 2.21 (br s, 1 H), 1.21 (s, 9 H), 0.99 (s, 9 H). **¹³C NMR (126 MHz, CDCl₃):** δ = 185.6, 148.0, 146.2, 143.9, 130.7, 74.3, 39.3, 34.8, 29.3, 25.5. **HRMS (ESI-MS):** calcd for C₁₄H₂₁O₂: 221.1547; found: 221.1552. **IR ν (cm⁻¹):** 3415, 2957, 2909, 2870, 1660, 1623, 1481, 1461, 1390, 1360, 1203, 990, 958, 846. **mp:** 65-66 °C

***N*-(2-Bromo-4-hydroxy-4-methylcyclohexa-2,5-dienylidene)-4-methylbenzenesulfonamide (38)**

White solid; yield: 30 mg (42%, Method A), 28 mg (38%, Method B); 30% *ee* (Method A), 34% *ee* (Method B) [HPLC (IC, CO₂/EtOH = 85:15, 1500 psi, 3 mL/min): *t_R* = 2.00 (major), 2.50 min (minor)]. **¹H NMR (400 MHz, CDCl₃):** δ = 7.91 (d, *J* = 8.3 Hz, 1 H), 7.44 (d, *J* = 10.1 Hz, 1 H), 7.37-7.30 (m, 1 H), 7.24 (d, *J* = 2.5 Hz, 1 H), 6.84 (dd, *J* = 10.1, 2.5 Hz, 1 H), 2.44 (s, 3 H), 2.42 (br s, 1 H), 1.48 (s, 3 H). **¹³C NMR (101 MHz, CDCl₃):** δ = 160.0, 152.5, 151.1, 144.1, 138.2, 129.7, 127.2, 122.0, 119.9, 69.9, 26.3, 21.8. **HRMS (ESI-MS):** calcd for C₁₄H₁₃BrNO₃S: 353.9805; found: 353.9797. **IR ν (cm⁻¹):** 3414, 3029, 2983, 2923, 1739, 1636, 1582, 1539, 1441, 1364, 1301, 1241, 1137, 1083, 1043, 870, 812. **mp:** 141-142 °C.

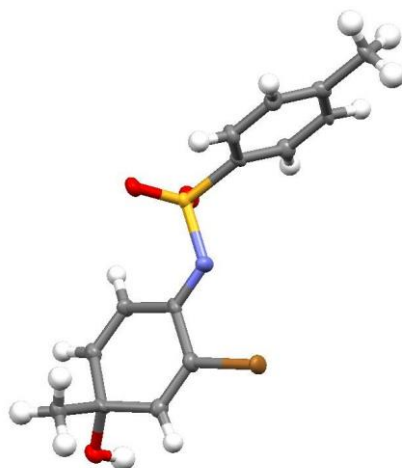


Table 4.11 Crystal data and structure refinement for **38**.

Identification code	CCDC1542367
Empirical formula	C14 H14 Br N O3 S
Formula weight	356.23
Temperature	100(2) K
Wavelength	0.71073 Å
Crystal system	Triclinic
Space group	P-1
Unit cell dimensions	a = 7.6867(7)Å α = 93.177(3)°. b = 8.2138(8)Å β = 98.936(3)° c = 24.524(2)Å γ = 107.624(3)°.
Volume	1449.1(2) Å ³
Z	4
Density (calculated)	1.633 Mg/m ³
Absorption coefficient	2.986 mm ⁻¹
F(000)	720
Crystal size	0.10 x 0.05 x 0.01 mm ³
Theta range for data collection	0.846 to 28.698°.
Index ranges	-6<=h<=10, -11<=k<=11, -32<=l<=27
Reflections collected	14584
Independent reflections	7103[R(int) = 0.0620]
Completeness to theta =28.698°	94.6%
Absorption correction	Multi-scan
Max. and min. transmission	0.971 and 0.72
Refinement method	Full-matrix least-squares on F ²
Data / restraints / parameters	7103/ 0/ 367
Goodness-of-fit on F ²	1.048
Final R indices [I>2sigma(I)]	R1 = 0.0653, wR2 = 0.1498
R indices (all data)	R1 = 0.1122, wR2 = 0.1678
Largest diff. peak and hole	1.163 and -0.907 e.Å ⁻³

Data for the chiral iodine(I) compound 28:

(2*R*,2'*R*)-2,2'-((2-iodo-1,3-phenylene)bis(oxy))bis(*N*-([1,1'-biphenyl]-2-yl)propanamide) (28) According to a published procedure,¹⁵¹ (2*R*,2'*R*)-2,2'-((2-iodo-5-methyl-1,3-phenylene)bis(oxy))dipropanoic acid (200 mg, 0.526 mmol, 1 equiv), oxalyl chloride (234 mg, 1.841 mmol, 3.5 equiv), and a catalytic amount of DMF were stirred in DCM (5 mL) for 3 h at room temperature under an argon atmosphere. The mixture was concentrated under reduced pressure and the crude product together with 2-aminobiphenyl (356 mg, 2.105 mmol, 4 equiv) and pyridine (166 mg, 2.105 mmol, 4 equiv) were stirred in DCM (3 mL) for 16 h at room temperature under an argon atmosphere. The reaction was quenched by addition of 3 M aq HCl. After extraction with DCM, the combined organic phases were dried (anhyd Na₂SO₄) and concentrated under reduced pressure. Purification by flash column chromatography (silica gel, *n*-hexane/EtOAc, 80:20) afforded the pure **28** (322 mg, 90%) as a white solid.

[α]_D²⁵: -136.3 (*c* = 1.00, CHCl₃). **¹H NMR (400 MHz, CDCl₃)**: δ = 8.36 (bs, 2H), 8.24 (dd, *J* = 8.3, 1.1 Hz, 2H), 7.39 (ddd, *J* = 8.7, 7.2, 2.0 Hz, 2H), 7.22-7.30 (m, 14H), 7.15 (t, *J* = 8.3 Hz, 1H), 6.39 (d, *J* = 8.3 Hz, 2H), 4.76 (q, *J* = 6.7 Hz, 2H), 1.65 (d, *J* = 6.7 Hz, 6H). **¹³C NMR (100 MHz, CDCl₃)**: δ = 169.6, 156.9, 138.0, 134.0, 133.6, 130.5, 130.1, 129.3, 129.1, 128.4, 128.1, 125.2, 122.3, 107.0, 80.8, 76.5, 18.9. **HRMS (ESI-MS)**: calcd for C₃₆H₃₁IN₂NaO₄: 705.1221, found: 705.1220. **IR ν (cm⁻¹)**: 3368, 1686, 1584, 1517, 1494, 1447, 1436, 1370, 1303, 1280, 1246, 1090, 1058, 1009. **m.p.**: 65-69 °C.

UNIVERSITAT ROVIRA I VIRGILI

NEW APPLICATIONS OF IODINE(III) REACTIVITY: SYNTHESIS AND FUNCTIONALIZATION OF HETEROCYCLES

Laura Fra Fernández

Chapter 5

Overall Conclusions and Outlook

5.1 Conclusions

The main scientific outcome of this doctoral Thesis has been the development of new synthetic methodology for indole syntheses using the unprecedented approach of hypervalent iodine(III) chemistry. In particular we have reported a new synthetic methodology towards the synthesis of either 2,3-unsubstituted indoles or 2,3-diarylated indoles. These scaffolds add to the generally available substitution pattern on the indole core, which constitutes one of the most ubiquitous heterocycles in medicinal and pharmaceutical chemistry. The main synthetic accomplishment thus lies with the substitution pattern at the indole product. In contrast to most common approaches, iodine(III) reactivity can promote the cyclization of unsubstituted 2-vinyl anilines to indoles that are non-substituted in its 2,3-positions and await subsequent further functionalization. The reaction is of broad scope demonstrating the high applicability of the present method.

As an alternative, an intramolecular cyclization employing a removable tether for reaction control provides selective access to 2,3-diarylated indoles. Four different protocols were successfully developed using stoichiometric or catalytic amounts of iodine(III) reagents.

In the final section, one of the first examples of enantioselective intermolecular dearomatization of phenols using a chiral iodine(III) catalyst is presented. The final 4-hydroxylated products were obtained with good enantiomeric excess, which resulted to be superior to the previously reported examples. These results open the door for the development of further new synthetic metal-free methodology in asymmetric transformations.

NEW APPLICATIVE FUNCTIONALIZATION OF HETEROCYCLES

Laura Fernández

UNIVERSITY OF NAVARRA

LEONARDO RODRÍGUEZ

LAURA FRA FERNÁNDEZ



UNIVERSITAT
ROVIRA i VIRGILI

